Visualisation and Detection of Latent DNA in the Wildlife Trade: Pangolins as a Model Species

By

CHAN Hee Joo, Amy

Bachelor of Science (Hons)

Thesis

Submitted to Flinders University

for the degree of

Master of Science by Research

College of Science and Engineering

31 March 2024

TABLE OF CONTENTS

TABLE OF CONTENTS ..... **I**
ABSTRACT ..... **V**
DECLARATION ..... **VII**
ACKNOWLEDGEMENTS ..... **VIII**
LIST OF FIGURES ..... **IX**
LIST OF TABLES ..... **XV**
ABBREVIATIONS ..... **XVII**
CHAPTER ONE: INTRODUCTION **1**
1.1 Wildlife Trade 1
1.1.1 Illegal Wildlife Trade (IWT) 2
1.1.2. The Convention on the International Trade in Endangered Species of Wild Fauna and Flora (CITES) 3
1.2 Pangolins 4
1.2.1 Different species of pangolins 4
1.2.2 Illegal Trade of Pangolins 5
1.2.3 Pangolins in Singapore 6
1.3 Molecular Techniques in Wildlife Forensics 8
1.3.1 Molecular Species Identification 9
1.3.2 Assignment of Geographical Origins 9
1.3.3 Determination of Number of Individuals 10
1.4 Visualisation of Latent DNA using Nucleic Acid Dyes 11
1.4.1 Latent DNA 11
1.4.2 Use of Nucleic Acid Stains for the Visualisation of Latent DNA 12
1.4.3 Types of Nucleic Acid Dyes 13
1.4.4 Ethidium Bromide 14
1.4.5 SYBR Green Nucleic Acid Stains 14
1.4.6 DAPI 15
1.4.7 Hoechst dye 15
1.4.8 GelRed® Nucleic Acid Gel Stain 16
1.4.9 Diamond™ Nuclei Acid Dye (DD) 16
1.5 Research Questions and Approach 16
1.5.1 Aims and Objectives 17
CHAPTER TWO: DEPOSITION OF LATENT DNA BY PANGOLIN SCALES: A PROOF-OF-CONCEPT STUDY **18**
2.1 Background 18
2.2 Material and Methods 18
2.2.1 Processing of Scales from *M. javanica* (Sunda Pangolin) 18
2.2.2 Surface Decontamination of Consumables and Tools Used 19

2.2.3 Deposition of Cellular Material onto Glass Slides 20
2.2.4 Staining and Visualisation of Latent DNA Using Diamond™ Nuclei Acid Dye 21
2.2.5 Quantification of Fluorescent Particles using ImageJ Software 21
2.2.6 Recovery of DNA using Tape-lifting 21
2.2.7 Extraction of DNA from Tapes Using Commercial Spin Columns 22
2.2.8 Quantification of Isolated DNA using Spectrometry 22
2.2.9 Molecular Species Identification of Isolated DNA Using Conventional PCR 23
2.3 Results 24
2.3.1 Morphological Observation of the Dried *M. javanica* Scales 24
2.3.2 Staining of Cellular Materials Deposited by *M. javanica* Scales via Friction 24
2.3.3 Staining of Cellular Material Deposited by *M. javanica* Scales via Pressure 34
2.3.4 Amplification and Sequencing of DNA Isolated via Conventional PCR 48
2.4 Discussion of results 55
2.4.1 The *M. javanica* Scales Used 55
2.4.2 Comparison of Fluorescent Particles Deposited by Human and *M. javanica* Scales 55
2.4.3 Molecular Species Identification using DNA Isolated from the Glass Slides 56
CHAPTER THREE: ESTABLISHMENT OF QUANTITATIVE PCR FOR THE QUANTITATION OF LATENT DNA DEPOSITED ON CONTACT SURFACES 59
3.1 Background 59
3.1.1 Types of Quantitative Polymerase Chain Reaction (qPCR) 59
3.1.2 Uses of qPCR in Wildlife Forensic Science 60
3.1.3 Objectives using qPCR 60
3.2 Materials and Methods 61
3.2.1 Samples Used 61
3.2.2 DNA Extraction from Dried Tissue Samples Using Commercial Spin Column Kit 61
3.2.3 Primers and Probe Design 62
3.2.3 Development and Optimisation 62
3.2.4 Assessing the Analytical Specificity 63
3.2.5 Assessing the Repeatability and Reproducibility 63
3.2.5 qPCR Amplification 63
3.3 Results 64
3.3.1 Primers and Probe Design 64
3.3.2 Preliminary Assessment of Primer sets: Determination of Annealing Temperature .. 65
3.3.3 Determination of Analytical Specificity of Primer and Probe set 67
3.3.4 Assay Optimization 68
3.3.5 Determination of Repeatability and Reproducibility of qPCR Assay 69
3.4 Discussion 70
3.4.1 The Selected Primers and Probe Set 70
3.4.2 Analytical Specificity of the Assay 71
3.4.3 Repeatability and Reproducibility of the Assay 71
3.4.4 Summary of Discussion 72

CHAPTER FOUR: COMPARISON OF DNA RECOVERY AND EXTRACTION METHODS FOR USE TO DETECT PANGOLIN LATENT DNA DEPOSITED ON GLASS SLIDES 73
4.1 Background 73
4.1.1 DNA Recovery Methods Used in Forensic Sciences 73
4.1.2 Objectives for Comparison of DNA Recovery and Extraction Methods 74
4.2 Materials and Methods 75
4.2.1 Samples Used 75
4.2.2 Staining and Visualisation of Latent DNA Deposited on Glass Slides Using Diamond™ Nuclei Acid Dye 76
4.2.3 Quantification of Fluorescent Particles using ImageJ Software 76
4.2.4 Latent DNA Recovery 76
4.2.5 DNA Extraction 77
4.2.6 DNA Amplification 78
4.3 Results 79
4.3.1 Visualisation of Latent DNA on Glass Slides 79
4.3.2 Distribution of Cellular Particles Deposited on Glass Slides 86
4.3.3 Comparison of Latent DNA Recovery and Extraction Methods using Conventional PCR 88
4.3.4 Comparison of Latent DNA Recovery and Extraction Methods using qPCR 90
4.4 Discussion 92
4.4.1 Distribution of *M. javanica* Cellular Materials Deposited on the Glass Slides 92
4.4.2 Optimal DNA recovery and DNA Extraction Method for Latent DNA Detection 93
CHAPTER FIVE: DEPOSITION OF LATENT DNA FROM *M. JAVANICA* SCALES ONTO TWO TYPES OF PLASTIC SHEETS VIA FRICTION 94
5.1 Background 94
5.1.1 Polyethylene (PE) 94
5.1.2 Objectives of this Experiment 94
5.2 Materials and Methods 95
5.2.1 Samples Used in this Experiment 95
5.2.2 Surface Substrates Used in this Experiment 95
5.2.3 Staining and Visualisation of Latent DNA Deposited on the Plastic Sheets Using Diamond™ Nuclei Acid Dye 95
5.2.4 DNA Recovery, Extraction and Amplification 96
5.3 Results 96
5.3.1 Visualisation of Latent DNA on Plastic Sheets 96
5.3.2 Comparison of Cellular Materials Deposited onto the HDPE (Transparent) and LDPE (Black) Bag 99
5.3.2 Amplification of DNA Samples Extracted from the Two Types of Plastic Sheets Using Conventional PCR 100
5.3.3 Comparison of Latent DNA Recovery and Extraction Methods for Plastic sheets using qPCR 105
5.4 Discussion 108
5.4.1 Deposition of *M. javanica* Cellular Materials on Plastic Sheets 108

5.4.2 Optimal DNA Recovery and Extraction Method for Latent *M. javanica* DNA Deposited on Plastic Sheets. 108

CHAPTER SIX: VISUALISATION AND DETECTION OF LATENT DNA DEPOSITED BY DRIED PANGOLIN SCALES ONTO PLASTIC PACKAGING BAGS 110

6.1 Background 110

6.1.1 DNA Extraction Methods 110

6.1.2 Objectives for this chapter 112

6.2 Publication and Presentation 112

6.3 Submitted Manuscript: Disrupting the illegal trade in pangolins: Visualisation and Detection of Latent DNA Deposited by Pangolin Scales 112

Title: Disrupting the illegal trade in pangolins: visualisation and detection of latent DNA deposited by pangolin scales 112

6.4 Further Materials and Methods 6

6.4.1 Deposition of Latent DNA onto Packaging Bags 6

6.4.2 Latent DNA Recovery via Tape – Lifting 6

6.4.3 Isolation of Latent DNA from Tapes via Commercial Spin Column Kits 6

6.4.3 Isolation of Latent DNA from Swabs or Tapes via Alkaline Lysis Extraction Method 6

6.5 Further Results and Discussion 7

6.5.1. Comparison of Various Latent DNA Samples Obtained Using Conventional PCR 7

6.5.2 DNA Quantification in Various Latent DNA Samples Using qPCR 11

6.5.3 Discussion of Results and the Optimal DNA Recovery and Extraction Workflow 13

CHAPTER SEVEN: CONCLUSION 15

7.1 Concluding Remarks 15

7.1.1 Limitations 16

7.2 Future Work 16

7.2.1 Deposition of Latent DNA on Different Contact Surface by Various Wildlife Products 16

7.2.2 Persistence of Latent DNA in Varying Environmental Conditions 17

7.2.3 Identification of Human Individuals from Latent DNA from IWT Casework 17

7.2.4 Validation of Latent DNA for IWT caseworks 17

BIBLIOGRAPHY 18

APPENDICES 28

Appendix A: Additional illustrations for Section 2.3.2: Staining of Cellular Material Deposited by *M. javanica* Scales via Friction 28

Appendix B: Additional illustrations for Section 2.3.3: Staining of Cellular Material Deposited by *M. javanica* Scales via Pressure 34

Appendix C: Co – Authorship Approval Form 39

ABSTRACT

This thesis detailed the detection and visualization of latent DNA deposited by pangolin scales using Diamond™ nucleic acid dye. Pangolins are the most illegally traded mammalian species with their scales commonly used in traditional medicines.

The ability of pangolin scales to shed cellular materials onto contact surfaces had not been investigated. In this project, the scales were removed from a roadkill Sunda pangolin (*Manis javanica*) and processed by drying to mimic the processing that pangolin scales undergo before distributing to the markets. A proof-of-concept study was first conducted using glass slides as a contact substrate. Two modes of cellular materials deposition, pressure, and friction were investigated and it was shown that more cellular materials were deposited onto the slides via friction than pressure. It was also deduced that much of the cellular materials deposited derived from the remnants of the dried tissues found on the ventral side of the scale as more cellular materials could be observed from the ventral side than the dorsal. DNA was then isolated from these cellular materials and identified to be of *M. javanica* origin using conventional PCR primers targeting the cyt b region of the mitochondrial DNA.

A *M. javanica* specific qPCR targeting the cyt b region of the mitochondrial DNA was also developed to quantify *M. javanica* latent DNA. The designed primer and probes set was determined to be specific by testing it against the DNA from *M. javanica*, *S. gigantea*, *S. temminckii*, *P. tricuspis*, *P. tetradactyla* and human. This qPCR was then used to compare the amount of latent *M. javanica* DNA recovered from glass slides using swabs or tape – lift and, extracted using commercial spin column or alkaline lysis DNA extraction method. It was found that swabbing was able to recover more DNA than tape – lifting. Swabbing followed by commercial spin column DNA extraction method also obtained the highest amount of DNA, indicating that this was the optimal workflow to be used when recovering and extracting latent *M. javanica* DNA from non – porous glass slides.

The experiment was then extended to recover latent *M. javanica* DNA from plastic bags used to store pangolin scales. *M. javanica* scales were packaged into five plastic bags and the presence of latent DNA was detected using Diamond™ Nucleic acid dye. Swabs were used to recover the stained cellular materials from various locations in the five bags, and isolated DNA was quantified using the established qPCR. As expected, a greater number of stained particles were found at the bottom of the bag than at the top. Latent *M. javanica* DNA were then recovered and extracted using a combination of swabbing or tape – lifting DNA recovery techniques followed by commercial spin column or alkaline lysis DNA extraction method and the qPCR results showed that using swabbing, followed by commercial spin column extraction method would recover and isolate the

highest amount of latent *M. javanica* DNA deposited on the plastic bags, correlating well with the results obtained previously from glass slides.

DECLARATION

I certify that this thesis does not incorporate without acknowledgment any material previously submitted for a degree or diploma in any university; and that to the best of my knowledge and belief it does not contain any material previously published or written by another person except where due reference is made in the text.

Signed:

Date: 31 August 2023

ACKNOWLEDGEMENTS

I would like to firstly express my gratitude to my supervisor, Professor Adrian Linacre for his patience and immense support for my project. Thank you for all the guidance provided throughout the two years. It was not easy to complete the project and thesis without being at the university physically, and without Prof. Linacre's clear, focused guidance and encouragement, I would not have done it.

Secondly, I would like to thank my supervisor at CWF, NParks – Dr Charlene Fernandez for her relentless support, guidance and understanding while I was working on the project in the NParks lab. Thank you for her total support in ensuring that I had all the resources I required to complete my project.

Next, I would also like to thank my co – supervisor, Prof Mike Gardner for his insightful comments and guidance during these two years; I had learnt a lot from our discussions.

Lastly, I would like to thank all my fellow lab-mates at the CWF laboratory in Singapore – you guys are the best! Thank you for covering my official NParks duties while I was "away" doing my Master course and keeping the laboratory running smoothly 😊. Not to mention all the stimulating discussions we had on my project – thank you for the discussions and help rendered, even though my project was not part of your job scope.

LIST OF FIGURES

Figure 1: Illustrating research effort in wildlife trade. Diagram obtained from Andersson et al., 2021. 1

Figure 2: Wildlife trade in terrestrial vertebrates (birds, mammals, amphibians, and reptiles) affects ~24% of species globally. Numbers in brackets are the total number of traded species. IUCN threat status codes: data deficient, DD; least concern, LC; near threatened, NT; vulnerable, VU; endangered, EN; and critically endangered, CR. Diagram obtained from Scheffers et al., 2019. 3

Figure 3: Picture extracted from surveillance camera video captured by National Parks Board, Singapore (NParks), showing a female M. javanica carrying her baby on her tail. Video obtained from NParks. Reproduced with permission. 7

Figure 4: Images of pangolin scales (left) and ivory (right) confiscated by NParks in 2019. Images obtained from NParks. Reproduced with permission. 8

Figure 5: A diagram showing various layers in human skin. Image obtained from Burrill et al (Burrill et al., 2019). 11

Figure 6: Schematic diagram showing the different binding modes of dyes (and other ligands) to DNA (ThermofisherScientific). 14

Figure 7: The chemical structure of SG [2-[N -(3-dimethylaminopropyl)- N -propylamino]-4-[2,3-dihydro-3-methyl-(benzo-1,3-thiazol-2-yl)-methylidene]-1-phenyl-quinolinium] as determined by MS and NMR studies. Image obtained from Zipper et al. (Zipper et al., 2004) 15

Figure 8: The chemical structure of 4',6-diamidino-2-phenylin-dole (DAPI). Image obtained from Kapuscinski, 1995 (Kapuscinski, 1995). 15

Figure 9: The chemical structure of Hoechst 33342, Hoechst 33258 and Hoechst 34580. Image obtained from Bucevičius et al. (Bucevičius et al., 2018). 16

Figure 10: Dorsal view of the respective scales used in this project. 19

Figure 11: View of the ventral side of the respective scale used. Red arrows indicate where dried tissues can be found. 19

Figure 12: Setup for cellular material deposition via pressure. Individual pangolin scales were placed on a clean glass plate ventral side downwards. A second clean glass plate was placed on top and a weight, of known mass, was placed on top of glass plate. 21

Figure 13: Overall view of negative control (N). The entire slide was divided into 7 columns and 4 rows to allow the field of the microscope to cover the entire slide. 25

Figure 14: Expanded image of the field highlighted in red in Figure 13 (blank slide), at 50x magnification. 25

Figure 15: Overall view of slide deposited with DNA from thumbprint. The entire slide was divided into 7 columns and 4 rows to allow the field of the microscope to cover the entire slide. 26

Figure 16: Expanded image of the field highlighted in red in Figure 15 (thumbprint), showing the length of a typical fluorescence staining from thumbprint (L-0.130 mm) at 50x magnification. 26

Figure 17: Overall view of slide deposited with DNA from scale A, via friction, 60 sec. The entire slide was divided into 7 columns and 4 rows to allow the field of the microscope to cover the entire slide. 27

Figure 18: Expanded image of the field highlighted in red in Figure 17 (scale A), showing the length of a typical fluorescence staining from scale A (L-0.196 mm) at 50x magnification. 27

Figure 19: Overall view of slide deposited with DNA from scale B, via friction, 60 sec. The entire slide was divided into 7 columns and 4 rows to allow the field of the microscope to cover the entire slide. 28

Figure 20: Expanded image of the field highlighted in red in Figure 19 (scale B), showing the length of a typical fluorescence staining from scale B (L-0.062 mm) at 50x magnification. 28

Figure 21: Overall view of slide deposited with DNA from scale C, via friction, 60 sec. The entire slide was divided into 7 columns and 4 rows to allow the field of the microscope to cover the entire slide. 29

Figure 22: Expanded image of the field highlighted in red in Figure 21 (scale C), showing the length of a typical fluorescence staining from scale C (L-0.062 mm) at 50x magnification. 29

Figure 23: Overall view of slide deposited with DNA from scale D, via friction, 60 sec. The entire slide was divided into 7 columns and 4 rows to allow the field of the microscope to cover the entire slide. 30

Figure 24: Expanded image of the field highlighted in red in Figure 23 (scale D), showing the length of a typical fluorescence staining from scale D (L-0.137 mm) at 50x magnification. 30

Figure 25: Overall view of slide deposited with DNA from scale E, via friction, 60 sec. The entire slide was divided into 7 columns and 4 rows to allow the field of the microscope to cover the entire slide. 31

Figure 26: Expanded image of the field highlighted in red in Figure 25 (scale E), showing the length of a typical fluorescence staining from scale E (L- 0.66 mm) at 50x magnification. 31

Figure 27: Box plot showing the 25%, 50% and 75% quantiles of the length of the fluorescent particles from the representative image of the slides (n = 20 for each slide). 33

Figure 28: Overall view of negative control (ventral) via pressure. The entire slide was divided into 7 columns and 4 rows to allow the field of the microscope to cover the entire slide..... 35

Figure 29: Overall view of negative control (dorsal) via pressure. The entire slide was divided into 7 columns and 4 rows to allow the field of the microscope to cover the entire slide..... 35

Figure 30: Overall view of slide deposited with DNA from scale A (ventral surface), via pressure. 36

Figure 31: Expanded image of the field highlighted in red in figure 22 (scale A, ventral), showing the length of a typical fluorescence staining from pangolin scale (L-0.086 mm) at 50x magnification. 36

Figure 32: Overall view of slide deposited with DNA from scale A (dorsal surface), via pressure. . 37

Figure 33: Expanded image of the field highlighted in red in Figure 24 (scale A, dorsal), showing the length of a typical fluorescence staining from pangolin scale (L-0.061 mm) at 50x magnification. 37

Figure 34: Overall view of slide deposited with DNA from scale B (ventral surface), via pressure. 38

Figure 35: Expanded image of the field highlighted in red in Figure 26 (scale B, ventral), showing the length of a typical fluorescence staining from pangolin scale (L-0.155 mm) at 50x magnification. 38

Figure 36: Overall view of slide deposited with DNA from scale B (dorsal surface), via pressure. . 39

Figure 37: Expanded image of the field highlighted in red in Figure 28 (scale B, dorsal), showing the length of a typical fluorescence staining from pangolin scale (L-0.086 mm) at 50x magnification. 39

Figure 38: Overall view of slide deposited with DNA from scale C (ventral surface), via pressure. 40

Figure 39: Expanded image of the field highlighted in red in Figure 30 (scale C, ventral), showing the length of a typical fluorescence staining from pangolin scale (L-0.135 mm) at 50x magnification. 40

Figure 40: Overall view of slide deposited with DNA from scale C (dorsal surface), via pressure. . 41

Figure 41: Expanded image of the field highlighted in red in Figure 32 (scale C, dorsal), showing the length of a typical fluorescence staining from pangolin scale (L-0.039 mm) at 50x magnification. 41

Figure 42: Overall view of slide deposited with DNA from scale D (ventral surface), via pressure. 42

Figure 43: Expanded image of the field highlighted in red in Figure 34 (scale D, ventral), showing the length of a typical fluorescence staining from pangolin scale (L-0.044 mm) at 50x magnification. 42

Figure 44: Overall view of slide deposited with DNA from scale D (dorsal surface), via pressure. . 43

Figure 45: Expanded image of the field highlighted in red in Figure 36 (scale D, dorsal), showing the length of a typical fluorescence staining from pangolin scale (L-0.066 mm) at 50x magnification. 43

Figure 46: Overall view of slide deposited with DNA from scale E (ventral surface), via pressure. 44

Figure 47: Expanded image of the field highlighted in red in Figure 38 (scale E, ventral), showing the length of a typical fluorescence staining from pangolin scale (L-0.116 mm) at 50x magnification. 44

Figure 48: Overall view of slide deposited with DNA from scale E (dorsal surface), via pressure. . 45

Figure 49: Expanded image of the field highlighted in red in Figure 40 (scale E, dorsal), showing the length of a typical fluorescence staining from pangolin scale (L-0.050 mm) at 50x magnification. 45

Figure 50: Box plot showing the 25%, 50% and 75% quantiles of the length of the fluorescent particles from the representative image of the slides (n = 10 for each slide). 46

Figure 51: Image of a 1.5% gel after electrophoresis. This shows the outcome from the PCR amplification of the: no template control (NTC), *M. javanica* positive control (extracted DNA), blank tape, blank slide, thumbprint and respective slides (A – E) with *M. javanica* scales. The scales had been in contact with the slides by friction. 50

Figure 52: Image of a 1.5% gel after electrophoresis. This shows the outcome of the PCR amplification from the: no template control (NTC), *M. javanica* positive control (Extracted DNA), blank tape, blank slide, thumbprint and respective slides (A – E) with *M. javanica* scales. The scales had been in contact with the slides via pressure. 52

Figure 53: The threshold level and Cq value on a qPCR amplification curve. (Oswald, 2015)..... 60

Figure 54: Picture of the qPCR conditions from the thermocycler. 64

Figure 55: Assessing optimal annealing temperature for primers Sunda2502A. Electrophoresis of a 1.5% agarose gel shows the PCR products from human, *M. javanica* and no template control (NTC)..... 66

Figure 56: Assessing optimal annealing temperature for primers Sunda2502B. Electrophoresis of a 1.5% agarose gel showed PCR products from human, *M. javanica* and no template control (NTC). 66

Figure 57: Assessing specificity of primer set Sunda2502B at 56°C. 1.5% gel electrophoresis showing PCR products from human, *M. javanica* and no template control (NTC)..... 66

Figure 58: Amplification plot for assessing analytical specificity of Sunda2502A primers and probe set, using DNA from *M. javanica*, *S. gigantea*, *S. temminckii*, *P. tricuspis*, *P. tetradactyla* and human..... 67

Figure 59: Amplification plot for assessing analytical specificity of Sunda2502B primers and probe set, using DNA from *M. javanica*, *S. gigantea*, *S. temminckii*, *P. tricuspis*, *P. tetradactyla* and human..... 68

Figure 60: Standard curve obtained using 0.1µM primers + 0.05µM probe. 69

Figure 61: Screenshot from PrimerQuest™ tool showing the binding locations of the selected primers/ probe set, Sunda2502B..... 71

Figure 62: Flowchart illustrating the downstream processes that each set of slides were subjected to. Set SE denotes sample set was subjected to swabbing followed by commercial spin column extraction; set SA denotes sample set was subjected to swabbing followed by alkaline lysis extraction; Set T denotes sample set was subjected to swabbing; TE denotes sample set was subjected to tape – lifting followed by commercial spin column extraction and, TA denotes sample set was subjected to tape – lifting followed by alkaline lysis extraction..... 75

Figure 63: Illustration of the positions where the fluorescence was imaged across the glass slides. Each dot indicated where 1 image was taken using the Dino-Lite digital microscope. A total of three fields were taken for each slide. 76

Figure 64: Images showing fluorescence staining of one of the clean slides (Negative control – N2) at 50x magnification. From left to right: - left of slide, centre of slide and right of slide. 81

Figure 65: Images showing fluorescence staining of one of the slides deposited with thumbprint (Positive staining control – T2) at 50x magnification. From left to right: - left of slide, centre of slide and right of slide. 81

Figure 66: Images showing fluorescence staining of one of the slides deposited with *M. javanica* scale A (A1) at 50x magnification. From left to right: - left of slide, centre of slide and right of slide. 82

Figure 67: Images showing fluorescence staining of one of the slides deposited with *M. javanica* scale B (B1) at 50x magnification. From left to right: - left of slide, centre of slide and right of slide. 82

Figure 68: Images showing fluorescence staining of one of the slides deposited with *M. javanica* scale C (C1) at 50x magnification. From left to right: - left of slide, centre of slide and right of slide. 83

Figure 69: Images showing fluorescence staining of one of the slides deposited with *M. javanica* scale D (D1) at 50x magnification. From left to right: - left of slide, centre of slide and right of slide. 83

Figure 70: Images showing fluorescence staining of one of the slides deposited with *M. javanica* scale E (E1) at 50x magnification. From left to right: - left of slide, centre of slide and right of slide. 84

Figure 71: Box plot showing the 25%, 50% and 75% quantiles of the length of the fluorescent particles from the representative image of the slides deposited with *M. javanica* cellular particles (n = 10 for each position). SA: set subjected to swabbing then alkaline lysis DNA extraction, SE: set subjected to swabbing then commercial spin column DNA extraction and T: set subjected to tape-lifting. 86

Figure 72: Image of a 1.5% gel after electrophoresis showing the outcome from the PCR amplification. The samples are: no template control (NTC), *M. javanica* positive control (extracted DNA), blank tape, blank slide (N1 and N2), thumbprint and respective slides (A – E) with M. *javanica* scales. The scales had been in contact with the slides by friction, recovered using *swabs* and DNA extracted using *commercial spin column kit*. 88

Figure 73: Image of a 1.5% gel after electrophoresis showing outcome from the PCR amplification. The samples are: no template control (NTC), *M. javanica* positive control (extracted DNA), blank tape, blank slide (N1 and N2), thumbprint and respective slides (A – E) with M. *javanica* scales. The scales had been in contact with the slides by friction, recovered using *swabs* and DNA extracted using *alkaline lysis extraction method*. 88

Figure 74: Image of a 1.5% gel after electrophoresis showing outcome from the PCR amplification. The samples are: no template control (NTC), *M. javanica* positive control (extracted DNA), blank tape, blank slide (N1 and N2), thumbprint and respective slides (A – E) with *M. javanica* scales. The scales had been in contact with the slides by friction, recovered using *tape lifting* and DNA extracted using *commercial spin column kit*. 89

Figure 75: Image of a 1.5% gel after electrophoresis, showing outcome from the PCR amplification. The samples are: no template control (NTC), *M. javanica* positive control (extracted DNA), blank tape, blank slide (N1 and N2), thumbprint and respective slides (A – E) with *M. javanica* scales. The scales had been in contact with the slides by friction, recovered using *tape lifting* and DNA extracted using *alkaline lysis extraction method*. 89

Figure 76: Box plot showing the 25%, 50% and 75% quantiles of the copy number of each DNA sample obtained from various combinations DNA recovery and extraction methods. 91

Figure 77: Black HDPE plastic sheets (left) and the transparent LDPE plastic sheets (right), each measuring approximately 7 cm x 20 cm, excluding plastic backing. 95

Figure 78: An illustration of the positions where the fluorescence was imaged across the plastic sheets. Each dot indicated where one image was taken using the Dino-Lite digital microscope. A total of three images were taken for each sheet. 96

Figure 79: Images showing fluorescence staining on clean transparent (left) and black (right) plastic sheets (negative controls), viewed under 50x UV microscope. 97

Figure 80: Images of showing fluorescence staining on transparent (left) and black (right) plastic sheet deposited with thumbprint (positive staining controls), viewed under 50x UV microscope. .. 97

Figure 81: Images of showing fluorescence staining transparent (left) and black (right) plastic sheet deposited with pangolin scale A, viewed under 50x UV microscope. 98

Figure 82: Images showing fluorescence staining on transparent (left) and black (right) plastic sheet deposited DNA with pangolin scale B, viewed under 50x UV microscope. 98

Figure 83: Images showing fluorescence staining on transparent (left) and black (right) plastic sheet deposited DNA with pangolin scale C, viewed under 50x UV microscope. 98

Figure 84: Images showing fluorescence staining on transparent (left) and black (right) plastic sheet deposited DNA with pangolin scale D, viewed under 50x UV microscope. 99

Figure 85: Images showing fluorescence staining on transparent (left) and black (right) plastic sheet deposited DNA with pangolin scale E, viewed under 50x UV microscope. 99

Figure 86: Box plot showing the 25%, 50% and 75% quantiles of the copy numbers obtained for each DNA samples from HDPE and LDPE plastic sheet (n = 20 for each group). 100

Figure 87: Image of a 1.5% gel after electrophoresis, showing outcome from the PCR amplification. The samples are: no template control (NTC), *M. javanica* positive control (Pos), clean plastic sheet (N1B and N2B), thumbprint and respective slides (A – E) with *M. javanica* scales. The scales had been in contact with the *HDPE (transparent) bag* by friction, recovered using *swabs* and DNA extracted using *alkaline lysis* extraction method. 101

Figure 88: Image of a 1.5% gel after electrophoresis, showing outcome from the PCR amplification. The samples are: clean plastic sheet (N1B and N2B), thumbprint and respective slides (A – E) with *M. javanica* scales. The scales had been in contact with the *LDPE (Black) bag* by friction, recovered using *swabs* and DNA extracted using *alkaline lysis* extraction method. Both positive control and no template control is shown in Figure 87 above. 101

Figure 89: Image of a 1.5% gel after electrophoresis, showing outcome from the PCR amplification. The samples are: no template control (NTC), *M. javanica* positive control (Pos), clean plastic sheet (N1B and N2B), thumbprint and respective slides (A – E) with *M. javanica* scales. The scales had been in contact with the *HDPE (transparent) bag* by friction, recovered using *swabs* and DNA extracted using *commercial spin column* extraction method. 102

Figure 90: Image of a 1.5% gel after electrophoresis, showing outcome from the PCR amplification. The samples are: no template control (NTC), *M. javanica* positive control (Pos), clean plastic sheet (N1B and N2B), thumbprint and respective slides (A – E) with *M. javanica* scales. The scales had been in contact with the *LDPE (black) bag* by friction, recovered using *swabs* and DNA extracted using *commercial spin column* extraction method. 102

Figure 91: Image of a 1.5% gel after electrophoresis, showing outcome from the PCR amplification. The samples are: no template control (NTC), *M. javanica* positive control (Pos), clean plastic sheet (N1B and N2B), thumbprint and respective slides (A – E) with *M. javanica* scales. The scales had been in contact with the *HDPE (transparent) bag* by friction, recovered using *tape - lifting* and DNA extracted using *alkaline lysis* extraction method. 103

Figure 92: Image of a 1.5% gel after electrophoresis, showing outcome from the PCR amplification. The samples are: no template control (NTC), *M. javanica* positive control (Pos), clean plastic sheet (N1B and N2B), thumbprint and respective slides (A – E) with *M. javanica* scales. The scales had been in contact with the *LDPE (black) bag* by friction, recovered using *tape - lifting* and DNA extracted using *alkaline lysis* extraction method. 103

Figure 93: Image of a 1.5% gel after electrophoresis, showing outcome from the PCR amplification. The samples are: no template control (NTC), *M. javanica* positive control (Pos), clean plastic sheet

(N1B and N2B), thumbprint and respective slides (A – E) with *M. javanica* scales. The scales had been in contact with the *HDPE (transparent) bag* by friction, recovered using *tape - lifting* and DNA extracted using *commercial spin column* extraction method..... 104

Figure 94: Image of a 1.5% gel after electrophoresis, showing outcome from the PCR amplification. The samples are: no template control (NTC), *M. javanica* positive control (Pos), clean plastic sheet (N1B and N2B), thumbprint and respective slides (A – E) with *M. javanica* scales. The scales had been in contact with the *LDPE (black) bag* by friction, recovered using *tape - lifting* and DNA extracted using *commercial spin column* extraction method..... 104

Figure 95: Box plot showing the 25%, 50% and 75% quantiles of the copy numbers obtained for each DNA samples from each treatment group. (n = 10 for each group)..... 106

Figure 96: Image of a 1.5% gel after electrophoresis, showing outcome from the PCR amplification. The samples are: no template control (Neg Ctrl), *M. javanica* positive control (Pos Ctrl), negative control bag (N1 – N6), respective bags (A1 – A6, B1 – B6, C1 – C6, D1 – D6, E1 – E6) with *M. javanica* scales. The scales had been contained in the HDPE (transparent) bag by friction, recovered using *swabs* and DNA extracted using the *commercial spin column extraction method*. 7

Figure 97: Image of a 1.5% gel after electrophoresis, showing outcome from the PCR amplification. The samples are: no template control (Neg Ctrl), *M. javanica* positive control (Pos Ctrl), negative control bag (N1 – N6), respective bags (A1 – A6, B1 – B6, C1 – C6, D1 – D6, E1 – E6) with *M. javanica* scales. The scales had been contained in the HDPE (transparent) bag by friction, recovered using *swabs* and DNA extracted using the *alkaline lysis extraction method*. 8

Figure 98: Image of a 1.5% gel after electrophoresis, showing outcome from the PCR amplification. The samples are: no template control (Neg Ctrl), *M. javanica* positive control (Pos Ctrl), negative control bag (N1TE – N6TE), respective bags (A1TE – A6TE, B1TE – B6TE, C1TE – C6TE, D1TE – D6TE, E1TE – E6TE) with *M. javanica* scales. The scales had been contained in the HDPE (transparent) bag, recovered using *tapes* and DNA extracted using the *commercial spin column extraction method*. 8

Figure 99: Image of a 1.5% gel after electrophoresis, showing outcome from the PCR amplification. The samples are: no template control (Neg Ctrl), *M. javanica* positive control (Pos Ctrl), negative control bag (N1TA – N6TA), respective bags (A1TA – A6TA, B1TA – B6TA, C1TA – C6TA, D1TA – D6TA, E1TA – E6TA) with *M. javanica* scales. The scales had been contained in the HDPE (transparent) bag, recovered using *tapes* and DNA extracted using the *alkaline lysis extraction method*..... 9

Figure 100: Image of a 1.5% gel after electrophoresis, showing outcome from the PCR amplification. The samples are: no template control (Neg Ctrl), *M. javanica* positive control (Pos Ctrl), as well as diluted samples from the negative control bag (N1 – N6) and respective bags (A1 – A6, B1 – B6, C1 – C6, D1 – D6, E1 – E6) with *M. javanica* scales. The scales had been contained in the HDPE (transparent) bag by friction, recovered using *swabs* and DNA extracted using the *alkaline lysis extraction method*..... 11

Figure 101: Box plot showing the 25%, 50% and 75% quantiles of the copy numbers obtained for each DNA samples from each treatment group. (n = 10 for each group)..... 12

LIST OF TABLES

Table 1: Composition of PCR master mix for conventional PCR 23

Table 2: Size of scales used in this experiment. The scales were measured point to point at its widest. 24

Table 3: Length (mm) of 20 particles from the representative image of slides deposited. A human thumbprint is included along with scales A – E. Cell deposition was via friction. The mean and standard deviation are included as the last two rows respectively. 32

Table 4: Total fluorescent particle count for each slide. 33

Table 5: Length (mm) of 10 particles from the representative image of slides deposited with ventral side of Scales A – E via pressure or thumbprint and, its respective mean and standard deviation. 46

Table 6: Raw data from One Way Anova analysis generated by RStudio for comparing length of fluorescent particles obtained via friction and pressure. 47

Table 7: Table comparing total fluorescent particle counts for slides exposed to ventral surfaces and dorsal surfaces. 48

Table 8: Table comparing total fluorescent particle counts for slides with cellular material deposited via friction and pressure. 48

Table 9: Concentration of DNA isolated from slides with cellular materials deposited via friction. . 48

Table 10: Concentration of DNA isolated from slides with cellular materials deposited via pressure. 49

Table 11: BLASTn results for DNA samples isolated from slides deposited with *M. javanica* cellular materials using friction. 51

Table 12: BLASTn results for DNA samples isolated from slides deposited with *M. javanica* cellular materials using pressure. 53

Table 13: Comparison of PCR success rate between DNA isolated from cellular materials deposited by friction and pressure. 55

Table 14: Details of 2 selected primers and probe sets. 64

Table 15: Efficiency % and R^2 values obtained for respective primers and probes concentrations. 68

Table 16:Cq value for each reaction of each diluted DNA standards. Each dilution of the DNA standard was tested over three runs and triplicates were performed for each run. The Cq values were obtained and the respective mean, sample standard deviation (SD), pooled SD, repeatability coefficient and P-value were calculated and shown in the table. 69

Table 17: Table showing fluorescent particle count obtained from each image for set SE (Swab, followed by spin column extraction): N1 and N2 – Negative control; T1 and T2 – human thumbprint; A1 and A2 – scale A, B1 and B2 – Scale B, C1 and C2 – Scale C; D1 and D2 – Scale D; and E1 and E2 – Scale E. 85

Table 18: Table showing fluorescent particle count obtained from each image for set SA (swab followed by alkaline lysis extraction): N1 and N2 – Negative control; T1 and T2 – human thumbprint; A1 and A2 – scale A, B1 and B2 – Scale B, C1 and C2 – Scale C; D1 and D2 – Scale D; and E1 and E2 – Scale E. 85

Table 19: Table showing fluorescent particle count obtained from each image for set T (tape – lift): N1 and N2 – Negative control; T1 and T2 – human thumbprint; A1 and A2 – scale A, B1 and B2 – Scale B, C1 and C2 – Scale C; D1 and D2 – Scale D; and E1 and E2 – Scale E. 85

Table 20: Raw data from One way ANOVA analysis generated by Rstudio for the analysis of fluorescent particle counts from each position of the glass slides. 87

Table 21: Raw data from Tukey post-hoc test generated by Rstudio, comparing the fluorescent particle counts obtained from each position of the glass slide. Potions highlighted in yellow indicated that there is statistical difference. 87

Table 22: Table summarising the total number of positive amplifications for DNA samples arising from various combinations (N = 10 for each combination). 90

Table 23: Copy numbers obtained for respective DNA samples using various DNA recovery and extraction methods. 90

Table 24: Raw data from One – way ANOVA analysis generated by Rstudio, for the comparison of CN obtained from DNA samples recovered and extracted using various combinations of DNA recovery and DNA extraction methods. 92

Table 25: Raw data from Tukey Post – hoc test generated by Rstudio, for the comparison of CN obtained from DNA samples recovered and extracted using various combinations of DNA recovery and DNA extraction methods. Portions highlight in yellow indicated that there is a statistical difference in CN obtained. 92

Table 26: Raw data from One – Way ANOVA analysis generated from Rstudio, comparing the TRFC obtained from HDPE and LDPE plastic sheets. 100

Table 27: Summary of conventional PCR results from DNA samples isolated from two types of plastic sheets – HDPE and LDPE. 104

Table 28: Copy numbers (CNs) and mean CNs of latent DNA samples obtained using different combinations of DNA recovery and DNA extraction methods. TA – Tape – lifting with alkaline lysis extraction, TE - Tape – lifting with commercial spin column extraction, SA – Swabbing with alkaline lysis extraction, SE - Swabbing with commercial spin column extraction. 105

Table 29: Raw data generated from One – Way ANOVA analysis in Rstudio, comparing CN of each DNA samples obtained from plastic sheets using different combinations of DNA recovery and DNA extraction methods. 107

Table 30: Raw data generated from Tukey Post – hoc test in Rstudio, comparing CN of each DNA samples obtained from plastic sheets using different combinations of DNA recovery and DNA extraction methods. 107

Table 31: Summary of conventional PCR results from DNA samples isolated from HDPE bags using different combinations of DNA recovery and DNA extraction methods. The number of positive amplications were indicated (rate of positive amplification in parentheses). 9

Table 32: Table showing copy numbers of DNA samples obtained using various combinations of DNA recovery and extraction methods. SA: Swab, followed by Alkaline Lysis Extraction, SE: Swab followed by Commercial Spin Column Extraction, TA: Tape - lift, followed by Alkaline Lysis Extraction, SE: Tape - lift followed by Commercial Spin Column Extraction. 11

Table 33: Raw data obtained for One – Way ANOVA analysis using RStudio, comparing the CNs obtained from samples from LDPE bags, subjected to different combinations of DNA recovery and DNA extraction workflow. 12

Table 34: Raw data obtained for Tukey Post – hoc test using RStudio, comparing the CNs obtained from samples from LDPE bags, subjected to different combinations of DNA recovery and DNA extraction workflow. SE denotes samples subjected to swabbing followed by commercial spin column DNA extraction, SA denotes samples subjected to swabbing followed by commercial alkaline lysis DNA extraction, TE denotes samples subjected to tape - lifting followed by commercial spin column DNA extraction, TA denotes samples subjected to tape - lifting followed by commercial alkaline lysis DNA extraction. 12

ABBREVIATIONS

°C	Degree celsius
µL	Microlitre(s)
µM	Micromolar
A	Adenine
ANOVA	Analysis of Variance
ATL buffer	Tissue lysis buffer
BLASTn	Nucleotide Basic Local Alignment Search Tool
bp	Base pair (s)
Buffer AW	Wash buffer
CITES	The Convention on the International Trade in Endangered Species of Wild Fauna and Flora
CN	Copy number(s)
COI	Cytochrome oxidase I
Cq	Quantification cycle
CWF	Centre of Wildlife Forensics, NParks
cyt b	Cytochrome b
DD	Diamond™ nucleic acid dye
DNA	Deoxyribonucleic acid
dNTPs	Deoxynucleoside triphosphate
dsDNA	Double stranded deoxyribonucleic acid
g	Gram(s)
hr	Hour(s)
IUCN	International Union of Conservation of Nature
IWT	Illegal Wildlife Trade
LDPE	Low-density polyethylene
LLDPE	Linear low-density polyethylene
$MgCl_2$	Magnesium chloride
Min	Minute(s)
mL	Mililitre(s)
mm	Milimetre(s)
mtDNA	Mitochondrial DNA
NCBI	National Center for Biotechnology Information
ng	Nanogram(s)
nm	Nanometer
NParks	National Parks Board, Singapore
PCR	Polymerase Chain Reaction
PE	Polyethelene
qPCR	Quantitative Polymerase Chain Reaction
RNA	Ribonucleic scid
rpm	Rounds per minute
Sec	Second(s)
STR	Short Tandem Repeats
T	Thymine
Tm	Melting temperature
TRFP	Total representative fluorescent particle count
v/v	Volume per volume
WT	Wildlife trade

CHAPTER ONE: INTRODUCTION

1.1 Wildlife Trade

Wildlife trade refers to the trade of any living organisms obtained from the wild, including vertebrates, invertebrates, plants and fungi (Fukushima et al., 2020), as well as products derived from these organisms (Hughes, 2021).

Wildlife trade comprises of both legal and illegal activities. The legal trade is typically regulated by national laws and, the international regulations and conventions. Internationally, the legal trade of wildlife species is regulated by The Convention on the International Trade in Endangered Species of Wild Fauna and Flora (CITES) while the vulnerability of all wildlife species to extinction is assessed through International Union of Conservation of Nature (IUCN). In contrast, the illegal wildlife trade involves unregulated poaching and trafficking of these vulnerable or endangered species and their derivatives that have been stipulated to be protected by the national and international legislations.

Figure 1: Illustrating research effort in wildlife trade. Diagram obtained from Andersson et al., 2021. [Removed due to copyright restriction]

The unregulated wildlife trade threatens biodiversity by overexploiting wildlife populations. The overexploitation of wildlife species undermines conservation efforts, drives wildlife species to extinction and poses a global threat to the balance of ecosystems. Additionally, unregulated wildlife trade of wildlife species can also facilitate the spread of pathogens by undermining biosecurity defences, causing global disease outbreak.

Although much of the focus in the trading of wildlife and associated products revolves around the impact it has on the eco-biodiversity, it is important to acknowledge that the trading of wildlife products derived from their natural environment, provides common necessities that are used in

daily lifestyle, such as the catching of food, such as fish from the wild, and traditional hunting. While implementing legislation to regulate wildlife trade, it is important to consider socio-economic and cultural factors as well as consumer's habits (Symes et al., 2018) in order to effectively enforce compliance with the legislation implemented.

Wildlife products are often associated with economic values and thus, is an important source of income for people living near the ranging regions of these wildlife species. These wildlife species can also serve as an important and cheap source of protein for these people. In regulating wildlife trade, it is important to take an integrated approach to ensure that the socio-economic needs of the surrounding human population are achieved together with the sustainable management of wildlife (Zain et al., 2017).

Demand for wildlife products is often linked to status of affluence. Products such as pangolin meat, shark fins, ivory and rhino horns are considered as luxury products to demonstrate high social economic status among emerging class, thus commanding high market prices (Challender et al., 2015; Eikelboom et al., 2020; Gao & Clark, 2014; Shea & To, 2017). Another contribution factor to the exploitation of wildlife products is the usage of wildlife products in traditional medicines. Examples include pangolin scales, saiga horns, bear bile, various herbs etc which are consumed as traditional medicine (Wang et al., 2022), with unproven health benefits. The demand of wildlife products for use in traditional medicines has also helped to drive demands for wildlife products (Andersson et al., 2021; Wang et al., 2022).

Lastly, the demand for live animals and plants as pets and ornamental plants is also driving the demand for trafficking of wildlife species from the wild, with amphibians, reptiles and birds most commonly traded as pets (Fukushima et al., 2020) and orchids as ornamental plants. Rising tourism also boosts the illegal trade of wildlife products when tourists unknowingly purchase souvenirs made of wildlife parts such as turtle shells or rhino horns to bring them back from their trips.

1.1.1 Illegal Wildlife Trade (IWT)

In wildlife forensic science, one of the most common legal concerns is the IWT, which includes the importing, exporting and sales of animals protected under national or international regulations (Johnson et al., 2014). IWT has led to an unsustainable exploitation of wildlife species; it is estimated that in 2016, IWT accounted for an annual value of USD$7-23 billion (TRAFFIC, 2022), making it one of the most profitable crimes in the world (Linacre, 2021).

IWT is a major threat to global biodiversity conservation and affects a wide range of species, with hotspots spanning across South America, Central to Southeast Africa, the Himalayas, Southeast Asia, and Australia, to the extent that 22.8% of mammals have been estimated to have been affected by wildlife trade (Scheffers et al., 2019). IWT is usually conducted by a well-organised network through complex interactions involving multi stakeholders, including conservation

organisations, enforcement agencies and the society (Xie, 2015). It poses serious consequences to biodiversity conservation efforts, driving wildlife species to extinction and ultimately poses serious threats to our ecosystem functions. Therefore, IWT requires a multi-disciplinary intervention effort between both exporting and importing countries to prevent further depletion of species at risk.

Figure 2: Wildlife trade in terrestrial vertebrates (birds, mammals, amphibians, and reptiles) affects ~24% of species globally. Numbers in brackets are the total number of traded species. IUCN threat status codes: data deficient, DD; least concern, LC; near threatened, NT; vulnerable, VU; endangered, EN; and critically endangered, CR. Diagram obtained from Scheffers et al., 2019.
[Removed due to copyright restriction]

1.1.2. The Convention on the International Trade in Endangered Species of Wild Fauna and Flora (CITES)

CITES is an international trade agreement on wildlife commodities between governments to ensure that the international trade of wild animals and plants does not threaten the survival of the species (CITES). CITES implements international trade control of certain animal or plant species selected through the assessment of risk of extinction faced by the wildlife species. Through subsequent continuous monitoring, the impact of the trade control to the selected protected species is then regularly reviewed. Since its inception on 1st July 1973, CITES has been the principal mechanism used for regulating international wildlife trade. At the date of writing, there are over 40,900 species listed in the CITES, including approximately 6,610 animal species and 34,310 plant species.

CITES applies varying degrees of protection to different wildlife species by including them in three different appendices based on their risk of extinction: I, II, and III. Appendix I includes animals that are threatened with extinction and therefore, the international commercial trade of these animals is generally prohibited. Appendix II includes animals that may not be threatened with extinction but may become so and therefore, international commercial trade is allowed but controlled to prevent

overexploitation. And lastly, animals that are subject to regulation within the jurisdiction of one Party and for which the assistance of other Parties is sought to control international trade are listed under Appendix III (CITES, 2019). Proposals to include / amend the list of species within the respective appendices will be determined by the parties to the Convention during regular meetings of the Conference of the Parties (CoP), based on a set of biological and trade criteria.

Countries that have voluntarily agreed to be bounded by the agreement of CITES are known as Parties to the Convention and to date, there are a total 184 parties (CITES). Parties are required to implement respective national legislations to ensure that they abide by the legal binding framework stipulated by the convention. Generally, the Parties fulfill their legal obligations to CITES by implementing a system comprising of (a) license and permits issuance to ban or regulate import and export of CITES listed species, (b) national enforcement legislations to investigate and seize illegally traded items and (c) national scientific agencies to inform the nation of the impact on the status of species.

Although CITES has largely been successful in curbing the international trade of various prominent at-risk species through collaboration among member countries, concerns of CITES regulations exacerbating the illegal trade and whether it has been effective in protecting at risk species have also been raised (Challender et al., 2015; Challender & O'Criodain, 2020). Implementation of CITES has been reported to possibly increase prices due to restricted supply and persistent demands of wildlife goods (Challender et al., 2015). This, in turn, drives the wildlife trade underground, making it difficult to control, monitor and circumvent, leading to an adverse effect on the survival of at-risk wildlife species. Therefore, economics, socio-cultural and consumers' habit should also be taken into consideration when implementing CITES regulations.

The effectiveness of implementing CITES at the national level has also been reported to be dependent on the low corruption rate, high income, and quality of enforcement in the member countries ('t Sas-Rolfes et al., 2019). This is mainly due to the availability of public funding used to carry out licensing and enforcement activities at the national level and to enact any regulation requirements as well as to ensure that any suspected IWT activity is thoroughly investigated (Morton et al., 2021). Additionally, through the support of national scientific agencies, sound decisions can be made based on the status of wildlife species and any evidence collected during an investigation can be admissible to legal proceedings to fully support enforcement of the national legislation without legal challenge.

1.2 Pangolins

1.2.1 Different species of pangolins

Pangolins, otherwise known as the "scaly anteaters", are solitary, nocturnal mammal (Order Pholidota; Family Manidae) that have been tragically labelled as one of the world's most heavily

trafficked wild mammal (H. Zhang et al., 2020). Pangolins feed exclusively on ants and termites and are easily recognisable by their unique scaled armour. The pangolin is the only mammal covered with overlapping keratinised, epidermal scales covering the dorsal surface of its body and tail. These scales are relied upon as the animal's only defence mechanism and when threatened with danger, it will curl up into a ball, leaving only their hard, sharp keratinised scales protruding outwards (Wang et al., 2016).

Pangolins are found only in Asia and Africa. There are eight extant species of pangolins - four species of Asian pangolins (*Manis crassicaudata*, *Manis culionensis*, *Manis javanica* and *Manis pentadactyla*) as well as four species of African pangolins (*Smutsia gigantea*, *Smutsia temminckii*, *Phataginus tricuspis* and *Phataginus tetradactyla*) (Gaubert et al., 2020).

Due to their elusive nature , the size of the population of wild pangolins in various countries cannot be accurately estimated, however, it has been reported that the population of all Asian and African pangolins have been declining severely over the decades (Heinrich et al., 2016). On the IUCN Red List of Threatened Species, three of the four Asian pangolins, *M. javanica* (Sunda Pangolin), *M. culionensis* (Philippine Pangolin) and *M. pentadactyla* (Chinese Pangolin), are listed as 'Critically Endangered', while the *M. crassicaudata* (Indian Pangolin) is listed as 'Endangered'. Two of the four African pangolins, *S. gigantea* (Giant Ground Pangolin) and *P. tricuspis* (White-bellied Pangolin) are listed as 'Endangered', while the *S. temminckii* (Temminck's Pangolin) and *P. tetradactyla* (Black-bellied Pangolin) are listed as 'Vulnerable' (IUCN, 2021). Additionally, in 2016, all eight species of pangolins were also transferred from Appendix II of the CITES to Appendix I of CITES, thereby prohibiting all international trade of severely threatened species (Challender et al., 2020).

1.2.2 Illegal Trade of Pangolins

Over the past decades, the populations of pangolins have been declining drastically. The Sunda Pangolin and Chinese Pangolin are reported to have declined more than 90% since 1960, while the African pangolins, although not as widely studied as the Asian pangolins, were also estimated to have a projected population at least 30 - 40% reduction over a 21 year period (seven years past, 14 years future; generation length estimated at seven years) (IUCN, 2016).

The pangolins are mainly exploited for consumption purposes, especially as bushmeats or for use in traditional medicines (Johnson et al., 2014). In Africa, the African pangolins are highly sought after in their native range country for their meat, as a cheap and easily accessible source of alternative protein. Coupled with a lack of conservation knowledge and awareness, as well as poor enforcement of animal protection regulation (Soewu & Sodeinde, 2015), the African pangolin population has been poached not only to fuel local demands but also the international trade.

In Asia, the pangolins are also exploited for both their meat and scales, with China and Vietnam as key consumers (Omifolaji et al., 2020). The meat of a pangolin is often deemed as a rarity and is therefore considered to be a luxury delicacy used to demonstrate high social status among consumers (Challender et al., 2015). The scales are usually consumed as traditional medicine with perceived medicinal benefits to improve a wide range of health conditions, such as blood circulation, skin diseases, milk secretion in lactating women, treating cancers etc. even though there is no proven evidence of any therapeutic benefit (Challender et al., 2015; Xing et al., 2020).

Due to the overexploitation of their meat and scales, Asian pangolin populations have declined drastically. Following the decline of Asian pangolin populations, the sources of pangolin meat and scales switched to the African pangolins, especially the *S. gigantea* (Giant Ground Pangolin) and the *P. tricuspis* (White bellied Pangolin) (Challender et al., 2020; Heinrich et al., 2016). These scales were generally transported by sea in shipping containers, from the Democratic Republic of the Congo (DRC) and Nigeria (Challender et al., 2020).

Even with a ban on the international trade of pangolin in place, the illegal trade of pangolin scales has continued to be fuelled by the consumption demands in Asia (Challender et al., 2015; Nash et al., 2018; Omifolaji et al., 2020). The demand for pangolin meat and scales has greatly impacted the conservation efforts of these insectivorous mammals, leading to an alarming decline in their populations globally (Xing et al., 2020).

1.2.3 Pangolins in Singapore

M. javanica (Mammalia: Pholidota), known as the Sunda Pangolin, is the only one of the eight species of pangolins that is known to be native in Singapore. Adults of this species of pangolin weigh between 4-7 kg on average, with a total length up to 140 cm (Chong et al., 2020). It is distributed throughout Southeast Asia, except in the Philippines (Lim & Ng, 2008). Due to its elusive nature, it had been difficult to accurately determine its total population and distribution within range countries (Chong et al., 2020). In Singapore, they are rarely seen and it was reported in 2019 that approximately 1046 *M. javanica* were estimated to be living in the wild; this was based on the use of camera traps surveys and microchip data on rescued and released pangolins, and other radio telemetry and pangolin tracking data (Nash et al., 2020).

Figure 3: Picture extracted from surveillance camera video captured by National Parks Board, Singapore (NParks), showing a female M. javanica carrying her baby on her tail. Video obtained from NParks. Reproduced with permission.

M. javanica are nocturnal and are excellent tree climbers. They typically live in tree hollows, burrows or tall grass (Lim & Ng, 2008). As Singapore is highly urbanised, they can be found living in both Singapore's fragmented forests and in various urban structures, such as housing estates and construction sites. They are solitary, and their young can sometimes be seen with the females. The gestation period is approximately 6 months with no specific breeding season and females typically give birth to one offspring at a time, but occasionally twins can be observed (Zhang et al., 2015). In Singapore, there is an absence of natural predators, and so, roadkill is the major threat faced by *M. javanica*. Illegal poaching is also not common in Singapore due to culture and socio-economic factors. Singapore is a small city state with strictly enforced legislation and tough penalties. Coupled with relatively high per capita income, illegal poaching is not lucrative or feasible (Nash et al., 2020). Although Singapore is one of the few countries with near zero poaching rate, Singapore is still implicated in the IWT of pangolin as it has one of the busiest shipping ports in the world and its strategic position on the shipping route, making it one of the most affected transit ports.

In 2019, Singapore seized a record haul of approximately 37.5 tonnes of pangolin scales, alongside approximately nine tonnes of ivory, in three separate seizures (AFP, 2019; Clarke, 2019; Griffiths, 2019). On all three occasions, the containers in which pangolin scales were stashed were enroute from DRC and Nigeria to Vietnam, transhipping through Singapore. In each of the containers, the pangolin scales were hidden behind frozen beef and/or timber within the containers and were declared as these legal products.

Figure 4: Images of pangolin scales (left) and ivory (right) confiscated by NParks in 2019. Images obtained from NParks. Reproduced with permission.

There is a need for Singapore to remain vigilant to the possibility of consignments of illegal wildlife goods using Singapore as a tranship port. Singapore has been a Party to CITES since November 1986 (NParks, 2020). National Parks Board of Singapore (NParks) is the CITES Management and Scientific Authority to implement and enforce the regulations stipulated under CITES within the jurisdiction of Singapore. Apart from conducting regular inspections and enforcement activities, in recognition of the need to use scientific methods to support the regulation framework, NParks established the Centre of Wildlife Forensics (CWF) in 2020. The CWF provides national in-house laboratory capabilities to conduct laboratory testing services to support investigations or enforcement activities when there is an allegation or information that legislation involving wildlife has been breached.

1.3 Molecular Techniques in Wildlife Forensics

Wildlife forensic science is the application of scientific techniques to address legal concerns involving wildlife with the main objectives of obtaining scientific evidence from crime scenes, persons of interest, suspects, and victims.

In the last decade, wildlife forensic science has been gaining significance in the field of forensic sciences (Linacre, 2021). The use of molecular techniques to support wildlife investigations has also been gaining much traction. As opposed to investigations in human crime investigations, where human witnesses can articulate the details of their involvement in the crimes, animals are unable to do so. As such, evidence used in wildlife forensic science needs to be subjected to molecular testing to provide the details required to support and aid in the investigations. Generally,

molecular techniques are applied in wildlife forensic science are to (1) identify the species involved, (2) identify the geographical origin of samples and (3) identify the number of individuals involved in a seizure (Linacre, 2021).

1.3.1 Molecular Species Identification

Molecular species identification is an important component of wildlife forensic science as it is often required to show whether the seized samples derive from a CITES regulated species and therefore is either legal or illegal. Unlike human forensic science where only one species is involved, wildlife forensic science encompasses many. Seized wildlife samples are also often highly processed to meet consumers' requirements and so, morphological traits that are used for species identification may no longer be present. In such cases, molecular analysis will need to be performed to identify the species involved.

Molecular species identification is widely carried out by DNA barcoding (Staats et al., 2016). DNA barcoding involves the amplification and sequencing of a short polymorphic sequence using universal primers. After amplification and sequencing, the obtained DNA sequence is then compared against a database comprised of sequences from known reference species (Gouda et al., 2020), such as NCBI's GenBank and BarCode of Life, to identify the species of the sample. For DNA barcoding, mitochondrial DNA (mtDNA) is often preferred over the nuclear DNA as it is present in hundreds of copies in the cell, allowing it to be more easily amplified in highly processed or degraded samples (Mitra et al., 2018). Regions in the mtDNA that are used commonly for molecular species identification includes the genes encoding cytochrome b (cyt b) (Ewart et al., 2018; Ewart et al., 2021; Wozney & Wilson, 2012) and cytochrome oxidase I (COI) (Hellberg et al., 2019), 12S and 16 ribosomal RNA segment (Kitano et al., 2007) as well as the control region (D loop) (Boscari et al., 2014). A crucial attribute with any locus used in species testing is that there should be little intra but sufficient inter sequence variability so that all members of the same species have almost the same targeted region but the targeted region have sufficient variability to distinguish two closely related species (Tobe et al., 2010).

1.3.2 Assignment of Geographical Origins

As the IWT may involve organised networks to coordinate the poaching, export and import of the wildlife commodities, the assignment of geographical origins is important to assist in identifying poaching hotspots and to understand how the network operates (Wasser et al., 2015).

One of the genetic analyses conducted for geographical origin assignment is through the analysis of variations in mitochondrial haplotypes. Genetic analysis to assign geographical origins of 1800 DNA samples from 30 seizures in Hong Kong of African pangolin scales during the period 2012-2016 using the cyt b region was reported in 2020 (H. Zhang et al., 2020). The data from these 1800 DNA samples were then compared to the genetic geographical map associated with

haplotype variations of the white bellied pangolins (Gaubert et al., 2016) from which it was deduced that pangolin scales are mainly poached from Cameroon, Equatorial Guinea, and Gabon (H. Zhang et al., 2020).

Apart from using the variations in mitochondrial DNA haplotypes from pangolin scales for geographical origin assignment, short tandem repeat (STR) profiling has also been used in genetic analysis to assign the geographical origins. STRs are short sequences of repetitive DNA that can be found scattered across the genome. These repetitive sequences are typically 2 – 6 base pair (bp) long and are highly polymorphic between individuals. And hence, they are very suitable to be used for genotyping. An example of the use of STR genotyping in wildlife forensics is the development of a 16 STR loci profiling system for the geographical assignment of elephant ivory. This STR profiling panel was developed by Wasser et al. to geographically assign African elephant ivory seized during the period of 1996 to 2014 (Wasser et al., 2015). The results from this analysis were then used to determine the poaching hotspots of the elephant and help to focus enforcement resources to the hotspots identified.

Although the assignment of geographical origins can play a key role in the investigation of alleged wildlife crime, much work is still required. First, the databases of known reference samples with geographical association are rarely available. Without the databases, scientists will not be able to associate the genotypes obtained from the seized samples to its geographical origins. Secondly, the analysis of large seizures can be time-consuming due to the large number of samples involved. A high throughput workflow is thereby required to aid in the genetic analysis.

1.3.3 Determination of Number of Individuals

Determination of identity through genetic analysis is also conducted to determine the number of individuals involved in a seizure. For example, two tusks can be linked together to indicate that these tusks belong to a particular elephant or in the case of pangolin scales, it can be used to estimate the numbers of pangolins involved in a seizure comprised of pangolin scales.

mtDNA has been widely used in wildlife forensic science for the purpose of species identification and geographical assignment. However, mtDNA may not be as effective for the purpose of individualisation determination due to its matrilineal mode of inheritance. In human forensic sciences where an identification of an individual is required, the typing of the STRs in the nuclear DNA will be more common (Mitra et al., 2018).

In human forensic science, STR panels are already well developed to identify individuals using well-established and validated STR libraries. STR panels have also been established and validated for domestic pets, such as dogs (Berger et al., 2014) and cats (Schury et al., 2014). However, the rarity of similar libraries for wildlife species can make genetic assignment to a particular individual extremely challenging in wildlife forensic science. Nonetheless, forensic STR panels have been

developed for some wildlife species such as the Eurasian badger (Dawnay et al., 2008), rhinoceros (Harper et al., 2013), North American black bear (Meredith et al., 2020) and falcons (Beasley et al., 2021). However, due to the inaccessibility to representative individuals within the populations and limited access to family groups, the development and validation of STR profiling system for individualisation of respective wildlife species remains challenging (Dawnay et al., 2008).

1.4 Visualisation of Latent DNA using Nucleic Acid Dyes

1.4.1 Latent DNA

Touch DNA is one of the most common DNA sample types used in human forensic casework. It refers to the transfer of an individual's DNA onto various surfaces through contact (Williamson, 2012). Touch DNA deposited is usually invisible (Panjaruang et al., 2022) and therefore, it is also referred to as latent DNA.

Latent DNA was suggested to derive mainly from the outermost cornified layer of the epidermis on the human skin surface. This layer consists of fully differentiated, anucleate keratinocytes that are constantly shed from the skin as the cells in this layer are eliminated through desquamation it was suggested that DNA in the cornified keratinocytes might not be completed degraded (Candi et al., 2016). It was also demonstrated that trace DNA could still be detected localised in the cornified layers (Kita et al., 2008), suggesting that touch DNA could indeed be derived from the anucleate keratinocytes (Burrill et al., 2020), and be deposited on contacted surfaces as the cells were shedding off continuously.

Figure 5: A diagram showing various layers in human skin. Image obtained from Burrill et al (Burrill et al., 2019). [Removed due to copyright restriction]

Latent DNA was also suggested to derive from cell free DNA (Burrill et al., 2021; Kaesler et al., 2022; Quinones & Daniel, 2012). Cell free DNA is generally present in the circulation of healthy

human individuals and was thought to be present due to various necrosis, apoptosis and active secretion mechanism present in the human body. Cell free DNA was detected to be present in the sweat of 80% of healthy individuals tests with an average concentration of 11.5 ng cell free DNA recovered per mL of cell free sweat, indicating that cell free DNA can also contribute to the latent DNA recovered from contact surfaces (Quinones & Daniel, 2012).

Typically, DNA from touched substrates is recovered in low amounts, and based on a compilation of various studies, the amount of DNA recovered from different contact surfaces (such as plastic, knives, cable ties, steering wheels and clothing) could range from 1 to 170 ng (Burrill et al., 2019). The amount of DNA recovered from the surfaces could also be affected by the environmental factors to which the DNA was exposed. It was reported that larger amounts of DNA could be recovered from cells exposed to laboratory conditions (indoor conditions) than cells exposed on a window frame or bag (outdoor conditions), both over the course of six weeks (Raymond et al., 2009). The amount of DNA recovered also decreased as the time between DNA deposition and collection increased (Raymond et al., 2009). The STR profiles generated from touch DNA deposited on rubber and steel substrates were adversely affected when these substrates were stored in an outside sheltered environment for up to three and six months respectively whereas STR profiles were generally not affected when the substrates were stored indoors for up to nine months (Kaesler et al., 2023).

1.4.2 Use of Nucleic Acid Stains for the Visualisation of Latent DNA

Touch or latent DNA has been used in forensic science as a powerful tool to associate a particular individual to a location or an object (Kanokwongnuwut et al., 2018a). Whilst latent DNA derived from the epidermal layer of the cornified layer of the human skin surface is constantly being shed (Kita et al., 2008). DNA is invisible to the naked eye, making a challenge for crime scene operatives to collect DNA samples at points where biological material may, or may not, be present. The samples, as part of a forensic investigation, are often collected on best assumptions and therefore result in majority not containing sufficient DNA for analysis (van Oorschot et al., 2012).

From the laboratory's perspective, the analysts often are unable to discern if the collected samples contain sufficient DNA for analysis until after DNA extraction (Mapes et al., 2015), thus wasting reagent and manpower processing samples with insufficient DNA. It would therefore be advantageous to be able to visualise these DNA-bearing items either during sample collection or prior to DNA extraction. By visualising the DNA during sample collection, it will allow the sampling officer to conduct more targeted sampling collected. Visualising the DNA on the collected samples, such as tape lifts or swabs, can also allow laboratory analysts to eliminate samples without sufficient DNA to reduce the number of samples to process (Kanokwongnuwut et al., 2018a).

Nucleic acid dyes can be used to visualise DNA deposited on surfaces of an object or in the environment. In one of the earliest work conducted by Haines *et al.,* it was demonstrated that DNA

could be visualised within hair follicles using Diamond™ nucleic acid dye (DD) (Haines et al., 2015a). Further evaluation was then conducted to compare the performance of six commonly used nuclei acid stains (EvaGreen™, RedSafe™, Diamond™ nucleic acid dye, SYBRGreen I, GelRed™ and GelGreen™) to detect DNA on biological materials as well as the effects of the dyes on DNA extraction, PCR amplification, and STR typing. This demonstrated that DD was the most suitable dye to be used for visualisation of DNA as it resulted in the least amount of DNA loss during DNA extraction (Haines et al., 2015b).

Subsequently, DD has been used to visualise DNA on the surfaces of improvised explosive devices (Tonkrongjun et al., 2017), credit cards, mobile phones (Kanokwongnuwut et al., 2018a), banknotes, fabric (Champion et al., 2021) etc. DD is also shown to be able to stain and detect DNA recovered on various latent DNA sample collection medium such as tapelifts (Kanokwongnuwut et al., 2020b) and swabs (Kanokwongnuwut et al., 2018b).

DD to visualise latent DNA is a valuable tool in human forensic science to ensure that targeted sampling can be conducted, so that samples collected contain sufficient DNA for genetic analysis. DD has not been studied for the detection of non-human mammalian DNA however, a recent study showed that DD could detect reptilian DNA after a boa constrictor had been kept in a glass tank (Deliveyne et al., 2022). DD in wildlife forensic science had also not been widely studied apart from to detect human cellular materials deposited on substrates commonly encountered in poaching, trapping and snaring of animals (Kanokwongnuwut et al., 2020a).

1.4.3 Types of Nucleic Acid Dyes

Nucleic acid dyes are commonly used in most molecular biology laboratories to visualise nucleic acid fragments (such as RNA and DNA) that have been separated (Borst, 2005). These nucleic acid dyes typically bind to the DNA or/and RNA molecules and when excited using certain wavelengths, they generate a fluorescent signal that can be detected, captured and analysed using various imaging devices. They are used in various molecular applications, such as gel electrophoresis, fluorescence *in situ* hybridization (FISH), flow cytometry, and microarray analysis for both diagnostic and research purposes.

Nucleic acid dyes can be broadly classified into two major groups based on their mechanism of action: (i) intercalating dyes and (ii) minor groove binding dyes (Haines et al., 2015b). Intercalating dyes, such as ethidium bromide and SYBR® Green, work by binding between adjacent base pairs of the double-stranded DNA (dsDNA) while minor groove binding dyes, such as DAPI and Hoechst dye, bind to minor grooves of DNA at A-T rich site through noncovalent bonds.

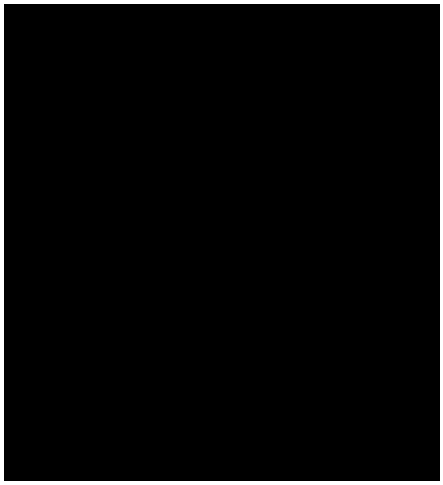

Figure 6: Schematic diagram showing the different binding modes of dyes (and other ligands) to DNA (ThermofisherScientific). [Removed due to copyright restriction]

1.4.4 Ethidium Bromide

Ethidium bromide is the one of the most commonly used nucleic acid dyes in molecular biology laboratories. It was first used to stain gels in the 1960s (Borst, 2005). It is an intercalating agent and can bind to both double stranded RNA and DNA. When bound, it was able to demonstrate an 21 – 25 fold increase in fluorescence when compared to its unbound state, making it an excellent candidate for visualising DNA in electrophoresis gels (Bourzac et al., 2003). However, due to its intercalating properties and its ability to permeate a cell membrane, ethidium bromide is a well-known mutagen and carcinogen (Haines et al., 2015d) and therefore, poses safety concerns to its users. Alternative nuclei acid dyes with less mutagenic and carcinogenic properties have been characterised to replace ethidium bromide for the use of staining nucleic acid bands in gel electrophoresis.

1.4.5 SYBR Green Nucleic Acid Stains

There are two types of SYBR Green nucleic acid stains - SYBR Green I and SYBR Green II. SYBR Green I is used for staining and visualisation of DNA while SYBR Green II is used for staining and visualisation of RNA.

SYBR Green I is a proprietary monomeric asymmetrical cyanine dye (Singer et al., 1999) developed for visualising nucleic acids in gel electrophoresis and solutions with higher sensitivity. It both intercalates and also binds to dsDNA at minor groove binding sites, particularly at A-T rich sequences (Zipper et al., 2004). Since the 1990s it has been used widely in various molecular analysis techniques, such as gel electrophoresis, quantitative PCR (qPCR) and flow cytometry and has been reported to demonstrate >1,000 fold increase in fluorescence when bound with dsDNA (Dragan et al., 2012)and, it has a higher affinity to dsDNA as compared to ethidium bromide. Due to its high sensitivity to dsDNA and a weaker mutagenic effect than ethidium bromide (Singer et al., 1999), SYBR Green I has been marketed as a safer replacement for ethidium bromide.

[redacted]

Figure 7: The chemical structure of SG [2-[N -(3-dimethylaminopropyl)- N -propylamino]-4-[2,3-dihydro-3-methyl-(benzo-1,3-thiazol-2-yl)-methylidene]-1-phenyl-quinolinium] as determined by MS and NMR studies. Image obtained from Zipper et al. (Zipper et al., 2004) [Removed due to copyright restriction]

1.4.6 DAPI

DAPI (4',6-diamidino-2-phenylindole) is a fluorescent dye commonly used for staining nucleic acids in fluorescence microscopy, flow cytometry, and chromosome staining. Binding to the A-T rich

regions in the minor groove of dsDNA leads to a ~20-fold enhancement in fluorescence upon the formation of the fluorescent complex (Kapuscinski, 1995). When excited by 405 nm wavelength to produce blue fluorescence, allowing for the visualisation and quantification of nucleic acids. Due to [redacted]genic (Bourzac et al., 2003).

Figure 8: The chemical structure of 4',6-[redacted]-2-phenylin-dole (DAPI). Image obtained from Kapuscinski, 1995 (Kapuscinski, 1995). [Removed due to copyright restriction]

1.4.7 Hoechst dye

The Hoechst dye consists of three chemically related bisbenzimide dyes: Hoechst 33258, Hoechst 33342 and Hoechst 34580 (Bucevičius et al., 2018). It is non-intercalating but binds the A-T rich regions at the minor grooves of the dsDNA through hydrogen bonding (Loontiens et al., 1990). When bound to dsDNA, its fluorescence will be enhanced by approximately 30-fold and when excited by UV light of approximately 360nm to emit a blue fluorescence of 460- 490 nm (Bucevičius et al., 2018). It is commonly used as a cytological stain to stain the nucleus of live and fixed cells to study gene expression (X. X. Zhang et al., 2020).

[redacted]

Figure 9: The chemical structure of Hoechst 33342, Hoechst 33258 and Hoechst 34580. Image obtained from Bucevičius et al. (Bucevičius et al., 2018). [Removed due to copyright restriction]

1.4.8 GelRed® Nucleic Acid Gel Stain

GelRed® Nucleic Acid Gel Stain was developed as a highly sensitive, stable and environmentally safe fluorescent nucleic acid dye to replace the highly mutagenic ethidium bromide for use in agarose and polyacrylamide gel electrophoresis. GelRed® is a bis-intercalating molecule with higher sensitivity as compared to ethidium bromide (Crisafuli et al., 2015). In addition, due to its inability to permeate cell membranes, it is non-cytotoxic and non-mutagenic at a level above the suggested working concentration (Biotium, 2021).

1.4.9 Diamond™ Nuclei Acid Dye (DD)

DD was developed as a safer alternative to ethidium bromide. It is a proprietary fluorescent nucleic acid dye that binds to the external grooves in the helical structure of DNA or RNA (Truman et al., 2013) and was shown to detect as little as 0.5 ng of DNA by gel electrophoresis (Haines et al., 2015d), thereby demonstrating that DD is a more sensitive and safer alternative compared to other nucleic acid stains for the visualization of DNA.

It has also been used as a quantitative dye in quantitative (qPCR) (Haines et al., 2016) as well as a visualisation dye for latent DNA.

1.5 Research Questions and Approach

First use of DD in the visualisation of latent DNA was reported in 2015 (Haines et al., 2015b) and research has since focused on its use to visualise latent DNA deposited by humans (Kanokwongnuwut et al., 2018a). It is well-established that humans can deposit DNA onto surfaces by touch, as humans are constantly shedding corneocytes from the epidermal, cornified layer of their skin (Kita et al., 2008).

DD has not been widely used for the visualisation of latent DNA in wildlife forensic science. In a 2020 paper by Kanokwongnuwut et al., DD was used to detect the presence of human cellular material deposited on five different types of substrates commonly used in the poaching, trapping and snaring of wild animals and, and to monitor the collection and transfer of the deposited cellular material from the substrate to the the adhesive tape used in tape – lifting (Kanokwongnuwut et al., 2020a).

In this project, it was hypothesised that wildlife products could shed cellular material onto surfaces they were in contact with and DD could be used to detect and visualise the cellular materials deposited in the environment; DD could then enable targeted DNA sampling to be carried out in order improve the rate of obtaining samples containing sufficient DNA for genetic analysis. Pangolin scales were used in this project as they are one of the most impacted animals in IWT.

1.5.1 Aims and Objectives

The aim of this project is to:

a. Determine if DD could be used to visualise the presence of DNA transferred by pangolin scales.
b. Determine an optimised workflow to recover, extract and amplify the pangolin DNA visualised.
c. Correlate the amount of fluorescence visualised using DD to the amount of pangolin DNA obtained and if the DNA was sufficient for amplification and other subsequent genetic analysis.

CHAPTER TWO: DEPOSITION OF LATENT DNA BY PANGOLIN SCALES: A PROOF-OF-CONCEPT STUDY

2.1 Background

A proof-of-concept study was conducted to determine if pangolin scales could deposit cellular materials onto contact surfaces and if the deposited cellular materials could be stained by DD and visualised under a fluorescent microscope. As it was hypothesized that the scales would deposit cellular materials onto contact surfaces via friction or pressure, even or a combination of both the mechanisms, these two mechanisms of cellular material deposition were used in this study. Glass slides were chosen as the surface substrate in this study as it is a non-porous substrate commonly found in the laboratory with a small exposed surface area. The small, exposed surface area makes it easy to standardise across the trials and to manoeuvre under a microscope.

2.2 Material and Methods

2.2.1 Processing of Scales from *M. javanica* (Sunda Pangolin)

2.2.1.1 Acquisition of Sunda Pangolin Carcass and Storage

NParks was notified by members of public that a pangolin was found dead by the roadside. The exact time of death was unknown. The carcass was picked up by the engaged transportation contractor within two hours from the time of notification and was sent to the Singapore Zoo. Internal organs were removed from the carcass by the veterinarians at the Singapore Zoo and the remaining carcass was submitted to our laboratory. Upon submission to the laboratory, the carcass was morphologically identified to be *M. javanica* (Sunda pangolin) and stored at 4°C, pending further processing.

2.2.1.2 Retrieval and Processing of Scales

The pangolin carcass was fully submerged in boiling water for five minutes to allow the scales to be easily removed. The scales were removed by using forceps and then they were air-dried at room temperature for 24 hours to allow surface moisture from the scales to be fully evaporated. The scales were then placed in an oven at 60°C, until the remnants of flesh attached to the scales were observed to be completely dried up (approximately 5 days). The dried scales were stored at room temperature in a low-density polyethylene (LDPE) bag till further use.

Five scales were retrieved from storage to be used in this experiment. An image of the five scales used is shown in Figures 10 and 11.

Figure 10: Dorsal view of the respective scales used in this project.

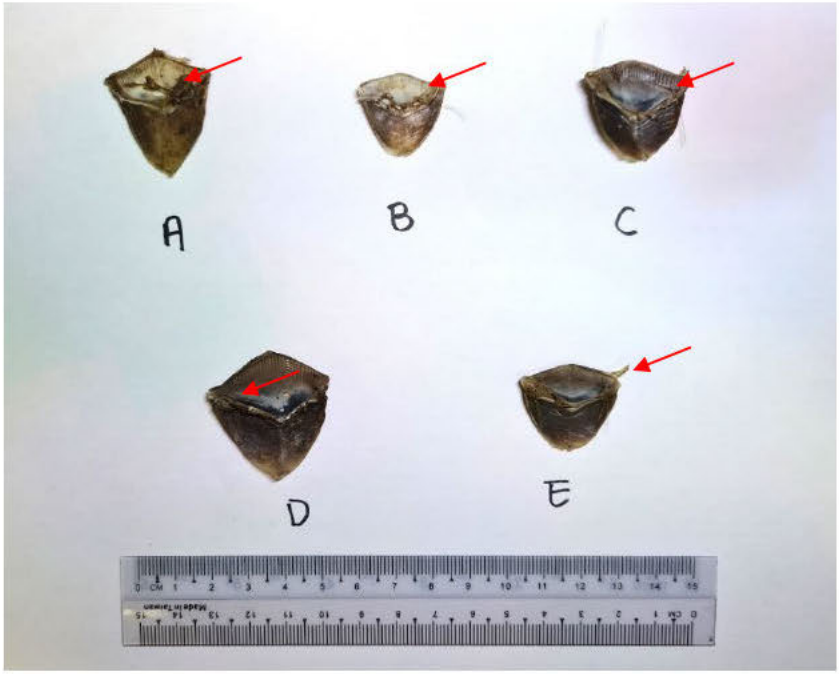

Figure 11: View of the ventral side of the respective scale used. Red arrows indicate where dried tissues can be found.

2.2.2 Surface Decontamination of Consumables and Tools Used

All consumables and tools, including glass slides, adhesive tapes, scissors, and scalpel blade holders used in this project were decontaminated before each experiment by first rinsing with tap water, then soaking in 3% sodium hypochlorite for 10 min, and lastly by wiping with absolute ethanol. The washed items were subsequently placed under ultraviolent (UV) light for 15 min to ensure that any remaining DNA contaminants could not be amplified.

Commercially available, individually packed sterile scalpel blades were used without undergoing further surface decontamination in the experiment.

2.2.3 Deposition of Cellular Material onto Glass Slides

It was anticipated that within a consignment or package of wildlife products such as the pangolin scales, latent cellular materials would be deposited onto the surface of the packaging via direct contact. Factors that affect transfer via contact include pressure and friction, and hence these two mechanisms of DNA deposition were examined in this project.

2.2.3.1 Cellular Material Deposition via Friction

Cellular materials from the scales of *M. javanica* were deposited onto glass slides by pressing and sliding the scale (ventral side down) firmly across the glass slide for 60 sec. Each of the five pieces of scales, shown in Figure 10, were used to deposit cellular materials onto their respective glass slides (labelled from A – E). One blank slide, without the application of a scale to transfer any cellular materials, was included in the experiment as a negative control (N). Thumbprints (T) were deposited onto a clean slide, as a control for positive staining, by pressing firmly down onto the slide for 5 sec.

2.2.3.2 Cellular Materials Deposition via Pressure

For deposition of any cellular materials from the scales via pressure, a piece of *M. javanica* scale was sandwiched between two pieces of glass slides. A weight of approximating 5 kg was placed on top of each set of the glass slides (Figure 12) and the set of glass slides was left on the benchtop for 7 days. The same setup was repeated for all five pieces of *M. javanica* scales. Two blank slides (N), without any scale in between and subjected to the same pressure over the same period, were included in the experiment as negative controls. In parallel, a human thumbprint (T) was deposited onto a clean slide, as a positive control positive staining, by pressing firmly down onto the slide for 5 sec.

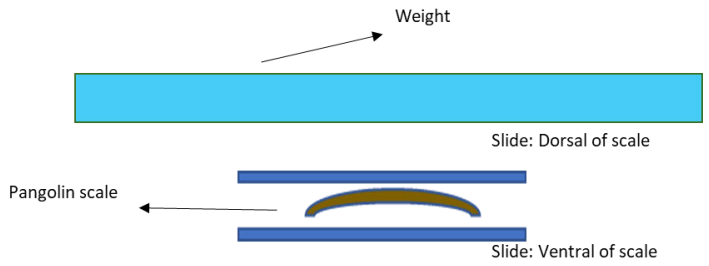

Figure 12: Setup for cellular material deposition via pressure. Individual pangolin scales were placed on a clean glass plate ventral side downwards. A second clean glass plate was placed on top and a weight, of known mass, was placed on top of glass plate.

2.2.4 Staining and Visualisation of Latent DNA Using Diamond™ Nuclei Acid Dye

A working stock of 20x DD (Promega Corporation, Madison, USA) was prepared by diluting 10,000x DD in 75% ethanol (v/v). The working stock was stored at 4°C for up to 7 days.

From the solution of 20x DD, 20 µL was pipetted onto each slide and spread evenly across the slide using a pipette tip, ensuring that the dye covered the entire surface of the slide evenly. The stained surfaces were then examined after at least 30 sec, using the Dino - Lite digital microscope (AnMo Electronics Corporation, Taipei, ROC) under blue light (480 nm) and at 50x magnification.

For ease of examination and capturing of images using the digital microscope, the slide was divided evenly into seven columns, (width of each column measuring approximately 8 mm), and four rows (height of each row measuring approximately 9 mm). The stage of the microscope was first moved horizontally across each field, ensuring that the end of each microscopic field slightly overlapped with the start of the next microscopic field; this captured images row-by-row. Images of fluorescence were recorded using the soft Dino-Capture 2.0. A total of 28 images were captured for each slide.

2.2.5 Quantification of Fluorescent Particles using ImageJ Software

The number of fluorescent particles in each image were quantified using ImageJ software (Schneider et al., 2012). Each of the images to be analysed were first converted into 8-bit images and then an auto-threshold, Maximum Entropy threshold algorithm, was applied to the image before quantifying the number of particles using the ImageJ software. The numbers of fluorescent particles counted from all 28 images from each slide were then totalled to generate a total fluorescent particle count.

2.2.6 Recovery of DNA using Tape-lifting

Cellular materials containing latent DNA deposited on the glass slides was recovered using tape-lifting. Brown adhesive packing tape was used for tape-lifting in this project. Tape sections of

approximately 10 mm x 10 mm were used for recovering DNA deposited on the glass slides, as per previously reported (Kanokwongnuwut et al., 2020b). Each piece of tape was pressed and lifted over each slide 20 times. After tape-lifting, the tape was examined under the digital fluorescent microscope to detect the presence of green, fluorescent spots, which was an indication that cellular materials had been successfully lifted onto the tape (Kanokwongnuwut et al., 2020b).

2.2.7 Extraction of DNA from Tapes Using Commercial Spin Columns

Latent DNA was then isolated from the tapes using commercial spin columns (solid phase extraction) using the QIAamp® DNA Investigator kit.

A piece 10 mm x 5 mm tape was cut out from the tape using a sterile scalpel blade and placed in an empty 1.5 mL microcentrifuge tube. For pre-treatment, 300 µL of Buffer ATL was added to the tube containing the tape and incubated at 85°C with shaking at 900 rpm for 30 min to dissolve the adhesive found on the tape. After incubation, the tube was allowed to cool to room temperature.

From a solution of proteinase K (10 mg/mL) 20 µL was added, mixed thoroughly and further incubated at 56°C with shaking at 900 rpm for at least 1 hr. After incubation, 300 µL of Buffer AL was added and incubated at 70°C with shaking at 900 rpm for 10 min. Ethanol (100% v/v) (150 µL) was added to the mixture. The solution, excluding the tape, was then transferred to the spin column provided with the test kit and centrifuged at 6000 x g for 1 min to allow liquid to pass through the column and DNA in the liquid to bind to the column.

After centrifugation, the column was transferred to a clean 2 mL collection tube for washing to remove any impurities present. The column was first washed in 500 µL of Buffer AW1 and centrifuging at 6000 x g (8000 rpm) for 1 min. The column was then placed into another clean 2 mL collection tube. Next, 700 µL of Buffer AW2 was added, and the tube was then centrifuged at 6000 x g (8000 rpm) for 1 min.

After washing, the column was transferred to a further clean 2 mL collection tube and 700 µL of absolute ethanol was added and centrifuged at 6000 x g (8000 rpm) for 1 min. The column was then placed in a clean 2 mL collection tube and dried by centrifuging at 20,000 x g for 3 min. To ensure that the membrane of the column had dried completely, the column was incubated at 56°C for 3 min with the lid open. Lastly, DNA was eluted with 30 µL of Buffer ATE. Eluted DNA was stored at -20°C until use.

2.2.8 Quantification of Isolated DNA using Spectrometry

In this experiment, isolated DNA was quantified using a Qubit™ Fluorometer (Life Technologies Corporation, Singapore), together with Qubit™ dsDNA HS kit (Life Technologies Corporation, Oregon, USA). Briefly, the 200x Qubit® dsDNA HS Reagent, provided in the kit, was diluted to 1x using the Qubit® dsDNA HS Buffer provided. Of the extracted DNA, 2 µL was then mixed with 198

µL of the 1x Qubit® dsDNA HS Reagent and incubated for 2 min. After 2 min, the DNA concentration was read using the fluorometer.

2.2.9 Molecular Species Identification of Isolated DNA Using Conventional PCR

Conventional PCR was conducted using primers as previously described (Ewart et al., 2021), using forward primer, PID-F (5'- CCCTCYAAYATCTCHGCATGATGRAA -3'), and reverse primer, PID-R (5'- GCNCCTCARRADGAYATYTGTCCTCA-3') which amplified a 350 bp segment of the cyt b region of the mitochondrial DNA. PCR master mix was prepared as indicated in Table 1 below.

PCR reagents	1 reaction (µL)
5x GoTaq® G2 Flexi PCR buffer (Promega Corporation)	5
dNTPs 10 mM (1st BASE)	2
$MgCl_2$ 25 mM (Promega Corporation)	2
GoTaq® G2 Flexi Taq polymerase (Promega Corporation)	0.125
PID-F Forward primer 10 mM (Integrated DNA Technologies, Inc.)	2
PID-R Reverse primer 10 mM (Integrated DNA Technologies, Inc.)	2
Nuclease free water (1st Base)	6.875
Sample template	5
Total	25

Table 1: Composition of PCR master mix for conventional PCR

All conventional PCR was conducted using the Applied Biosystems Proflex® PCR thermocyler (ThermoFisher Scientific, Singapore) with the following PCR conditions: initial denaturation step at 95°C for 3 min, followed by 40 cycles of denaturing at 95°C for 30 sec, annealing at 57°C for 30 sec and elongation at 72°C for 30 sec, with a final extension at 72°C for 5 min.

PCR products were then visualised on a 1.5% agarose gel stained with 1x GelRed® (Biotium, Fremont, USA). Samples showing positive PCR amplicons then were sequenced via Sanger Sequencing. Sanger sequencing were conducted by a commercial DNA sequencing provider (Bio Basic Asia Pacific Pte Ltd., Singapore). Both forward and reverse strands were sequenced for each positive amplicon.

Sequence data obtained were aligned and trimmed using BioEdit Sequence Alignment Editor and then compared and matched to the most closely related sequence in the National Center for Biotechnology Information (NCBI) GenBank database using the megablast program on Nucleotide Basic Local Alignment Search Tool (BLASTn) with an expected threshold of 0.05 and word size of 28.

2.3 Results

2.3.1 Morphological Observation of the Dried *M. javanica* Scales

A total of five scales (A, B, C, D and E) were used to demonstrate the deposition of cellular materials onto the glass slides. From Figures 10 and 11, it could be observed that the scales used in this project were concave in shape and dried tissue could be seen attaching onto the ventral side of the scales. The presence of dried tissues on the ventral side of the scales is a common phenomenon observed from pangolin scales seized in Singapore in 2019. It was hypothesised that most of the cellular material deposited onto the glass slides would be coming from these dried tissues.

The size of each scale is recorded in Table 2 below. All sizes of the scales used in this experiment fall within the expected measurement of scales from *M. javanica* (Cota-Larson, 2017).

Table 2: Size of scales used in this experiment. The scales were measured point to point at its widest.

Scale	Width (cm)	Height (cm)
A	2.7	3.4
B	2.2	2.1
C	3.1	2.5
D	3.3	3.5
E	2.6	2.3

2.3.2 Staining of Cellular Materials Deposited by *M. javanica* Scales via Friction

2.3.2.1 Distribution of fluorescence staining

Almost all areas of the negative control slide (N) were devoid of any fluorescence and any fluorescence detected was not the size or morphology expected for cellular materials (Figure 13 and 14). This indicated that the slide used in this experiment were clean and free from auto-fluorescence and therefore were suitable for use.

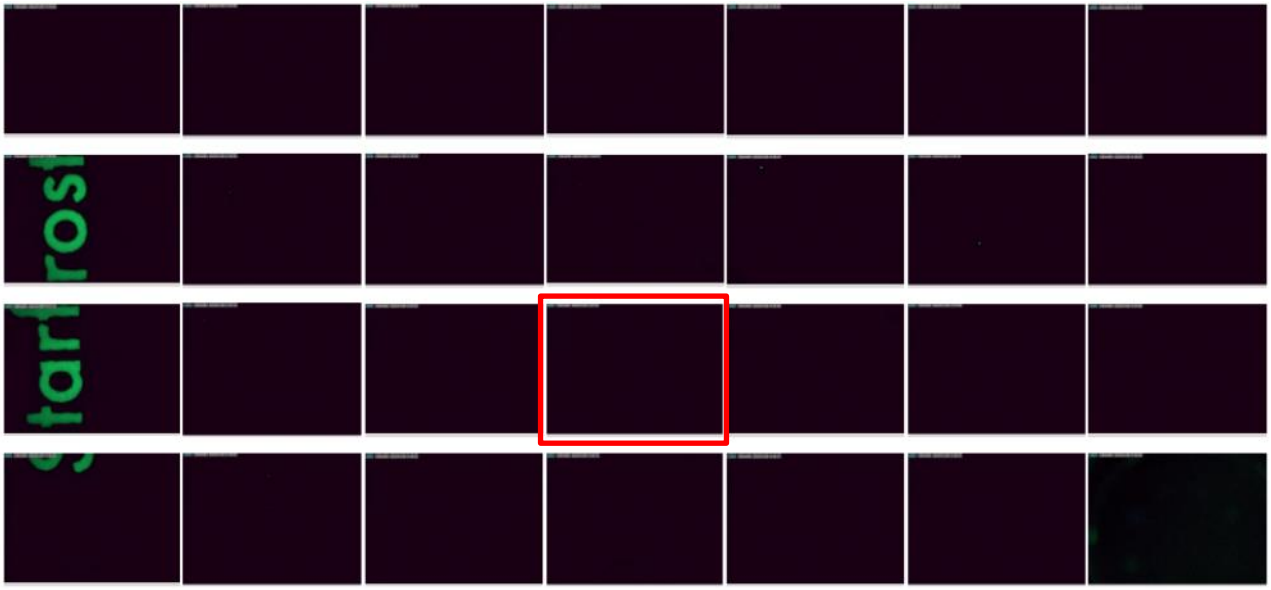

Figure 13: Overall view of negative control (N). The entire slide was divided into 7 columns and 4 rows to allow the field of the microscope to cover the entire slide.

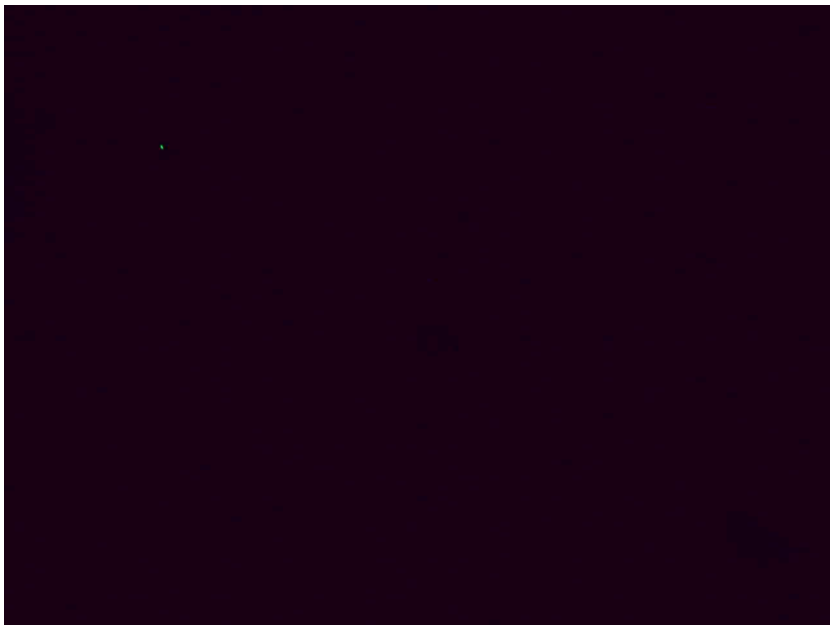

Figure 14: Expanded image of the field highlighted in red in Figure 13 (blank slide), at 50x magnification.

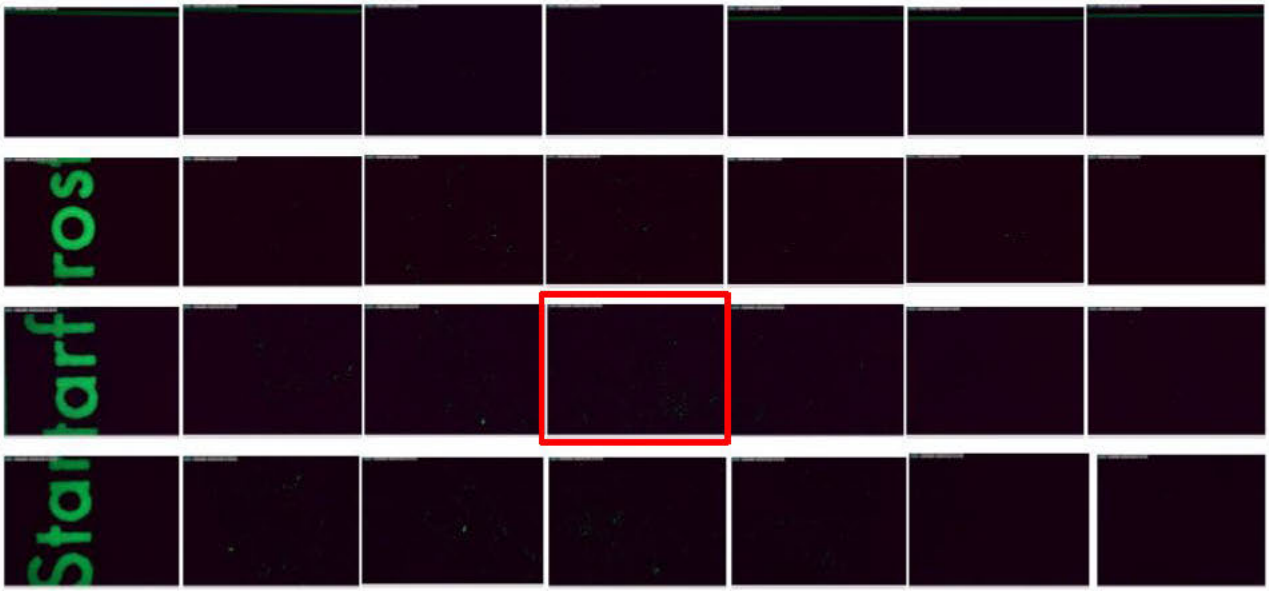

Figure 15: Overall view of slide deposited with DNA from thumbprint. The entire slide was divided into 7 columns and 4 rows to allow the field of the microscope to cover the entire slide.

Figure 16: Expanded image of the field highlighted in red in Figure 15 (thumbprint), showing the length of a typical fluorescence staining from thumbprint (L-0.130 mm) at 50x magnification.

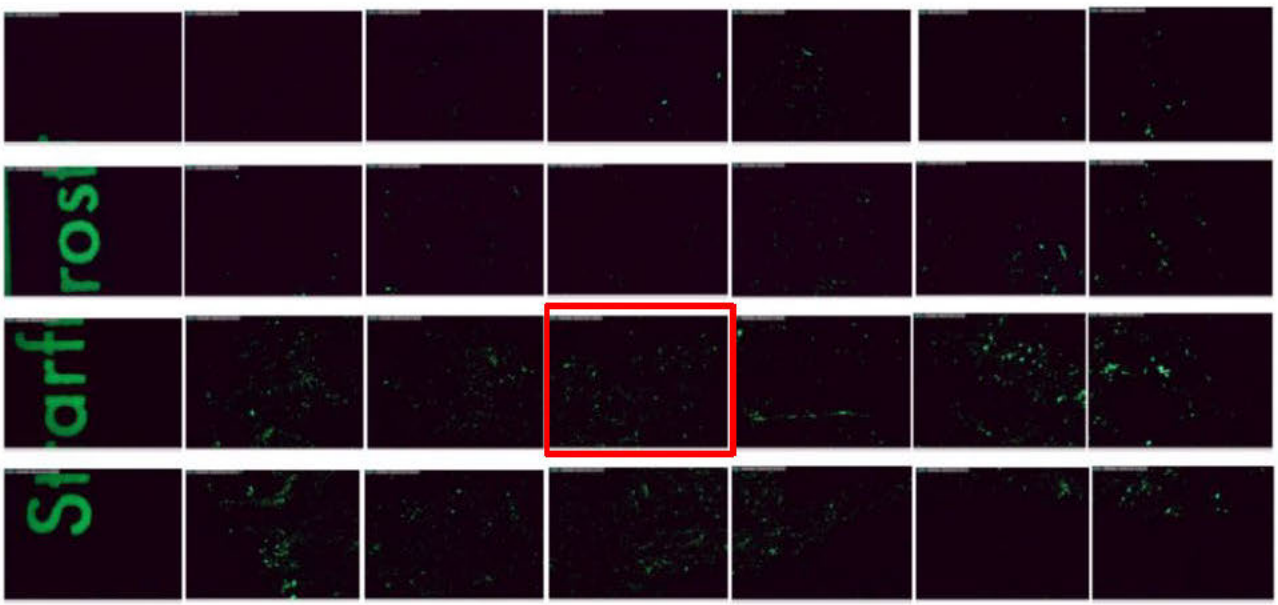

Figure 17: Overall view of slide deposited with DNA from scale A, via friction, 60 sec. The entire slide was divided into 7 columns and 4 rows to allow the field of the microscope to cover the entire slide.

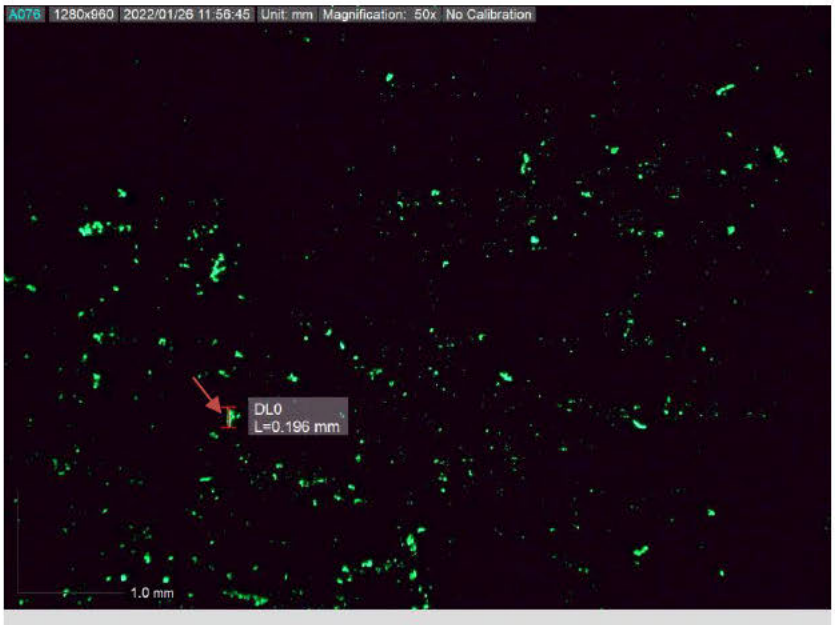

Figure 18: Expanded image of the field highlighted in red in Figure 17 (scale A), showing the length of a typical fluorescence staining from scale A (L-0.196 mm) at 50x magnification.

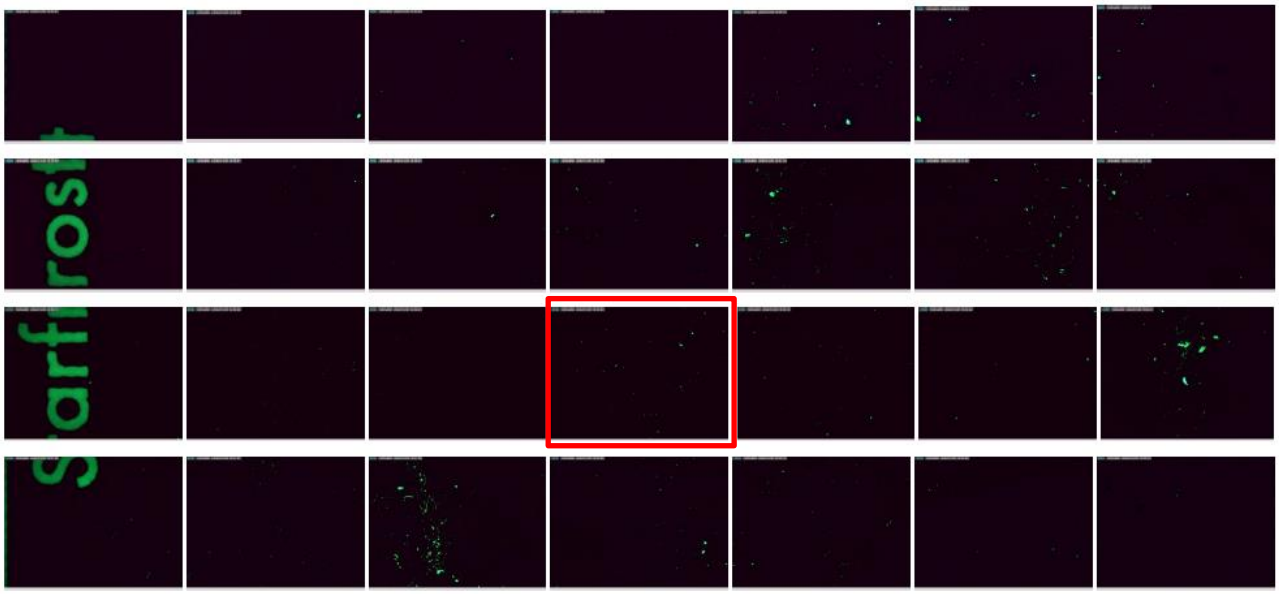

Figure 19: Overall view of slide deposited with DNA from scale B, via friction, 60 sec. The entire slide was divided into 7 columns and 4 rows to allow the field of the microscope to cover the entire slide.

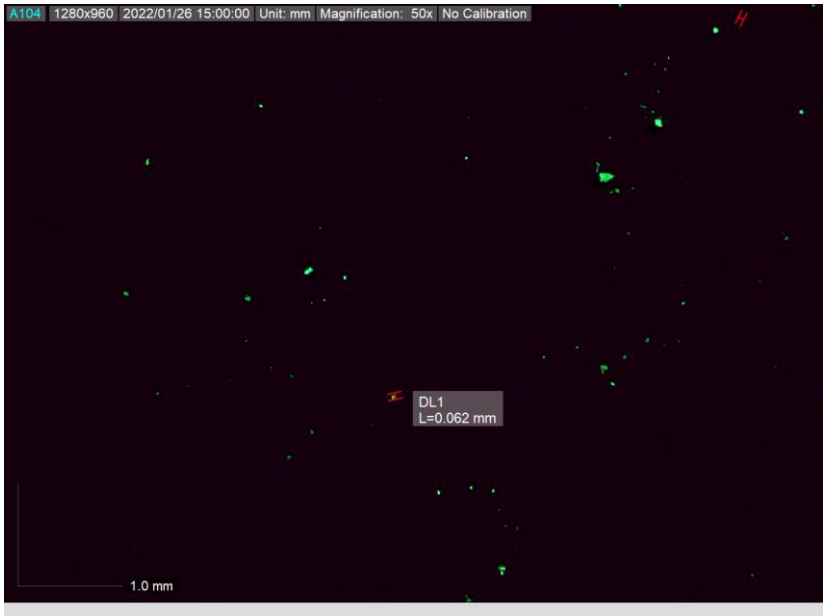

Figure 20: Expanded image of the field highlighted in red in Figure 19 (scale B), showing the length of a typical fluorescence staining from scale B (L-0.062 mm) at 50x magnification.

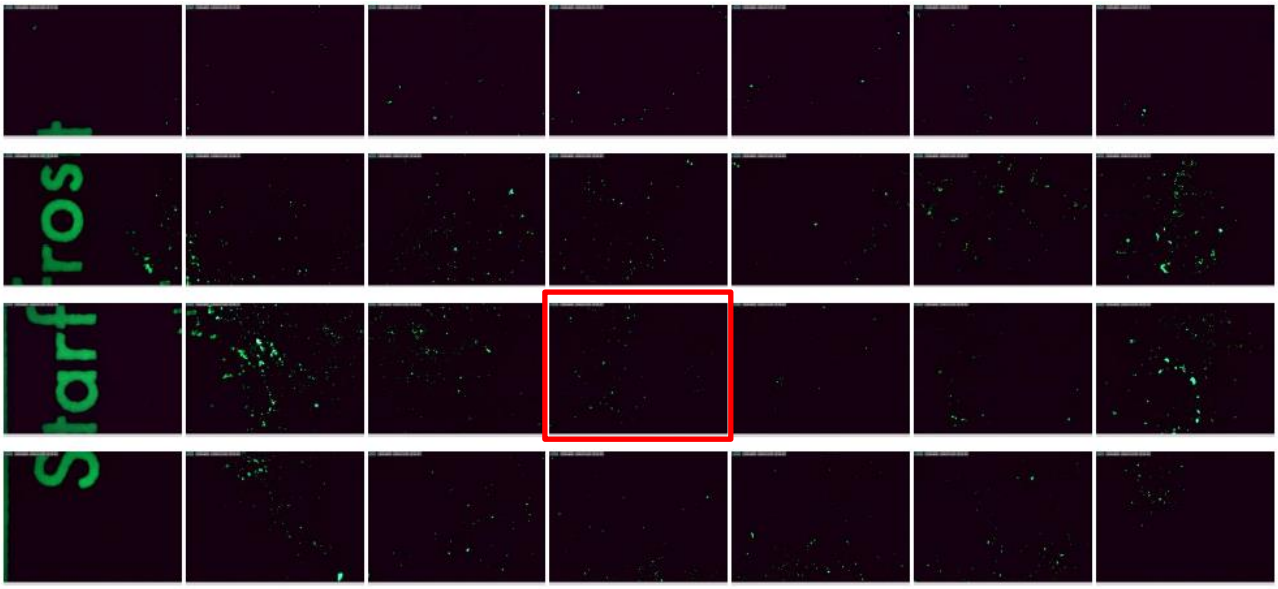

Figure 21: Overall view of slide deposited with DNA from scale C, via friction, 60 sec. The entire slide was divided into 7 columns and 4 rows to allow the field of the microscope to cover the entire slide.

Figure 22: Expanded image of the field highlighted in red in Figure 21 (scale C), showing the length of a typical fluorescence staining from scale C (L-0.062 mm) at 50x magnification.

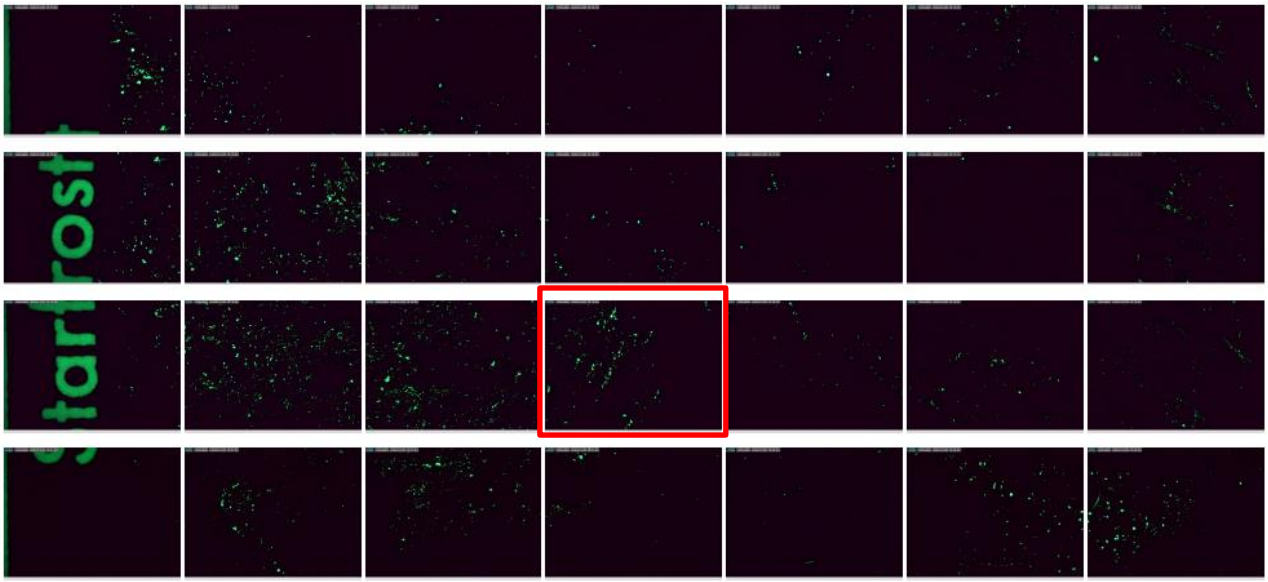

Figure 23: Overall view of slide deposited with DNA from scale D, via friction, 60 sec. The entire slide was divided into 7 columns and 4 rows to allow the field of the microscope to cover the entire slide.

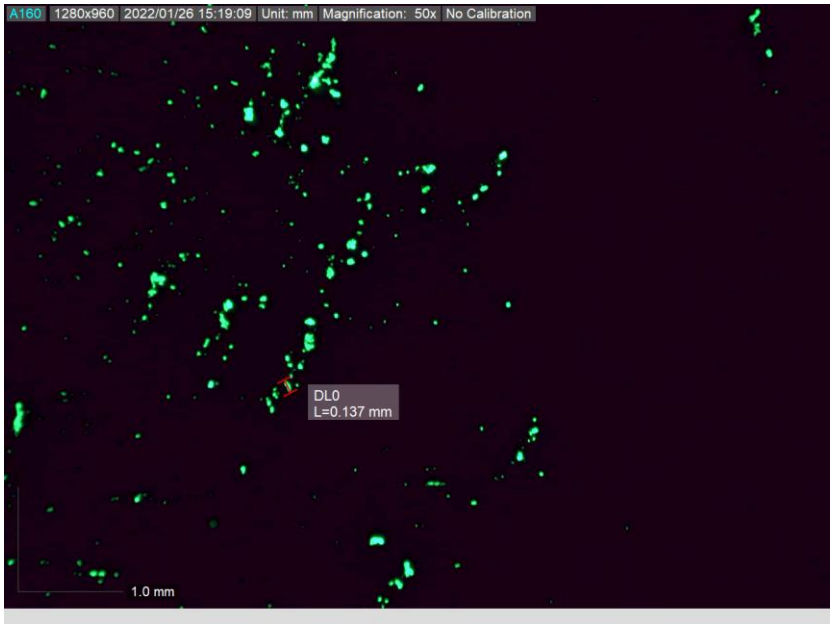

Figure 24: Expanded image of the field highlighted in red in Figure 23 (scale D), showing the length of a typical fluorescence staining from scale D (L-0.137 mm) at 50x magnification.

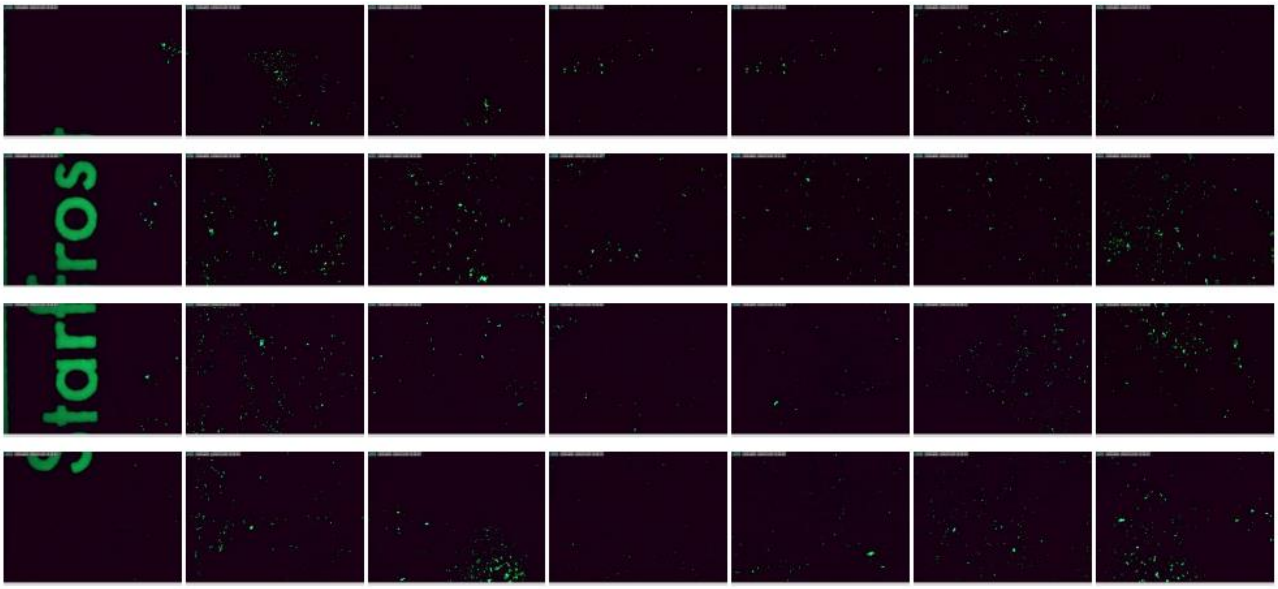

Figure 25: Overall view of slide deposited with DNA from scale E, via friction, 60 sec. The entire slide was divided into 7 columns and 4 rows to allow the field of the microscope to cover the entire slide.

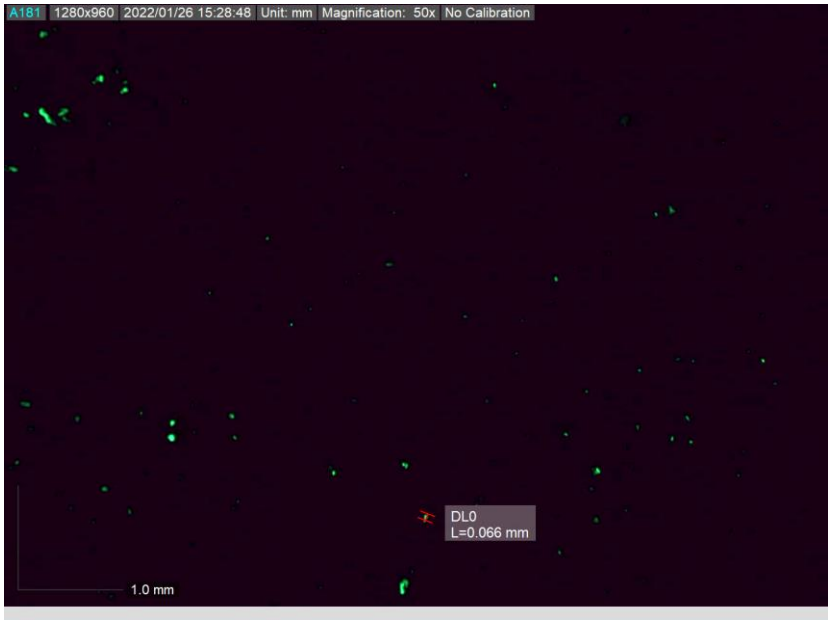

Figure 26: Expanded image of the field highlighted in red in Figure 25 (scale E), showing the length of a typical fluorescence staining from scale E (L- 0.66 mm) at 50x magnification.

Bright, green, fluorescent particles could be seen in all slides that had been in contact with the pangolin scales, indicating that cellular materials had been transferred from the respective scales onto the slides via friction. Fluorescence staining was seen to be unevenly distributed throughout the slides, with a visually higher concentration of fluorescence staining observed at the two ends of the slides: A, B, C and E (Figures 17, 19, 21 and 25). This could be attributed to the sliding motion when introducing friction; the cellular materials may be pushed to the sides when sliding the scales across the slides.

As shown in Figures 16 and 18, the size of a single green, fluorescent particles appeared to be larger for that from pangolin scales (length = 0.196 mm) (Figure 18) as compared to the fluorescent stain from human thumbprint (length = 0.130 mm) (Figure 16).

2.3.2.2 Comparison of the size of fluorescent particles from thumbprint and M. javanica scales

In order to determine if the size of fluorescent particles from pangolin scales was indeed larger than that of the thumbprint, the lengths of 20 fluorescent particles from one representative image of each slide (Figures 16, 18, 20, 22, 24 and 26) were randomly selected and measured, The mean and standard deviation of the measured lengths were calculated (Table 3). The measured lengths of the 20 fluorescent particles were also plotted into a whiskered boxplot (Figure 27).

The mean length of the fluorescent particles obtained from the thumbprint was the shortest (Table 3). A similar result was also demonstrated by the boxplot, indicating that the fluorescent particles from thumbprints had the shortest length.

Table 3: Length (mm) of 20 particles from the representative image of slides deposited. A human thumbprint is included along with scales A – E. Cell deposition was via friction. The mean and standard deviation are included as the last two rows respectively.

	THUMBPRINT	A	B	C	D	E
1	0.13	0.196	0.055	0.062	0.137	0.066
2	0.052	0.071	0.062	0.143	0.139	0.164
3	0.039	0.115	0.055	0.071	0.098	0.074
4	0.049	0.069	0.088	0.13	0.132	0.055
5	0.05	0.074	0.139	0.115	0.135	0.061
6	0.027	0.191	0.113	0.101	0.086	0.088
7	0.061	0.082	0.061	0.086	0.089	0.039
8	0.037	0.111	0.061	0.086	0.061	0.143
9	0.05	0.086	0.05	0.088	0.086	0.066
10	0.073	0.149	0.086	0.113	0.113	0.061
11	0.069	0.061	0.095	0.049	0.05	0.05
12	0.077	0.039	0.071	0.035	0.074	0.069
13	0.052	0.061	0.061	0.086	0.055	0.062
14	0.055	0.055	0.049	0.062	0.086	0.055
15	0.039	0.099	0.062	0.055	0.11	0.05
16	0.039	0.115	0.035	0.099	0.062	0.074
17	0.039	0.055	0.05	0.071	0.073	0.088
18	0.061	0.089	0.05	0.05	0.069	0.061
19	0.027	0.049	0.062	0.049	0.061	0.044
20	0.055	0.062	0.044	0.044	0.061	0.044
MEAN	0.0541	0.0915	0.0675	0.0798	0.0889	0.0707
SD	0.0220	0.0430	0.0246	0.0294	0.0288	0.0306

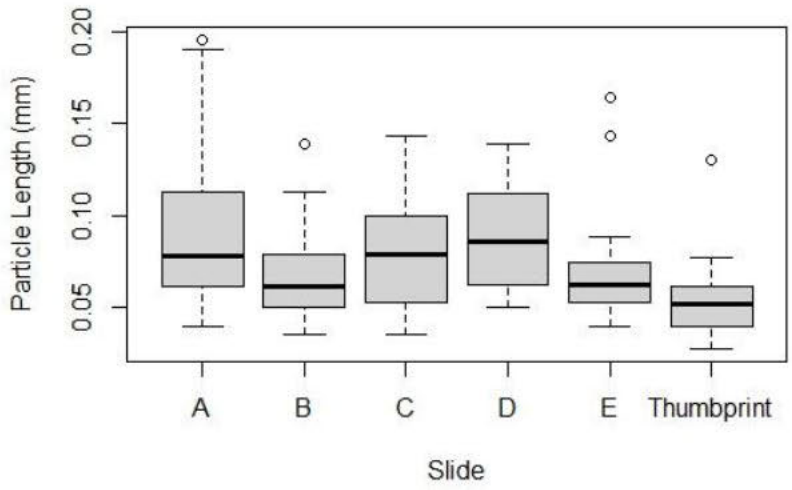

Figure 27: Box plot showing the 25%, 50% and 75% quantiles of the length of the fluorescent particles from the representative image of the slides (n = 20 for each slide).

Data obtained were then analysed statistically. Using a one-way ANOVA test, there was evidence to show that the length of fluorescent particles collected varied (F-value = 4.087, p = 0.00189) between the various slides (thumbprint: n=20, A: n=20, B: n=20, C: n= 20, D: n=20, E: n=20). A Tukey post-hoc test was then conducted to determine pairwise relationship between the length of fluorescent particles obtained from each slide, and there was evidence to indicate that the length of fluorescent particles collected from thumbprint were shorter from those of A (p = 0.00332) and D (0.00797). However, the difference in the length of fluorescent particles obtained from thumbprint was not evident between B (p = 0.75319), C (p = 0.10569), and E (p = 0.54495).

2.3.2.3 Quantification of fluorescent particles

The number of fluorescent particles on each slide was also quantified using the ImageJ particle counting function. The total number of fluorescent particles from each slide is shown in Table 4 below. The first image of each row of each slide was excluded from the calculation of total fluorescent particle count as the brand marking of the slide interfered with the particle counting function of ImageJ.

Table 4: Total fluorescent particle count for each slide.

	Blank Slide	Thumbprint	A	B	C	D	E
Total Fluorescent Particle Count	22	3191	11373	1896	3326	5911	4160

From Table 4, it can be seen that slide A has the highest number of fluorescent particles while slide B has the lowest number of fluorescent particles among the slides deposited with cellular

materials from *M. javanica* scales. Although some fluorescent particles were observed on the negative control slide, the number was much lower than the rest of the slides. These fluorescent particles were either: cellular materials that might have been deposited during manufacturing, storage, or handling process; or not cellular in origin but scored erroneously by ImageJ.

2.3.3 Staining of Cellular Material Deposited by *M. javanica* Scales via Pressure

2.3.3.1 Distribution of fluorescence staining

Cellular materials deposited were stained by DD and visualised using the digital microscope under 50x magnification to determine the presence of green, fluorescent particles. Two slides were obtained for each scale; one slide that was in contact with ventral side of the scales and the other slide that was in contact with dorsal side of the scale.

From each slide, 4 x 7 images were taken to ensure that all fluorescent particles present were captured. The 28 images were then pieced together to provide an overall presentation of the fluorescent particle staining patterns on each slide.

Fluorescent staining could be seen in all slides (Figures 28 – 49) although it was visually observed to be much fewer and smaller in length when compared to the slides where cellular materials had been deposited via friction. Much more fluorescent staining could be observed on slides in contact with the ventral side of the scales (Figures 30, 34, 38, 42 and 46) than the slides in contact with the dorsal side of the scales (Figures 32, 36, 40, 44 and 48). The fluorescent staining was also observed to concentrate mainly at certain areas of each slide instead of being evenly distributed. For slides in contact with ventral surface of the scales, this could be due to the contact between the dried tissues present on the scales and the slides indicating that the number of cellular materials deposited on the slide would likely to be dependent on the presence of dried tissues on the scales that were in contact with the slides.

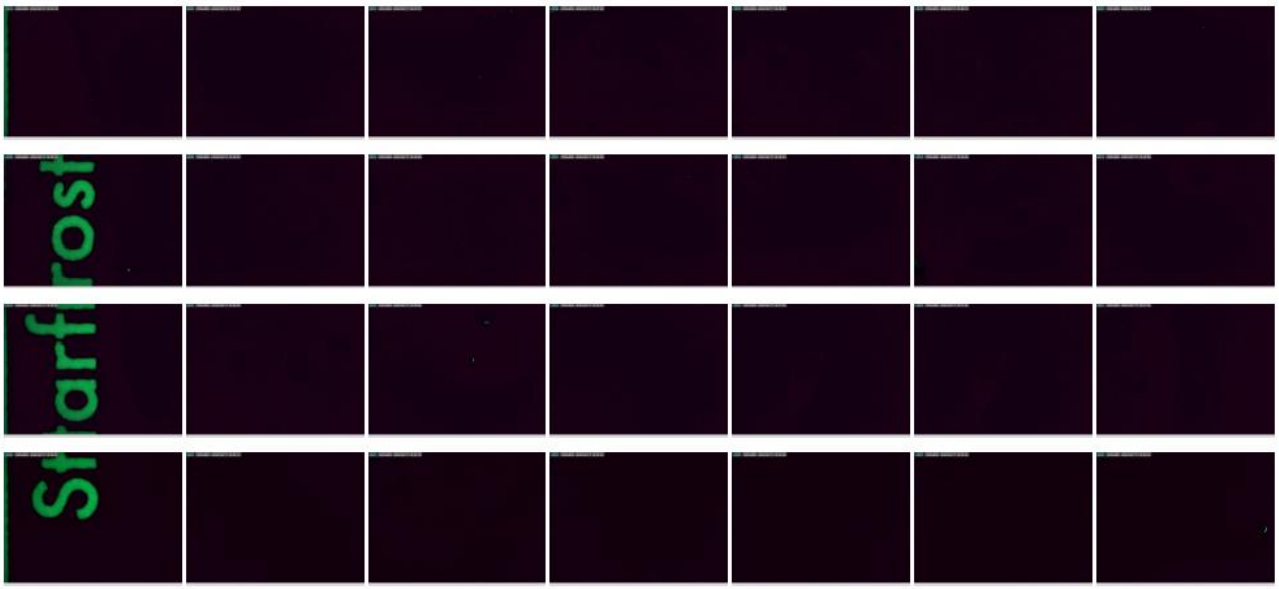

Figure 28: Overall view of negative control (ventral) via pressure. The entire slide was divided into 7 columns and 4 rows to allow the field of the microscope to cover the entire slide.

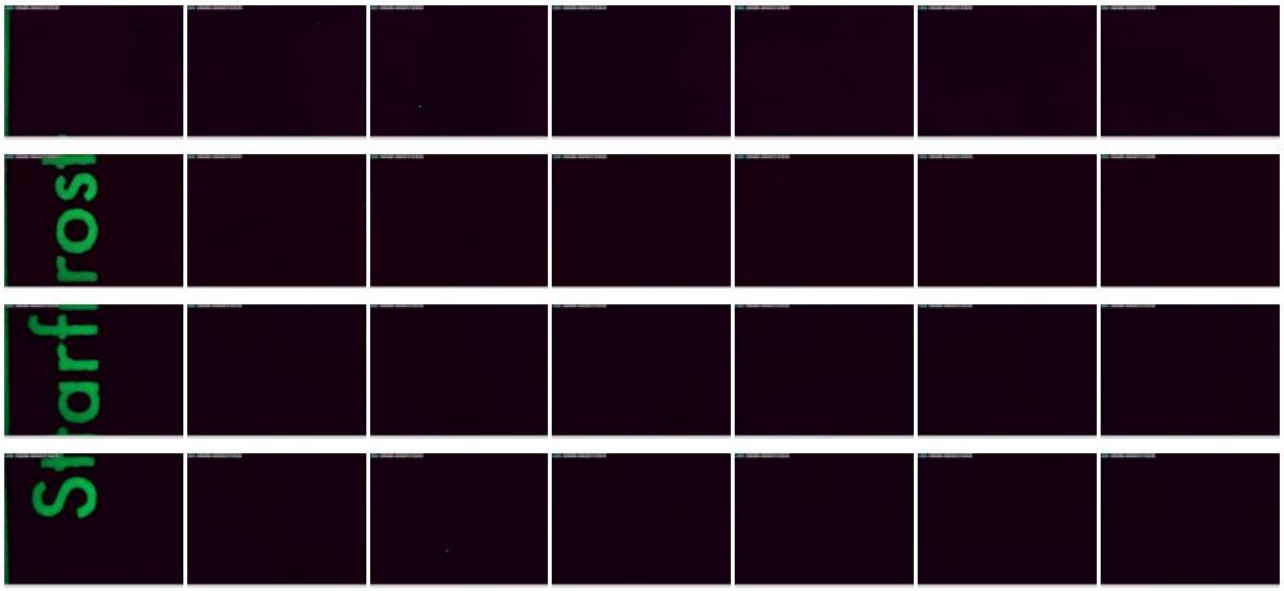

Figure 29: Overall view of negative control (dorsal) via pressure. The entire slide was divided into 7 columns and 4 rows to allow the field of the microscope to cover the entire slide.

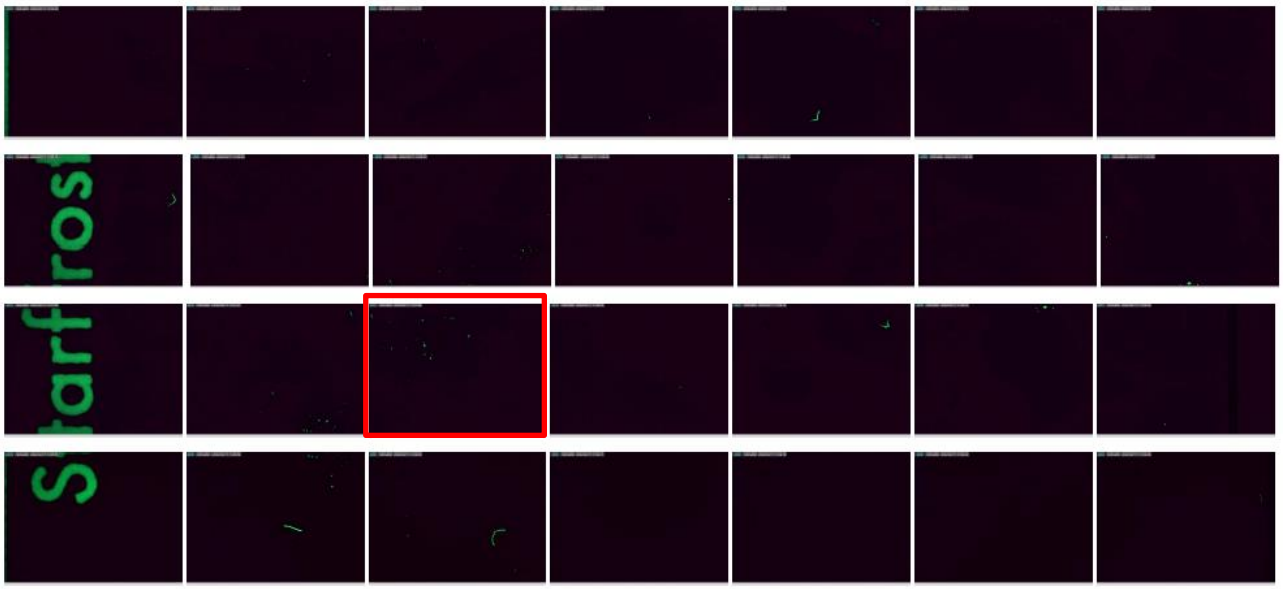

Figure 30: Overall view of slide deposited with DNA from scale A (ventral surface), via pressure.

Figure 31: Expanded image of the field highlighted in red in figure 22 (scale A, ventral), showing the length of a typical fluorescence staining from pangolin scale (L-0.086 mm) at 50x magnification.

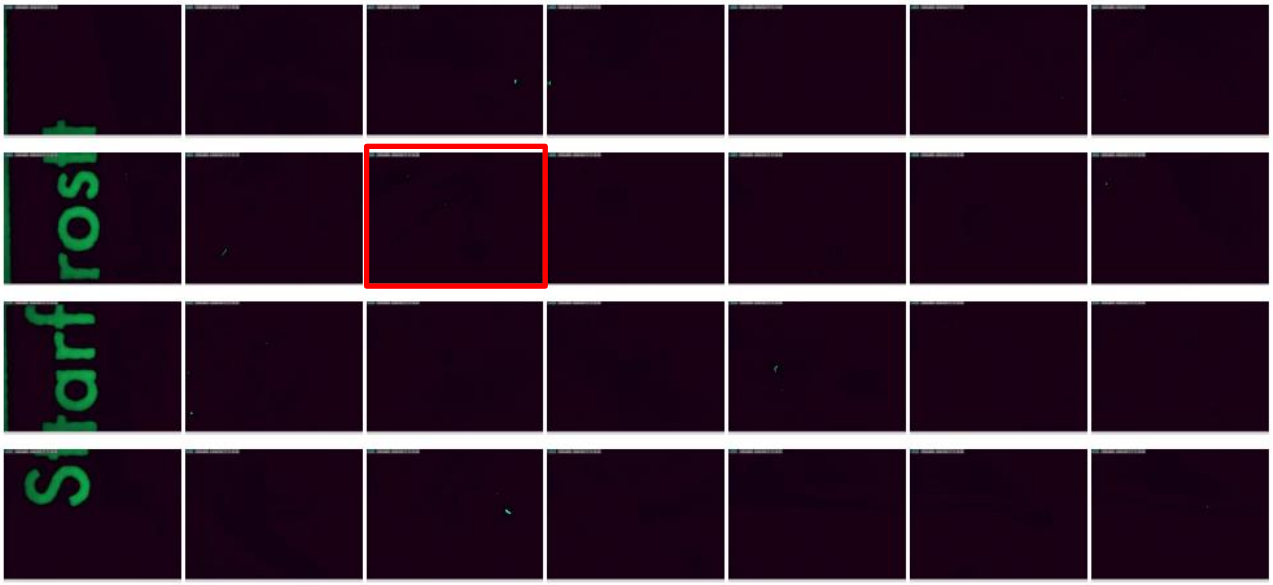

Figure 32: Overall view of slide deposited with DNA from scale A (dorsal surface), via pressure.

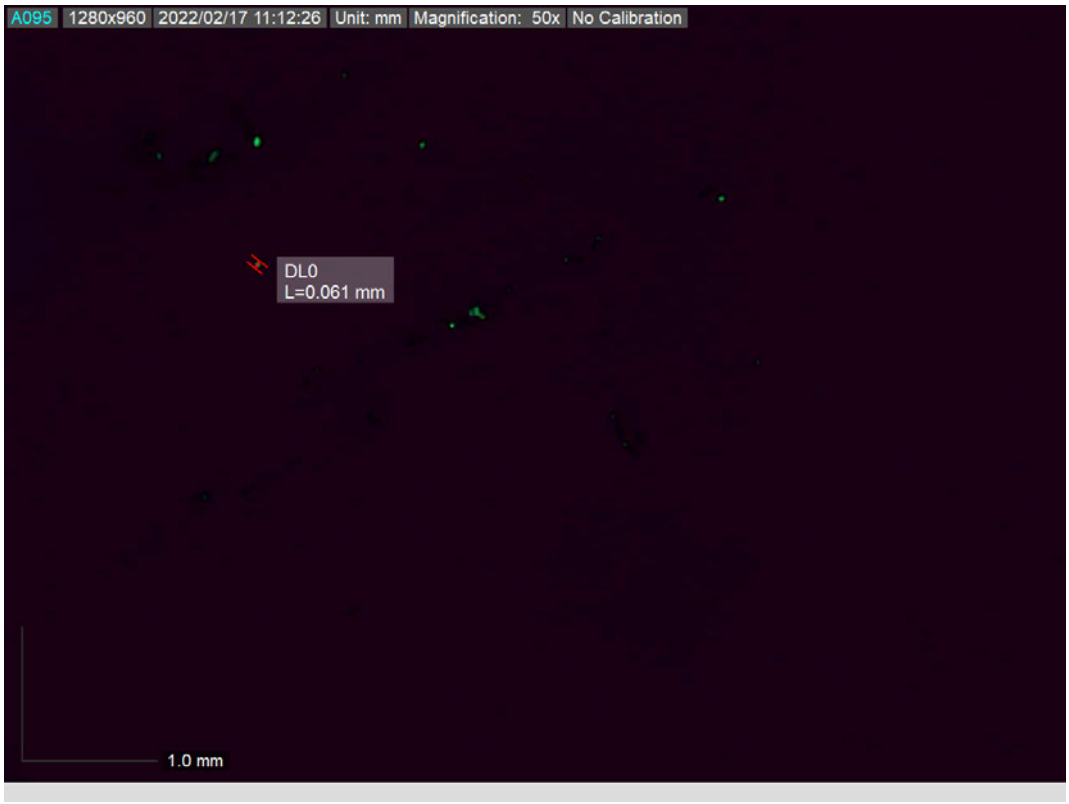

Figure 33: Expanded image of the field highlighted in red in Figure 24 (scale A, dorsal), showing the length of a typical fluorescence staining from pangolin scale (L-0.061 mm) at 50x magnification.

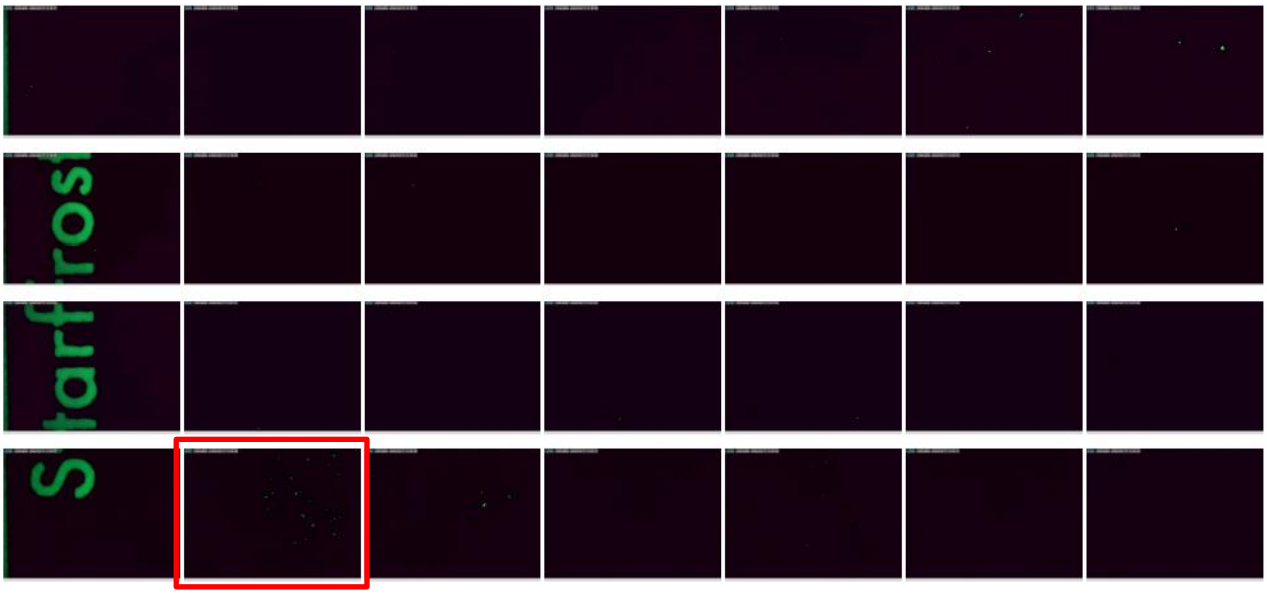

Figure 34: Overall view of slide deposited with DNA from scale B (ventral surface), via pressure.

Figure 35: Expanded image of the field highlighted in red in Figure 26 (scale B, ventral), showing the length of a typical fluorescence staining from pangolin scale (L-0.155 mm) at 50x magnification.

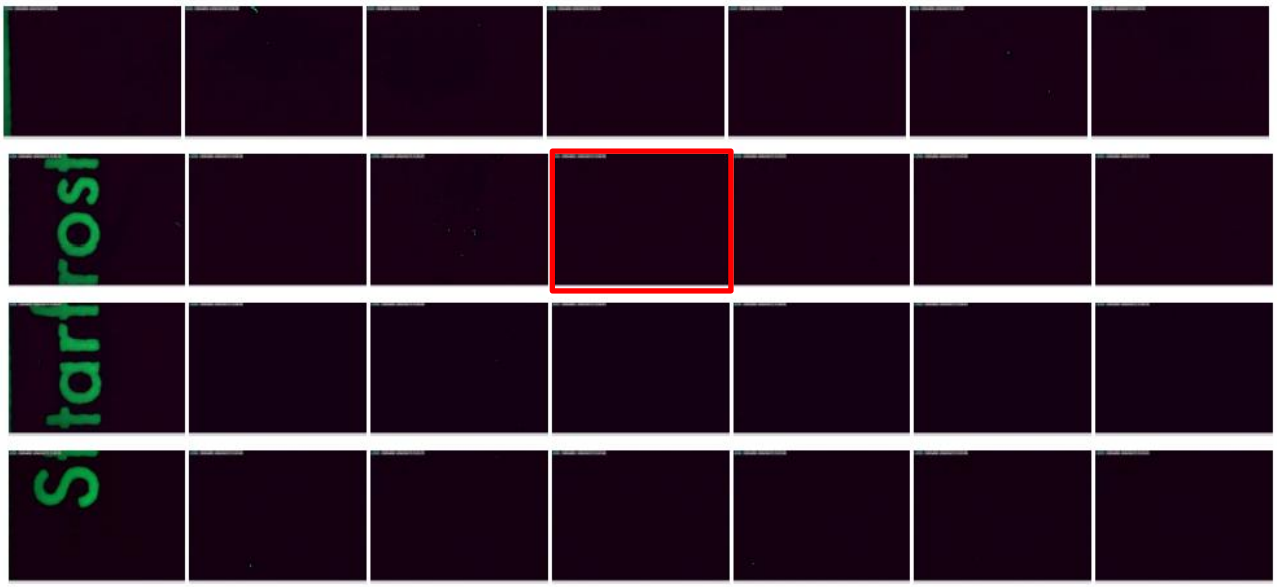

Figure 36: Overall view of slide deposited with DNA from scale B (dorsal surface), via pressure.

Figure 37: Expanded image of the field highlighted in red in Figure 28 (scale B, dorsal), showing the length of a typical fluorescence staining from pangolin scale (L-0.086 mm) at 50x magnification.

Figure 38: Overall view of slide deposited with DNA from scale C (ventral surface), via pressure.

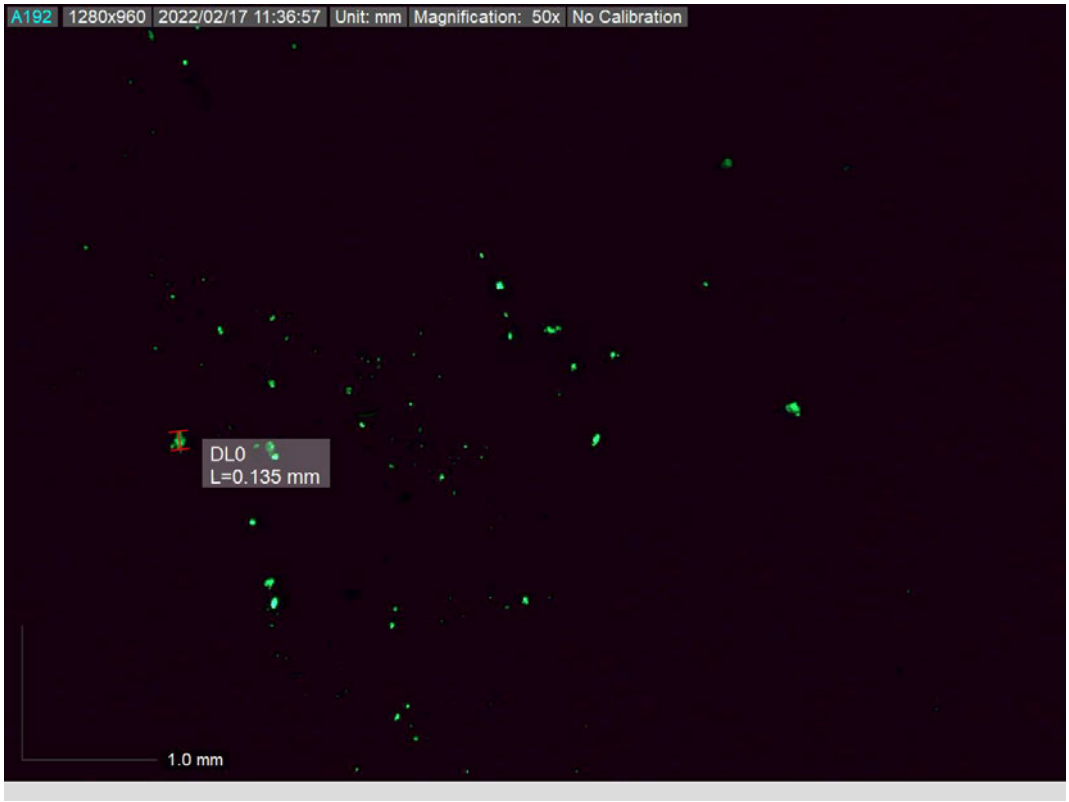

Figure 39: Expanded image of the field highlighted in red in Figure 30 (scale C, ventral), showing the length of a typical fluorescence staining from pangolin scale (L-0.135 mm) at 50x magnification.

Figure 40: Overall view of slide deposited with DNA from scale C (dorsal surface), via pressure.

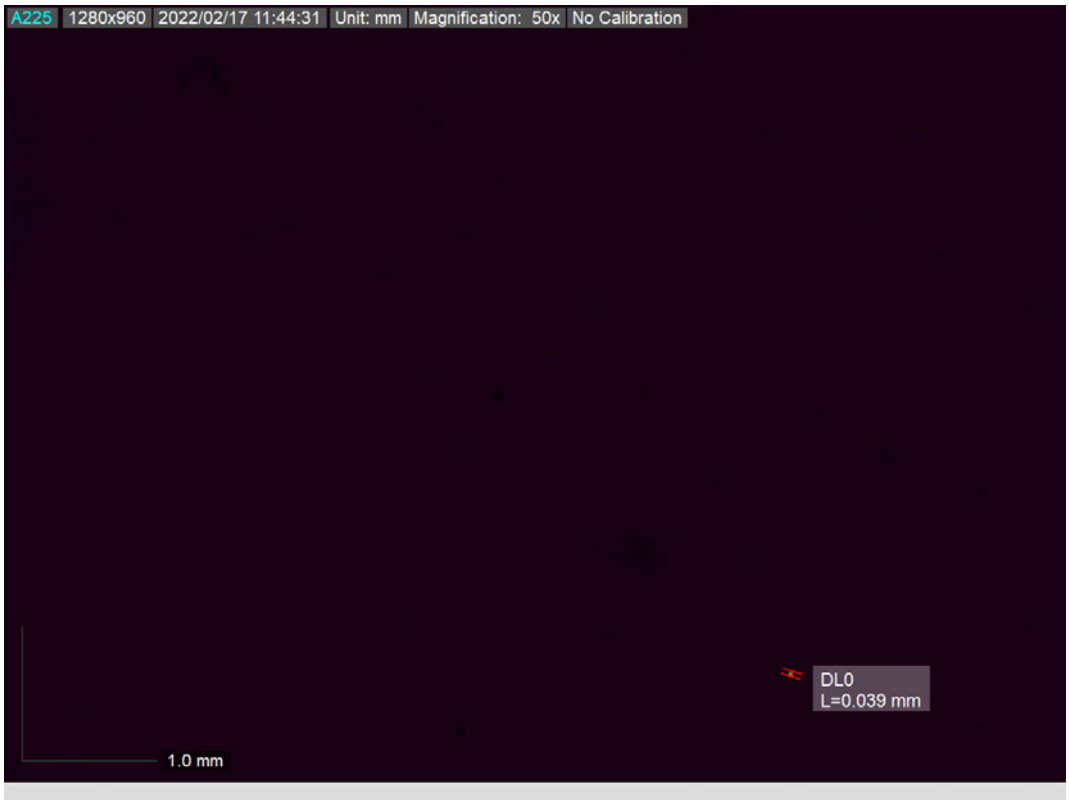

Figure 41: Expanded image of the field highlighted in red in Figure 32 (scale C, dorsal), showing the length of a typical fluorescence staining from pangolin scale (L-0.039 mm) at 50x magnification.

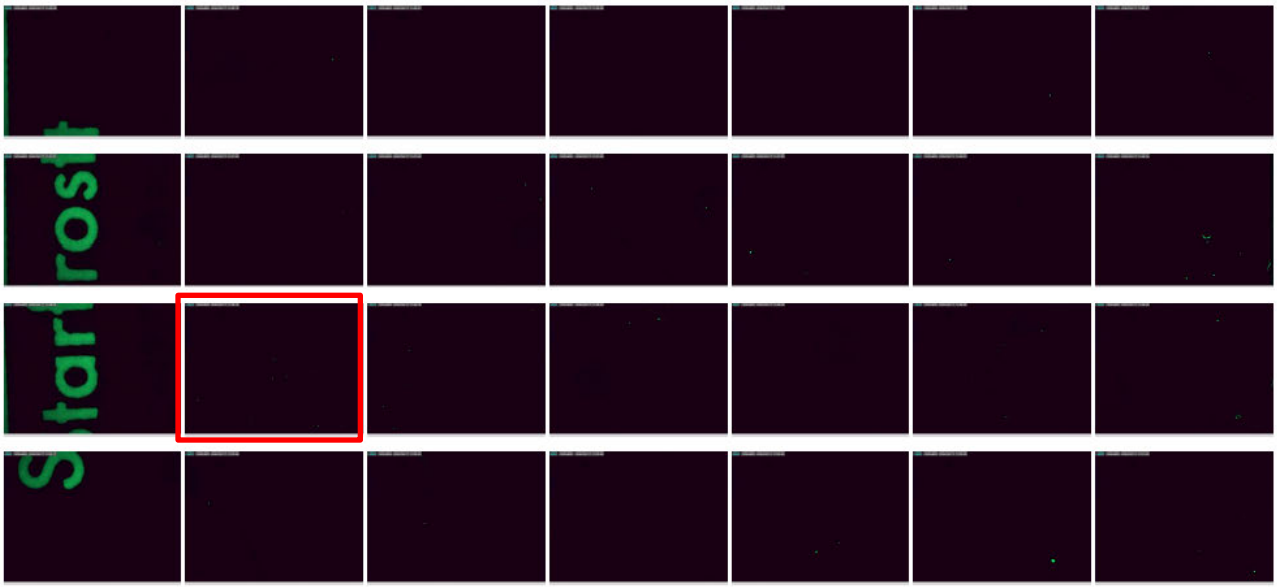

Figure 42: Overall view of slide deposited with DNA from scale D (ventral surface), via pressure.

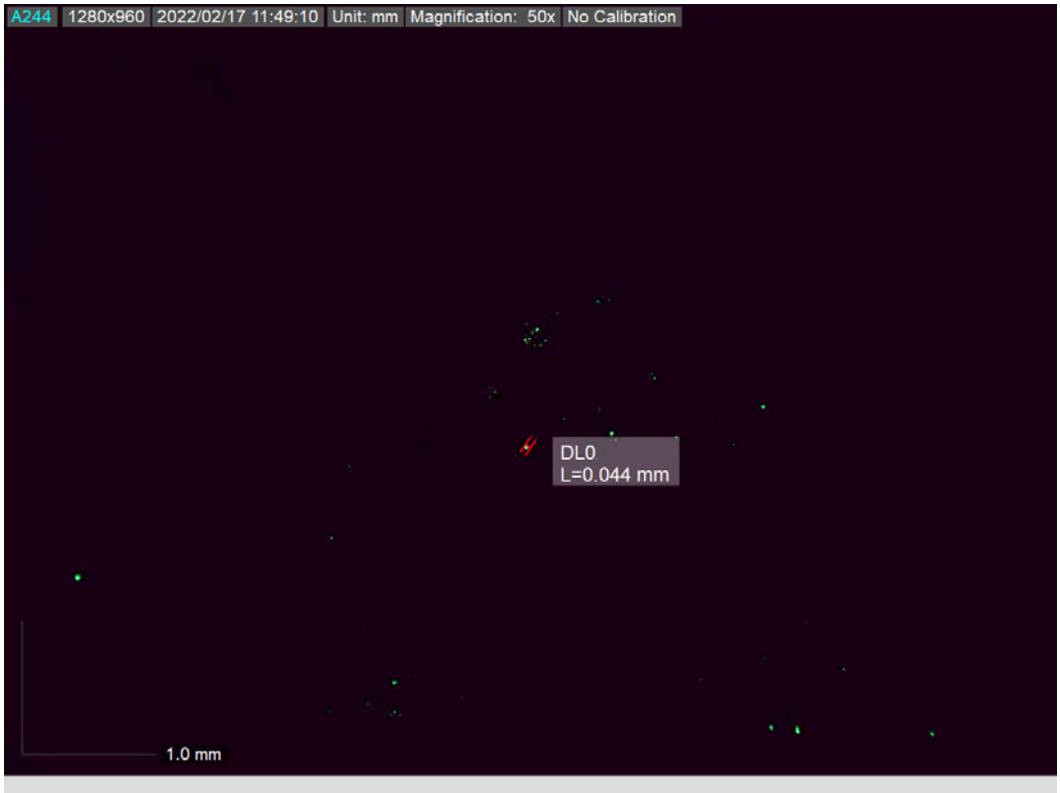

Figure 43: Expanded image of the field highlighted in red in Figure 34 (scale D, ventral), showing the length of a typical fluorescence staining from pangolin scale (L-0.044 mm) at 50x magnification.

Figure 44: Overall view of slide deposited with DNA from scale D (dorsal surface), via pressure.

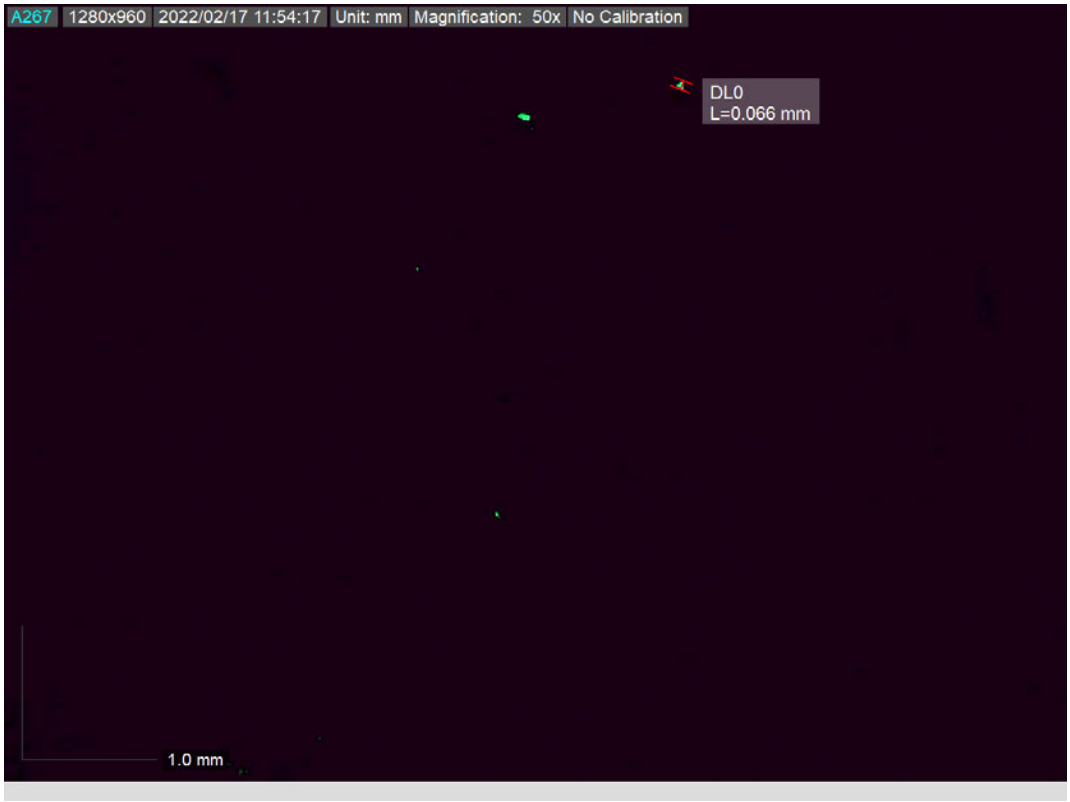

Figure 45: Expanded image of the field highlighted in red in Figure 36 (scale D, dorsal), showing the length of a typical fluorescence staining from pangolin scale (L-0.066 mm) at 50x magnification.

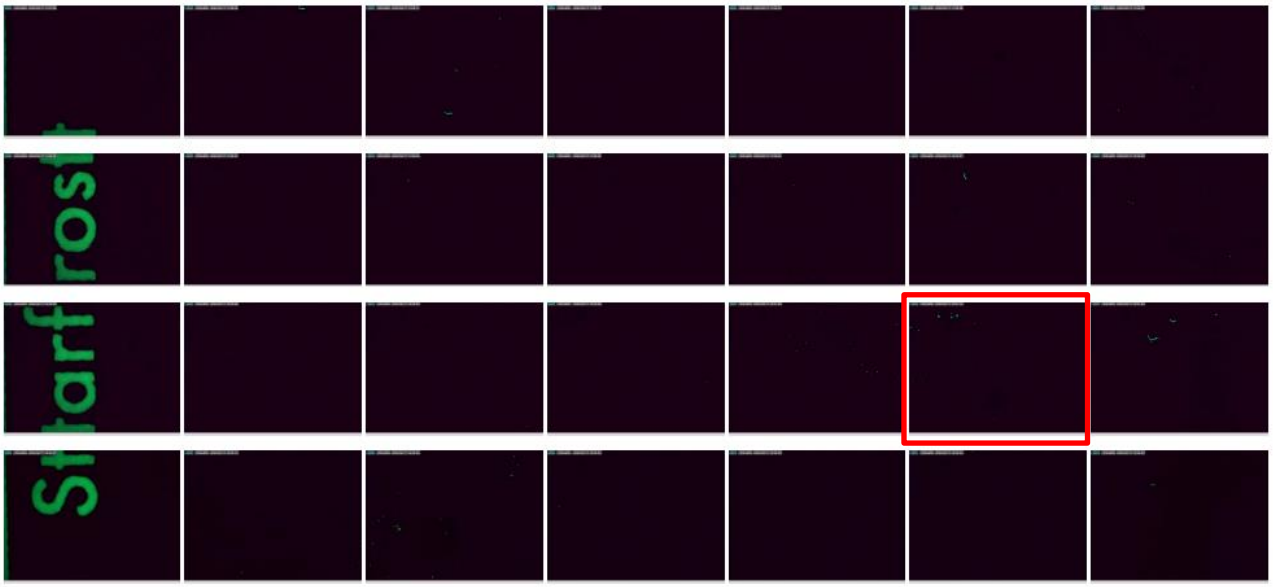

Figure 46: Overall view of slide deposited with DNA from scale E (ventral surface), via pressure.

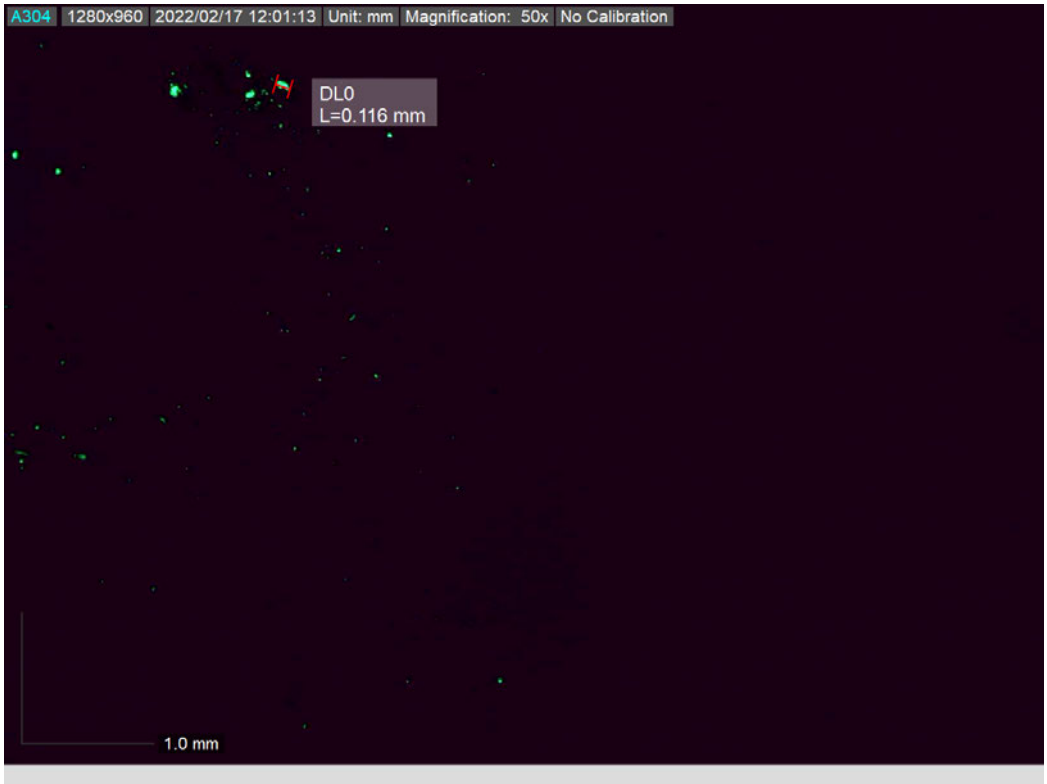

Figure 47: Expanded image of the field highlighted in red in Figure 38 (scale E, ventral), showing the length of a typical fluorescence staining from pangolin scale (L-0.116 mm) at 50x magnification.

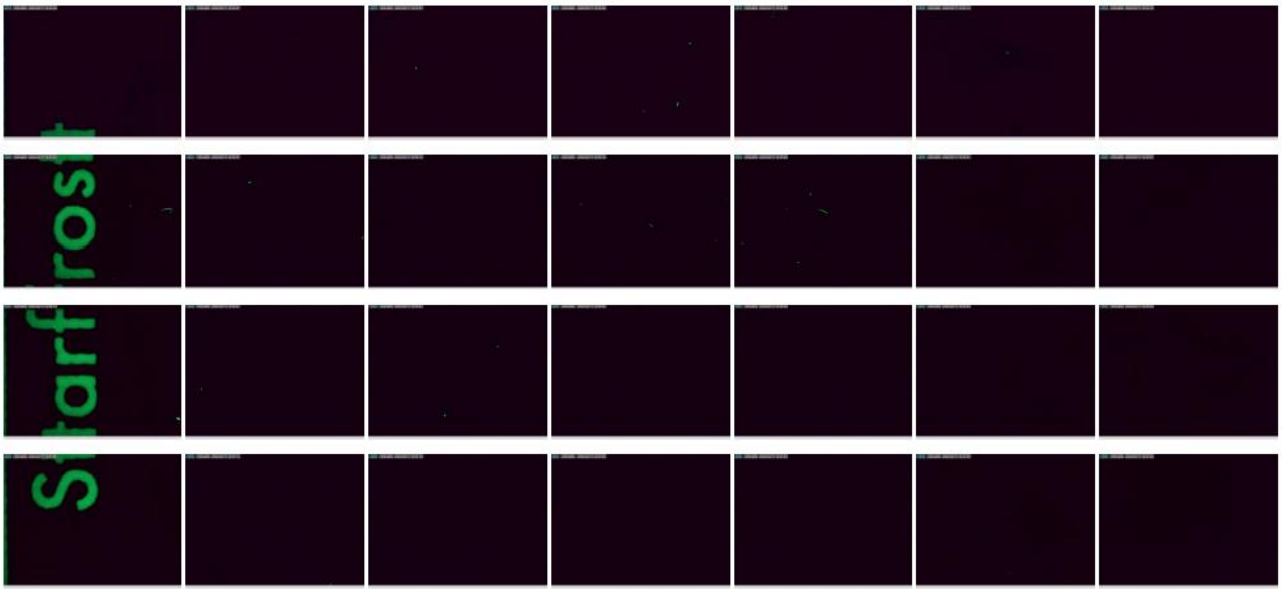

Figure 48: Overall view of slide deposited with DNA from scale E (dorsal surface), via pressure.

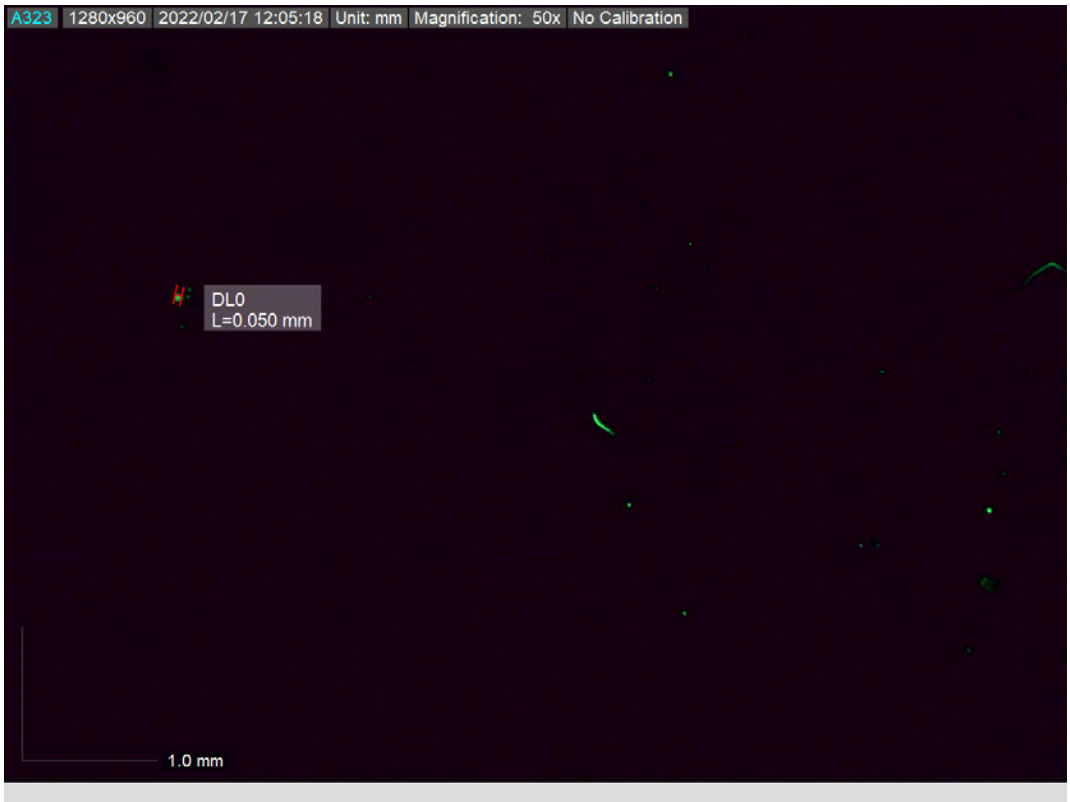

Figure 49: Expanded image of the field highlighted in red in Figure 40 (scale E, dorsal), showing the length of a typical fluorescence staining from pangolin scale (L-0.050 mm) at 50x magnification.

2.3.3.2 Comparison of the size of fluorescent particles from cellular materials deposited via pressure and thumbprints

The length of 10 fluorescent particles from one representative image of each slide deposited with cellular materials from ventral side of the scales (Figures 23, 27, 31, 35, and 39) were measured and the mean and standard deviation of the measured length were calculated (Table 3). The fluorescent particles obtained from the dorsal side of the scales were not measured as the number of fluorescent particles was very low (see Section 2.3.3.4). In this trial, only 10 measurements were taken as the number of fluorescent particles was lower than the number of fluorescent particles deposited via friction.

The measured length of the fluorescent particles was plotted into a whiskered boxplot (Figure 42).

Table 5: Length (mm) of 10 particles from the representative image of slides deposited with ventral side of Scales A – E via pressure or thumbprint and, its respective mean and standard deviation.

	THUMBPRINTS	AV	BV	CV	DV	EV
1	0.063	0.155	0.155	0.135	0.044	0.11
2	0.053	0.062	0.071	0.050	0.047	0.095
3	0.047	0.077	0.082	0.121	0.066	0.074
4	0.047	0.116	0.098	0.113	0.044	0.054
5	0.038	0.086	0.078	0.086	0.044	0.053
6	0.038	0.049	0.055	0.073	0.052	0.043
7	0.043	0.069	0.086	0.071	0.053	0.042
8	0.060	0.095	0.061	0.044	0.032	0.057
9	0.053	0.055	0.061	0.077	0.042	0.038
10	0.057	0.074	0.037	0.052	0.053	0.047
MEAN	0.050	0.084	0.078	0.082	0.048	0.061
SD	0.007925219	0.028784	0.02899	0.028447	0.008147	0.021876

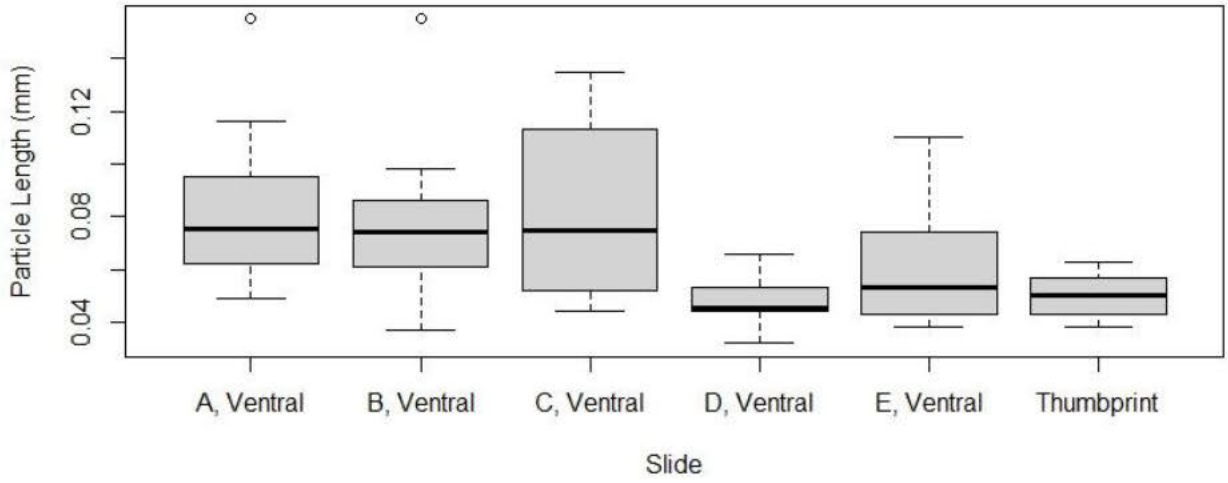

Figure 50: Box plot showing the 25%, 50% and 75% quantiles of the length of the fluorescent particles from the representative image of the slides (n = 10 for each slide).

The mean length of the fluorescent particles obtained from the scale D was the shortest (Table 5). However, the mean length of the fluorescent particles from thumbprint was similar to that of scale D. The mean lengths of fluorescent particles from other scales were longer than that of scale D and the thumbprint. These data are provided in a boxplot (Figure 50) which also indicated similar results.

Data obtained for the lengths of the fluorescent particles were then analysed statistically. Using a one-way ANOVA test, there was evidence that the lengths of fluorescent particle collected varied (F-value = 4.265, p = 0.00243) between the various slides (thumbprint: n=10, A: n=10, B: n=10, C: n= 10, D: no=10, E: n=10).

A Tukey post-hoc test was then conducted to determine pairwise relationship between the length of fluorescent particles obtained from each slide, and there was evidence to indicate that length of fluorescent particle collected from thumbprint were different from that of only A (p = 0.04202) and C (p = 0.00599720). However, the difference in the length of fluorescent particles obtained from thumbprint was not evident between B (p = 0.13024), D (p = 0.99995), and E (p = 0.91034). These results indicated that the length of fluorescent particles obtained from especially D and E has no difference from that of the thumbprint.

2.3.3.3 Comparison of the size of fluorescent particles from cellular materials deposited via friction and pressure

One-way ANOVA test was also conducted to determine if there was a difference between the lengths of fluorescent particles obtained via friction and pressure.

Results from the One-way ANOVA test (Table 6) indicated that there was no evidence (F-value = 2.575, p = 0.111) that the length of fluorescent particle obtained through friction was different (n = 100) from that obtained through pressure (n = 50).

Table 6: Raw data from One Way Anova analysis generated by RStudio for comparing length of fluorescent particles obtained via friction and pressure.

```
                                        Df  Sum Sq  Mean Sq F value Pr(>F)
factor(Mode_of_deposition$Mode.of.Deposition)   1 0.00268 0.002676   2.575  0.111
Residuals                                     148 0.15382 0.001039
```

2.3.3.4 Quantification of fluorescent particles

The number of fluorescent particles on each slide in contact with the ventral and dorsal side of the scales was also quantified using ImageJ particle counting function. The total number of fluorescent particles from each slide is shown in Table 7 below. The first image of each column of each slide was excluded from the calculation of total fluorescent particle count as the brand marking of the slide interfered with the particle counting function of ImageJ.

Table 7: Table comparing total fluorescent particle counts for slides exposed to ventral surfaces and dorsal surfaces.

	Negative Control	A	B	C	D	E	Total
Ventral	11	153	78	572	202	360	1376
Dorsal	11	45	80	34	68	45	283

From Table 7, the number of fluorescent particles was seen to be lower on slides that were in contact with the dorsal side of the scales than the ventral side of the scales. As fragments of dried tissues were found attaching to the ventral side of the scales, it was therefore deduced that the presence of these dried tissues could increase the number of cellular materials being deposited on the slides.

Table 8: Table comparing total fluorescent particle counts for slides with cellular material deposited via friction and pressure.

	Negative Control	A	B	C	D	E	Total
Friction	22	11373	1896	3326	5911	4160	26688
Pressure (Ventral)	11	153	78	572	202	360	1376
Pressure (Dorsal)	11	45	80	34	68	45	283

When compared to the number of fluorescent particles deposited via friction (Table 8), fewer fluorescent particles were observed from the slides deposited via pressure, indicating that the introduction of friction would allow more cellular materials to be deposited on contact surfaces.

2.3.4 Amplification and Sequencing of DNA Isolated via Conventional PCR

2.3.4.1 Quantification of Isolated DNA using Qubit™ Fluorometer

Cellular materials deposited onto glass slides via friction were recovered using tape lifting and isolated DNA was quantified using the Qubit™ Fluorometer. Results from the Qubit™ Fluorometer were shown in Tables 9 and 10 below.

Table 9: Concentration of DNA isolated from slides with cellular materials deposited via friction.

Sample	Concentration (ng/mL)
Blank Tape	Too low to be detected
Blank Slide	0.067
Thumbprint	0.056
Scale A	0.076
Scale B	0.052
Scale C	0.056
Scale D	0.054
Scale E	0.087

Table 10: Concentration of DNA isolated from slides with cellular materials deposited via pressure.

Sample	Concentration (ng/mL)
Blank Tape	Too low to be detected
Blank Slide (Ventral)	Too low to be detected
Blank Slide (Dorsal)	Too low to be detected
Thumbprint	Too low to be detected
Scale A (Ventral)	Too low to be detected
Scale A (Dorsal)	Too low to be detected
Scale B (Ventral)	Too low to be detected
Scale B (Dorsal)	Too low to be detected
Scale C (Ventral)	Too low to be detected
Scale C (Dorsal)	0.053
Scale D (Ventral)	Too low to be detected
Scale D (Dorsal)	Too low to be detected
Scale E (Ventral)	Too low to be detected
Scale E (Dorsal)	Too low to be detected

The concentration of DNA samples recovered from slides with cellular materials deposited via friction was higher than of DNA samples obtained from slides with cellular materials deposited via pressure. To note that DNA was isolated from blank slide (table 9); this indicates that blank slides might be contaminated with human DNA or pangolin DNA as the blank slide was placed together with the other sample slides. Qubit™ Fluorometer was unable to differentiate or confirm the source of contamination at this point.

The DNA concentrations of all recovered DNA samples from slides with cellular materials deposited via pressure, except scale C (dorsal), were too low to be detected by the Qubit™ Fluorometer.

This result seems to correlate well with the total fluorescent particle counts where total fluorescent particle counts from slides with cellular materials deposited via friction was much higher than from slides with cellular materials deposited via pressure.

2.3.4.2 Species Identification of cellular materials deposited onto glass slides via friction

Conventional PCR amplifications of the DNA samples recovered from all five slides with *M. javanica* cellular material deposited via friction showed a band of approximately 350 bp, indicating that PCR amplification was successful for all slides obtained via friction (Figure 51). Extracted DNA from *M. javanica* tissue was used as a positive control and had yielded a PCR amplicon of the expected size. All negative controls, including no template control (NTC), blank tape and blank slides yielded negative PCR amplifications; this indicated that the PCR reagents, brown tapes and slides used in this experiment was free from contamination.

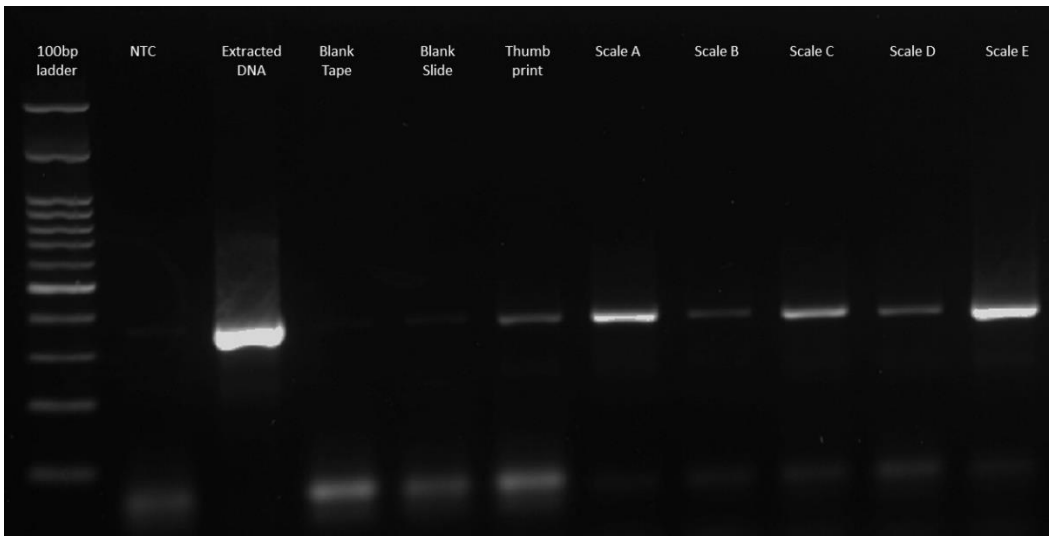

Figure 51: Image of a 1.5% gel after electrophoresis. This shows the outcome from the PCR amplification of the: no template control (NTC), *M. javanica* positive control (extracted DNA), blank tape, blank slide, thumbprint and respective slides (A – E) with *M. javanica* scales. The scales had been in contact with the slides by friction.

Positive PCR amplicons were then sequenced and subjected to BLASTn analysis. Sequence data from all slides A – E matched to the sequence from *M. javanica* reference sequences on BLASTn, with at least 98% identity, indicating that the cellular materials deposited onto these slides were indeed of *M. javanica* origins (Table 11).

Table 11: BLASTn results for DNA samples isolated from slides deposited with *M. javanica* cellular materials using friction.

Sample description	Sequence obtained	Matched description	Sequence ID	Query Cover	Identities
Thumbprint	CACCACAGGATTATTCCTAGGCATGCACTACTCACCAGACGCCTCAACCGCCTTTTCATCAATCGCCCACATCACTCGAGACGTAAATTATGGCTGAATCATCCGCTACCTTCACGCCAATGGCGCCTCAATATTCTTTATCTGCCTCTTCCTACACATCGGACGAGGCCTATATTACGGATCATTTCTCTACTCAGAAACCTGAAACATCGGCATTATCCTCCTG	*Homo sapiens* isolate NU27 haplogroup Q1 mitochondrion, complete genome	MN849543.1	100%	99.56%
Scale A	ATTCTCACAGGACTATTTCTAGCCATACACTACACAGCAGACACAACAACCGCATTCTCATCAGTAACTCACATCTGCCGAGATGTAAACTACGGATGAATTATCCGATACATACACGCTAACGGAGCTTCCCTGTTCTTCATCTGCCTATTCGCACACATCGGACGAGGCATCTACTACGGATCCTTTGCCTACAAAGAGACATGAAACATCGGTATCCTGCTCCTATTTGCAGTAA	*Manis javanica* isolate S4 cytochrome b (cyt b) gene, partial cds; mitochondrial	MW197447.1	100%	100%
Scale B	ATTCTCACAGGACTATTTCTAGCCATACACTACACAGCAGACACAACAACCGCATTCTCATCAGTAACTCACATCTGCCGAGATGTAAACTACGGATGAATTATCCGATACATACACGCTAACGGAGCTTCCCTGTTCTTCATCTGCCTATTCGCACACATCGGACGAGGCATCTACTACGGATCCTTTGCCTACAAAGAGACATGAAACATCCGGTATCCTGACTCCTAT	*Manis javanica* isolate S4 cytochrome b (cyt b) gene, partial cds; mitochondrial	MW197447.1	100%	99.13%
Scale C	TTCTCACAGGACTATTTCTAGCCATACACTACACAGCAGACACAACAACCGCATTCTCATCAGTAACTCACATCTGCCGAGATGTAAACTACGGATGAATTATCCGATACATACACGCTAACGGAGCTTCCCTGTTCTTCATCTGCCTATTCGCACACATCGGACGAGGCATCTACTACGGATCCTTTGCCTACAAAGAGACATGAAACATCGGTATCCTGCTCCTATTTGCAGTAATAGCA	*Manis javanica* isolate S4 cytochrome b (cyt b) gene, partial cds; mitochondrial	MW197447.1	100%	100%
Scale D	TCTCACAGGACTATTTCTAGCCATACACTACACAGCAGACACAACAACCGCATTCTCATCAGTAACTCACATCTGCCGAGATGTAAACTACGGATGAATTATCCGATACATACACGCTAACGGAGCTTCCCTGTTCTTCATCTGCCTATTCGCACACATCGGACGAGGCATCTACTACGGATCCTTTGCCTACAAAGAGACATGAAACATCGGTATCCTG	*Manis javanica* isolate S4 cytochrome b (cyt b) gene, partial cds; mitochondrial	MW197447.1	100%	100%
Scale E	AATTCTCACAGGACTCTTTCTCGCCATCCACTACACAGCAGACACAACAACCGCATTCTCATCAGTAACTCACATCTGCCGAGATGTAAACTACGGATGAATTATCCGATACATACACGCTAACGGAGCTTCCCTGTTCTTCATCTGCCTATTCGCACACATCGGACGAGGCATCTACTACGGATCCTTTGCCTACAAAGAGACATGAAACATCGGTATCCTGCTCCTATTTGC	*Manis javanica* isolate S4 cytochrome b (cyt b) gene, partial cds; mitochondrial	MW197447.1	100%	98.72%

2.3.4.3 Species identification of cellular materials deposited onto glass slides via pressure

Cellular materials deposited onto glass slides via pressure were also recovered using a tape-lift and DNA was isolated from these samples.

Conventional PCR amplifications of the DNA samples from three out of five slides in contact with the dorsal surface of the *M. javanica* scales showed a band of approximately 350 bp. Similarly, three out of five slides in contact with the ventral surface of the *M. javanica* scales showed a band of approximately 350 bp (Figure 52). Extracted DNA from *M. javanica* tissue and thumbprint was used as a positive control and both had yielded positive PCR amplifications. All negative controls including no template control (NTC), and blank slide (dorsal – top) yielded negative PCR amplifications, indicating that the PCR reagents, brown tapes, and slides used in this experiment were free from contamination. Blank slide (ventral) yielded a very faint band; however, this PCR amplicon cannot be sequenced successfully.

All positive PCR amplicons were then sequenced and subject to BLASTn analysis. Sequence data from all six DNA samples matched to the sequences from *M. javanica* reference sequences on BLASTn, with at least 99% identity, indicating that the cellular materials deposited onto these slides were indeed of *M. javanica* origins (Table 12).

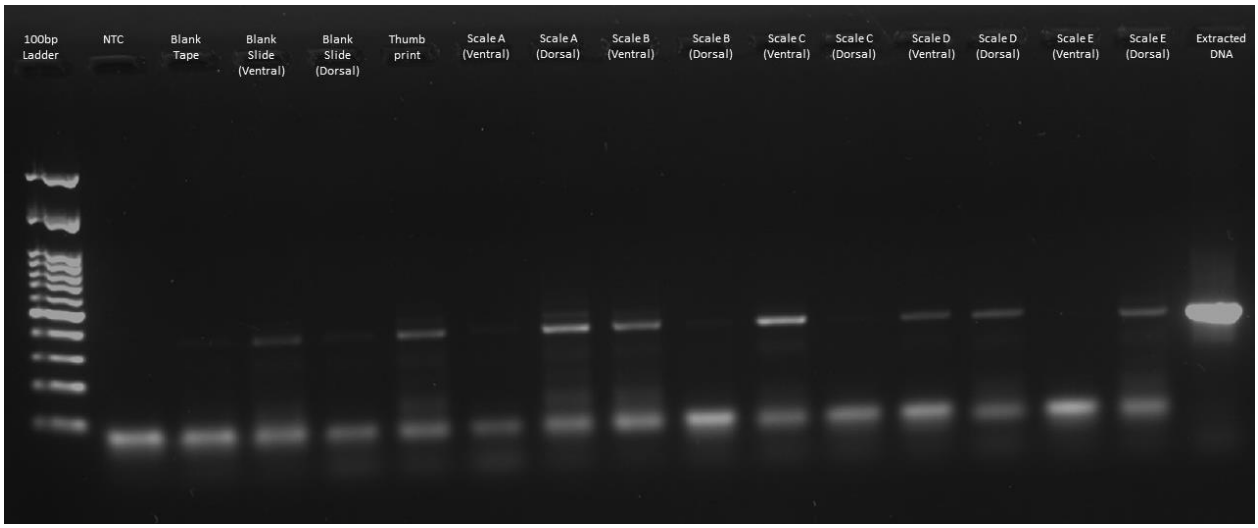

Figure 52: Image of a 1.5% gel after electrophoresis. This shows the outcome of the PCR amplification from the: no template control (NTC), *M. javanica* positive control (Extracted DNA), blank tape, blank slide, thumbprint and respective slides (A – E) with *M. javanica* scales. The scales had been in contact with the slides via pressure.

Table 12: BLASTn results for DNA samples isolated from slides deposited with *M. javanica* cellular materials using pressure.

Sample description	Sequence obtained	Matched description	Sequence ID	Query Cover	Identities
Thumbprint	CCAAATCACCACAGGACTATTCCTAGCCATGCACTACTCACCAGACGCCTCAACCGCCTTTTCATCAATCGCCCACATCACTCGAGACGTAAATTATGGCTGAATCATCCGCTACCTTCACGCCAATGGCGCCTCAATATTCTTTATCTGCCTCTTCCTACACATCGGACGAGGCCTATATTACGGATCATTTCTCTACTCAGAAACCTGAAACATCGGCATTATCCTCCTG	*Homo sapiens* isolate MST403 mitochondrion, complete genome	OQ731990.1	100%	100%
Scale A, Dorsal	TTCTCACAGGACTATTTCTAGCCATACACTACACAGCAGACACAACAACCGCATTCTCATCAGTAACTCACATCTGCCGAGATGTAAACTACGGATGAATTATCCGATACATACACGCTAACGGAGCTTCCCTGTTCTTCATCTGCCTATTCGCACACATCGGACGAGGCATCTACTACGGATCCTTTGCCTACAAAGAGACATGAAACATCGGTATCATGCTCCTATT	*Manis javanica* isolate S2 cytochrome b (cyt b) gene, partial cds; mitochondrial	MW197445.1	100%	99.56%
Scale B, Ventral	AATTCTCACAGGACTATTTCTAGCCATACACTACACAGCAGACACAACAACCGCATTCTCATCAGTAACTCACATCTGCCGAGATGTAAACTACGGATGAATTATCCGATACATACACGCTAACGGAGCTTCCCTGTTCTTCATCTGCCTATTCGCACACATCGGACGAGGCATCTACTACGGATCCTTTGCCTACAAAGAGACATGAAACATCGGTATCCTGCTCCTAT	*Manis javanica* isolate S2 cytochrome b (cyt b) gene, partial cds; mitochondrial	MW197445.1	100%	99.56%
Scale C, Ventral	TCTCACAGGACTATTTCTAGCCATACACTACACAGCAGACACAACAACCGCATTCTCATCAGTAACTCACATCTGCCGAGATGTAAACTACGGATGAATTATCCGATACATACACGCTAACGGAGCTTCCCTGTTCTTCATCTGCCTATTCGCACACATCGGACGAGGCATCTACTACGGATCCTTTGCCTACAAAGAGACATGAAACATCGGTATCATGCT	*Manis javanica* isolate S2 cytochrome b (cyt b) gene, partial cds; mitochondrial	MW197445.1	100%	99.55%
Scale D, Ventral	CTCACAGGACTATTTCTAGCCATACACTACACAGCAGACACAACAACCGCATTCTCATCAGTAACTCACATCTGCCGAGATGTAAACTACGGATGAATTATCCGATACATACACGCTAACGGAGCTTCCCTGTTCTTCATCTGCCTATTCGCACACATCGGACGAGGCATCTACTACGGATCCTTTGCCTACAAAGAGACATGAA	*Manis javanica* isolate S2 cytochrome b (cyt b) gene, partial cds; mitochondrial	MW197445.1	100%	100%
Scale D, Dorsal	AGGAATCTGCTTAGTCCTACAAATTCTCACAGGACTATTTCTAGCCATACACTACACAGCAGACACAACAACCGCATTCTCATCAGTAACTCACATCTGCCGAGATGTAAACTACGGATGAATTATCCGATACATACACGCTAACGGAGCTTCCCTGTTCTTCATCTGCCTATTCGCACACATCGGACGAGGCATCTACTACGGATCCTTTGCCTACAAAGAGACATGAAGCACCT	*Manis javanica* isolate S2 cytochrome b (cyt b) gene, partial cds; mitochondrial	MW197445.1	97%	100%

Scale E, Dorsal	CCTACGCATTCTCACAGGACTATTTCTAGCCATACACTACACAGCAGACACAACAACCGCATTCTCATC AGTAACTCACATCTGCCGAGATGTAAACTACGGATGAATTATCCGATACATACACGCTAACGGAGCTT CCCTGTTCTTCATCTGCCTATTCGCACACATCGGACGAGGCATCTACTACGGATCCTTTGCCTACAAA GAGACATGAAACATCGGTATCCTGCTCCTATTTGCAGTAATAGCAA	*Manis javanica* isolate S2 cytochrome b (cyt b) gene, partial cds; mitochondrial	MW197445.1	100%	99.20%

Additionally, it can also be seen that the number of positive PCR amplification was lower from the DNA isolated from slides with cellular materials deposited via pressure than friction (Table 14). This could suggest that the amount of DNA isolated from slides deposited with cellular materials deposited via pressure was lower than that of friction.

Table 13: Comparison of PCR success rate between DNA isolated from cellular materials deposited by friction and pressure.

	No of samples	Positive amplicons	Success Rate
Friction	5	5	100%
Pressure (ventral)	5	3	60%
Pressure (dorsal)	5	3	60%
Total	15	11	73.33%

2.4 Discussion of results

2.4.1 The *M. javanica* Scales Used

The processing done to the pangolin scales done in this project mimicked what would have been done to the pangolin scales in the IWT. The resultant dried scales were therefore, in a form that were similar to the pangolin scales seized in an illegal wildlife consignment. Due to the extensive drying process and long-term storage (about 6 months) at room temperature prior to using the scales for this experiment, it was hypothesized that the DNA from these scales would be highly degraded. As seen in Figure 11, despite the time interval and the processing of the scales, small pieces of dried tissues could still be observed attached to the ventral surface of the scales. These pieces of dried tissues could be a better source of DNA as compared to keratinised structure of the scales itself.

The scales were also observed not to be in complete contact with the glass slides during the trial involving the deposition of DNA via pressure, due to the concave shape and hard keratinised nature of the scales. This inevitably resulted in less cellular materials deposited onto the glass slides. As this is a first study involving the visualization of cellular materials deposited by pangolin scales onto surfaces of packaging materials, we could only hypothesized that this effect would be mitigated in a real case scenario by the much larger number of pangolin scales that would be usually involved. The amount of surface area not being covered with scales would be greatly reduced as these scales would be densely packed into their packaging during transport.

2.4.2 Comparison of Fluorescent Particles Deposited by Human and *M. javanica* Scales

DD was shown to be able to stain eukaryotic cellular materials deposited by humans (Kanokwongnuwut et al., 2018a), likely through the binding to minor grooves in the backbone of

double-stranded DNA (Haines et al., 2015d). In this chapter, DD was used to stain the cellular material deposited by *M. javanica*.

Bright, green, fluorescent particles could be observed on glass slides deposited with cellular materials from *M. javanica* via friction. These stained cellular materials (Figure 18) were observed to be bigger than that of deposited by a human thumbprint – the positive staining control (Figure 16).

The length of 20 fluorescent particles were collected from each of the slide deposited with thumbprint and scale A-E via friction, so that comparison could be made. As with the visual observation, the mean length of fluorescent particle was indeed the shortest and statistical analysis showed the length of the fluorescent particles from thumbprint was shorter only than slides deposited by scale A and D, but there was no evidence to show that the length of thumbprint was different from that deposited by scale B, C and E.

The stained cellular material from deposited by *M. javanica* scales via pressure was observed to be smaller than deposited via friction – in this trial, the shortest mean fluorescent particle length was obtained from scale D, then followed by thumbprint. However, statistical analysis indicated that there was no difference between the lengths of fluorescent particles obtained via friction and pressure.

The results from this trial therefore deduced that the size of fluorescent particles deposited by pangolin scales was similar to the cellular materials deposited by humans and that the size of fluorescent particles deposited by *M. javanica* scales is not affected by the two modes of deposition studied in this experiment: friction and pressure.

2.4.3 Molecular Species Identification using DNA Isolated from the Glass Slides

2.4.3.1 DNA quantification using spectrometry

The stained cellular materials on the glass slides were recovered using tape-lifts and DNA was extracted from the tapes using a QIAamp® DNA Investigator kit. Quantification of the DNA isolated was attempted using the Qubit™ Fluorometer together with Qubit™ dsDNA HS (High Sensitivity) kit.

All the six samples, including thumbprint, from the friction trial yielded DNA concentrations of less than 0.1 ng/µL (Table 9), while 10 of the 11 samples, including thumbprint, from the pressure trial yielded DNA concentration that were too low to be measured by Qubit™ Fluorometer (Table 10). The only sample that had a reading from the pressure trial - scale C (dorsal), yielded a DNA concentration of 0.053 ng/µL. As the quantitation range for the Qubit™ dsDNA HS (High Sensitivity) kit is from 0.1 ng to 120 ng (ThermoFisherScientificInc., 2018), the Qubit™ Fluorometer was not an accurate method for quantifying DNA isolated from these trials. However, the results

did indicate that the amount of DNA isolated from the cellular materials deposited by contact with *M. javanica* scales was lower than the detection range of the Qubit™ fluorometer.

2.4.3.2 PCR Amplification and sequencing of isolated DNA

PCR amplification was conducted using a set of universal primers targeting the mammalian Cyt b region, however with a preference for pangolin species (Ewart et al., 2021). The primers were able to amplify human DNA at a 20:1 ratio (human: *M. tricuspis*).

All five DNA samples isolated from the slides deposited with *M. javanica* cellular material using friction yielded positive amplicons of *M. javanica* origin, while six out of 10 DNA samples isolated from the slides deposited with *M. javanica* cellular materials using pressure yielded positive amplicons of *M. javanica* origin (Table 13). This indicated that the cellular materials deposited on the glass slides indeed originated from the *M. javanica* scales and it also suggested that the amount of latent DNA deposited via friction was higher than via pressure.

The experiment conducted in this chapter therefore showed that pangolin scales, although highly dehydrated and stored for a long period of time, could deposit latent DNA onto the surfaces that they were in contact with, and this latent DNA could be visualised using DD. Although the latent DNA deposited were likely to be in very small amount as it could not be measured accurately using spectrometry, it was sufficient to be used for downstream molecular species identification.

Between the two modes of latent DNA deposition, friction or pressure, our results suggested that friction would likely to be the main contributor of latent pangolin scale DNA deposition in an illegal pangolin scale consignment. However, this could not be confirmed at the time of this study as more detailed trials involving a higher number of scales would have to be set up so as to minimise that effect of DNA reduction through using the same scales repeatedly. The amount of cellular materials might also be required to determine the exact amount of cellular materials dislodged from the scales after each trial, however, this may pose some technical challenges as this process was comprises of many uncontrolled factors such as strength involved in introducing friction, the thickness and exposed surface area of the dried tissues etc.

,

CHAPTER THREE: ESTABLISHMENT OF QUANTITATIVE PCR FOR THE QUANTITATION OF LATENT DNA DEPOSITED ON CONTACT SURFACES

3.1 Background

3.1.1 Types of Quantitative Polymerase Chain Reaction (qPCR)

Real-time PCR or quantitative PCR (qPCR) a well-established molecular method used for the measurement and quantification of DNA or RNA present in a sample. In a qPCR, the amount of PCR amplicons accumulated real time is monitored by measuring the change in emission of fluorescence from either fluorescent DNA-binding dyes or target-specific fluorescently labelled primers or probes added to the PCR. There are several different types of qPCR. Two of the most common qPCR techniques are the Taqman probe-based qPCR and the intercalating dye-based qPCR.

The Taqman probe-based qPCR often utilises a DNA-based probe with a fluorescent reporter dye at the 5’ end and a quencher at the 3’ end. When the reporter dye is in close proximity to the quencher, the energy from the high energy reporter dye is transferred to the low energy quencher, resulting in an diminution of the emission of the fluorescence from the reporter dye. As DNA polymerisation takes place during PCR amplification, the reporter dye is being cleaved by the 5' to 3' exonuclease activity of the *Taq* polymerase, thus breaking away from the quencher, allowing the reporter dye to emit its fluorescence signal. This fluorescence signal can then be detected by the qPCR thermocycler (Arya et al., 2005).

The intercalating dye-based qPCR typically utilises an DNA intercalating dye - SYBR Green. SYBR Green dye binds to double-stranded DNA, emitting fluorescence upon binding. As this dye intercalates with any double-stranded DNA product generated during PCR amplification, it therefore allows PCR amplicons to be detected and measured during PCR amplification.

During the initial phase of the qPCR amplification, the fluorescence signals are not detected as the signals are below the background level. As amplification progresses and the amount of PCR products increase significantly, the fluorescent signals will accumulate and increase exponentially and eventually rise above the background level (Schefe et al., 2006). The point where the fluorescence signal reaches ten-times above the standard deviation of the average signal of the background level is known as the threshold and the PCR cycle that crosses the threshold is known as the quantification cycle – Cq value. Due to PCR inhibiting factors and the limitation of PCR enzymes and reagents, the generation of PCR products will start to taper off until the PCR reaches a saturation level where the reaction no longer generates PCR products (Kubista et al., 2006).

The level of fluorescence generated during the PCR is directly proportional to the amount of amplified DNA or RNA present in the sample and the Cq is inversely proportional to the initial quantity of target DNA. By comparing the fluorescence signals to a standard curve generated using known concentrations of the target DNA or RNA, the initial amount of the target DNA or RNA can then be accurately determined (Farrell, 2017).

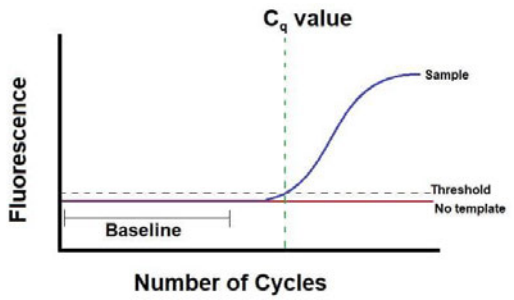

Figure 53: The threshold level and Cq value on a qPCR amplification curve. (Oswald, 2015)

3.1.2 Uses of qPCR in Wildlife Forensic Science

Being a rapid, sensitive and reliable method, qPCR has been commonly used for a wide range of molecular studies in areas including gene expression (Cicinnati et al., 2008), disease diagnostics (Davoust et al., 2014; Goncharova et al., 2021; McCartney et al., 2003; Xu et al., 2017), food safety (Heymans et al., 2018) , microbial ecology (Fey et al., 2004; Zemb et al., 2020) and forensic sciences (Fu & Allen, 2019; Funes-Huacca et al., 2011; Sauer et al., 2016) etc.

In wildlife forensic science, qPCR had been established for use in the molecular species identification of a limited number of wildlife species, such as turtles (Cardeñosa et al., 2021), elephants (Bourgeois et al., 2019; Conte et al., 2019; Wozney & Wilson, 2012) and sharks (Cardenosa et al., 2018). In these studies, qPCR was the choice of laboratory method for molecular species identification due to its short turnaround time and adaptability to be deployed on site (Cardeñosa et al., 2021; Cardenosa et al., 2018). Additionally, qPCR was also more advantageous when used on degraded samples as it was a more sensitive method compared to conventional PCR (Bourgeois et al., 2019).

3.1.3 Objectives using qPCR

The use of qPCR for species identification of pangolins is not common. For this project, a *M. javanica* specific qPCR was established for use in quantifying the amount of *M. javanica* latent DNA isolated from the samples recovered from contact surfaces.

In Chapter Two, latent DNA was isolated from the glass slides deposited with cellular materials from *M. javanica*. latent DNA from these samples was identified to be of *M. javanica* origin using conventional PCR amplifications and Sanger sequencing. An attempt to quantify the amount of

DNA extracted was made using the Qubit™ fluorometer. However, the fluorometer was unable to accurately determine the amount of DNA in the DNA samples as it was below the assay range of the equipment and reagent kit used.

This chapter describes the establishment of a qPCR to detect specifically *M. javanica* DNA in these DNA samples and to quantify the initial amount of DNA materials in the samples. As it was likely that the DNA from these samples was highly degraded due to the long exposure to heat and long-term storage at room temperature, qPCR might be also more effective in detecting *M. javanica* DNA than conventional PCR as the target DNA region was shorter than that of the conventional PCR.

3.2 Materials and Methods

3.2.1 Samples Used

Dried scales from various pangolin species were obtained from NParks, Singapore. These dried scales were part of the consignments seized by the Singapore authorities in 2019. The scales had been morphologically and molecularly identified to be from the four African species - *S. gigantea*, *S. temminckii*, *P. tricuspis*, *P. tetradactyla* by NParks and were stored at room temperature till use.

Dried tissue samples from the scale of each of the four African pangolin species as well as *M. javanica* scales from section 2.2.1 were used in this experiment. Human DNA was also extracted from a human thumbprint deposited on glass slide as described in section 2.2.3.

3.2.2 DNA Extraction from Dried Tissue Samples Using Commercial Spin Column Kit

DNA was extracted from the dried pangolin tissue samples using DNeasy® Blood & Tissue Kits (Qiagen) following manufacturer's recommendations. Approximately 15 ng of dried tissue samples were removed from one scale of each pangolin species, using a scalpel blade.

For pre-treatment, 180 µL of Buffer ATL and 20 µL of proteinase K (10 mg/mL) were added to each of the tube containing the dried tissue and mixed thoroughly. The tube was then incubated at 56°C with shaking at 900 rpm overnight to lyse the tissue. After the overnight incubation, the samples were checked to be completely lysed prior to proceeding to the next step. Subsequently, 200 µL of Buffer AL and 200 µL of ethanol (100% v/v) was added to the mixture and the mixture was then transferred to the spin column provided and then centrifuged at 6000 x g for 1 min to allow liquid to pass through the column and DNA in the liquid to bind to the column. After centrifugation, the column was transferred to a clean 2 mL collection tube for washing to remove any impurities present. The column was first washed by using 500 µL of Buffer AW1 and centrifuging at 6000 x g (8000 rpm) for 1 min. After which, the column was then placed in a clean 2 mL collection tube. Next, 500 µL of Buffer AW2 was added, and the tube was then centrifuged at 20,000 x g (14,000 rpm) for 3 min. After washing, the column was transferred to a clean 2 mL microcentrifuge tube

and DNA was eluted by adding 200 µL of Buffer AE to the column and then centrifuging at 6000 x g (8000 rpm) for 1 min. The extracted DNA samples were then quantified using NanoDrop™ One Microvolume UV-Vis Spectrophotometer (ThermoFisher Scientific Inc.). Eluted DNA samples were stored at -20°C until use.

3.2.3 Primers and Probe Design

Primers, targeting the cyt b region of the mitochrondrial DNA, were designed using the program, PrimerQuest™ Tool (Integrated DNA Technologies, Iowa, USA).

First, mitochondrial DNA sequences corresponding to the cyt b region for *S. gigantea*, *S. temminckii*, *P. tricuspis* and *M. javanica* were downloaded from the NCBI GenBank database. The downloaded sequences were aligned using Bioedit Sequence Alignment Editor version 7.2.5. A region with variable sequence information among the different species was selected visually so that the target region could be used to differentiate between the various species of pangolins.

The selected sequence region was then used to generate the primer/probe set using the PrimerQuest™ tool (Owczarzy et al., 2008) with the following parameters: a minimum and maximum PCR product size of 75 bp to 150 bp respectively, a minimum and maximum primer melting temperature of 59˚C to 65˚C and a minimum and maximum probe melting temperature of 64˚C to 72˚C.

Five sets of primers/probe were generated by the software and were screened for nonspecific binding using the online PrimerBLAST tool in NCBI database (https://www.ncbi.nlm.nih.gov/Blast.cgi). The primers/probe sets designed by the program were then visually screened for hairpin and dimer structures. The shortlisted primers/probe sets were also further screened using NCBI Primer-BLAST program to identify non-target binding. Two primer sets with no potential non-target binding were then selected and sent for synthesis by a third-party oligo-synthesis company (Integrated DNA Technologies).

3.2.3 Development and Optimisation

A synthesised DNA plasmid control, comprising of the target cyt b mitochondrial DNA fragment in a pUC57 vector, was used as a DNA standard for the qPCR in this experiment. The DNA standard was diluted to 10^9 copies per 2 µL and a standard curve comprising of serial dilutions from 10^1 to 10^6 copies were generated from serial dilutions. This standard curve was conducted in triplicates and used to determine the optimal concentration of the reagents to be used.

A linear regression curve was generated automatically by the thermocycler software - QuantStudio™ Design and Analysis Software, and the efficiency values as well as the R^2 value were determined from the linear regression curve. An optimum qPCR should generate an

efficiency value between 80% - 120% with a R^2 value of >0.98. The concentrations of primers and probe were adjusted to generate a reaction with the optimal efficiency and R^2 values.

3.2.4 Assessing the Analytical Specificity

To assess the analytical specificity of the assay, the assay was performed on DNA extracted from the scales of *M. javanica* and the four species of African pangolin species (*S. gigantea*, *S. temminckii*, *P. tricuspis* and *P. tetradactyla*) to detect any non-target binding. Human DNA extracted from a human thumbprint deposited on the glass slide was also included in this assessment to determine the specificity of the primers/probe set as human DNA contamination was common in wildlife product due to human manipulation during the processing of the products.

3.2.5 Assessing the Repeatability and Reproducibility

To assess the repeatability and reproducibility of the assay, qPCR assay was performed on the serial dilutions of the DNA standard in section 3.2.3 on three different runs, each of the dilutions were repeated three times during each run.

The mean, standard deviations and repeatability coefficient was then calculated to determine the repeatability of the assay. The differences between Cq values obtained within each run and Cq values obtained inter-run were evaluated using one way ANOVA analysis to determine the reproducibility of the assay.

3.2.5 qPCR Amplification

qPCR was conducted on Quantstudio 3 real-time PCR system (ThermoFisher Scientific), in a 20 µL reaction volume using 1 x Applied Biosystems™ TaqMan™ Fast Advanced Master Mix (ThermoFisher Scientific), 0.1 µM of each forward and reverse primer, 0.05 µM of MGB probe and 2 µL of DNA samples. The reactions conditions used for all reactions were as follows: 2 min activation at 95°C, followed by 40 cycles of 15 sec at 95°C, and 45 sec at 56°C. Analysis of run data were performed using the thermocycler software - QuantStudio™ Design and Analysis Software.

A standard curve as detailed in section 3.2.3 was generated with every run in order to assess the run quality and quantify the copies number of initial DNA template.

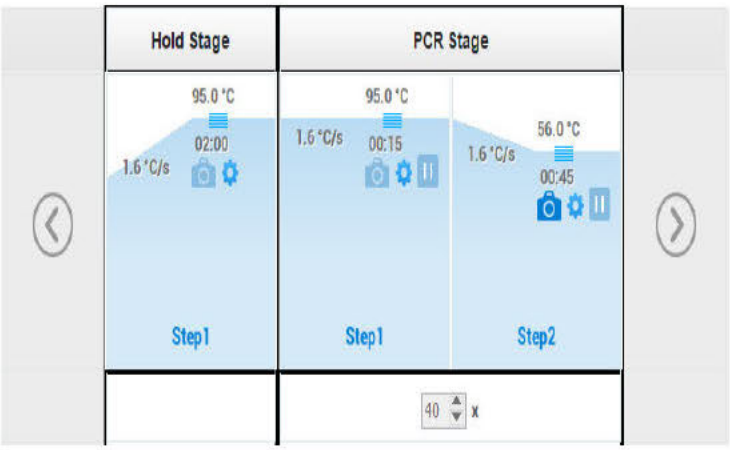

Figure 54: Picture of the qPCR conditions from the thermocycler.

3.3 Results

3.3.1 Primers and Probe Design

Two primers/probe sets were selected from the five primers/probe sets generated by the the PrimerQuest™ Tool. It can be seen from Table 14 that the melting temperature (Tm) of the forward and reverse primers in both sets were similar to each other and the Tm of respective probes was slightly higher than its respective primers set. This indicated that the primers and probe within each particular set were compatible to be used together in a single assay. The sizes of the target amplicons for both sets ranged from 110 – 120 bp, which was shorter than that of a conventional PCR and therefore would ensure that the assay would have an advantage of higher PCR efficiency. It was also anticipated that the latent DNA samples would be degraded and hence, it would also be more advantageous for a shorter target region.

Table 14: Details of 2 selected primers and probe sets.

Primer / Probe name	Type	Sequence (5'-3')	Length (bp)	Tm (°C)	GC %	Amplicon Size (bp)	Hairpin Tm (°C)
Sunda2502AF	Forward Primer	CTCGGTAGACAAAGCAACTCTC	22	62.306	50		
	Probe	CGCTCTTCACTTCATCCTTCCCTTCG	26	67.916	53.846		-14.6
Sunda2502AR	Reverse Primer	TTGGATCCGGTTTCGTGTAAG	21	62.317	47.619		13.8
	Product	CTCGGTAGACAAAGCAACTCTCACTCGATTCTTCGCTCTTCACTTCATCCTTCCCTTCGTAATTCTTGCCTTAGTACTAGTACACTTACTATTCTTACACGAAACCGGATCCAA				114	

Sunda2502BF	Forward Primer	CCTGCTCCTGTTTGCAGTAA	20	62.376	50		45.5
	Probe	AGGACGTATCCCATAAAGGCTGTTGC	26	67.999	50		42.6
Sunda2502BR	Reverse Primer	CGATGTAGGGTATTGCGGATAAA	23	62.316	43.478		13.1
	Product	CCTGCTCCTGTTTGCAGTAATAGCAACAGCCTTTATGGGATACGTCCTACCATGAGGACAAATGTCCTTCTGAGGTGCTACAGTAATTACAAACCTTTTATCCGCAATACCCTACATCG				119	

3.3.2 Preliminary Assessment of Primer sets: Determination of Annealing Temperature

Two sets of primers and probe - Sunda 2502A and Sunda 2502B, targeting the cyt b region of the *M. javanica* mitochrondrial DNA were synthesised, and a suitable annealing temperature for each of the primers and probe sets was first determined using a conventional PCR, without the inclusion of a probe. The annealing temperatures tested ranged from 52°C to 58°C.

Primers set Sunda2502A was shown to be able to amplify human DNA at all annealing temperatures tested and therefore, might not be suitable this experiment (Figure 55). Whereas the primers set Sunda2502B was shown not to amplify human DNA at 52°C and 56°C (Figure 56). As 56°C was closer to the melting points of the forward and reverse primers, 56°C was selected to be used to optimise the qPCR assay.

Do note that PCR amplification for human DNA had fail to amplify as the reaction mix dried up in ther thermocycler due defective reaction tubes. Conventational PCR was not repeated as human DNA was already amplifying with a strong band at the lower temperature. Further validation would be conducted using qPCR.

Do also note that contamination was observed in No Template Control (NTC) for reactions conducted using 56°C. Reaction would be repeated using conventional PCR in Figure 57 and qPCR for confirmation.

Figure 55: Assessing optimal annealing temperature for primers Sunda2502A. Electrophoresis of a 1.5% agarose gel shows the PCR products from human, *M. javanica* and no template control (NTC).

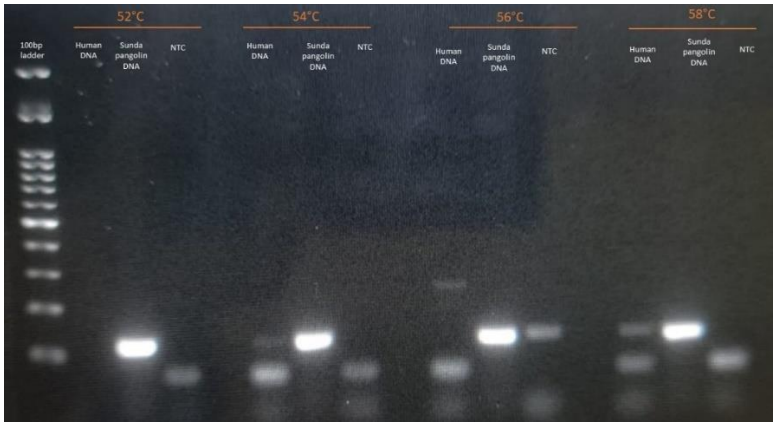

Figure 56: Assessing optimal annealing temperature for primers Sunda2502B. Electrophoresis of a 1.5% agarose gel showed PCR products from human, *M. javanica* and no template control (NTC).

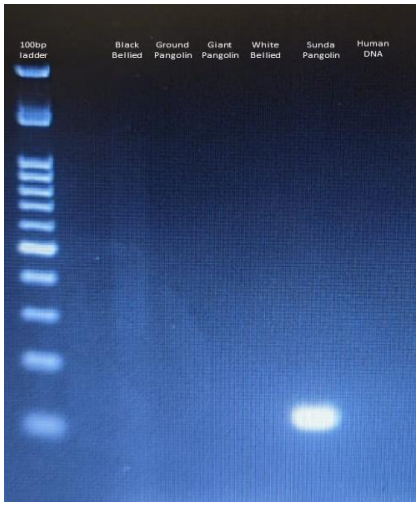

Figure 57: Assessing specificity of primer set Sunda2502B at 56°C. 1.5% gel electrophoresis showing PCR products from human, *M. javanica* and no template control (NTC).

The primer set, Sunda2502B, was also further assessed to determine if it would be able to amplify DNA from other African Pangolin species at the selected annealing temperature of 56°C. From Figure 57, it showed that Sunda2502B only amplified *M. javanica* DNA.

3.3.3 Determination of Analytical Specificity of Primer and Probe set

The cross reactivity of the primers and probe sets - Sunda 2502A and Sunda 2502B, with other pangolin species and human DNA were determined using qPCR. Figures 58 and 59 show the amplification plots of the qPCR assays conducted using Sunda 2502A and Sunda 2502B respectively. Figure 58 shows that Sunda2502A primers/probe set was amplifying human DNA, together with *M. javanica* DNA. In contrast, Sunda2502B primers/probe set was amplifying specifically only *M. javanica* (Figure 59).

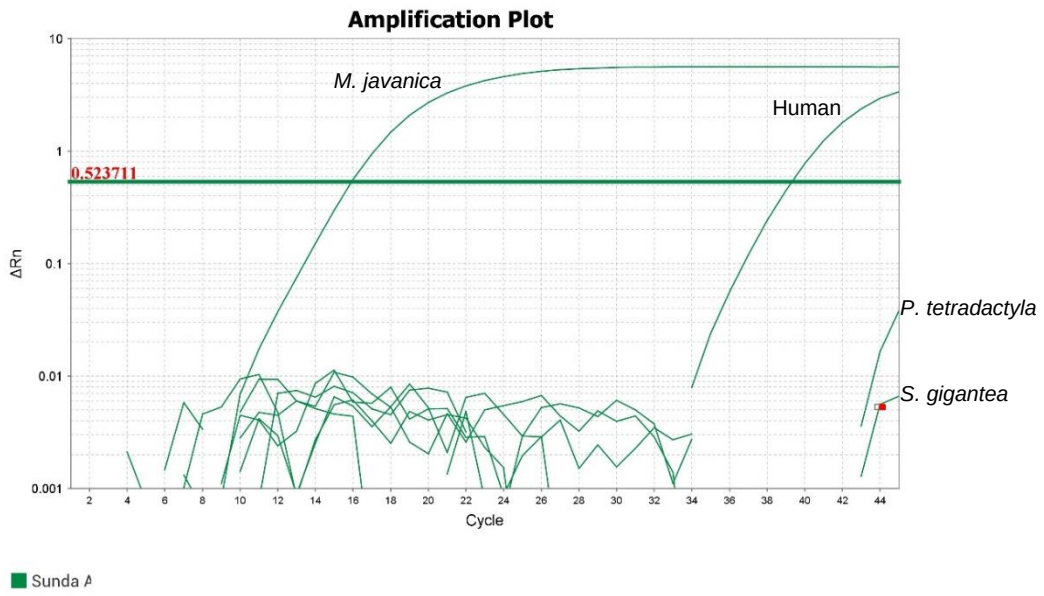

Figure 58: Amplification plot for assessing analytical specificity of Sunda2502A primers and probe set, using DNA from *M. javanica*, *S. gigantea*, *S. temminckii*, *P. tricuspis*, *P. tetradactyla* and human.

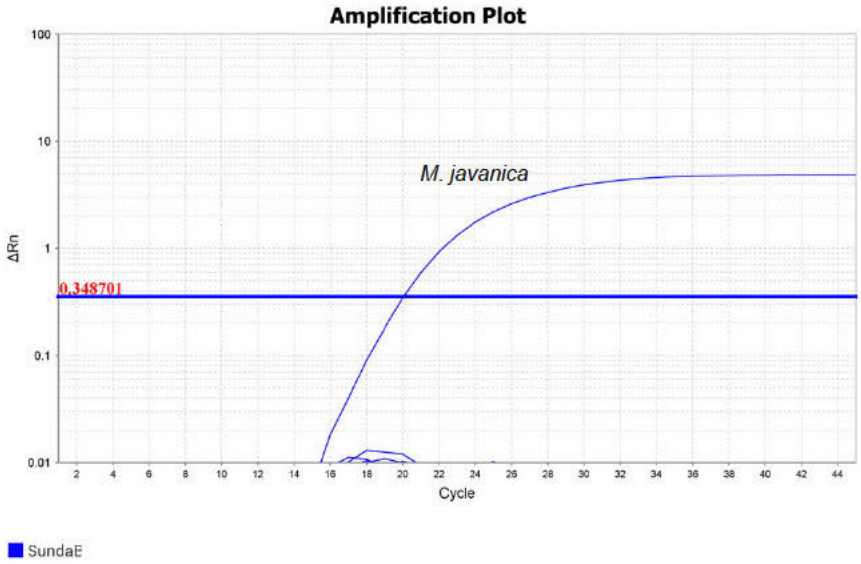

Figure 59: Amplification plot for assessing analytical specificity of Sunda2502B primers and probe set, using DNA from *M. javanica*, *S. gigantea*, *S. temminckii*, *P. tricuspis*, *P. tetradactyla* and human.

3.3.4 Assay Optimization

An optimal concentration of Sunda2502B primers and probes were then determined using primers concentrations ranging from 0.5 µM to 0.1 µM and probe concentrations ranging from 0.25 µM to 0.05 µM. Table 15 below showed the primers and probes concentrations and their respective efficiency % and R^2 value obtained. From the values obtained, the optimal concentration of primers and probe to be used was determined to be 0.1 µM for each primer and 0.05 µM for the probe as the efficiency value obtained was between 80% - 120% with a R^2 value of >0.98.

Table 15: Efficiency % and R^2 values obtained for respective primers and probes concentrations.

Primer concentration (µM)	Probe concentration (µM)	Efficiency (%)	R^2 values
0.5	0.25	120.344	0.985
0.3	0.15	120.793	0.984
0.2	0.10	113.625	0.991
0.1	0.05	105.413	0.994

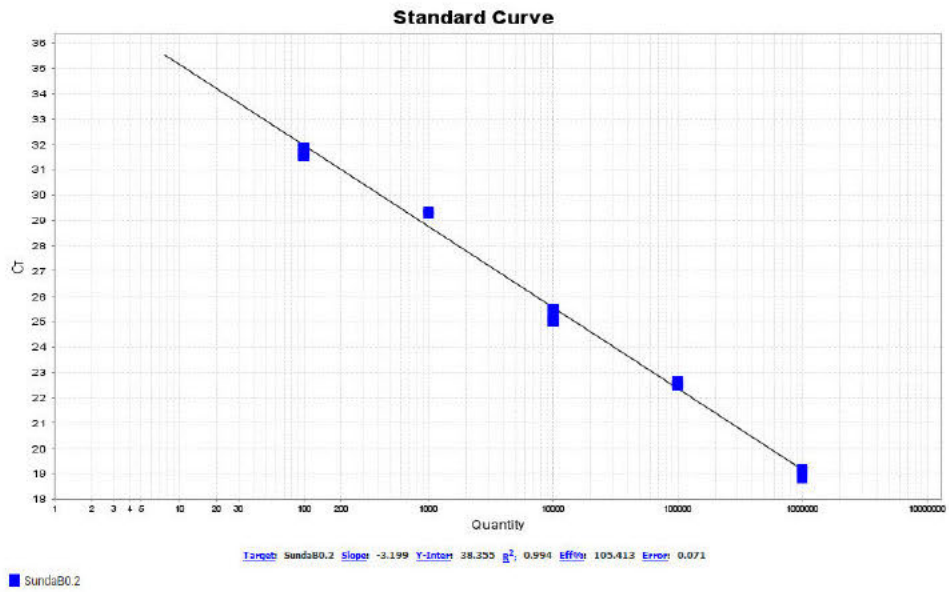

Figure 60: Standard curve obtained using 0.1µM primers + 0.05µM probe.

3.3.5 Determination of Repeatability and Reproducibility of qPCR Assay

Cq values of each dilution of the DNA standard, ranging from 10^1 to 10^6 were obtained over three different runs and during each run, triplicates were performed for each dilution. Cq values for each reaction and their respective calculated values are detailed in Table 16 below.

Table 16:Cq value for each reaction of each diluted DNA standards. Each dilution of the DNA standard was tested over three runs and triplicates were performed for each run. The Cq values were obtained and the respective mean, sample standard deviation (SD), pooled SD, repeatability coefficient and P-value were calculated and shown in the table.

DNA standard: 10 copies								
	Replicate per run			**Mean**	**SD**	**Pooled SD**	**Repeatability Coefficient**	**P-value**
Run no.	**1**	**2**	**3**					
1	37.131	37.759	37.640	37.510	0.334	0.159	0.439	0.832
2	36.867	36.599	35.921	36.462	0.488			
3	36.867	36.778	36.664	36.770	0.102			
DNA standard: 100 copies								
	Replicate per run			**Mean**	**SD**	**Pooled SD**	**Repeatability Coefficient**	**P-value**
Run	**1**	**2**	**3**					
1	35.224	34.270	34.664	34.719	0.479	0.050	0.139	0.724
2	33.368	34.280	33.388	33.679	0.521			
3	34.777	35.562	35.039	35.126	0.400			
DNA standard: 1,000 copies								
	Replicate per run			**Mean**	**SD**	**Pooled SD**	**Repeatability Coefficient**	**P-value**
Run	**1**	**2**	**3**					
1	31.825	31.448	31.649	31.641	0.189	0.034	0.094	0.999
2	29.294	29.564	29.709	29.522	0.211			
3	31.278	31.444	31.188	31.303	0.130			

DNA standard: 10,000 copies								
	Replicate per run			**Mean**	**SD**	**Pooled SD**	**Repeatability Coefficient**	**P-value**
Run	**1**	**2**	**3**					
1	27.952	27.908	27.857	27.906	0.048	0.034	0.095	1.000
2	26.329	26.258	26.212	26.266	0.059			
3	28.450	28.606	28.698	28.585	0.125			
DNA standard: 100,000 copies								
	Replicate per run			**Mean**	**SD**	**Pooled SD**	**Repeatability Coefficient**	**P-value**
Run	**1**	**2**	**3**					
1	25.276	25.965	25.831	25.691	0.365	0.155	0.429	0.580
2	24.573	24.609	24.733	24.638	0.084			
3	24.602	24.764	25.441	24.936	0.445			
DNA standard: 1,000,000 copies								
	Replicate per run			**Mean**	**SD**	**Pooled SD**	**Repeatability Coefficient**	**P-value**
Run	**1**	**2**	**3**					
1	22.536	22.542	22.572	22.550	0.019	0.021	0.059	0.990
2	21.257	21.358	21.360	21.325	0.059			
3	20.902	20.996	21.035	20.978	0.068			

The repeatability for each dilution obtained was less than 0.5, indicating that the assay was repeatable within each run. Using the one-way ANOVA, P-value obtained for all the dilutions were >0.1, indicating that there was no difference between the results obtained from over three runs and the results obtained within a single run. This showed that results from the qPCR assay established were reproducible.

3.4 Discussion

3.4.1 The Selected Primers and Probe Set

Based on the results obtained, the primers and probe set, Sunda2502B was found to be suitable for use in the qPCR assay to specifically detect *M. javanica* cyt b mitochondrial DNA, generating an amplicon length of 119 bp. The optimal primers and probe concentration to be used was determined to be 0.1 µM of each of the forward and reverse primers together with 0.05 µM MGB probe. The annealing location of the probe (Figure 61) was also suitable for use as it was as close to the forward primer as possible without overlapping (Smith & Osborn, 2009).

Sequence 1 Assay Set 4 Details

BACK TO RESULTS

Parameter Set: RT-qPCR (Primers with Probe)
Sequence Name: Sequence 1
Amplicon Length: 119

		Start	Stop	Length	Tm	GC%
Forward	CCTGCTCCTGTTTGCAGTAA (Sense)	88	108	20	62	50
Probe	AGGACGTATCCCATAAAGGCTGTTGC (AntiSense)	110	136	26	68	50
Reverse	CGATGTAGGGTATTGCGGATAAA (AntiSense)	184	207	23	62	43.5

Base	Sequence
1	CCTGTTCTTCATCTGCCTATTCGCACACATCGGACGAGGCATCTACTACGGATCCTTTGCCTACAAAGAGACATGAAACATCGGTATCCTGCTCCTGTTT
101	GCAGTAATAGCAACAGCCTTTATGGGATACGTCCTACCATGAGGACAAATGTCCTTCTGAGGTGCTACAGTAATTACAAACCTTTTATCCGCAATACCCT
201	ACATCGGGTCTAGCCTAGTAGAGTGAGTCTGAGGGGGATTCTCGGTAGACAAAGCAACTCTCACTCGATTCTTCGCTCTTCACTTCATCCTTCCCTTCGT
301	AATTCTTGCCTTAGTACTAGTACACTTACTATTCTTACACGAAACCGGATCCAACAACCCAATAGGAATCGTATCCAACCCCGACGTAATCCCCTTCCAC
401	CCATACTACACAGCCAAGGACACCCTTGGCCTATTCATCATGCTCACAGCACTAATATCCTTAGCCCTATTCTTCCCCGACCTACTAGGAGACCCAGACA
501	ATTATACACCCGCAAACCCCCTAAACACACCACCCCACATCAAACCAGAATGGTACTTCCTATTCGCATACGCAATCCTACGCTCAATTCCCAACAAATT
601	GGGAGGGGTACTAGCACTAATCCTATCCATCCTCGTACTAGCACTAATCCCACTACTACACACATCAAAACAACGAACTATGATGTTCCGACCCCTGAGC
701	CAAACCATCTTCTGACTCCTGGTGGCCGACCTACTAGTTCTCACATGAATCGGAGGAC

Figure 61: Screenshot from PrimerQuest™ tool showing the binding locations of the selected primers/ probe set, Sunda2502B.

3.4.2 Analytical Specificity of the Assay

In this experiment, the analytical specificity of the qPCR was determined using DNA extracted from *M. javanica*, *S. gigantea*, *S. temminckii*, *P. tricuspis*, *P. tetradactyla* and human thumbprint. It was shown that the selected primer and probe set – Sunda2502B was able to detect *M. javanica* DNA, but not DNA from the four African pangolins and human DNA. Although it was not possible to obtain DNA from the other three species of Asian pangolins, the Sunda2502B primer and probe set was also analysed using the NCBI PrimerBLAST program to detect any non-target binding. The results from the program indicated that the probe might be able to bind non-specifically to the antlion (*Myrmeleon* sp.) and the reverse primer may be able to bind non-specifically to the large headed rice rat (*Hylaeamys megacephalus*). However, as the forward primer did not return with any nonspecific match, it was therefore not possible for the qPCR to non-specifically bind to other mammals when they were used as a set.

3.4.3 Repeatability and Reproducibility of the Assay

The repeatability of the assay was determined using a synthesised DNA standard diluted from 10^1 to 10^6 copies; three replicates of each serial dilution was performed, and the repeatability coefficient for each of the dilution showed that the assay was repeatable, indicating that the results from each replicate did not vary within the run.

Cq values of each dilution over three runs were also analysed using the one-way ANOVA and the results ($p = >0.5$) for all the dilutions ($n = 9$) indicated that there was no difference between results obtained from over three runs and the results obtained within a single run, and hence, the assay was reproducible.

It was also noted that only three runs and three replicates in each run were performed. The repeatability coefficients for dilutions of 10 copies and 100,000 copies were very close to 0.5. The P-value obtained for the dilution of 100,000 copies was also very close to 0.5; more replicates and more runs will be able to improve these values.

3.4.4 Summary of Discussion

The results from this chapter showed that a qPCR specific to the detection of a *M. javanica* cyt b mitochondrial DNA has been developed and tested. Using the primers and MGB probe set – Sunda2502B, at a concentration of 0.1 and 0.05 µM respectively, the Cq values obtained indicated that the qPCR assay established was able to detect *M. javanica* specifically and results obtained were repeatable and reproducible. The established assay could therefore be used reliably in this project for the quantification of *M. javanica* latent DNA.

qPCR is not commonly used for the species identification of pangolins. However, qPCR was shown to be a more rapid molecular species identification method compared to a conventional PCR method. Additionally, due to the shorter target DNA region, qPCR will be a more sensitive method to be used for degraded samples that are frequently encountered in illegal wildlife trade.

CHAPTER FOUR: COMPARISON OF DNA RECOVERY AND EXTRACTION METHODS FOR USE TO DETECT PANGOLIN LATENT DNA DEPOSITED ON GLASS SLIDES

4.1 Background

4.1.1 DNA Recovery Methods Used in Forensic Sciences

The optimal DNA recovery method to be used for recovering latent or touch DNA is highly dependent on the type of surfaces involved. Various methods have been applied to recover touch or latent DNA from surfaces, including cutting (Sewell et al., 2008), swabbing and tape-lifting. Swabbing and tape – lifting will be discussed in the following section.

4.1.1.1 Swabbing techniques

DNA recovery using the swabbing technique can be conducted by using a dry swab, a wet swab or a combination of wet swab followed by a dry swab (as known as double swabbing). The dry swabbing technique involved the use of a dry swab consists of a bud made of usually cotton, rayon, polyester or calcium alginate with a shaft usually made of wood, plastic or wire. (Hansson et al., 2009) to recover DNA from surfaces directly. Wet swabbing requires the dry swab to be moistened with sterile water or buffer prior to being used (Hartless et al., 2019) while double swab techniques involved using first a wet swab followed by a dry swab to recover the DNA deposited on surfaces (Sweet et al., 1997). Studies have shown that the quality and quantity of the DNA recovered can be affected by various factors such as the type of target biological samples, the type of contact surfaces, the type of swabs used, the swabbing techniques used as well as the downstream extraction process (Alketbi & Goodwin, 2019; Bruijns et al., 2018; Hartless et al., 2019).

The optimal type of swabs to be used had been widely studied. While some studies have shown that nylon swabs performed the best in recovering DNA (Bruijns et al., 2018; Comte et al., 2019), there are also studies showing that cotton swabs are more effective in DNA recovery (Comment et al., 2023; Verdon et al., 2014b). Some studies even demonstrated that there were no difference in the effectiveness of both cotton and nylon swabs (Wood et al., 2017). It was also reported that swabs of foam composition were more suitable for recovering DNA from rough or porous surfaces while swabs of polyester or cotton materials were more effective to be used for recovering DNA from smoother surfaces (Hartless et al., 2019). And therefore, it remains debatable on which type of swabs is the most effective for DNA recovery and the choice of swabs to be used for DNA recovery depends greatly on the various factors mentioned above.

Double swabbing was introduced in 1997 by Sweet et al. and was reported to be more effective than wet swabbing by various studies (Castella & Mangin, 2008; Hess & Haas, 2017; Sweet et al., 1997). The double swabbing technique entails the swabbing contact surface first using a wet

swab and then swabbing the same contact area again using a dry swab to absorb any excess liquid that has been left behind by the wet swabbing. Although double swabbing was able to recover more DNA than a single wet swab, it has also been deduced that most of the DNA from a non – porous surface will have been recovered using the first wet swab.Therefore, the application of the second dry swab, , it might be too excessive, leading to an increase of workload, even if it is able to slight increase the DNA recovery rate (Hedman et al., 2020).

4.1.1.2 Tape – lifting technique

Tape-lifting had been reported to be more effective in recovering DNA from fabric materials as compared to swabbing (Hansson et al., 2009; Hess & Haas, 2017; Verdon et al., 2014a) and can be applied more easily to fabric materials as compared to other methods (Hess & Haas, 2017). The different types of adhesive tapes to be used in tape-lifting had also been studied. A study conducted by Vendon *et al*. showed that the quantity of DNA recovered could be affected by the stickiness of the tape and hence, the stickier the adhesive tape, the more effective it was in recovering the DNA from surface. Additionally, it also shown that a loss in adhesion might result in a loss of effectiveness in DNA removal and hence, tape-lifting might not be suitable for recovering from surfaces that would cause the adhesive on the tape to be lost, such as flannelette (due to its easily removed fibres) (Verdon et al., 2014a). Again, this study also demonstrated that the optimal DNA recovery method to be used for recovering latent or touch DNA is highly dependent on the type of surfaces involved.

A wider range of adhesive tapes to be used for tape-lifting was also studied by Kanokwongnuwaut *et al.* where it was shown that the off the shelf brown packing tape and clear adhesive tape were more effective in recovering DNA than forensic crime scene sampling tape (Kanokwongnuwut et al., 2020b). Although the off-the shelf tapes were not DNA free, the adhesive properties of these off the shelf tapes were more effective than the forensically used tapes.

The selection of the DNA extraction method used for isolating the latent DNA from the swabs and tapes had also been shown to affect the quantity of DNA recovered (Joël et al., 2015) and hence, it is also important to determine the appropriate DNA extraction method to be applied to the swab or tape used for latent DNA recovery.

4.1.2 Objectives for Comparison of DNA Recovery and Extraction Methods

The objective of this experiment is to determine the optimised workflow for recovering latent DNA deposited on glass slides which maximises the quantity of the latent DNA isolated. Two commonly used DNA recovery method, tape-lifting and swabbing were selected as they are generally easy to obtain and handle. Two DNA extraction methods were also tested in this experiment – a solid phase DNA extraction method and alkaline lysis DNA extraction method. The commercial spin column extraction kit, QIAamp® DNA Investigator kit (Qiagen) was tested as it was a DNA extraction kit intended for forensic casework with a wide variety of in-house protocols for handling

various sample types. The alkaline lysis DNA extraction method was a cheap and relatively easy and convenient method to use for extracting DNA.

4.2 Materials and Methods

4.2.1 Samples Used

The scales used in this experiment were the same dried *M. javanica* scales as detailed in section 2.2.1. Cellular materials from these five scales were deposited onto their respective glass slides via friction as detailed in section 2.2.3.1.

A total of three sets of glass slides with *M. javanica* cellular materials were generated for this experiment. Cellular materials from each of the five pieces of *M. javanica* scales (section 2.2.1.2) were deposited onto two respective glass slides via friction, generating a total of 10 slides with *M. javanica* cellular materials for each set. Two clean slides and two slides with thumbprints were also included into each set as negative control and positive staining control respectively. Cellular materials were recovered from the slides using either swabbing or tape-lifting technique. Two sets of swabs bearing the recovered cellular materials were subjected to commercial spin column extraction and alkaline lysis extraction respectively while each piece of the tape obtained from tape-lifting was divided into two portions, each measuring 10mm x 5mm. One portion of the tape was subjected to commercial spin column extraction and the other portion to be subjected to alkaline lysis extraction. Figure 62 below depicts the processes that each set was subjected to.

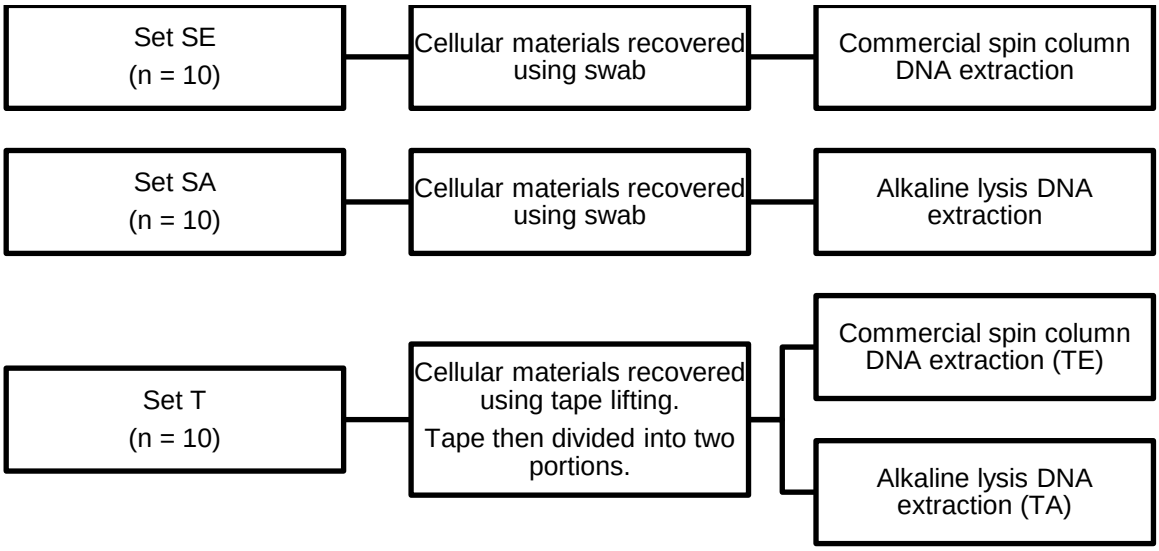

Figure 62: Flowchart illustrating the downstream processes that each set of slides were subjected to. Set SE denotes sample set was subjected to swabbing followed by commercial spin column extraction; set SA denotes sample set was subjected to swabbing followed by alkaline lysis extraction; Set T denotes sample set was subjected to swabbing; TE denotes sample set was subjected to tape – lifting followed by commercial spin column extraction and, TA denotes sample set was subjected to tape – lifting followed by alkaline lysis extraction.

4.2.2 Staining and Visualisation of Latent DNA Deposited on Glass Slides Using Diamond™ Nuclei Acid Dye

A working stock of 20x DD (Promega Corporation, Madison, USA) was prepared by diluting 10,000x DD in 75% ethanol (v/v). The working stock was stored at 4°C for up to 7 days.

From the solution of 20x DD, 20 µL was pipetted onto each slide and spread evenly across the slide using a pipette tip to ensure that the dye covered the entire surface of the slide evenly. The stained surfaces were then examined after at least 30 sec, using the Dino-Lite digital microscope (AnMo Electronics Corporation) under blue light (480 nm) and at 50x magnification. Each slide was examined at 3 different fields spread evenly across middle of each slide, as shown in Figure 63. Images of fluorescent staining were recorded using the software, Dino-Capture 2.0.

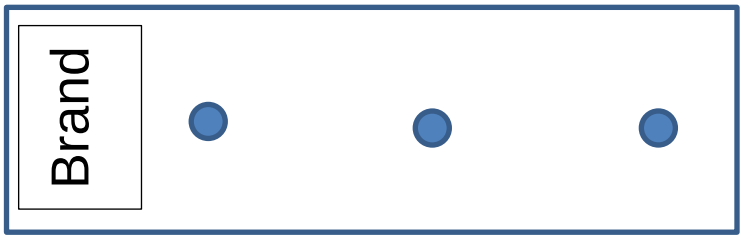

Figure 63: Illustration of the positions where the fluorescence was imaged across the glass slides. Each dot indicated where 1 image was taken using the Dino-Lite digital microscope. A total of three fields were taken for each slide.

4.2.3 Quantification of Fluorescent Particles using ImageJ Software

The number of fluorescent particles in each image were quantified using ImageJ software (Schneider et al., 2012). Each of the images to be analysed were first converted into 8-bit images and then an auto-threshold, Maximum Entropy threshold algorithm, was applied to the image before quantifying the number of particles using the ImageJ software. The numbers of fluorescent particles counted from the three images from each slide were then totalled to generate a total representative fluorescent particle count (TRFP).

4.2.4 Latent DNA Recovery

Latent DNA deposited on the various substrates was recovered using a tape-lift or nylon flocked swab as detailed below.

4.2.4.1 Latent DNA Recovery from Glass Slides Using Tape Lifting

Cellular material containing latent DNA deposited on the glass slides was recovered by tape-lifting. Brown adhesive packing tape was for tape-lifting in this project. Tape sections of approximately 10 mm x 10 mm were used for recovering DNA deposited on the glass slides, as per previously reported (Kanokwongnuwut et al., 2020b). Each piece of tape was pressed and lifted over each slide 20 times. After tape-lifting, the tape was examined under the digital microscope to detect the presence of green, fluorescent spots, which was an indication that cellular material had been successfully lifted onto the tape (Kanokwongnuwut et al., 2020b).

4.2.4.2 Latent DNA Recovery from Glass Slides Using Swabbing

Regular nylon flocked swabs (FLOQswabs®, Copan Diagnostic Inc) were used to recover DNA from the glass slides. Each swab was first moistened with 10 µL of nuclease free water (1st BASE) and then used to wipe over the entire area of the respective glass slide first latitudinally across, followed by longitudinally across. Each swab was then placed into an empty a 2 mL microcentrifuge tube prior to DNA extraction.

4.2.5 DNA Extraction

DNA extraction from the brown adhesive tapes or swabs was performed using a commercial spin column DNA extraction kit or alkaline lysis extraction method.

4.2.5.1 DNA Extraction from Tapes Using Commercial Spin Column DNA Extraction Kit

A piece of 10 mm x 5 mm of tape was cut out from the tape using a sterile scalpel blade and placed in a 1.5 mL microcentrifuge tube. 300 µL of Buffer ATL was then added to the tube containing the tape and was incubated at 85°C with shaking at 900 rpm for 30 min to dissolve the adhesive found on the tape. After incubation, the tube was allowed to cool to room temperature in order not to inactivate the proteinase K to be added in the next step.

Next, 20 µL of proteinase K (10 mg/mL) was added, mixed thoroughly and further incubated at 56°C with shaking at 900 rpm for at least 1hr to allow for digestion to occur. After the 1hr incubation, 300 µL of Buffer AL was added and incubated at 70°C with shaking at 900 rpm for 10 min. After the 10 min incubation, ethanol (100% v/v) (150 µL) was added to the mixture. The solution, excluding the tape, was then transferred to the spin column provided with the test kit and centrifuged at 6000 x g for 1 min to allow liquid to pass through the column and DNA in the liquid to bind to the column. After centrifugation, the column was transferred to a clean 2 mL collection tube for washing to remove any impurities present. The supernatant was discarded.

The column was first washed by adding 500 µL of Buffer AW1 to it and centrifuging at 6000 x g (8000 rpm) for 1 min. After the centrifugation, the column was then placed in a clean 2 mL collection tube. A second wash was then performed by adding 700 µL of Buffer AW2. The tube was then centrifuged at 6000 x g (8000 rpm) for 1 min. After the centrifugation, the column was then transferred in another clean 2 mL collection tube, and 700 µL of absolute ethanol was added and centrifuged at 6000 x g (8000 rpm) for 1 min. The column was then placed in a clean 2 mL collection tube and dried by centrifuging at 20,000 x g for 3 min. To ensure that the membrane of the column had dried completely, the column was at 56°C for 3 min with lid open. Lastly, DNA was eluted with 30 µL of Buffer ATE. Eluted DNA was stored at -20°C until use.

4.2.5.2 DNA Extraction from Swabs Using Commercial Spin Column DNA Extraction Kit

DNA was extracted from the nylon flocked swabs using QIAamp® DNA Investigator kit (Qiagen) following manufacturer's recommendations.

The swab was removed from the shaft and placed into a 2 mL microcentrifuge tube. For the pre-treatment, 400 µL of Buffer ATL and 20 µL of proteinase K (10 mg/mL) was added to the tube. The tube was then incubated at 56°C with shaking at 900 rpm for at least 1hr. After incubation, 400 µL of Buffer AL was added and incubated at 70°C with shaking at 900 rpm for 10 min. Lastly, 200 µL of absolute ethanol was added to the mixture.

The solution was then transferred to the column provided in the test kit and centrifuged at 6000 x g for 1 min to allow DNA to bind to the column. After centrifugation, the column was transferred to a clean 2 mL collection tube. The column was first washed by adding 500 µL of Buffer AW1 and centrifuging at 6000 x g (8000 rpm) for 1 min. After which, the column was then placed in a clean 2 mL collection tube. Next, 700 µL of Buffer AW2 was added, and the tube was centrifuged at 6000 x g (8000 rpm) for 1 min. After washing, the column was transferred in a clean 2 mL collection tube and 700 µL of absolute ethanol was added and centrifuged at 6000 x g (8000 rpm) for 1 min. The column was then placed in a clean 2 mL collection tube and dried by centrifuging at 20,000 x g for 3 min. To ensure that the membrane of the column had dried completely, the column was at 56°C for 3 min with lid open. Lastly, DNA was eluted with 50 µL of Buffer ATE. Eluted DNA was stored at -20°C until use.

4.2.5.3 DNA Extraction from Tapes Using Alkaline Lysis Method

Tape measuring approximately 10 mm x 5 mm was cut out using a sterile scalpel blade for alkaline lysis extraction and placed in a 0.5 mL microtube. Briefly, 50 µL of alkaline lysis solution containing 0.025 M sodium hydroxide and 0.2 mM ethylene-diamine-tetra-acetic acid (EDTA), was added. The tube was then incubated at 85°C for 30 min. After incubation, the tube was allowed to cool down to room temperature and 50 µL of neutralising buffer, containing 0.04 M Tris-hydrochloride, was added to neutralise the alkaline lysis buffer. This solution was then subsequently used as the sample template in PCR amplifications.

4.2.5.4 DNA Extraction from Swabs Using Alkaline Lysis Method

The swabs used in section 4.2.3.2 was cut out using a sterile scissors for alkaline lysis extraction and placed in a 0.5 mL microtube. Briefly, 150 µL of alkaline lysis solution containing 0.025 M sodium hydroxide and 0.2 mM ethylene-diamine-tetra-acetic acid (EDTA), was added. The tube was then incubated at 85°C for 30 min. After incubation, the tube was allowed to cool down to room temperature and 150 µL of neutralising buffer, containing 0.04 M Tris-hydrochloride, was added to neutralise the alkaline lysis buffer. This solution was then subsequently used as the sample template in PCR amplifications.

4.2.6 DNA Amplification

The Cyt b region of the *M. javanica* mitochondrial DNA was amplified using conventional PCR for molecular species identification or qPCR for the quantification of the *M. javanica* mitochondrial DNA as detailed below.

4.2.6.1 Conventional PCR

Conventional PCR was conducted as described in section 2.2.8, with 5 µL of respective DNA template used in each reaction. Extracted DNA from *M. javanica* fresh tissue was used as a positive control in each PCR and a no template control was included in each PCR.

4.2.6.2 qPCR

qPCR was conducted as described in section 3.2.5 with 2 µL of respective DNA template used in each reaction. Extracted DNA from *M. javanica* fresh tissue was used as a positive control in each PCR and a no template control was included in each PCR.

A DNA standard curve was included in every run. A synthesised DNA plasmid control, comprising of the target cyt b mitochondrial DNA fragment in a pUC57 vector, was used as the DNA standard. The DNA standard was diluted to 10^9 copies per 2 µL and a standard curve comprising of serial dilutions from 10^1 to 10^6 copies was generated from serial dilutions. This standard curve was conducted in triplicates and used for the quantification of the starting DNA template.

4.3 Results

4.3.1 Visualisation of Latent DNA on Glass Slides

DD was used to visualize cellular materials that might be deposited by the *M. javanica* scales on the glass slides. The negative control slide (Figure 64) was observed to be devoid of any fluorescence staining indicating that there was no background contamination and the slide used did not auto fluorescent. The positive staining control showed that DD had stained the cellular materials deposited by human thumbprint and the fluorescence could be detected at 50x magnificent.

All slides which had been subjected to friction with *M. javanica* scales A – E (Figure 66 – 70) showed positive fluorescent staining when observed under the digital fluorescent microscope. The fluorescent particles were observed from left, centre, and right side of the slides, with no obvious difference in degree of fluorescence, suggesting that cellular materials were deposited evenly across the slide when the scales were slide across the slide. The amount of fluorescent particles deposited also appeared to be somewhat similar between all five scales

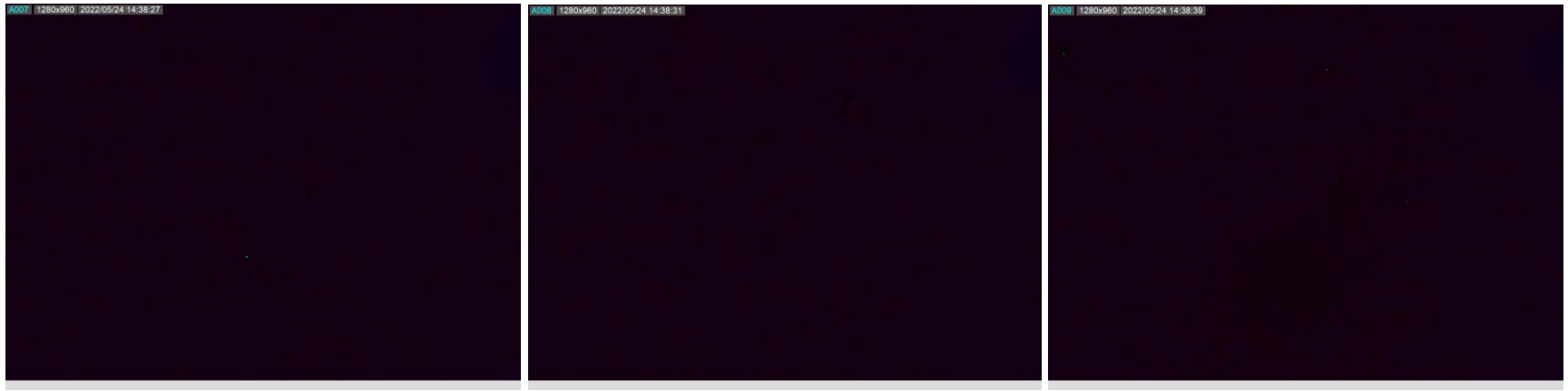

Figure 64: Images showing fluorescence staining of one of the clean slides (Negative control – N2) at 50x magnification. From left to right: - left of slide, centre of slide and right of slide.

Figure 65: Images showing fluorescence staining of one of the slides deposited with thumbprint (Positive staining control – T2) at 50x magnification. From left to right: - left of slide, centre of slide and right of slide.

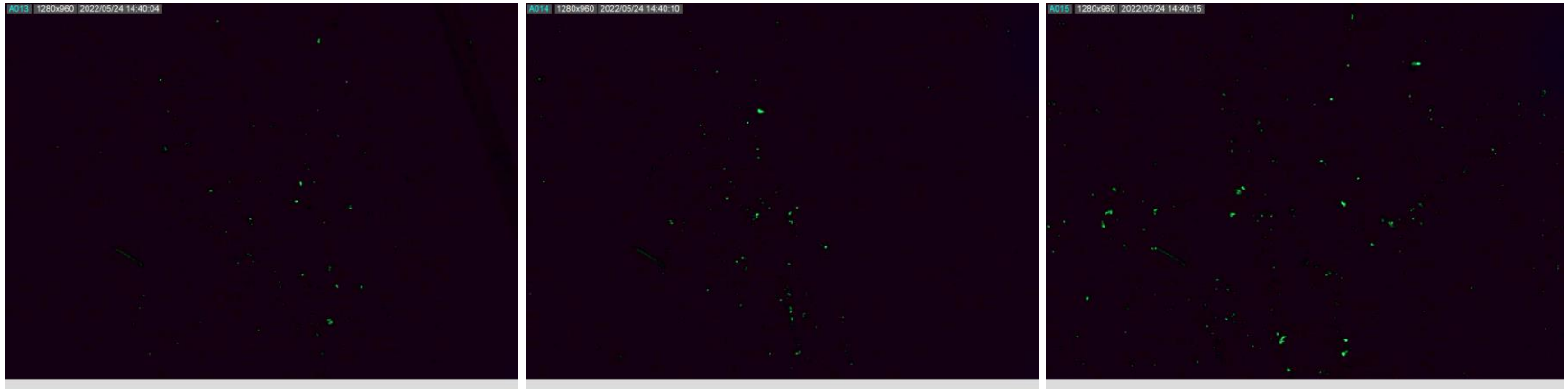

Figure 66: Images showing fluorescence staining of one of the slides deposited with *M. javanica* scale A (A1) at 50x magnification. From left to right: - left of slide, centre of slide and right of slide.

Figure 67: Images showing fluorescence staining of one of the slides deposited with *M. javanica* scale B (B1) at 50x magnification. From left to right: - left of slide, centre of slide and right of slide.

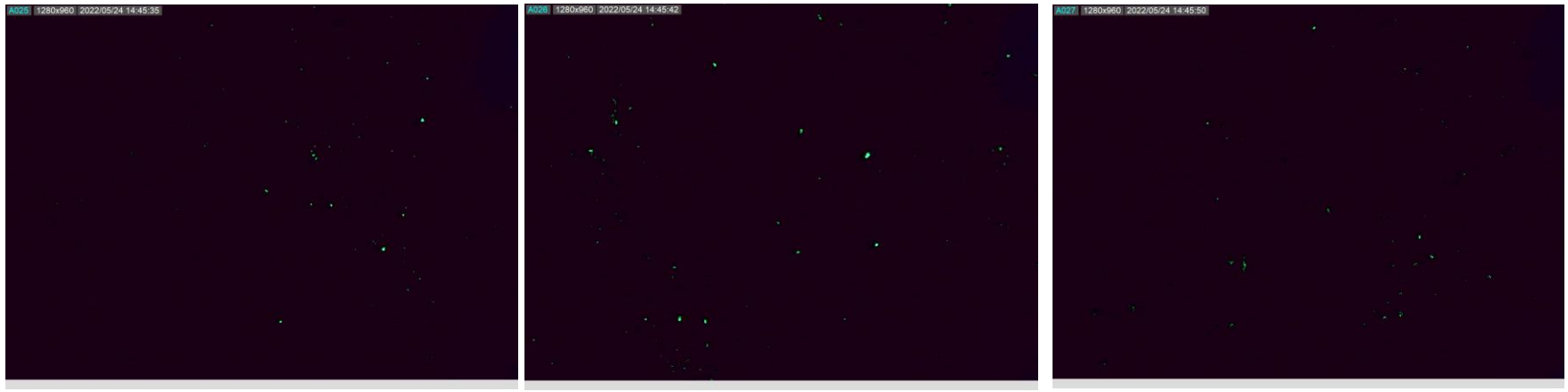

Figure 68: Images showing fluorescence staining of one of the slides deposited with *M. javanica* scale C (C1) at 50x magnification. From left to right: - left of slide, centre of slide and right of slide.

Figure 69: Images showing fluorescence staining of one of the slides deposited with *M. javanica* scale D (D1) at 50x magnification. From left to right: - left of slide, centre of slide and right of slide.

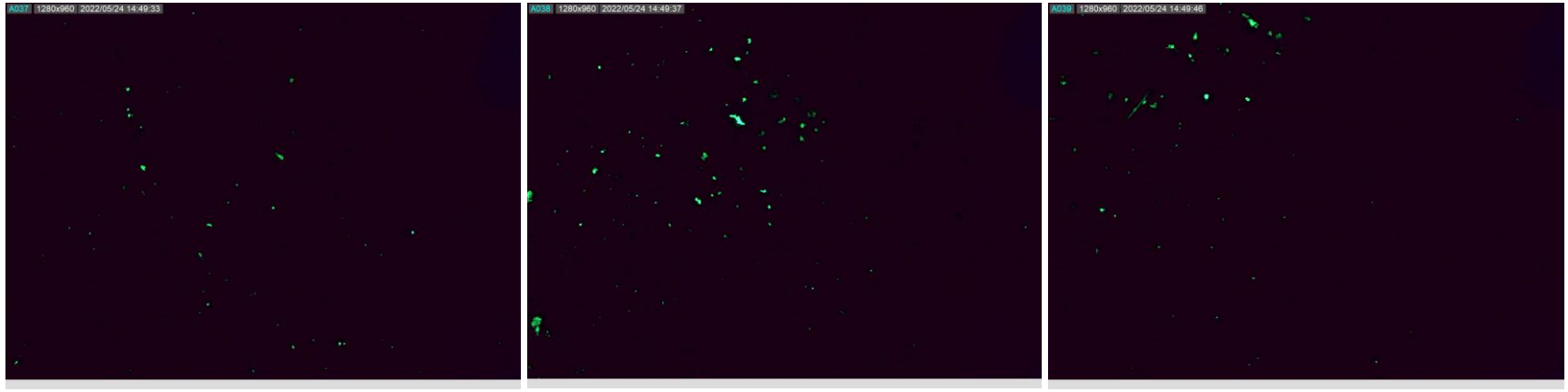

Figure 70: Images showing fluorescence staining of one of the slides deposited with *M. javanica* scale E (E1) at 50x magnification. From left to right: - left of slide, centre of slide and right of slide.

Table 17: Table showing fluorescent particle count obtained from each image for set SE (Swab, followed by spin column extraction): N1 and N2 – Negative control; T1 and T2 – human thumbprint; A1 and A2 – scale A, B1 and B2 – Scale B, C1 and C2 – Scale C; D1 and D2 – Scale D; and E1 and E2 – Scale E.

	N1	N2	T1	T2	A1	A2	B1	B2	C1	C2	D1	D2	E1	E2	Mean
Left	1	0	43	44	56	127	34	11	71	108	60	65	73	50	65.5
Centre	0	1	98	90	75	613	12	9	99	149	8	35	125	81	120.6
Right	3	3	34	64	158	248	11	10	61	235	38	73	83	289	120.6
Total	4	4	175	198	289	988	57	30	231	492	106	173	281	420	

Table 18: Table showing fluorescent particle count obtained from each image for set SA (swab followed by alkaline lysis extraction): N1 and N2 – Negative control; T1 and T2 – human thumbprint; A1 and A2 – scale A, B1 and B2 – Scale B, C1 and C2 – Scale C; D1 and D2 – Scale D; and E1 and E2 – Scale E.

	N1	N2	T1	T2	A1	A2	B1	B2	C1	C2	D1	D2	E1	E2	Mean
Left	3	0	46	83	473	71	726	2454	902	3027	149	110	613	748	927.3
Centre	4	0	370	278	214	533	1146	4288	1643	5669	182	288	216	2521	1670
Right	4	3	161	278	355	379	149	566	913	3141	314	1452	366	639	827.4
Total	11	3	577	639	1042	983	2021	7308	3458	11837	645	1850	1195	3908	

Table 19: Table showing fluorescent particle count obtained from each image for set T (tape – lift): N1 and N2 – Negative control; T1 and T2 – human thumbprint; A1 and A2 – scale A, B1 and B2 – Scale B, C1 and C2 – Scale C; D1 and D2 – Scale D; and E1 and E2 – Scale E.

	N1	N2	T1	T2	A1	A2	B1	B2	C1	C2	D1	D2	E1	E2	Mean
Left	1	0	7	62	199	1738	91	97	299	114	40	75	212	139	300.4
Centre	0	2	56	289	144	1234	35	46	155	4	27	136	493	54	232.8
Right	0	0	31	16	229	760	21	160	194	142	318	206	429	84	254.3
Total	1	2	94	367	572	3732	147	303	648	260	385	417	1134	277	

4.3.2 Distribution of Cellular Particles Deposited on Glass Slides

The number of fluorescent particles seen on each image were counted using ImageJ and are displayed in Table 17 (set SE), 18 (set SA), and 19 (set T). These fluorescent particle counts were plotted into a boxplot according to their position on the slide within the set (Set SA, SE or T, see figure 71). From figure 71, it can be seen that set SA had the greatest number of cellular materials deposited onto it.

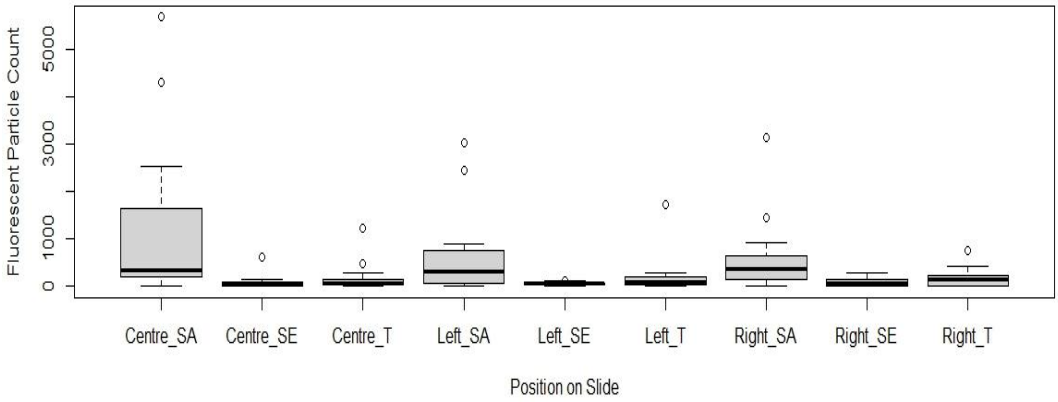

Figure 71: Box plot showing the 25%, 50% and 75% quantiles of the length of the fluorescent particles from the representative image of the slides deposited with *M. javanica* cellular particles (n = 10 for each position). SA: set subjected to swabbing then alkaline lysis DNA extraction, SE: set subjected to swabbing then commercial spin column DNA extraction and T: set subjected to tape-lifting.

One-way ANOVA test was also conducted to determine if there was a difference between fluorescent particle count obtained at each position. Results from the One-way ANOVA test (Table 20) indicated that there was evidence (F-value = 3.92, $p > 0.001$) that the fluorescent particle count obtained for each position from each set of the slides was different (n = 10).

A Tukey post-hoc test was then conducted to determine pairwise relationship between each position from each set of slides. From the pairwise comparison, there was evidence to indicate that fluorescent particle counts from the centre of the set SA were higher ($p < 0.01$) than that from all three positions of set SE and set T (Table 21, highlighted in yellow). However, there was no evidence to show that there was a difference in the fluorescent particle count from each of the position within a set ($p > 0.1$). These results showed that the centre position of set SA had the highest number of fluorescent particles even though that all three sets were subjected to similar conditions. The results also suggested that the cellular

materials were deposited evenly across the slides via friction as there was no difference in fluorescent particle count between each position with a set.

Table 20: Raw data from One way ANOVA analysis generated by Rstudio for the analysis of fluorescent particle counts from each position of the glass slides.

```
> summary(anova_PC)

                                Df   Sum Sq Mean Sq F value   Pr(>F)
factor(PC_slides_4.2$Position)   8 17493013 2186627    3.92 0.000391 ***
Residuals                      117 65261991  557795
---
Signif. codes:  0 ‘***’ 0.001 ‘**’ 0.01 ‘*’ 0.05 ‘.’ 0.1 ‘ ’ 1
```

Table 21: Raw data from Tukey post-hoc test generated by Rstudio, comparing the fluorescent particle counts obtained from each position of the glass slide. Portions highlighted in yellow indicated that there is statistical difference.

```
> TukeyHSD(anova_PC)

  Tukey multiple comparisons of means
    95% family-wise confidence level

Fit: aov(formula = PC_slides_4.2$Count ~ factor(PC_slides_4.2$Position))

$`factor(PC_slides_4.2$Position)`
                          diff        lwr       upr     p adj
Centre_SE-Centre_SA -1139.785714 -2031.9991 -247.5723 0.0030207
Centre_T-Centre_SA  -1048.357143 -1940.5706 -156.1437 0.0092315
Left_SA-Centre_SA    -567.642857 -1459.8563  324.5706 0.5390713
Left_SE-Centre_SA   -1186.357143 -2078.5706 -294.1437 0.0016562
Left_T-Centre_SA    -1019.857143 -1912.0706 -127.6437 0.0128404
Right_SA-Centre_SA   -616.571429 -1508.7849  275.6420 0.4227989
Right_SE-Centre_SA  -1145.857143 -2038.0706 -253.6437 0.0027964
Right_T-Centre_SA   -1054.428571 -1946.6420 -162.2151 0.0085948
Centre_T-Centre_SE     91.428571  -800.7849  983.6420 0.9999962
Left_SA-Centre_SE     572.142857  -320.0706 1464.3563 0.5281424
Left_SE-Centre_SE     -46.571429  -938.7849  845.6420 1.0000000
Left_T-Centre_SE      119.928571  -772.2849 1012.1420 0.9999691
Right_SA-Centre_SE    523.214286  -368.9991 1415.4277 0.6465967
Right_SE-Centre_SE     -6.071429  -898.2849  886.1420 1.0000000
Right_T-Centre_SE      85.357143  -806.8563  977.5706 0.9999978
Left_SA-Centre_T      480.714286  -411.4991 1372.9277 0.7435646
Left_SE-Centre_T     -138.000000 -1030.2134  754.2134 0.9999096
Left_T-Centre_T        28.500000  -863.7134  920.7134 1.0000000
Right_SA-Centre_T     431.785714  -460.4277 1323.9991 0.8393229
Right_SE-Centre_T     -97.500000  -989.7134  794.7134 0.9999938
Right_T-Centre_T       -6.071429  -898.2849  886.1420 1.0000000
Left_SE-Left_SA      -618.714286 -1510.9277  273.4991 0.4179004
Left_T-Left_SA       -452.214286 -1344.4277  439.9991 0.8019100
Right_SA-Left_SA      -48.928571  -941.1420  843.2849 1.0000000
Right_SE-Left_SA     -578.214286 -1470.4277  313.9991 0.5134391
Right_T-Left_SA      -486.785714 -1378.9991  405.4277 0.7303380
Left_T-Left_SE        166.500000  -725.7134 1058.7134 0.9996298
Right_SA-Left_SE      569.785714  -322.4277 1461.9991 0.5338644
Right_SE-Left_SE       40.500000  -851.7134  932.7134 1.0000000
Right_T-Left_SE       131.928571  -760.2849 1024.1420 0.9999358
Right_SA-Left_T       403.285714  -488.9277 1295.4991 0.8844893
Right_SE-Left_T      -126.000000 -1018.2134  766.2134 0.9999548
Right_T-Left_T        -34.571429  -926.7849  857.6420 1.0000000
Right_SE-Right_SA    -529.285714 -1421.4991  362.9277 0.6320977
Right_T-Right_SA     -437.857143 -1330.0706  454.3563 0.8286236
Right_T-Right_SE       91.428571  -800.7849  983.6420 0.9999962
```

4.3.3 Comparison of Latent DNA Recovery and Extraction Methods using Conventional PCR

DNA templates obtained via different combinations of DNA recovery and extraction methods were subjected to conventional PCR amplification and samples showing detectable amplicons were sequenced. Figures 72 – 75 show the 1.5% gel electrophoresis outcome of DNA samples subjected to four different combinations of DNA recovery methods and extraction methods: (a) swab with commercial spin column extraction kit, (b) swab with alkaline lysis extraction, (c) tape lift with commercial spin column extraction kit and (d) tape with alkaline lysis extraction. PCR amplification results were summarised in Table 22.

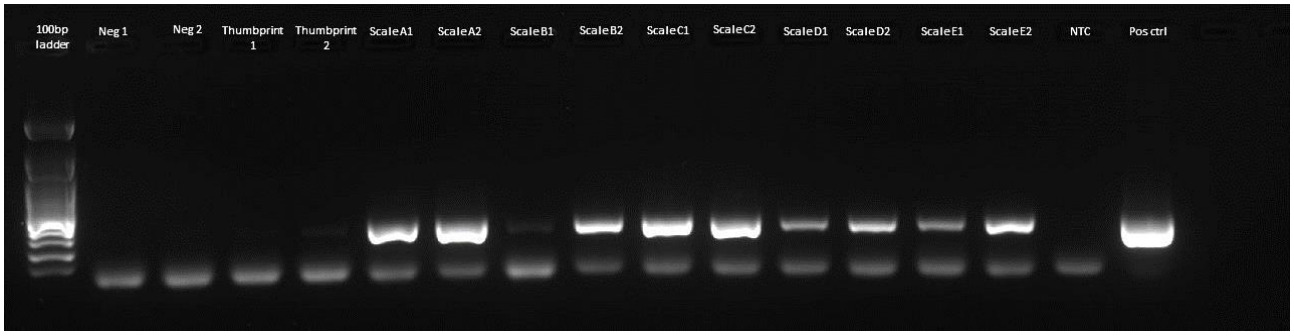

Figure 72: Image of a 1.5% gel after electrophoresis showing the outcome from the PCR amplification. The samples are: no template control (NTC), *M. javanica* positive control (extracted DNA), blank tape, blank slide (N1 and N2), thumbprint and respective slides (A – E) with M. *javanica* scales. The scales had been in contact with the slides by friction, recovered using *swabs* and DNA extracted using *commercial spin column kit*.

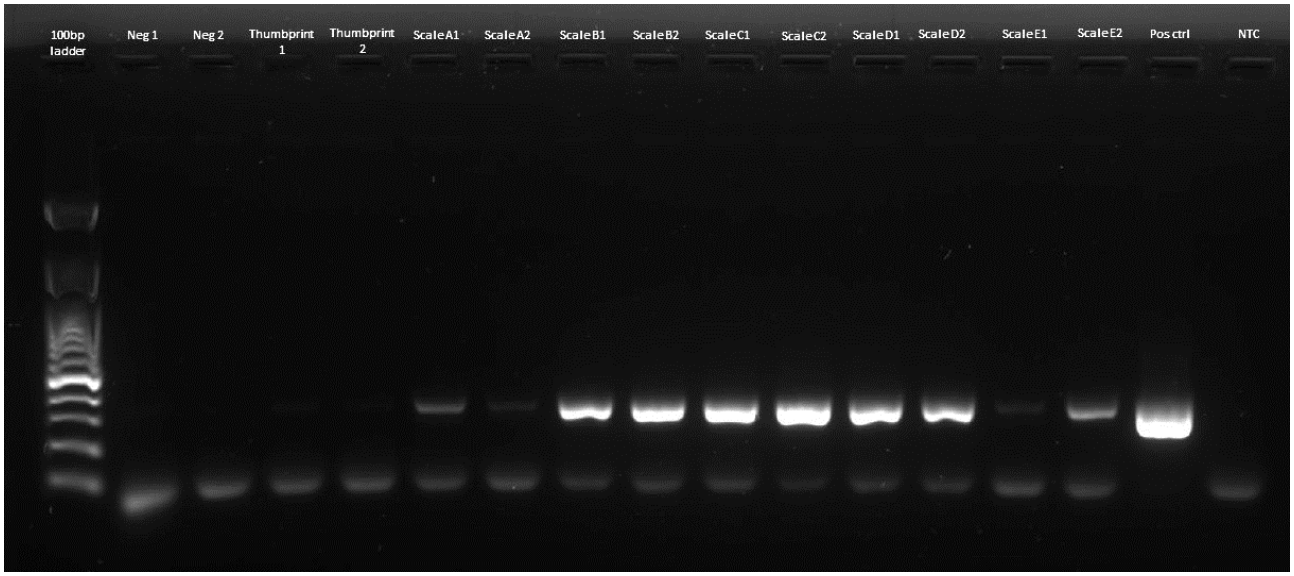

Figure 73: Image of a 1.5% gel after electrophoresis showing outcome from the PCR amplification. The samples are: no template control (NTC), *M. javanica* positive control (extracted DNA), blank tape, blank slide (N1 and N2), thumbprint and respective slides (A – E)

with M. *javanica* scales. The scales had been in contact with the slides by friction, recovered using *swabs* and DNA extracted using *alkaline lysis extraction method*.

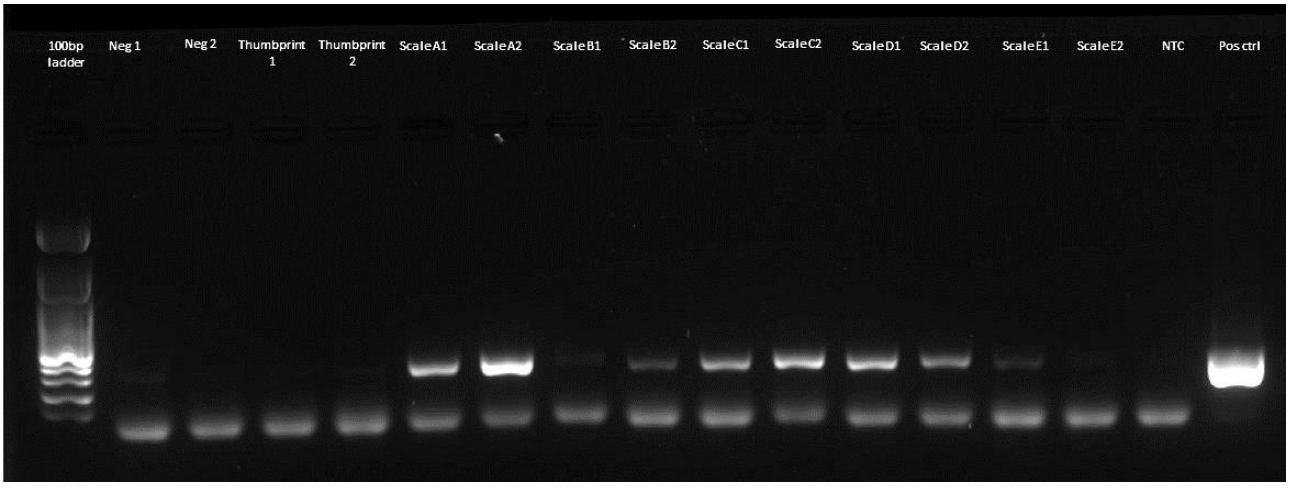

Figure 74: Image of a 1.5% gel after electrophoresis showing outcome from the PCR amplification. The samples are: no template control (NTC), *M. javanica* positive control (extracted DNA), blank tape, blank slide (N1 and N2), thumbprint and respective slides (A – E) with *M. javanica* scales. The scales had been in contact with the slides by friction, recovered using *tape lifting* and DNA extracted using *commercial spin column kit*.

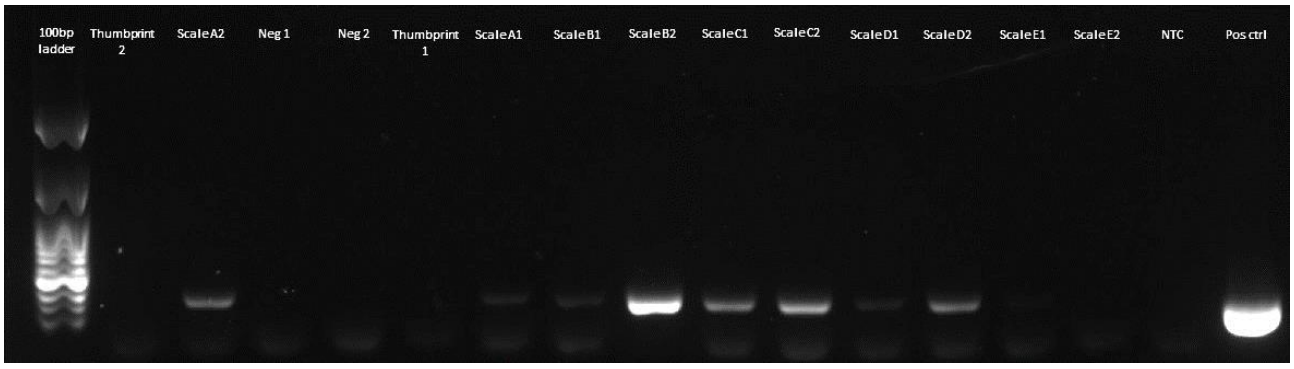

Figure 75: Image of a 1.5% gel after electrophoresis, showing outcome from the PCR amplification. The samples are: no template control (NTC), *M. javanica* positive control (extracted DNA), blank tape, blank slide (N1 and N2), thumbprint and respective slides (A – E) with *M. javanica* scales. The scales had been in contact with the slides by friction, recovered using *tape lifting* and DNA extracted using *alkaline lysis extraction method*.

Table 22: Table summarising the total number of positive amplifications for DNA samples arising from various combinations (N = 10 for each combination).

	Commercial spin column	Alkaline lysis	Total
Swab	10	10	20
Tape lift	9	8	17
Total	19	18	

From Table 22, it can be seen that out of the 20 DNA samples that were recovered using swabbing, all 20 samples yielded positive PCR amplifications, while out of the 20 DNA samples that were recovered using tape-lifting, only 17 samples yielded positive amplifications, suggesting that swabbing might be a better DNA recovery method for use in this scenario. The number of positive amplifications yielded for DNA samples isolated using commercial spin column kit and alkaline lysis extraction method were 19 and 18 respectively, suggesting that both DNA extraction methods were effective in producing satisfactory DNA samples for conventional PCR amplifictions.

4.3.4 Comparison of Latent DNA Recovery and Extraction Methods using qPCR

Copy numbers (CN) of the DNA samples were extrapolated using the standard curve results run on the same qPCR. Table 23 below showed the CN obtained from each sample. The CN obtained for each DNA sample was also plotted into a boxplot based on the respective combinations of DNA recovery and DNA extraction methods used (Figure 76). From Figure 76, it can be seen that DNA samples obtained from swabs had higher CN than that of DNA samples obtained from tapes.

Table 23: Copy numbers obtained for respective DNA samples using various DNA recovery and extraction methods.

	DNA recovery, DNA extraction method			
	Swab, Spin column	Swab, Alkaline lysis	Tape, Spin column	Tape, Alkaline lysis
A1	51,563	1,455	5,122	13,988
A2	144,569	572	20,003	12,837
B1	1,395	9,074	637	1,731
B2	14,170	48,505	1,297	12,503
C1	44,525	31,979	4,737	6,779
C2	79,109	83,908	9,041	6,977
D1	11,708	11,388	10,196	3,978
D2	15,299	11,869	4,456	3,736
E1	5,679	1,326	948	373
E2	27,509	3,867	350	145

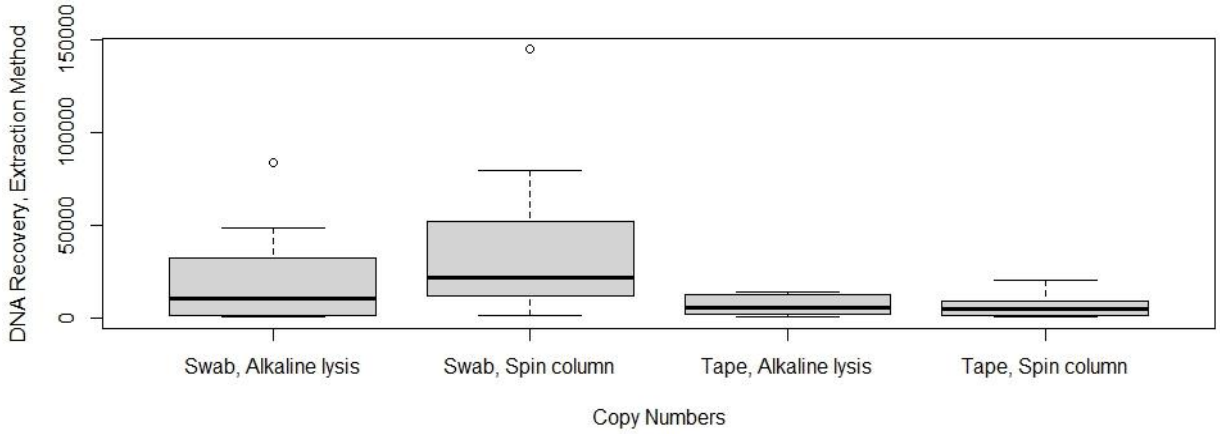

Figure 76: Box plot showing the 25%, 50% and 75% quantiles of the copy number of each DNA sample obtained from various combinations DNA recovery and extraction methods.

The CNs obtained were also subjected to One-way ANOVA analysis to determine if there was a difference between the CNs from different DNA recovery and extraction method combination. Results from the One-way ANOVA test (Table 24) indicated that there was evidence (F-value = 3.68, $p > 0.0207$) that there was a difference between the CN of the DNA samples obtained from different combinations of DNA recovery and extraction methods.

A Tukey post-hoc test was then conducted to determine pairwise relationship between each combination of DNA recovery and extraction methods. From the pairwise comparison, there was evidence to indicate that CN of DNA samples obtained using tape-lifting with commercial spin column extraction method and DNA samples obtained using tape-lifting with alkaline lysis extraction method were lower than that of DNA samples obtained from swabbing with commercial spin column extraction method ($p<0.05$). However, there was no evidence to indicate that there was a difference between the copy number of DNA samples obtained using swabbing with commercial spin column extraction method and swabbing with alkaline lysis extraction method. These results suggested that using swabbing to recover latent DNA from the glass slides and subsequently extract the DNA from the swab using a commercial spin column extraction kit would yield the highest amount of DNA that was amplifiable using the *M. javanica* specific qPCR.

Table 24: Raw data from One – way ANOVA analysis generated by Rstudio, for the comparison of CN obtained from DNA samples recovered and extracted using various combinations of DNA recovery and DNA extraction methods.

```
> summary(anova)
                    Df    Sum Sq   Mean Sq F value Pr(>F)
factor(qpcr_4.3$V1)  3 7.588e+09 2.529e+09   3.682 0.0207 *
Residuals           36 2.473e+10 6.869e+08
---
Signif. codes:  0 ‘***’ 0.001 ‘**’ 0.01 ‘*’ 0.05 ‘.’ 0.1 ‘ ’ 1
```

Table 25: Raw data from Tukey Post – hoc test generated by Rstudio, for the comparison of CN obtained from DNA samples recovered and extracted using various combinations of DNA recovery and DNA extraction methods. Portions highlighted in yellow indicated that there is a statistical difference in CN obtained.

```
> TukeyHSD(anova)
  Tukey multiple comparisons of means
    95% family-wise confidence level

Fit: aov(formula = qpcr_4.3$V2 ~ factor(qpcr_4.3$V1))

$`factor(qpcr_4.3$V1)`
                                                diff       lwr       upr     p adj
Swab, Spin column-Swab, Alkaline lysis      19158.3 -12409.18 50725.784 0.3727134
Tape, Alkaline lysis-Swab, Alkaline lysis -14089.6 -45657.08 17477.884 0.6295376
Tape, Spin column-Swab, Alkaline lysis     -14715.6 -46283.08 16851.884 0.5964869
Tape, Alkaline lysis-Swab, Spin column     -33247.9 -64815.38 -1680.416 0.0357717
Tape, Spin column-Swab, Spin column        -33873.9 -65441.38 -2306.416 0.0314795
Tape, Spin column-Tape, Alkaline lysis       -626.0 -32193.48 30941.484 0.9999442
```

4.4 Discussion

4.4.1 Distribution of *M. javanica* Cellular Materials Deposited on the Glass Slides

Fluorescent particles could be seen on all glass slides deposited with *M. javanica* cellular materials, indicating that the cellular materials from the *M. javanica* scales had transferred from the scales to the slides via friction. Three sets of glass slides were deposited with *M. javanica* cellular materials in this experiment and out of these three sets, one set of the glass slides showed to have more cellular materials present even though the conditions of deposition (such as same operator, timing of friction generated, type of glass slides and the pangolin scales) were similar for all three sets. This might indicate that the transfer of cellular materials could be affected by other uncontrollable conditions not measured in this experiment such as strength / force of the operator, humidity of the environment etc..

This experiment also showed that cellular materials was deposited evenly across the surfaces that the scales were in contact with via friction. As the contact time used in this experiment was only 60 sec, this implied that contact time for sufficient cellular materials to be transferred was very low.

4.4.2 Optimal DNA recovery and DNA Extraction Method for Latent DNA Detection

Two DNA recovery methods, namely swabbing and tape-lifting, and two DNA extraction methods, namely alkaline lysis extraction method and commercial spin column extraction method, were compared in this experiment. *M. javanica* cellular materials deposited on the glass slides were subjected to a combination of these DNA recovery and DNA extraction methods. Each of the four combinations were tested on 10 sample glass slides: (a) swabbing with alkaline lysis extraction, (b) swabbing with commercial spin column extraction, (c) tape-lifting with alkaline lysis extraction and (d) tape-lifting with commercial spin column extraction.

All 20 latent DNA samples recovered using the nylon flocked swabs were able to be amplified using conventional PCR as compared to 17 samples that were recovered using tape-lifting (Table 22), indicating that swabbing is a better DNA recovery method in this instance. The results from qPCR had also indicated that more DNA was recovered using the nylon flocked swabs than tape-lifting (Figure 76). The results from Tukey Post-hoc test further showed that the amount of DNA isolated from samples subjected to swabbing then commercial spin column extract kit yielded the highest amount of DNA, indicating that recovering latent DNA using swabbing followed by DNA extraction using the commercial spin column extraction kit was the optimal workflow in this instance.

CHAPTER FIVE: DEPOSITION OF LATENT DNA FROM *M. JAVANICA* SCALES ONTO TWO TYPES OF PLASTIC SHEETS VIA FRICTION

5.1 Background

5.1.1 Polyethylene (PE)

Polyethylene (PE) is one of the most commonly used plastic materials. It is a very versatile polymer exhibiting a wide range of physical properties, ranging from stiff/brittle to ductile/tough to different degree of elasticity, depending upon the degree of crystallinity of its polymer (Dobbin, 2017). Due to its versatility, it is used in many diverse applications ranging from electronics / electricals, constructions, household essentials etc.

PE is sorted into different categories based on the branches in the polymer and their melting index (Kissin, 2020). PE are generally categorised into three broad categories: high-density polyethylene (HDPE), low-density polyethylene (LDPE) and linear low-density polyethylene (LLDPE). The two most common type of polyethylene that we encountered in packaging materials are the high-density polyethylene (HDPE) and low-density polyethylene (LDPE).

While all PE resins are made up of linear polymer chains, containing carbon and hydrogen, (chemical formula: –(CH2–CH2)n–, where n ranges from ~1,000 to ~100,000), some PE resins can contain branches along their polymer backbones (Patel, 2017). LDPE are made up of such branches whereas HDPE has a more crystallised structure in the polymer. Due to their highly branched composition, LDPE exhibits excellent elasticity and melt strength properties but has inferior impact, tear, abrasion, and environmental stress-cracking resistance (ESCR) properties (Patel, 2017). LDPE also exhibits good optic and high clarity. These properties make LDPE suitable in applications where elasticity and/or optics are important (Wooster & Martin, 2017), such as wire and cable casings, food wraps etc.

Generally, PE with density higher than 0.940 g/cm^3 are known as HDPE (Kissin, 2020). The crystalised structure of HDPE provides HDPE with better rigidity and durability as well as better chemical resistance than LDPE (Patel, 2017). And hence, HDPE is the preferred material for rigid or strong packaging applications (Mure, 2017), such as containers for chemical products, outdoor furniture or structures, plumbing pipes etc.

5.1.2 Objectives of this Experiment

The objective of this experiment is to determine if the *M. javanica* scales could deposit latent DNA onto the surfaces of a packaging material that are more commonly used in packaging

wildlife products, such as plastic bags (plastic bags). Two types of polyethylene material, high-density polyethylene (HDPE) and low-density polyethylene (LDPE) were chosen as plastic bags are commonly made of these two materials.

5.2 Materials and Methods

5.2.1 Samples Used in this Experiment

The scales used in this experiment were the dried *M. javanica* scales as detailed in section 2.2.1. Cellular materials from these five scales were deposited onto their respective plastic sheets via friction as detailed in section 2.2.3.1.

5.2.2 Surface Substrates Used in this Experiment

Small pieces of plastic sheets were cut from two different types of plastic bags: the black HDPE garbage bag and the transparent LDPE plastic bags. The plastic sheets measured approximately 7 cm x 20 cm each and were fixed onto a thicker plastic backing for the ease of handling (Figure 77). Three sets of these plastic sheets were subjected to cellular material deposition as described in section 2.2.3.1. Each set containing the five pieces of *M. javanica* scales (section 2.2.1.2) were deposited onto two plastic sheets each, generating a total of 10 plastic sheets with *M. javanica* cellular materials for each set. Two clean plastic sheets and two sheets with thumbprints were also included as negative control and positive staining control respectively in each set.

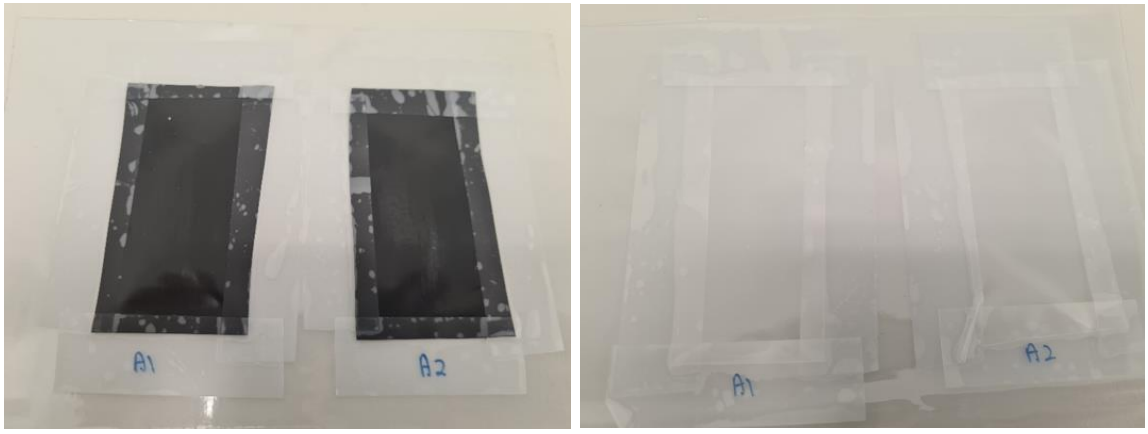

Figure 77: Black HDPE plastic sheets (left) and the transparent LDPE plastic sheets (right), each measuring approximately 7 cm x 20 cm, excluding plastic backing.

5.2.3 Staining and Visualisation of Latent DNA Deposited on the Plastic Sheets Using Diamond™ Nuclei Acid Dye

A working stock of 20x DD (Promega Corporation, Madison, USA) was prepared by diluting 10,000x DD in 75% ethanol (v/v). The working stock was stored at 4°C for up to 7 days.

From the solution of 20x DD, 150 µL was pipetted onto each plastic sheet and spread evenly across the sheet using a pipette tip to ensure that the dye covered the entire surface of the sheet evenly. The stained surfaces were then examined after at least 30 sec, using the Dino-Lite digital microscope (AnMo Electronics Corporation) under blue light (480 nm) and at 50x magnification. Each sheet was examined at three different fields spread evenly across middle of each sheet, as shown in Figure 69. Images of fluorescent staining were recorded using the software Dino-Capture 2.0.

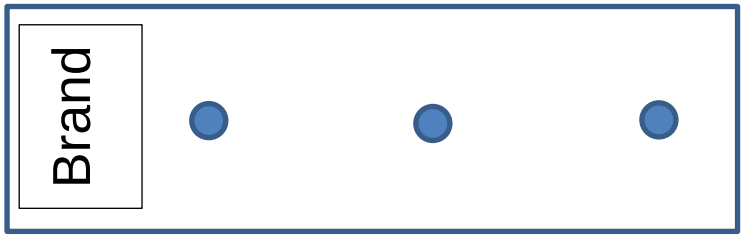

Figure 78: An illustration of the positions where the fluorescence was imaged across the plastic sheets. Each dot indicated where one image was taken using the Dino-Lite digital microscope. A total of three images were taken for each sheet.

5.2.4 DNA Recovery, Extraction and Amplification

DNA sample was recovered from each plastic sheet using swabbing and tape-lifting, as described in section 4.2.4 and DNA was subsequently extracted using commercial spin column extraction kit and alkaline lysis extraction as per section 4.2.5. Each DNA sample obtained was subjected to conventional PCR, as described in section 2.2.9, and qPCR, as described in section 4.2.6.

5.3 Results

5.3.1 Visualisation of Latent DNA on Plastic Sheets

Figures 70 – 76 showed representative images from the plastic sheets used in this experiment. Positive fluorescence staining can be seen on plastic sheets deposited with pangolin scales A – E (Figures 81 – 85), indicating that the cellular materials from the pangolin scales were deposited onto both the transparent and black plastic sheets when friction was introduced. The morphology of the fluorescent particles seen on these plastic sheets were similar to those seen on glass slides.

No or minimal positive fluorescent staining could be seen in the negative controls (Figure 79), indicating that the plastic sheets used were clean with minimal cellular materials found on them.

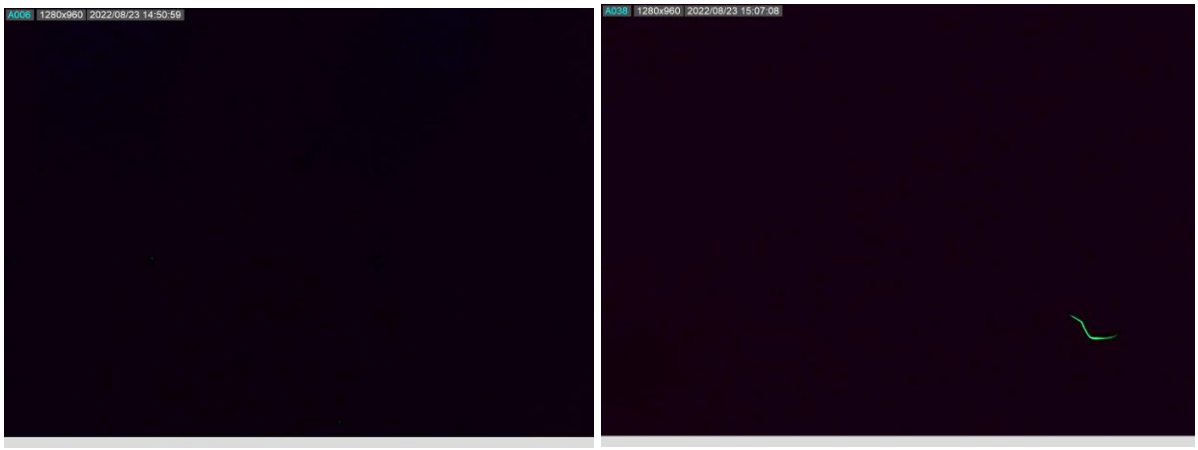

Figure 79: Images showing fluorescence staining on clean transparent (left) and black (right) plastic sheets (negative controls), viewed under 50x UV microscope.

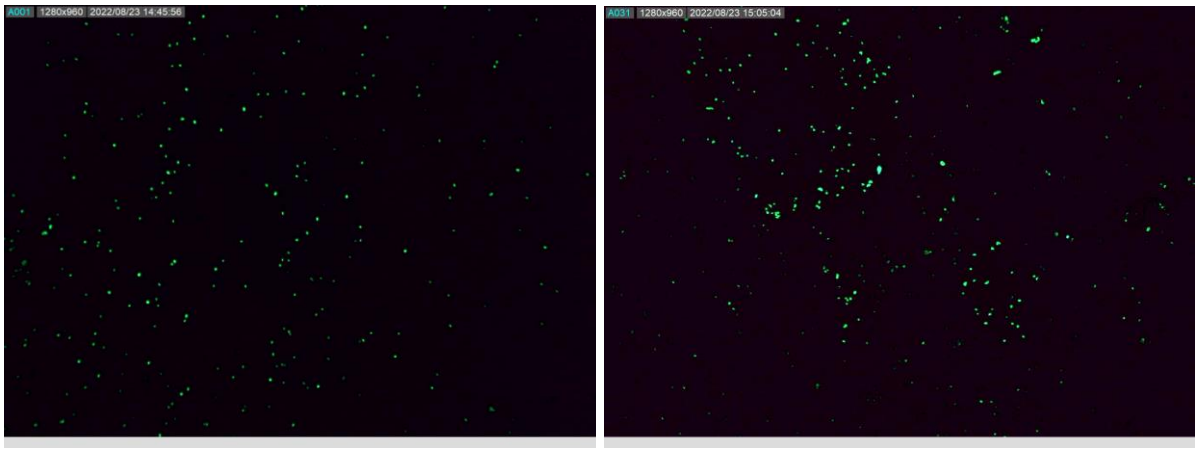

Figure 80: Images of showing fluorescence staining on transparent (left) and black (right) plastic sheet deposited with thumbprint (positive staining controls), viewed under 50x UV microscope.

Figure 81: Images of showing fluorescence staining transparent (left) and black (right) plastic sheet deposited with pangolin scale A, viewed under 50x UV microscope.

Figure 82: Images showing fluorescence staining on transparent (left) and black (right) plastic sheet deposited DNA with pangolin scale B, viewed under 50x UV microscope.

Figure 83: Images showing fluorescence staining on transparent (left) and black (right) plastic sheet deposited DNA with pangolin scale C, viewed under 50x UV microscope.

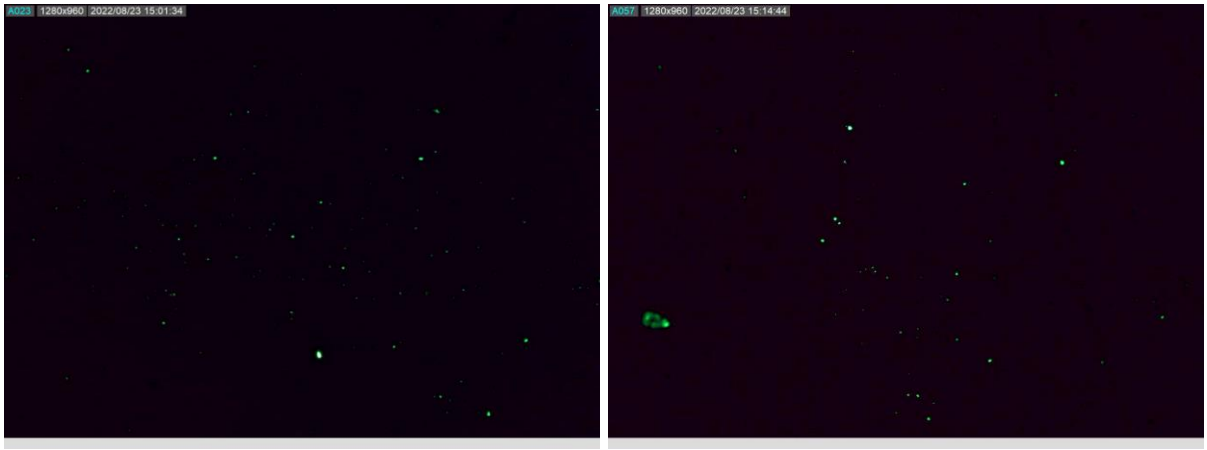

Figure 84: Images showing fluorescence staining on transparent (left) and black (right) plastic sheet deposited DNA with pangolin scale D, viewed under 50x UV microscope.

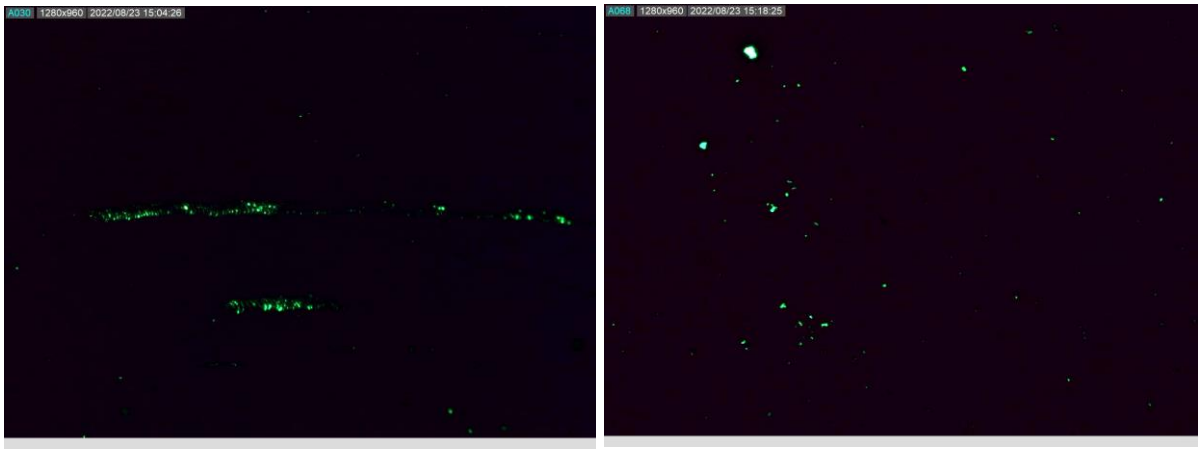

Figure 85: Images showing fluorescence staining on transparent (left) and black (right) plastic sheet deposited DNA with pangolin scale E, viewed under 50x UV microscope.

5.3.2 Comparison of Cellular Materials Deposited onto the HDPE (Transparent) and LDPE (Black) Bag

The total representative fluorescent particle count (TRFC) was obtained for each sheet for two sets of the HDPE and LDPE plastic sheets to determine if more cellular materials were deposited on one type of plastic sheet over the other. The TRFC was then plotted into a box plot (Figure 86) and analysed using One-Way ANOVA analysis (Table 26) to determine if there is a difference between the number of fluorescent counts from HDPE and LDPE plastic sheets. Results from the One-way ANOVA test (Table 26) indicated that there was no evidence (F-value = 2.794, p = 0.103) that the numbers of fluorescent counts obtained from HDPE and LDPE plastic sheets were different from each other. However, from the boxplot, it can be observed that the TRFC obtained from the LDPE plastic sheets seemed to spread over a wider and higher range than that of the HDPE plastic sheet.

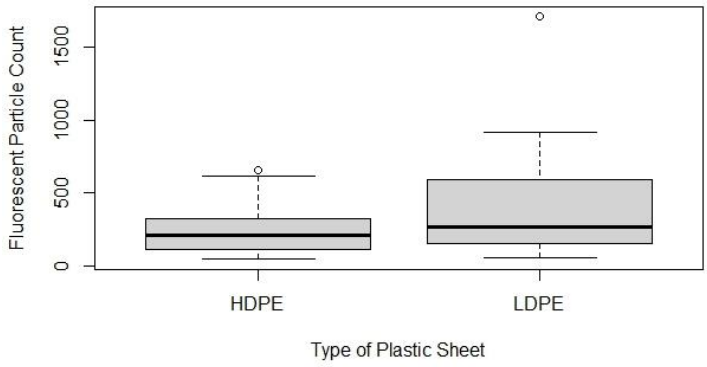

Figure 86: Box plot showing the 25%, 50% and 75% quantiles of the copy numbers obtained for each DNA samples from HDPE and LDPE plastic sheet (n = 20 for each group).

Table 26: Raw data from One – Way ANOVA analysis generated from Rstudio, comparing the TRFC obtained from HDPE and LDPE plastic sheets.

```
> summary(anova)
                              Df  Sum Sq Mean Sq F value Pr(>F)
factor(ParticleCount_sheets$V1)  1  280228  280228   2.794  0.103
Residuals                       38 3810892  100287
```

5.3.2 Amplification of DNA Samples Extracted from the Two Types of Plastic Sheets Using Conventional PCR

Cellular materials deposited on the two types of plastic sheets were then recovered and extracted using different combinations of methods. Each combination of DNA recovery and DNA extraction methods resulted in 10 samples with cellular materials from *M. javanica* scales. The DNA isolated was subsequently subjected to conventional PCR.

Figures 87 to 94 show the images of gel electrophoresis of each conventional PCR amplification for the different combinations of DNA recovery and DNA extraction methods and Table 27 summarises the conventional PCR results obtained.

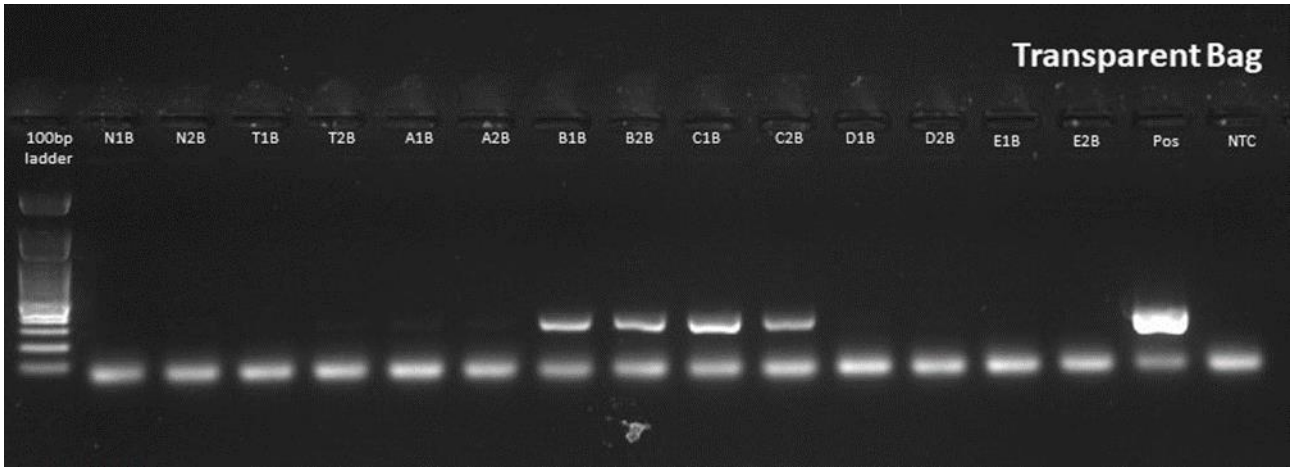

Figure 87: Image of a 1.5% gel after electrophoresis, showing outcome from the PCR amplification. The samples are: no template control (NTC), *M. javanica* positive control (Pos), clean plastic sheet (N1B and N2B), thumbprint and respective slides (A – E) with *M. javanica* scales. The scales had been in contact with the *HDPE (transparent) bag* by friction, recovered using *swabs* and DNA extracted using *alkaline lysis* extraction method.

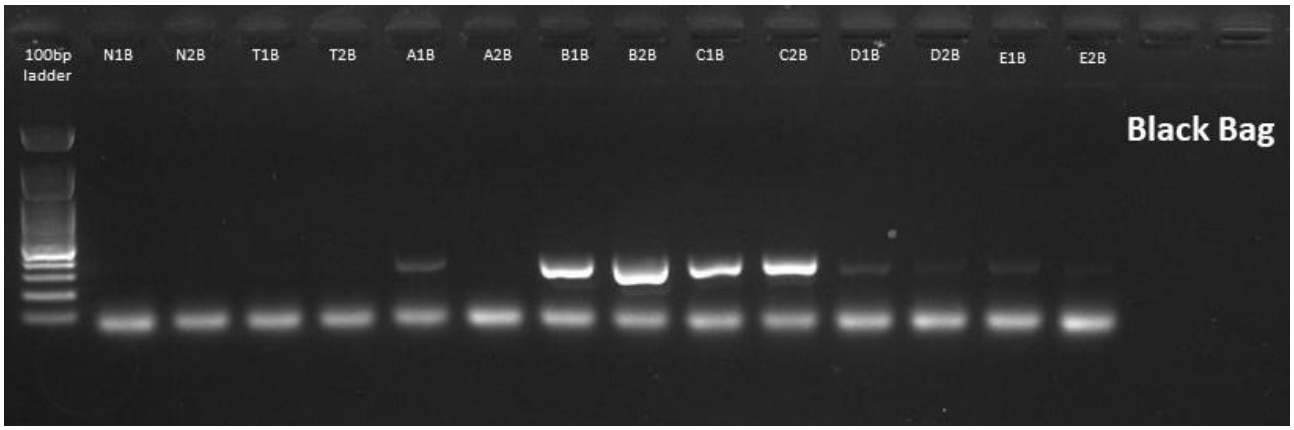

Figure 88: Image of a 1.5% gel after electrophoresis, showing outcome from the PCR amplification. The samples are: clean plastic sheet (N1B and N2B), thumbprint and respective slides (A – E) with *M. javanica* scales. The scales had been in contact with the *LDPE (Black) bag* by friction, recovered using *swabs* and DNA extracted using *alkaline lysis* extraction method. Both positive control and no template control is shown in Figure 87 above.

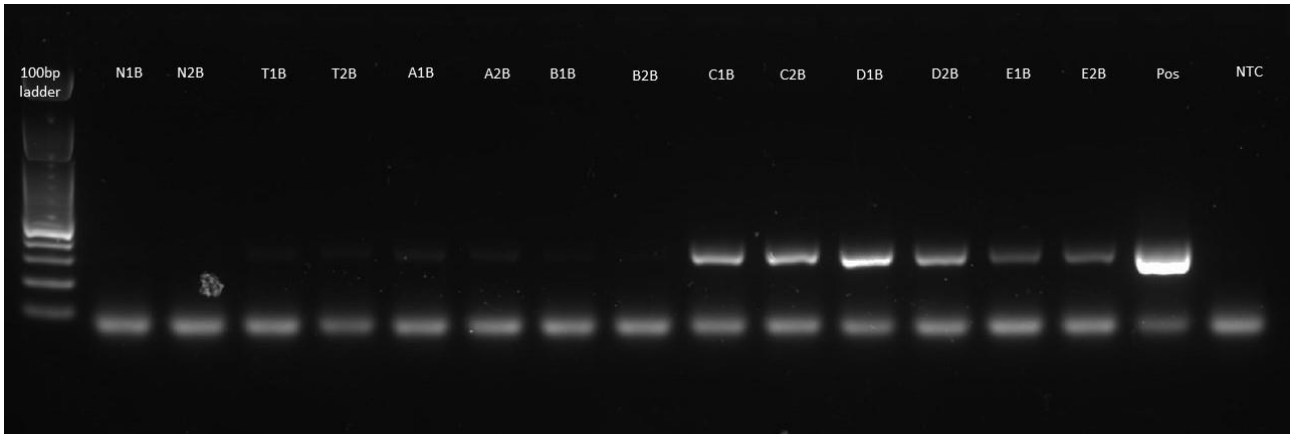

Figure 89: Image of a 1.5% gel after electrophoresis, showing outcome from the PCR amplification. The samples are: no template control (NTC), *M. javanica* positive control (Pos), clean plastic sheet (N1B and N2B), thumbprint and respective slides (A – E) with *M. javanica* scales. The scales had been in contact with the *HDPE (transparent) bag* by friction, recovered using *swabs* and DNA extracted using *commercial spin column* extraction method.

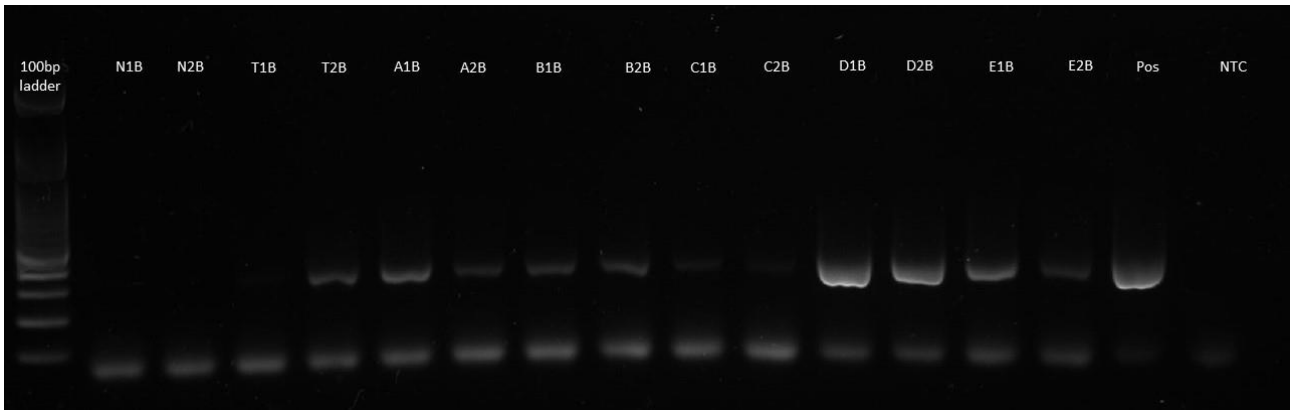

Figure 90: Image of a 1.5% gel after electrophoresis, showing outcome from the PCR amplification. The samples are: no template control (NTC), *M. javanica* positive control (Pos), clean plastic sheet (N1B and N2B), thumbprint and respective slides (A – E) with *M. javanica* scales. The scales had been in contact with the *LDPE (black) bag* by friction, recovered using *swabs* and DNA extracted using *commercial spin column* extraction method.

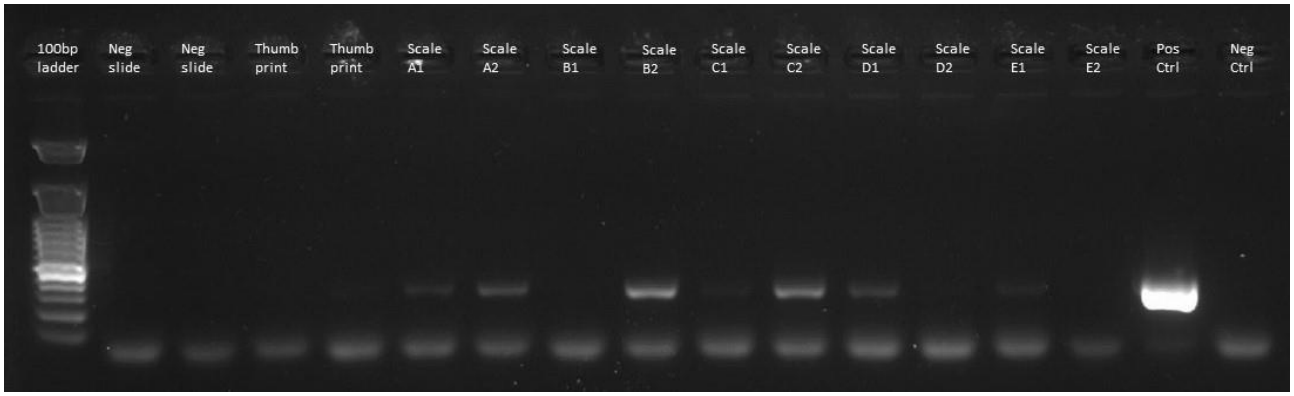

Figure 91: Image of a 1.5% gel after electrophoresis, showing outcome from the PCR amplification. The samples are: no template control (NTC), *M. javanica* positive control (Pos), clean plastic sheet (N1B and N2B), thumbprint and respective slides (A – E) with *M. javanica* scales. The scales had been in contact with the *HDPE (transparent) bag* by friction, recovered using *tape - lifting* and DNA extracted using *alkaline lysis* extraction method.

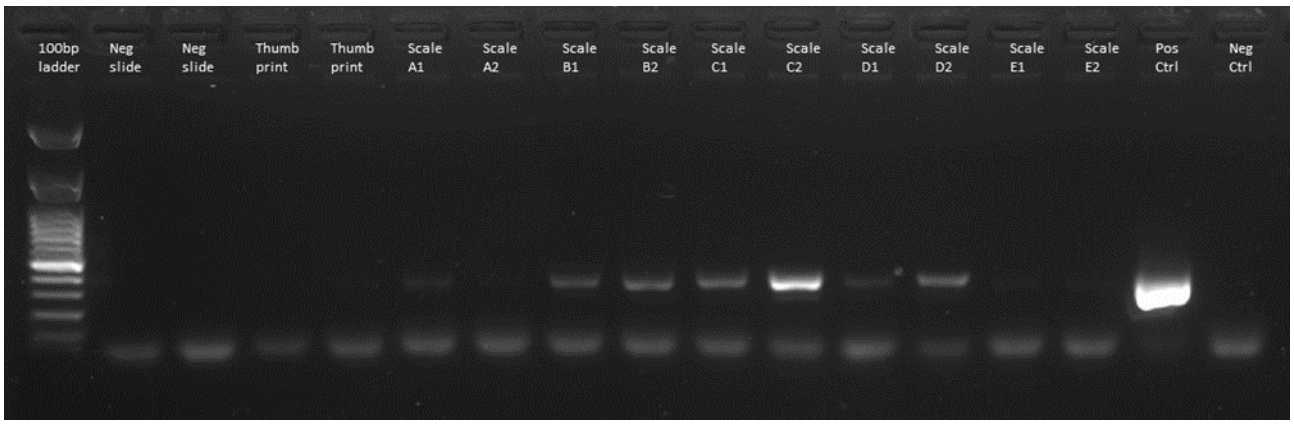

Figure 92: Image of a 1.5% gel after electrophoresis, showing outcome from the PCR amplification. The samples are: no template control (NTC), *M. javanica* positive control (Pos), clean plastic sheet (N1B and N2B), thumbprint and respective slides (A – E) with *M. javanica* scales. The scales had been in contact with the *LDPE (black) bag* by friction, recovered using *tape - lifting* and DNA extracted using *alkaline lysis* extraction method.

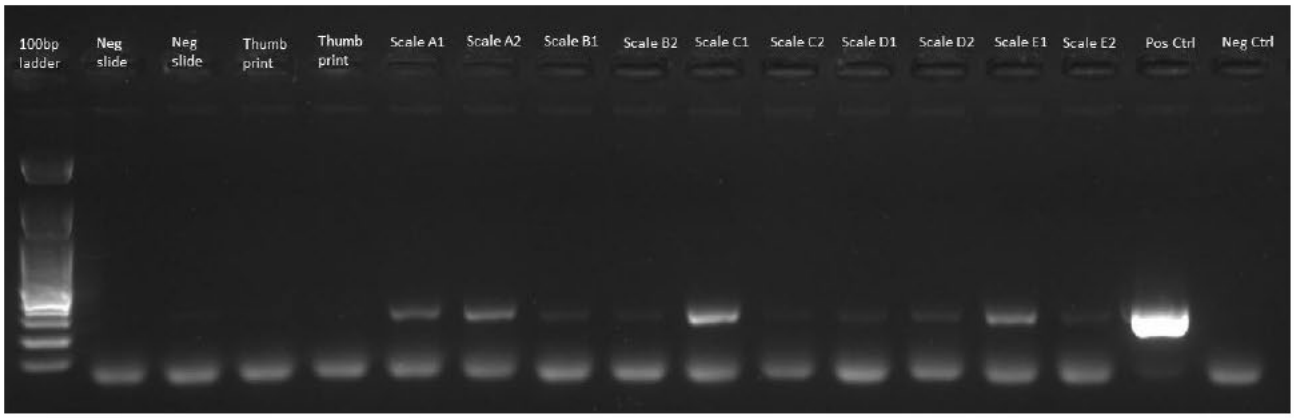

Figure 93: Image of a 1.5% gel after electrophoresis, showing outcome from the PCR amplification. The samples are: no template control (NTC), *M. javanica* positive control (Pos), clean plastic sheet (N1B and N2B), thumbprint and respective slides (A – E) with *M. javanica* scales. The scales had been in contact with the *HDPE (transparent) bag* by friction, recovered using *tape - lifting* and DNA extracted using *commercial spin column* extraction method.

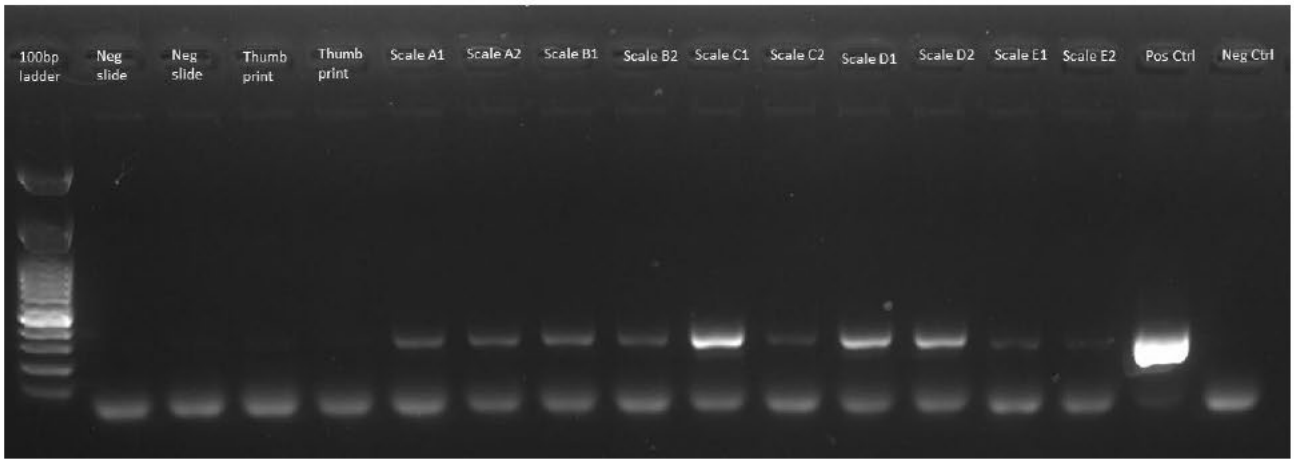

Figure 94: Image of a 1.5% gel after electrophoresis, showing outcome from the PCR amplification. The samples are: no template control (NTC), *M. javanica* positive control (Pos), clean plastic sheet (N1B and N2B), thumbprint and respective slides (A – E) with *M. javanica* scales. The scales had been in contact with the *LDPE (black) bag* by friction, recovered using *tape - lifting* and DNA extracted using *commercial spin column* extraction method.

Table 27: Summary of conventional PCR results from DNA samples isolated from two types of plastic sheets – HDPE and LDPE.

	Swabs		Tapes		
	LDPE plastic sheets	**HDPE plastic sheets**	**LDPE (black) plastic sheets**	**HDPE plastic sheets**	**Total**
Spin column	0.8 (8/10)	0.7 (7/10)	1 (10/10)	1 (10/10)	0.875 (35/40)
Alkaline lysis	1 (10/10)	0.6 (6/10)	0.7 (7/10)	0.7 (7/10)	0.75 (30/40)
Total	0.9 (18/20)	0.65 (13/20)	0.85 (17/20)	0.85 (17/20)	

As shown in Table 27, it can be seen that out of the 40 DNA samples extracted using spin column extraction method, 35 of these samples yielded a positive PCR amplification. This is higher than those extracted using the alkaline lysis extraction method (30/40), indicating that the commercial spin column extraction method was a more effective method to be used for the extraction of latent *M. javanica* DNA recovered from plastic sheets. This is in agreement with the results obtained in Chapter Four.

All 20 DNA samples that were recovered using tapes and extracted using commercial spin column kits yielded positive PCR amplifications. This indicates that DNA recovery using tape-lifting with commercial spin column DNA extraction seems to work the best for latent *M. javanica* DNA deposited on plastic sheets. Additionally, the results also indicate that latent DNA deposition on the LDPE (black) plastic sheets were able to yield more positive amplifications (35/40) than the HDPE (transparent) plastic sheets (30/40).

5.3.3 Comparison of Latent DNA Recovery and Extraction Methods for Plastic sheets using qPCR

The DNA samples were also subjected to qPCR amplifications using the Sunda2502B primers and probe set, and CN of the DNA samples were extrapolated using the standard curve run on the same qPCRs. Table 28 below showed the CN obtained from the DNA samples for the different combinations of DNA recovery and DNA extraction methods.

Table 28: Copy numbers (CNs) and mean CNs of latent DNA samples obtained using different combinations of DNA recovery and DNA extraction methods. TA – Tape – lifting with alkaline lysis extraction, TE - Tape – lifting with commercial spin column extraction, SA – Swabbing with alkaline lysis extraction, SE - Swabbing with commercial spin column extraction.

	LDPE plastic sheets				HDPE plastic sheets			
	TA	TE	SA	SE	TA	TE	SA	SE
A1	456	2,988	2,311	17,672	894	4,742	555	1,959

A2	112	2,441	204	4,731	1,454	5,146	631	54,118
B1	1,634	5,158	15,521	5,144	38	755	6,731	626
B2	2,714	7,450	42,205	4,580	3,156	1,284	5,456	360
C1	3,957	19,422	14,765	1,013	362	9,545	12,948	8,783
C2	20,963	3,110	35,640	1,262	3,300	315	6,290	12,226
D1	1,947	10,877	725	77,426	414	349	208	21,849
D2	10,994	15,460	419	6	82	805	152	12,255
E1	89	1,298	6	16,385	336	3,074	68	5,038
E2	260	1,051	330	4,636	304	349	55	7,453
Mean	4,313	6,925	11,212	13,286	1,034	2,636	3,309	12,467

When comparing the mean CNs of the DNA samples obtained from either LDPE or HDPE plastic sheets, using the same DNA recovery and extraction method, it can be seen that DNA samples from the LDPE plastic sheets generally yielded a higher mean CN than the HDPE plastic sheets. The mean CNs of DNA samples recovered using swabs were also higher than that of DNA samples recovered using tape-lifting and the mean CN of DNA samples extracted using commercial spin column kits were higher than the corresponding DNA samples extracted using alkaline lysis. The DNA samples obtaining using swabs with commercial spin column kit also yielded the highest mean CN.

The CN obtained for each DNA sample was also plotted in the boxplot, however, no difference in copy number between each group can be observed. This could be due to the large spread in copy numbers obtained for each group. More samples might be needed to provide better differentiation and resolution between the groups.

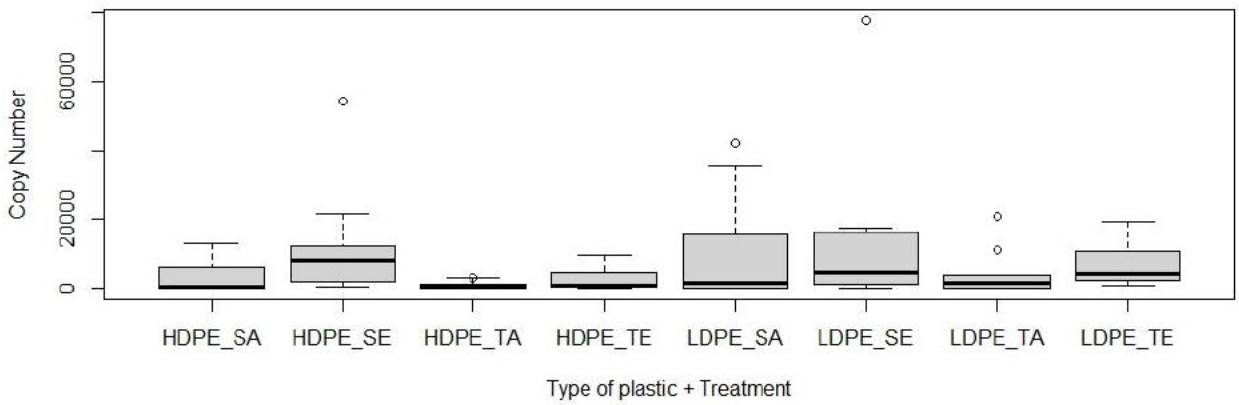

Figure 95: Box plot showing the 25%, 50% and 75% quantiles of the copy numbers obtained for each DNA samples from each treatment group. (n = 10 for each group).

The copy numbers obtained were also subjected to One-way ANOVA analysis to determine if there was a difference between the copy numbers from different combinations of DNA recovery and extraction methods. Results from the One-way ANOVA test (Table 29) indicated that there was no evidence (F-value = 1.59, p = 0.152) to show that there was a difference between the CN of the DNA samples obtained from different combinations of DNA recovery and extraction methods. A Tukey post-hoc test (Table 30) was then conducted to determine pairwise relationship between each combination of DNA recovery and extraction methods and likewise, the pairwise comparison showed that there was no evidence to indicate that copy numbers of the various DNA samples obtained from different combinations of DNA recovery and extraction methods were different. As qPCR indicated positive detection of *M. javanica* mitochondrial DNA in these samples, the statistical results suggested that all DNA recovery and extraction methods tested in this experiment were suitable to be used to recover and extract latent *M. javanica* DNA from plastic sheets.

Table 29: Raw data generated from One – Way ANOVA analysis in Rstudio, comparing CN of each DNA samples obtained from plastic sheets using different combinations of DNA recovery and DNA extraction methods.

```
> summary(anova)
                      Df    Sum Sq   Mean Sq F value Pr(>F)
factor(qPCR_sheets$V1)  7 1.625e+09 232194852    1.59  0.152
Residuals              72 1.052e+10 146065815
```

Table 30: Raw data generated from Tukey Post – hoc test in Rstudio, comparing CN of each DNA samples obtained from plastic sheets using different combinations of DNA recovery and DNA extraction methods.

```
> TukeyHSD(anova)
  Tukey multiple comparisons of means
    95% family-wise confidence level

Fit: aov(formula = qPCR_sheets$V2 ~ factor(qPCR_sheets$V1))

$`factor(qPCR_sheets$V1)`
                       diff        lwr       upr     p adj
HDPE_SE-HDPE_SA   9157.3365  -7715.790 26030.463 0.6908438
HDPE_TA-HDPE_SA  -2275.3893 -19148.516 14597.738 0.9998821
HDPE_TE-HDPE_SA   -673.1195 -17546.246 16200.007 1.0000000
LDPE_SA-HDPE_SA   7902.9856  -8970.141 24776.113 0.8244883
LDPE_SE-HDPE_SA   9976.0921  -6897.035 26849.219 0.5917087
LDPE_TA-HDPE_SA   1003.2235 -15869.903 17876.350 0.9999996
LDPE_TE-HDPE_SA   3615.9341 -13257.193 20489.061 0.9975531
HDPE_TA-HDPE_SE -11432.7258 -28305.853  5440.401 0.4153483
HDPE_TE-HDPE_SE  -9830.4560 -26703.583  7042.671 0.6096538
LDPE_SA-HDPE_SE  -1254.3509 -18127.478 15618.776 0.9999980
LDPE_SE-HDPE_SE    818.7556 -16054.371 17691.883 0.9999999
LDPE_TA-HDPE_SE  -8154.1130 -25027.240  8719.014 0.8003326
LDPE_TE-HDPE_SE  -5541.4024 -22414.529 11331.725 0.9690349
HDPE_TE-HDPE_TA   1602.2698 -15270.857 18475.397 0.9999891
LDPE_SA-HDPE_TA  10178.3749  -6694.752 27051.502 0.5667088
LDPE_SE-HDPE_TA  12251.4814  -4621.646 29124.608 0.3261118
LDPE_TA-HDPE_TA   3278.6128 -13594.514 20151.740 0.9986892
LDPE_TE-HDPE_TA   5891.3234 -10981.804 22764.450 0.9569314
```

LDPE_SA-HDPE_TE	8576.1051	-8297.022	25449.232	0.7565428
LDPE_SE-HDPE_TE	10649.2116	-6223.915	27522.339	0.5087000
LDPE_TA-HDPE_TE	1676.3430	-15196.784	18549.470	0.9999852
LDPE_TE-HDPE_TE	4289.0536	-12584.073	21162.181	0.9929622
LDPE_SE-LDPE_SA	2073.1065	-14800.020	18946.233	0.9999371
LDPE_TA-LDPE_SA	-6899.7621	-23772.889	9973.365	0.9045156
LDPE_TE-LDPE_SA	-4287.0515	-21160.178	12586.075	0.9929821
LDPE_TA-LDPE_SE	-8972.8686	-25845.996	7900.258	0.7122627
LDPE_TE-LDPE_SE	-6360.1580	-23233.285	10512.969	0.9359761
LDPE_TE-LDPE_TA	2612.7106	-14260.416	19485.838	0.9997030

5.4 Discussion

5.4.1 Deposition of *M. javanica* Cellular Materials on Plastic Sheets

Fluorescence staining could be observed from both the HDPE and LDPE plastic sheets deposited with *M. javanica* cellular materials via friction, indicating that *M. javanica* cellular materials could be transferred onto both types of PE materials.

The *M. javanica* scales deposited a wider and higher number of fluorescent particles on the LDPE plastic sheets. This could be due to that, when the scales were slided across the surfaces of the LDPE plastic sheets, the elastic and flexible nature of the LDPE material created longer and closer contact between the scales and the surface. And therefore, more cellular materials from the scales were deposited onto the surface of the LDPE plastic sheets. It is however important to note that the statistical analysis showed that there was no difference between the fluorescent particle counts obtained from HDPE and LDPE plastic sheets, indicating that cellular materials from *M. javanica* scales could be transferred onto both HDPE and LDPE plastic sheets through friction.

5.4.2 Optimal DNA Recovery and Extraction Method for Latent *M. javanica* DNA Deposited on Plastic Sheets.

It was demonstrated that both swabs and tape – lifts could be used to effectively recover *M. javanica* cellular materials from the plastic sheets.

Using conventional PCR, the tape-lifts (34 out of 40) yielded more positive PCR amplifications than swabs (31 out of 40). In constrast, the same DNA samples extracted from tape - lifts tended to yield a lower mean CN than those from swabs when amplifications were conducted using qPCR. , indicating that although more DNA samples recovered from tape – lifts contained succificent DNA amount for positive PCR amplifications to take place, the amount of DNA available for PCR amplification to take place is less than those from swab recovery method. This may be due to the adhesive nature of the tape used in tape-liftingwhere the double-stranded DNA in the samples recovered from tape – lifts might be still adhering tightly onto the tape, and when subjected to high heat treatment during the pre-

treatment stage of the DNA extraction, only a one strand of the double-stranded DNA dissociated, releasing only one strand of the DNA into the mixture for extraction, leading to a lower starting DNA amount.

Both conventional PCR and qPCR results yielded more positive amplifications and higher mean CNs respectively from samples extracted using commercial spin column kits than alkaline lysis extraction methods. This result is in agreement with the results obtained in Chapter Four. It is likely that commercial spin column matrixes were able to better remove PCR inhibitors from the DNA samples, leading to a better PCR efficiency than the DNA samples from alkaline lysis extraction method.

Although the results from the mean CNs of the DNA samples might indicate that recovering DNA using swabbing, followed by DNA extraction using commercial spin column extraction method was the optimal workflow, the statistical analysis indicated that all combinations of the DNA recovery and extraction methods tested in this experiment was suitable for use to recover and extract latent *M. javanica* DNA from both HDPE and LDPE plastic sheets.

CHAPTER SIX: VISUALISATION AND DETECTION OF LATENT DNA DEPOSITED BY DRIED PANGOLIN SCALES ONTO PLASTIC PACKAGING BAGS

6.1 Background

6.1.1 DNA Extraction Methods

DNA extraction is a crucial technique used in molecular biology laboratories to purify and isolate DNA from biological materials. Generally, the DNA extraction process include lysis of cell, inactivation of nucleases and other enzymes, removal of macromolecules, lipids, RNA, or proteins and other contaminants, and lastly precipitation or elution of the DNA. The efficiency and effectiveness of the DNA extraction methods significantly affects the quality and quantity of the DNA isolated for downstream molecular analysis. The type of DNA extraction method to be used is determined by the nature of the biological sample involved, the technical requirements, cost effectiveness, time efficiency, storage requirement etc (Carpi et al., 2011). DNA extraction methods can be broadly classified into two categories – the liquid-based DNA extraction methods and solid-phase DNA extraction methods (Finaughty et al., 2023).

6.1.1.1 Liquid based DNA extraction methods

Liquid-based methods utilises either organic or inorganic extraction procedures. The organic extraction methods include techniques such as phenol chloroform precipitation or ethanol precipitation. As these techniques use organic chemicals that are toxic and corrosive, personnel safety is of paramount importance when carrying out the organic extraction method. Personal protective equipment and a chemical fume hood must be available when using this technique and personnel must also be adequately trained in chemical handling procedures (Griffiths & Chacon-Cortes, 2014).

Due to the hazardous nature of the chemicals used in the organic extraction methods, modifications to replace the chemicals in organic extraction method have been developed over the years. Inorganic chemical extraction methods typically involve the salting out technique that utilises a high salt content solution to remove impurities instead of the organic solvents in the organic extraction method. Generally, in the salting out technique, the cell is first lysed using SDS – proteinase K. The proteins are then removed through precipitation using a high salt content solution such as sodium chloride, leaving behind a mixture containing the DNA. The DNA will then be precipitated out using ethanol or isopropanol (Mardan-Nik et al., 2019; Nasiri et al., 2005; Shaik et al., 2016).

6.1.1.2 Solid phase DNA extraction methods

The use of commercially available DNA extraction kits has been gaining popularity over the years. Most of these kits utilise the solid phase DNA method which generally involves the lysis of the cell, DNA adsorption to a solid phase due to the presence of required pH and salt conditions, washing to remove impurities and lastly, DNA release and elution through a change of pH and salt conditions to the solid phase. Many solid-phase techniques involve the use of a spin column to bind to the DNA and such spin column matrices can be made of silica matrices, glass particles or powder, diatomaceous earth, or anion exchange carriers (Carpi et al., 2011; Griffiths & Chacon-Cortes, 2014).

Spin column DNA extraction methods takes up to 1 hour (excluding pre-treatment) to extract the DNA from the biological materials. The use of commercially available DNA extraction kits ensure that the DNA extraction is conducted quickly and free of contamination through the use of a standardised platform. The use of these commercially available DNA extraction kits has also been incorporated into automated robotic platforms to provide an operator free DNA extraction option (Gehrig et al., 2009; Phillips et al., 2012; Zhao et al., 2020). Although such robotic platforms reduce the amount of manpower, the risk of pipetting error, and provide higher throughput (Phillips et al., 2012), these platforms are typically very expensive.

DNA extraction method using magnetic beads has also been commonly incorporated into the automated DNA extraction platforms (Nylund et al., 2010; Zhao et al., 2020). The magnetic beads are made of one or several magnetic cores, such as magnetite (Fe_3O_4) or maghemite (gamma Fe_2O_3), coated with a matrix of polymers, silica, or hydroxyapatite with terminal functionalized groups (Carpi et al., 2011) . After cell lysis, the DNA will bind to the magnetic beads. The impurities in the mixture will be removed after the DNA bound magnetic bead is immobilised and after which, the DNA will be eluted from the magnetic beads (McGaughey et al., 2018).

Chelex extraction is a rapid and simple solid phase DNA extraction method that has been commonly used in forensic testing purposes (Phillips et al., 2012; Walsh et al., 2013). It involves the addition of a chelex resin to the biological sample, before cell lysis. The chelex resin has a high affinity for polyvalent metal ions and can chelate metal ions that may catalyse the breakdown of DNA at high temperatures in low ionic strength solutions. The mixture is then subjected to heat treatment to lyse the cell and release the DNA. The metal ions and other contaminants released will then bind to the chelex resin and be removed subsequently, leaving behind only the DNA (Idris & Goodwin, 2015). That the chelex DNA extraction technique requires the sample to be heated to about 100°C and therefore, the resultant DNA samples may degrade and hence, is not suitable for certain downstream

molecular processes requiring DNA of a higher quality (Singh et al., 2018; Walsh et al., 2013).

6.1.2 Objectives for this chapter

It has been demonstrated in the previous chapters that although dehydrated, the dried *M. javanica* scales could deposit latent DNA onto their contact surfaces via friction or pressure. These latent DNA could then be stained and visualised using Diamond™ Nuclei Acid Dye.

In this chapter, the ability to deposit latent DNA by the dried *M. javanica* scales onto contact surfaces in a more realistic environment was investigated. We aim to determine if *M. javanica* scales could deposit latent DNA onto surfaces of plastic bags that they were contained in, and to determine the optimal workflow for the recovering and extracting the latent DNA from the plastic bags.

6.2 Publication and Presentation

Part of this study has been submitted for publication as a research paper in Forensic Science International: Genetics on 10 May 2023 and is currently under review. Results from this study has also been accepted as a poster presentation in the 23rd Triennial Meeting of the International Association of Forensic Sciences to be held on 20 – 24 November 2023 at International Convention Centre Sydney, Australia.

Completed co – authorship approval form can be found in Appendix X.

6.3 Submitted Manuscript: Disrupting the illegal trade in pangolins: Visualisation and Detection of Latent DNA Deposited by Pangolin Scales

Refer to Appendix C for Co – authorship approval form.

Title: Disrupting the illegal trade in pangolins: visualisation and detection of latent DNA deposited by pangolin scales

Names of Authors: Amy H.J. Chan[1,2], Michael G. Gardner[1,3], Adrian Linacre[1]

[1]College of Science and Engineering, Flinders University, Adelaide, Australia

[2]Centre of Wildlife Forensics, National Parks Board of Singapore, Singapore

[3]Evolutionary Biology Unit, South Australian Museum, Adelaide, Australia

Corresponding author: Amy Chan (amy_chan@nparks.gov.sg)

Corresponding address: Centre of Wildlife Forensics, 6 Perahu Road, Singapore 718827

Highlights

- The outer surface of pangolin scales can transfer DNA in detectable quantities to the surface of plastic bags used in their transportation.
- Transferred cellular material from the pangolin scales can be detected and scored using a DNA staining dye.
- The accumulation of DNA from processed pangolin scales varied depending on the position of the bag in which they were stored.
- There was a correlation between the fluorescence and amount of DNA collected.
- The trace DNA from processed pangolin scales was sufficient to allow molecular species identification.

Keywords (3 – 6 items): Pangolin scales, latent DNA, Diamond™ nuclei acid dye, cytochrome b, qPCR, species identification, illegal wildlife trade

Abstract

We report on the identification and analyses of pangolin DNA by use of a DNA binding dye. Pangolins are the most illegally traded mammalian species due to their scales being used in traditional medicines. The scales are transported via sea routes from the country where they are poached in the wild, to where they are processed and distributed into markets in other countries. The illegal consignments of pangolin scales are usually hidden behind legal products, rendering them difficult to access or detect. This is the first report detailing the detection of trace latent DNA from processed wildlife products. Prior to this report it was not known if the outer surface of pangolin scales contained transferable quantities of biological material for DNA analyses. To address this, scales were removed from a roadkill Sunda pangolin (*Manis javanica*) and processed by drying and packaging into one of five bags to mimic the mode of transportation by illegal traders. The presence of latent DNA was detected and visualised using Diamond™ nucleic acid dye. The fluorescent particles from the pangolin scales were similar in size to those of human corneocytes. Swabs were used to recover

stained biological material from various locations in the five bags. The DNA was isolated and quantified using a newly designed quantitative PCR (qPCR) specific to *M. javanica* to amplify a fragment of the mtDNA cytochrome b gene. There was a positive correlation between the number of stained particles and DNA quantity, and a greater number of stained particles were found at the bottom of the bag than were found at the top. PCR targeting part of the cytochrome b gene amplified a product from all 30 samples taken from the bags and in all cases, sequence data generated matched that of the Sunda pangolin, as expected. All negative controls yielded no results. The method described here is the very first use of a staining dye to detect latent DNA from a mammalian species, other than humans, and highlights the opportunity for further use of Diamond™ nucleic acid dye in wildlife forensic science. It is anticipated that this method will be invaluable in retrieving latent DNA deposited by wildlife products from the environment in which they were contained, to determine the presence of these illegal wildlife products even when previously hidden, inaccessible, or no longer present physically. Further research is required understand if the use on non-mammalian wildlife species is feasible.

Introduction

Pangolins are the most illegally traded mammals in the world (Challender et al., 2014; Johnson et al., 2014). They are seized from the wild for their meat and scales, which is consumed based on their perceived—but unfounded—health benefits. The scales are often processed in preparation for use in a wide range of traditional medicinal applications (Challender et al., 2015; Soewu & Sodeinde, 2015; Xing et al., 2020). Currently, all eight species of pangolins are afforded the highest international protection, the prohibition of trade, under Appendix I of the Convention on International Trade in Endangered Species of Flora and Fauna (CITES) ("Consideration of Proposals for Amendment of Appendices I and II," 2016).

Pangolin scales are commonly transported by sea where they are packed in bags, stacked into containers, and shipped across the world (Challender et al., 2020). These packages of pangolin scales are usually falsely declared as legal products, such as plant products and meats, and are also often hidden behind these legal products, blocking access to the pangolin scales. As just one example, in 2019 National Parks Board of Singapore seized a record haul of approximately 37.5 tonnes of pangolin scales, alongside approximately nine tonnes of ivory, in three separate seizures (AFP, 2019; Clarke, 2019; Griffiths, 2019). The pangolin scales were hidden behind frozen beef and timber within the containers of otherwise declared, legal products. Tremendous manpower and money are required to firstly identify the container and then to unload the legal products at the front to gain access to the hidden pangolin scales. Techniques to provide evidential identity of the illegal goods without necessitating direct access to the hidden wildlife products would be beneficial to support enforcement activity by reducing the manpower and monetary cost required.

Molecular techniques used in wildlife forensic science primarily are derived from techniques used in genetics and biodiversity conservation and then validated for use in human forensic science (Maxwell et al., 2016). One important tool in human forensic science is the use of latent DNA to associate a particular individual to a location or an object (Haines et al., 2015c; Hughes et al., 2022; Kanokwongnuwut et al., 2018a; Tonkrongjun et al., 2017). It is now well-established that humans deposit latent DNA onto surfaces by touch as humans are constantly

shedding corneocytes found on the epidermal, cornified, layer of their skin (Kita et al., 2008). Cellular material and DNA deposited by touch is latent, hence when examining items of forensic relevance, it is not known if DNA is present. To overcome this limitation, the detection of DNA can be enhanced by using compounds that bind to nucleic acids, such as Diamond™ nuclei acid dye (Kanokwongnuwut et al., 2018a).

The use of Diamond™ nuclei acid dye for the visualisation of latent DNA was first reported in 2015 (Haines et al., 2015a). Diamond™ nuclei acid dye is an external groove binding nucleic acid (Truman et al., 2013) that was initially developed to stain DNA in gel electrophoresis. Much research has been conducted since then to show that Diamond™ nuclei acid dye could be used to visualise latent DNA deposited by humans to allow for targeted sampling of DNA from forensically significant items such as credit cards, mobile phones etc. (Haines et al., 2015a, 2015b; Kanokwongnuwut et al., 2018a; Kanokwongnuwut et al., 2020b; Kanokwongnuwut et al., 2021). The use of latent DNA has not yet been widely applied in wildlife forensic science. There has been only one report, as a proof-of-concept study, detecting latent DNA deposited by a boa after keeping the snake in a glass tank. Diamond™ nuclei acid dye was then used to study the deposition of this latent reptilian DNA to provide information on the movements of the snakes (Deliveyne et al., 2022).

Although Diamond™ nuclei acid dye has been shown to be useful for visualising latent DNA from live snakes, it was unknown if wildlife products commonly involved in the illegal wildlife trade, such as pangolin scales, could deposit latent DNA into the environment in which they were contained, including packing materials and shipping containers.

This paper provides the first proof-of-concept study examining processed pangolin scales, to show that although wildlife products were processed, they could still deposit sufficient latent DNA onto contact surfaces. Furthermore, Diamond™ nuclei acid dye could be used to visualise the DNA to provide information on the distribution of the latent DNA on these surfaces and to allow targeted sampling to be carried out. This paper also aims to determine if the latent DNA could then be isolated and used in the confirmation of species identification. The process developed in this study thus offers a potential tool to use latent DNA in the enforcement of

legislation relating to the illegal wildlife trade, especially in the absence of a direct access to the hidden wildlife product consignment.

Materials and Methods

Processing of scales from Manis javanica (Sunda pangolin)

A pangolin carcass was collected from a roadkill within two hours of notification by a member of the public; the actual time of death of the pangolin was unknown. The carcass was subsequently morphologically identified to be *M. javanica* at the Centre of Wildlife Forensics, National Parks Board of Singapore (NParks). Scales were removed from the carcass after it was submerged in boiling water for 5 min. The removed scales were placed in an oven at 60°C until the remnants of flesh attached to the scales were observed to be completely dried up (approximately 5 days). The dried scales were stored at room temperature in a low-density polyethylene (LDPE) bag until use.

Deposition of latent DNA onto surfaces of transparent LDPE bags

Five transparent LDPE bags (labelled as A – E) were used in this experiment, each containing approximately 100 g of dried *M. javanica* scales. Each of these bags, measuring 20 cm x 25 cm, were then sealed using transparent sticky tape (Figure 1) and placed on an orbital shaker at 90 rpm for 1 hr on the first day to simulate the friction between the surfaces of the LDPE bags and the scales that might occur during the transportation of the wildlife products. Subsequently, the bags were placed on a tabletop at room temperature for a period totalling seven days. Bags acting as negative controls were treated the same as the others but had no pangolin scales placed inside, to account for any contamination of cellular material onto the bag from the environment.

Figure 1: Image of one of the LDPE bags showing how pangolin scales were packed. The highly processed scales were packaged to mimic typical seizures. The bags were stored for a total of seven days to mimic typical transportation.

After seven days, the pangolin scales were removed from each of the five bags. Each bag was cut into six sections, as illustrated in Figure 2, with section 1 and 2 from the bottom of the LDPE bag, section 3 and 4 from the middle and lastly, section 5 and 6 from the top.

6	5
4	3
2	1

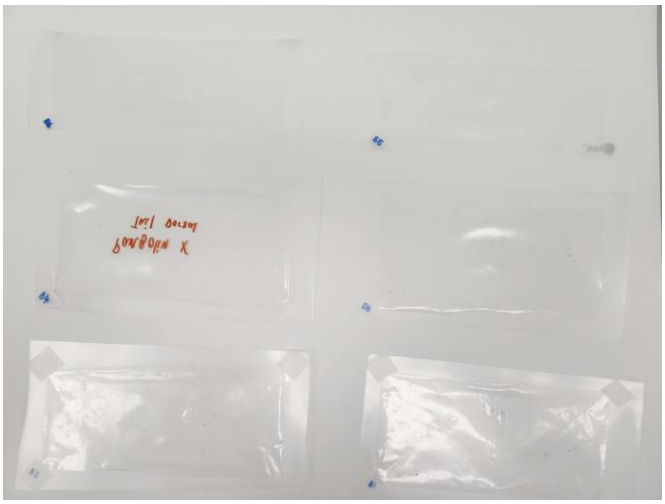

Figure 2: (Left - right) A: An illustration depicting how the LDPE bag was divided into six sections. B: An image of the LDPE bag after it had been cut into six sections. The sections were fixed onto a plastic backing for easy handling after cutting.

Visualisation of latent DNA using Diamond™ nuclei acid dye

Using a pipette tip, 150 µL of the 20x Diamond™ nuclei acid dye (Promega Corporation, Madison, USA) was spread over each section evenly. Thumbprints from a human volunteer were made by pressing their thumb firmly onto the surface for five seconds; this acted as a positive control for the staining process. The stained surfaces were then examined after at least 30 sec using a Dino-Lite digital microscope (AnMo Electronics Corporation, Taipei, ROC) under blue light (480 nm) and at 50x magnification. Each section of the plastic bag was examined at nine different points (one image at each point) spread across the section of the LDPE bag. Images of fluorescence due to the staining were captured and recorded using the software Dino-Capture 2.0, version 1.5.44 (AnMo Electronics Corporation, Taipei, ROC). A total of nine images were captured from each of the six sections of the LDPE bags, resulting in a total of 54 images per bag.

Quantification of fluorescent particles using ImageJ software

The number of fluorescent particles in each image was quantified using the software ImageJ (Schneider et al., 2012). Each of the images were first converted into 8-bit images and then an auto-threshold, Maximum Entropy threshold algorithm, was applied. The number of fluorescent particles counted from the nine images in each section of each bag were then totalled to generate a total representative fluorescent particle count (TRFC) for each section. Next, the mean fluorescent particle count for each location of the bags was then calculated using the TRFC for each similar section of the five different LDPE bags (A-E).

Recovery of DNA via swabbing

Regular nylon flocked swabs (FLOQswabs®, Copan Diagnostic Inc., Brescia, Italy), moistened with 10 µL of nuclease-free water (1st BASE, Singapore), were used to recover DNA from the respective six sections of the LDPE bag.

Extraction of DNA using commercial spin column kit

Swabs were pre-treated by incubating them in a mixture consisting of 400 µL of Buffer ATL (Qiagen, Hilden, Germany) and 20 µL of proteinase K (10 mg/mL) at 56°C with shaking at 900 rpm for at least 1 hr. After pre-treatment, DNA extraction was conducted using QIAamp® DNA Investigator kit (Qiagen) following manufacturer's recommended protocol. DNA was eluted in 30 µL of ATE solution.

Conventional PCR amplification

Conventional PCR to amplify a region of the cytochrome b (cyt b) mtDNA gene was conducted using forward primer, PID-F (5'- CCCTCYAAYATCTCHGCATGATGRAA -3'), and reverse primer, PID-R (5'- GCNCCTCARRADGAYATYTGTCCTCA -3') as described in (Ewart et al., 2021). Conventional PCR was conducted in a volume of 25 µL, each containing 5 µL of sample template, 1x GoTaq® G2 Flexi DNA Polymerase Master Mix (Promega Corporation), 2 mM $MgCl_2$ (Promega Corporation), 0.8 µM of each primer, 0.2 mM dNTP mix (Promega Corporation), 0.08 mM of bovine serum albumin solution and 0.625 units of *Taq* polymerase (Promega Corporation). All conventional PCR was conducted with the following PCR conditions: initial denaturation step at 95°C for 3 min, followed by 40 cycles of denaturing at 95°C for 30 sec, annealing at 57°C for 30 sec and elongation at 72°C for 30 sec, with a final extension at 72°C for 5 min. Samples showing positive PCR amplicons were sequenced via Sanger Sequencing in both forward and reverse directions using the forward primer, PID-F, and the reverse primer, PID-R, respectively. All PCR clean-up and Sanger sequencing was conducted by a commercial DNA sequencing provider (Bio Basic Asia Pacific Pte Ltd., Singapore).

Sequences obtained were aligned and trimmed using BioEdit Sequence Alignment Editor (Hall, 1999)and then compared and matched to the most closely related sequence in the National Center for Biotechnology Information (NCBI) GenBank database using the megablast program on Nucleotide Basic Local Alignment Search Tool (BLASTn) with an expected threshold of 0.05 and word size of 28.

Design of primers and probes for quantitative PCR (qPCR)

A qPCR was designed to quantify the starting DNA template. Briefly, cyt b sequences for *M. javanica* were downloaded from GenBank (www.ncbi.nlm.nih.gov/genbank) and these sequences were then aligned using BioEdit, to identify a highly conserved region. Cyt b sequences for other pangolin species were also aligned to the identified conserved region of *M. javanica* and the aligned regions were visually screened for dissimilarity. The identified region was used for primer/probe design using PrimerQuest™ tool (Owczarzy et al., 2008) with the following parameters: a minimum and maximum PCR product size of 75 bp to 150 bp respectively, a minimum and maximum primer melting temperature of 59˚C to 65˚C and a minimum and maximum probe melting temperature of 64˚C to 72˚C. Five sets of primer/probes were generated by the software and were screened for nonspecific binding using the online PrimerBLAST tool in NCBI database (https://www.ncbi.nlm.nih.gov/Blast.cgi). The selected primer/probes set was synthesised by Integrated DNA Technologies Inc (Singapore). To further assess the specificity, the synthesised primers/probe set was tested against extracted DNA from four species of African pangolins (*Smutsia gigantea*, *Smutsia temminckii*, *Phataginus tricuspis* and *Phataginus tetradactyla*) and human DNA (thumbprint) using qPCR conditions described in this paper.

qPCR amplification

qPCRs were conducted in a volume of 20 µL, each containing 2 µL of sample template, 1X Applied Biosystems™ TaqMan™ Fast Advanced Master Mix (Thermo Fisher Scientific), 0.16 µM forward primer (5'-CTGCTCCTGTTTGCAGTAA-3'), 0.16 µM reverse primer (5'-CGATGTAGGGTATTGCGGATAAA-3') and 0.08 µM hydrolysis probe (5' FAM–AGGACGTATCCCATAAAGGCTGTTGC–MGB 3'). qPCR amplifications were conducted using the following cycling condition: 95 °C for 2 min, followed by 45 cycles of 95°C for 15 sec, and 56°C for 45 sec. A standard curve was generated for every reaction to quantify the copy number of target DNA using a plasmid DNA standard that was synthesized commercially (Bio Basic Inc., Ontario) containing the target DNA sequence. The lyophilised DNA was

resuspended in 40 µL of 1x Tris – EDTA buffer and diluted to a concentration of 10^9 copies/µL. A standard curve was constructed using three replications of the serially 10-fold diluted synthesized DNA with concentrations spanning from 10^6 to 10^1 copies per 2 µL. The qPCR was assessed to be efficient when assay efficiency ranges from 90% to 110% and coefficient of determination (R^2) was >0.98.

Results and Discussion

Latent DNA visualisation on each section of the transparent LDPE bag

Both the positive staining control (human thumbprint) and the bags where *M. javanica* scales had been contained recorded bright, green, fluorescent particles/deposits. At the position where the *M. javanica* scales had been in contact with the bag, single green, fluorescent deposits measuring approximately 0.196 mm in length were recorded. This contrasts with the size of the fluorescent deposits from a human thumbprint (length = 0.130 mm). The human deposits in Figure 3 were also approximately the same size as those reported as human corneocytes (Kanokwongnuwut et al., 2021). The similar, albeit larger, staining pattern seen for pangolin scales gives confidence that the presence of fluorescence staining is due to the presence of biological material rather than auto-fluorescence or any other artefacts. Prior to this report, it was not known if there was any cellular material, or DNA, on the outer surface of pangolin scales.

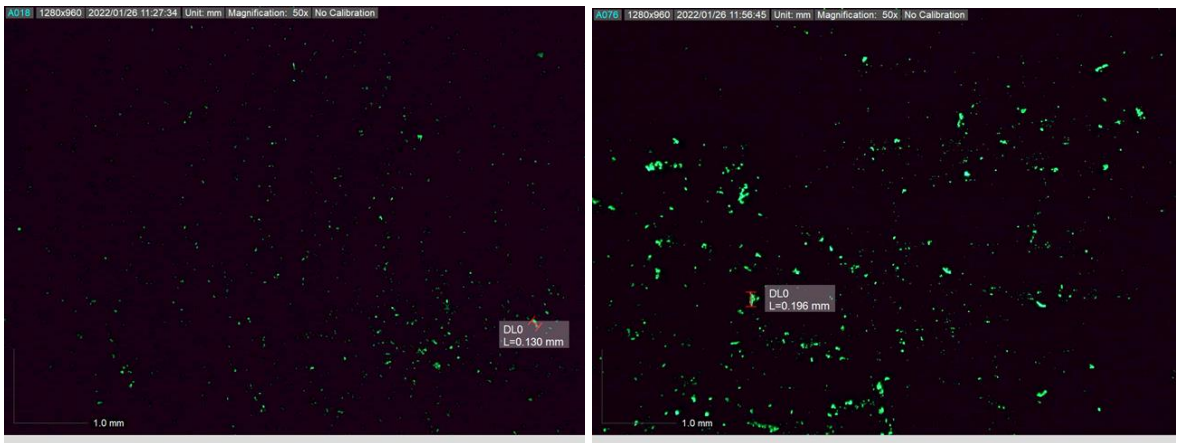

Figure 3: Images showing the fluorescent particles viewed under 50x magnification. (Left) Positive staining control (human thumbprint), length of a fluorescent particle = 0.130 mm. (Right) *M. javanica* scales, length of a fluorescent particle = 0.196 mm.

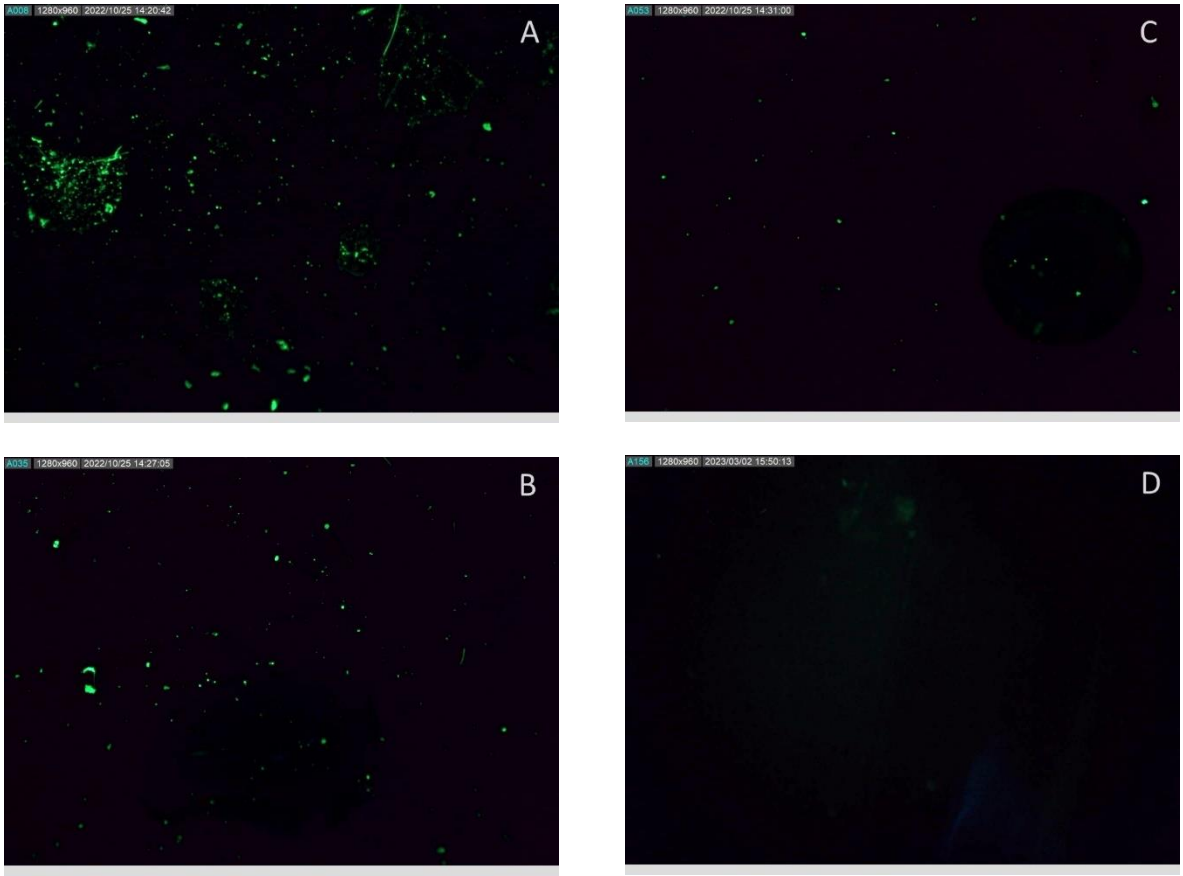

Figure 4: Images showing the fluorescent particles on the different positions of the LDPE bags, onto which pangolin scales may have transferred. A, B and C designate the bottom, middle and top section of the treatment LDPE bags respectively, and D designates the bottom section of the negative control LDPE bag (50x magnification).

All 30 total representative fluorescent particle counts (TRFC) obtained from the various locations (bottom; n=10, middle; n=10, top; n=10) of the LDPE are represented in a boxplot (Figure 5). The bottom of the bag (section 1 and 2) yielded the highest TRFCs while the top of the bag (section 5 and 6) yielded the lowest TRFCs, suggesting that most of the biological material was found at the bottom of the LDPE bag, followed by the middle of the bag, and lastly the top of the bag.

The one-way ANOVA test showed that there was strong evidence that the TRFCs varied (F-value = 40.76, $p < 0.0001$) between the various locations (top: n=10, middle: n=10, and bottom: n=10) of the LDPE bag. A Tukey post-hoc test was then conducted to determine the pairwise relationship between each group, and the result indicates that TRFCs obtained from the bottom of the LDPE bag were higher than that of the middle and top of the LDPE bag ($p < 0.0001$). However, a difference in TRFCs was not evident ($p = 0.29$) between the middle and top of the LDPE bag, where the scales did not have any direct contact with the LDPE during the storage period.

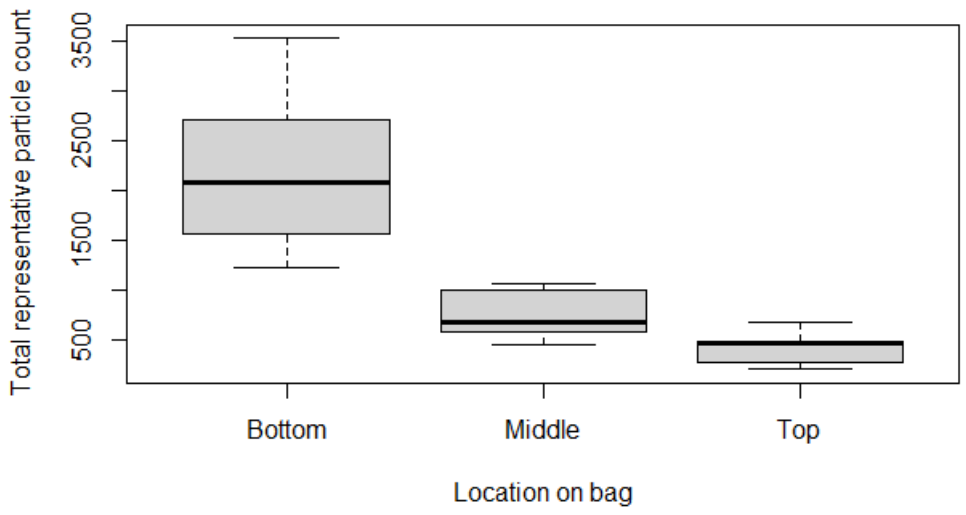

Figure 5: Box plots showing the 25%, 50% and 75% quantiles of the total representative fluorescent particle counts (TRFCs) from all 3 locations on the LDPE bag. TRFCs for section 1 and 2 (n=10) were collated as “Bottom”, section 3 and 4 (n=10) were collated as “Middle” and section 5 and 6 (n=10) were collated as “Top” on the LDPE bag.

Amplification of DNA recovered using conventional PCR

All 30 swabs generated from the five LDPE bags (A – E) which had contained pangolin scales, produced positive PCR amplifications from the cyt b locus, and resulted in DNA sequences of approximately 190 bp per sample. The cellular material on the outer surface of the pangolin scales appears not to be similar to corneocytes and the amount of genomic DNA in each particle is unknown. Despite this, all 30 samples generated an amplicon of the expected size. The sequence data from all 30 samples matched to the cyt b sequence from *M. javanica* reference sequences on BLASTn, with at least 99% identity, confirming that the DNA recovered from all 30 samples were of *M. javanica* origin.

Quantification of DNA recovered using qPCR

The mean copy number from qPCR for sections 1 and 2 (bottom of the LDPE bag) were higher than that of 3 and 4 (middle), whereas sections 5 and 6 (top) yielded the least mean copy number. The mean copy numbers (CN) obtained for each section of the LDPE bags was shown to strongly correlate to the mean fluorescent particle count for each of the section of the LDPE bags (Figure 8: $R^2 = 0.9563$; $p < 0.005$, n=30). In order to assess the strength of association between the respective TRFCs and CNs, the Spearman’s rank correlation was applied and it showed that the respective TRFCs and CNs obtained from each section were strongly positively correlated ($\rho(28) = 0.77$, $p < 0.001$). From these results, it could then be deduced that the bottom of the LDPE bags (section 1 and 2) had the highest mean fluorescent particle counts, therefore yielded the greatest amount of DNA, followed by the middle of the bag. The top of the bag, with which the pangolin scales would have had the least direct contact, yielded the least number of copies of DNA, along with the lowest mean fluorescent particle counts.

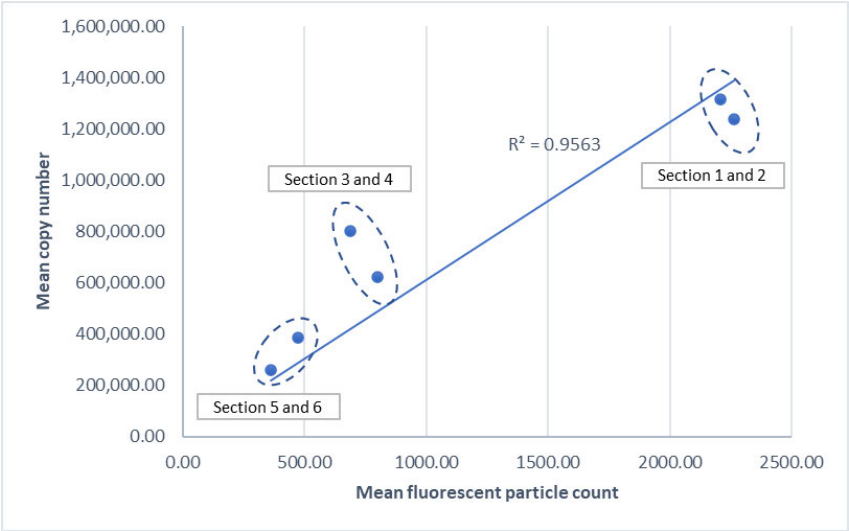

Figure 8: Scatterplot illustrating the relationship between the mean total representative fluorescent particle counts (TRFCs) from the various sections of the bags (n=5) and its respective mean copy number (CN) obtained from *M. javanica* specific qPCR. X-axis shows the mean TRFCs of each section of the LDPE bags and, Y-axis shows the mean CN of starting DNA template for each section of the LDPE bags.

Our results indicated that the greatest cell transfer took place at the bottom of the bag (section 1 and 2) where the highest total representative fluorescent particle count and the highest mean copy number was obtained. This is the part of the bag where there was the greatest amount of direct contact between the pangolin scales and the LDPE bags during the agitation and the seven days storage period. However, although the middle and top portions of the LDPE bags did not have any direct contact with the pangolin scales during the storage period, a significant number of fluorescent particles could still be observed and had transferred onto the surfaces of these sections in sufficient quantity to produce positive PCR amplicons. Sequence data confirmed the DNA to be from *M. javanica*. The inference is that prolonged direct contact, both during shaking on the orbital shaker and storage, was not the only mode of interaction that deposited the DNA onto the surfaces of these bags. It was therefore deduced that apart from prolonged direct contact, the pangolin scales might also be able to deposit DNA onto the surfaces of the LDPE during only the brief moments of friction that were introduced when pangolin scales were poured in and out of the bags.

Conclusion

In this report, *M. javanica* scales used were treated to mimic the pangolin scales seen typically in illegal wildlife trade and despite the dehydration that the scales were subjected to, the presence of fluorescent cellular particles on these contact surfaces could be visualised, indicating that the trace amounts of cellular material on the outer surface of the *M. javanica* pangolin scales had been transferred to the inside of a bag. We demonstrated here that the process of DNA recovery, extraction and amplification of latent DNA that has been applied for use in human forensic science (Hefetz et al., 2019; Kanokwongnuwut et al., 2021; Wood et al., 2017) was shown to be applicable to wildlife samples as well.

The visualisation of latent DNA may be useful to determine if illegal wildlife products were concealed in areas that are not easily accessible for sampling, such as the back of a fully packed shipping container. In such cases, the entryway of the container may be examined for the presence of latent DNA and targeted sampling can be conducted to detect the presence of concealed wildlife goods. Additionally, latent DNA can provide an important piece of evidence to aid in investigations where the wildlife products are not present at the crime scene, leaving behind only the containers and packaging that may once held the wildlife goods.

This proof-of-concept study is the first to show that: there is biological material on the outer surface of pangolin scales; the cellular material contains DNA; the DNA within cellular material transferred by pangolin scales creates similar fluorescence to human corneocytes but larger in length; the trace amounts of cellular material from the pangolin scales is sufficient to generate a PCR product; and even the briefest contact of moving scales into and out of a bag results in sufficient transfer to allow species identification. More study will need to be conducted to examine the factors affecting cell transfer and the effect of various surface substrates on the amount of DNA deposited, and the feasibility in non-mammalian species. This study opens up the opportunity to use latent DNA detection in the fight against the illegal trading of wildlife products.

References

[1] Johnson RN, Wilson-Wilde L, Linacre A. Current and future directions of DNA in wildlife forensic science. Forensic Science International Genetics. 2014;10:1-11.

[2] Challender DWS, Waterman C, M. BJE. Scaling up pangolin conservation. UCN SSC Pangolin Specialist Group Conservation Action Plan. London, UK: Zoological Society of London; 2014.

[3] Xing S, Bonebrake TC, Cheng W, Zhang M, Ades G, Shaw D, et al. Meat and Medicine: Historic and Contemporary Use in Asia. Pangolins 2020. p. 227-39.

[4] Soewu DA, Sodeinde OA. Utilization of pangolins in Africa: Fuelling factors, diversity of uses and sustainability. International Journal of Biodiversity and Conservation. 2015;7:1-10.

[5] Challender DWS, Harrop SR, MacMillan DC. Understanding markets to conserve trade-threatened species in CITES. Biological Conservation. 2015;187:249-59.

[6] Consideration of Proposals for Amendment of Appendices I and II. CITES: Seventeenth meeting of the Conference of the Parties. Johannesburg (South Africa)2016. p. 1-26.

[7] Challender DWS, Heinrich S, Shepherd CR, Katsis LKD. International trade and trafficking in pangolins, 1900–2019. Pangolins2020. p. 259-76.

[8] AFP. Singapore in second major pangolin seizure in a week. AFP International Text Wire in English; Washington. Washington: Agence France-Presse; 2019.

[9] Griffiths J. 14 tons of pangolin scales seized in Singapore in a single smuggling bust. CNN Wire Service; Atlanta. Atlanta: CNN Newsource Sales, Inc.; 2019.

[10] Clarke S. Singapore Officials Seize Elephant Ivory, Pangolin Scales in Record Haul. University Wire; Carlsbad. Carlsbad: Uloop, Inc.; 2019.

[11] Maxwell S, Fuller R, Brooks T, Watson J. Biodiversity: The ravages of guns, nets and bulldozers. Nature. 2016;536:143–5.

[12] Kanokwongnuwut P, Kirkbride P, Linacre A. Detection of latent DNA. Forensic Science International Genetics. 2018;37:95-101.

[13] Tonkrongjun P, Thanakiatkrai P, Phetpeng S, Asawutmangkul W, Sotthibandhu S, Kitpipit T. Touch DNA localization and direct PCR: An improved workflow for STR typing from improvise explosive devices. Forensic Science International: Genetics Supplement Series. 2017;6:e610-e2.

[14] Hughes DA, Szkuta B, van Oorschot RAH, Conlan XA. "Technical Note:" Optimisation of Diamond Nucleic Acid Dye preparation, application, and visualisation, for latent DNA detection. Forensic Science International. 2022;330:111096.

[15] Haines AM, Tobe SS, Kobus HJ, Linacre A. Finding DNA: Using fluorescent in situ detection. Forensic Science International: Genetics Supplement Series. 2015;5:e501-e2.

[16] Kita T, Yamaguchi H, Yokoyama M, Tanaka T, Tanaka N. Morphological study of fragmented DNA on touched objects. Forensic Science International Genetics. 2008;3:32-6.

[17] Haines AM, Tobe SS, Kobus HJ, Linacre A. Duration of in situ fluorescent signals within hairs follicles. Forensic Science International: Genetics Supplement Series. 2015;5:e175-e6.

[18] Truman A, Hook B, Hendricksen A. Diamond™ Nucleic Acid Dye: A Sensitive Alternative to SYBR® Dyes. 2013.

[19] Kanokwongnuwut P, Martin B, Taylor D, Kirkbride KP, Linacre A. How many cells are required for successful DNA profiling? Forensic Science International Genetics. 2021;51:102453.

[20] Haines AM, Tobe SS, Kobus HJ, Linacre A. Effect of nucleic acid binding dyes on DNA extraction, amplification, and STR typing. Electrophoresis. 2015;36:2561-8.

[21] Kanokwongnuwut P, Kirkbride PK, Linacre A. An assessment of tape-lifts. Forensic Science International Genetics. 2020;47:102292.

[22] Deliveyne N, Cassey P, Linacre A, Delean S, Austin JJ, Young JM. Recovering trace reptile DNA from the illegal wildlife trade. Forensic Science International: Animals and Environments. 2022;2.

[23] Schneider CA, Rasband WS, Eliceiri KW. NIH Image to ImageJ: 25 years of image analysis. Nature methods. 2012;9:671-5.

[24] Ewart KM, Lightson AL, Sitam FT, Rovie-Ryan J, Nguyen SG, Morgan KI, et al. DNA analyses of large pangolin scale seizures: Species identification validation and case studies. Forensic Science International: Animals and Environments. 2021;1.

[25] Hall TA. BioEdit: A User-Friendly Biological Sequence Alignment Editor and Analysis Program for Windows 95/98/NT. Nucleic Acids Symposium Series. 1999;41:95-8.

[26] Owczarzy R, Tataurov AV, Wu Y, Manthey JA, McQuisten KA, Almabrazi HG, et al. IDT SciTools: a suite for analysis and design of nucleic acid oligomers. Nucleic Acids Research. 2008;36:W163-9.

[27] Wood I, Park S, Tooke J, Smith O, Morgan RM, Meakin GE. Efficiencies of recovery and extraction of trace DNA from non-porous surfaces. Forensic Science International: Genetics Supplement Series. 2017;6:e153-e5.

[28] Hefetz I, Einot N, Faerman M, Horowitz M, Almog J. Touch DNA: The effect of the deposition pressure on the quality of latent fingermarks and STR profiles. Forensic Science International Genetics. 2019;38:105-12.

6.4 Further Materials and Methods

6.4.1 Deposition of Latent DNA onto Packaging Bags

Four different combinations of DNA recovery and extraction methods were tested in this chapter – (i) swabbing followed by commercial spin column extraction method, (ii) swabbing followed by alkaline lysis extraction method, (iii) tape – lifting followed by commercial spin column extraction method and lastly, (ii) tape – lifting followed by alkaline lysis extraction method. For each workflow, one set of plastic bags, consisting of five transparent LDPE bags (labelled as A – E), each containing approximately 100 g of dried *M. javanica* scales was prepared. One negative control bag (clean bag without *M. javanica* scales) was also included within each set to ensure that the experiments were free from cross contamination.

6.4.2 Latent DNA Recovery via Tape – Lifting

Apart from recovering latent DNA using swabbing as detailed in section 6.3, latent DNA was also recovered using tape – lifting. Brown adhesive packing tape was used for tape-lifting in this chapter. Tape sections of approximately 10 mm x 10 mm were used for recovering DNA deposited on the glass slides, as per previously reported (Kanokwongnuwut et al., 2020b). Each piece of tape was pressed and lifted over each plastic section for 50 times. After tape-lifting, the tape used was examined under the digital microscope to detect the presence of green, fluorescent spots, which was an indication that cellular material had been successfully lifted onto the tape (Kanokwongnuwut et al., 2020b).

6.4.3 Isolation of Latent DNA from Tapes via Commercial Spin Column Kits

Latent DNA was also isolated from tapes using commercial spin column kits as described in section 4.2.5.1.

6.4.3 Isolation of Latent DNA from Swabs or Tapes via Alkaline Lysis Extraction Method

Apart from extracting latent DNA using the commercial spin column kits, latent DNA was also extracted from the swabs or tapes using alkaline lysis extraction methods as described in section 4.2.5.4 and 4.2.5.3 respectively.

6.5 Further Results and Discussion

6.5.1. Comparison of Various Latent DNA Samples Obtained Using Conventional PCR

DNA samples obtained using the four different DNA recovery and extraction workflow were subjected to conventional PCR. Each set of DNA samples consists of 30 samples (six sections from each of the five bags) and six negative samples (six sections from one negative control bag).

Figures 96 to 99 show the PCR results for the different combinations of DNA recovery and DNA extraction methods and Table 31 summarises the PCR results obtained.

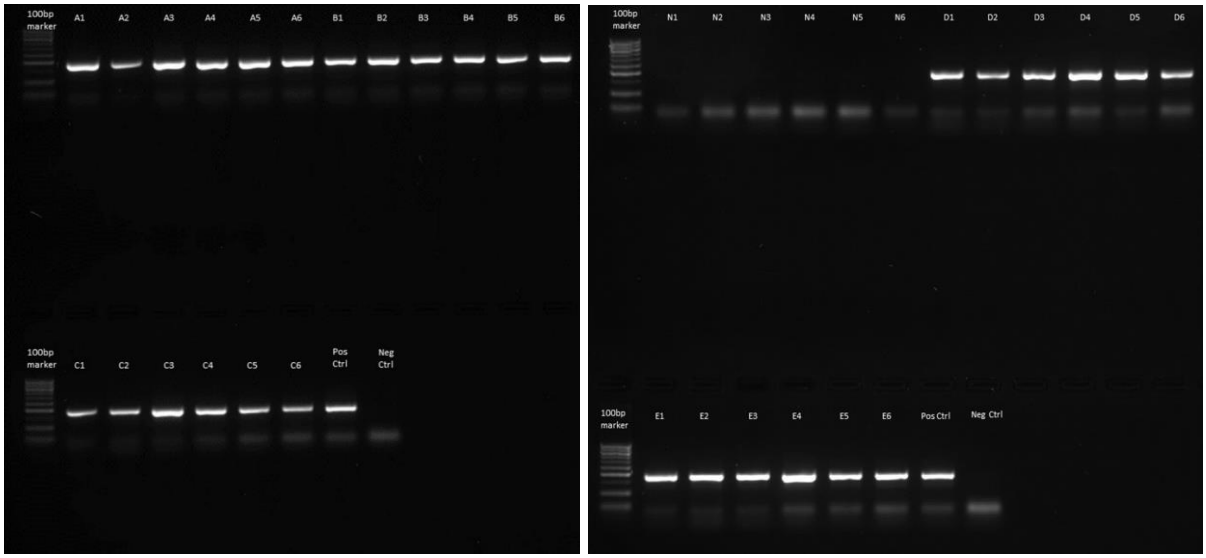

Figure 96: Image of a 1.5% gel after electrophoresis, showing outcome from the PCR amplification. The samples are: no template control (Neg Ctrl), *M. javanica* positive control (Pos Ctrl), negative control bag (N1 – N6), respective bags (A1 – A6, B1 – B6, C1 – C6, D1 – D6, E1 – E6) with *M. javanica* scales. The scales had been contained in the HDPE (transparent) bag by friction, recovered using *swabs* and DNA extracted using the *commercial spin column extraction method*.

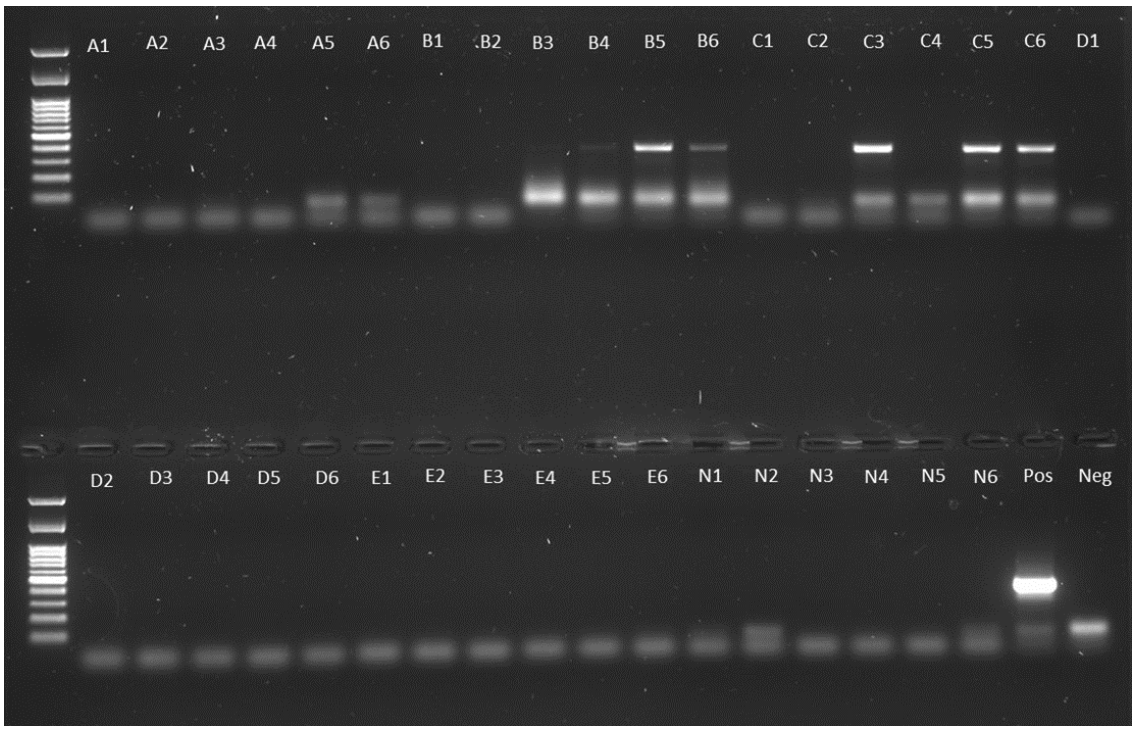

Figure 97: Image of a 1.5% gel after electrophoresis, showing outcome from the PCR amplification. The samples are: no template control (Neg Ctrl), *M. javanica* positive control (Pos Ctrl), negative control bag (N1 – N6), respective bags (A1 – A6, B1 – B6, C1 – C6, D1 – D6, E1 – E6) with *M. javanica* scales. The scales had been contained in the HDPE (transparent) bag by friction, recovered using *swabs* and DNA extracted using the *alkaline lysis extraction method*.

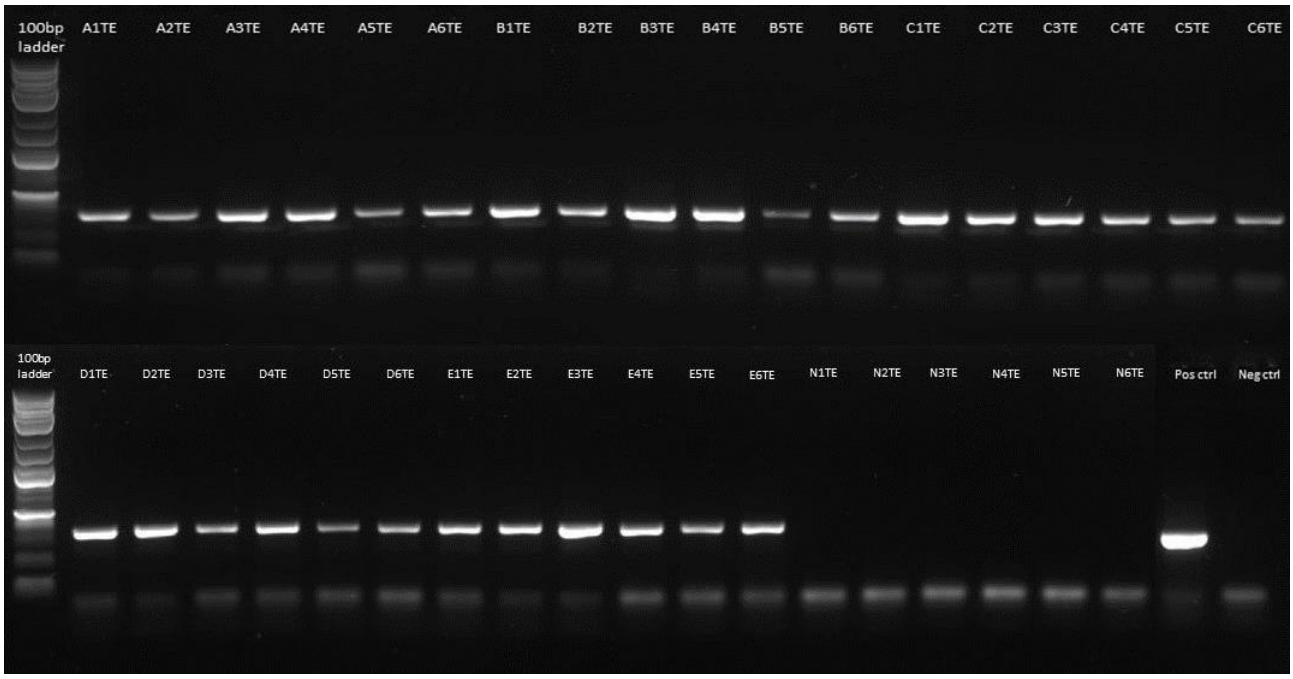

Figure 98: Image of a 1.5% gel after electrophoresis, showing outcome from the PCR amplification. The samples are: no template control (Neg Ctrl), *M. javanica* positive control (Pos Ctrl), negative control bag (N1TE – N6TE), respective bags (A1TE – A6TE, B1TE – B6TE, C1TE – C6TE, D1TE – D6TE, E1TE – E6TE) with *M. javanica* scales. The scales had been contained in the HDPE (transparent) bag, recovered using *tapes* and DNA extracted using the *commercial spin column extraction method*.

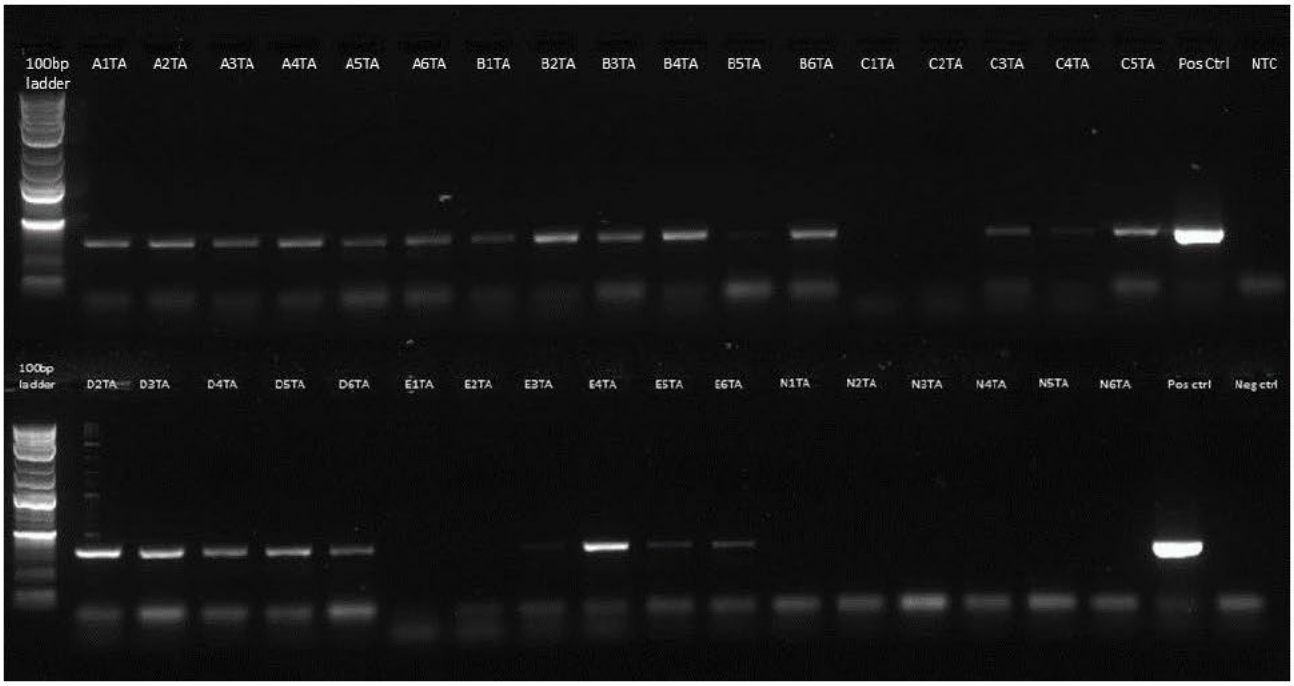

Figure 99: Image of a 1.5% gel after electrophoresis, showing outcome from the PCR amplification. The samples are: no template control (Neg Ctrl), *M. javanica* positive control (Pos Ctrl), negative control bag (N1TA – N6TA), respective bags (A1TA – A6TA, B1TA – B6TA, C1TA – C6TA, D1TA – D6TA, E1TA – E6TA) with *M. javanica* scales. The scales had been contained in the HDPE (transparent) bag, recovered using *tapes* and DNA extracted using the *alkaline lysis extraction method*.

Table 31: Summary of conventional PCR results from DNA samples isolated from HDPE bags using different combinations of DNA recovery and DNA extraction methods. The number of positive amplications were indicated (rate of positive amplification in parentheses).

	Commercial Spin Column	Alkaline Lysis	Total
Swabs	30 (100%)	6 (20%)	36 (60%)
Tape lifts	30 (100%)	26 (86.67%)	56 (93.33%)
Total	60 (100%)	32 (53.33%)	

All 60 samples (comprising of 30 samples recovered using swabs and 30 samples recovered using tape – lifting) that were extracted using commercial spin column kitswere amplified successfully using conventional PCR while only 53.33% of the DNA samples extracted using alkaline lysis extraction methods were positive (Table 31). This showed that the commercial spin column DNA extraction method was more effective in extracting viable DNA for conventional PCR than the alkaline lysis extraction method. The commercial spin column DNA extraction method was able to extract viable DNA samples from both the swabs and tape – lifts, The alkaline lysis extraction method, on the other hand, was able to extract more viable samples from the tape – lifts than swabs.

The samples that were recovered using swabs and extracted alkaline lysis extraction produced the least number of positive PCR amplifications. It was likely that dirt / soil on the the pangolin scales was also deposited onto the surfaces of the bags alongside with the cellular material. This dirt / soil was then recovered by the swab method and was directly transferred into the alkaline lysis solution during the alkaline lysis DNA extraction. The dirt was subsequently added into the PCR tubes as the alkaline lysis solution was used directly as the DNA sample in PCR, causing the PCR inhibition.

In order to eliminate the effects of PCR inhibition due to the presence of dirt, the DNA samples recovered using swabs followed by alkaline lysis extraction method were diluted 10 times using nuclease free water before conventional PCR amplification. Out of the 30 diluted samples, 28 samples were able to generate positive conventional PCR results (Figure 100), indicating that PCR inhibitors were indeed present in the extracted DNA samples using alkaline lysis extraction method from swabs. It was also speculated that that the PCR inhibition was due to the presence of dirt or soil recovered from the surfaces of the bags.

PCR clean-up and Sanger sequencing was conducted was conducted for all PCR positive samples by a commercial DNA sequencing provider (Bio Basic Asia Pacific Pte Ltd., Singapore).DNA sequences obtained were matched to the sequence from *M. javanica* reference sequences on BLASTn, with at least 99% identity. These results confirmed that the DNA recovered from all 30 samples, six from each of the five LDPE bags, were indeed of *M. javanica* origin.

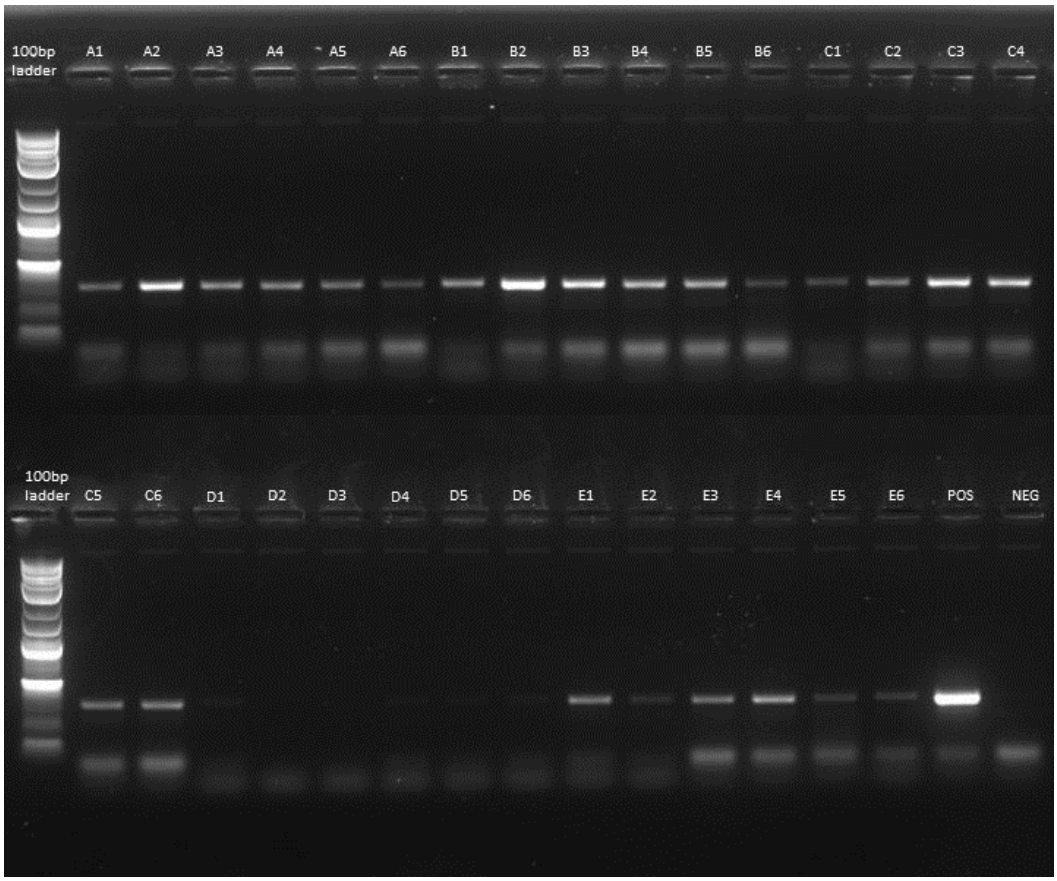

Figure 100: Image of a 1.5% gel after electrophoresis, showing outcome from the PCR amplification. The samples are: no template control (Neg Ctrl), *M. javanica* positive control (Pos Ctrl), as well as diluted samples from the negative control bag (N1 – N6) and respective bags (A1 – A6, B1 – B6, C1 – C6, D1 – D6, E1 – E6) with *M. javanica* scales. The scales had been contained in the HDPE (transparent) bag by friction, recovered using *swabs* and DNA extracted using the *alkaline lysis extraction method*.

6.5.2 DNA Quantification in Various Latent DNA Samples Using qPCR

As shown in 6.3, there was a difference in the copy numbers obtained from the various positions of the bags – bottom, middle and top. And hence, for the ease of comparison, we would only be using the CN from the bottom of the bags in this chapter, as this was where the highest amount of latent *M. javanica* DNA was isolated from.

Table 32 shows the CNs and mean CNs of the DNA samples obtained using various combinations of DNA recovery and extraction methods. The CN obtained for each DNA sample was also plotted into a boxplot based on the various combinations of DNA recovery and DNA extraction methods used (Figure 101).

When comparing the mean CNs of DNA samples obtained using the various DNA recovery and extraction methods, it could be seen that the highest mean CN was obtained when DNA samples was recovered using swabbing followed by commercial spin column extraction method. The next highest mean CN was obtained from DNA samples recovered using tape - lifting followed by commercial spin column extraction method and the lowest mean CN was obtained from DNA samples recovered using tape - lifting followed by alkaline lysis extraction method.

Table 32: Table showing copy numbers of DNA samples obtained using various combinations of DNA recovery and extraction methods. SA: Swab, followed by Alkaline Lysis Extraction, SE: Swab followed by Commercial Spin Column Extraction, TA: Tape - lift, followed by Alkaline Lysis Extraction, SE: Tape - lift followed by Commercial Spin Column Extraction.

	SA	SE	TA	TE
A1	44,258.26	1,924,270.38	9,402.68	156,465.55
A2	43,539.57	1,303,892.75	9,300.29	86,313.40
B1	198,788.95	2,308,489.75	7,203.51	180,064.98
B2	245,590.92	2,373,193.00	12,042.79	205,913.25
C1	247,004.16	442,752.81	5,674.49	974,494.00
C2	294,902.06	786,378.69	4,276.24	142,595.42
D1	18,718.73	290,479.47	87,013.01	302,235.50
D2	18,286.13	416,544.47	37,587.61	384,478.75
E1	74,607.11	1,218,895.50	1,971.25	103,913.36
E2	90,665.97	1,697,183.25	1,770.15	90,253.91
Mean	127,636.19	1,276,208.01	17,624.20	262,672.81

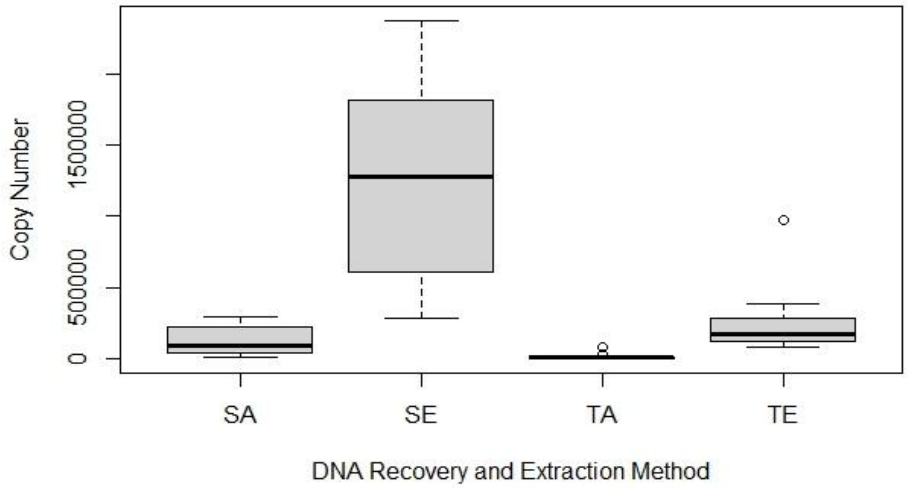

Figure 101: Box plot showing the 25%, 50% and 75% quantiles of the copy numbers obtained for each DNA samples from each treatment group. (n = 10 for each group)

The CNs obtained were also subjected to One-way ANOVA analysis to determine if there was a difference between the copy numbers from the various combinations of DNA recovery and extraction methods. Results from the One-way ANOVA test (Table 33) indicated that there was evidence (F-value = 23.51, p = <0.001) that the copy number of the DNA samples obtained from different combinations of DNA recovery and extraction methods were different. A Tukey post-hoc test (Table 34) was then conducted to determine pairwise relationship between each combination of DNA recovery and extraction methods and likewise, the pairwise comparison showed that there was evidence to indicate that copy numbers of the DNA samples obtained using swabbing followed by commercial spin column extraction method was higher compared to those obtained using the other three combinations of DNA recovery and extraction methods (highlighted in yellow).

Table 33: Raw data obtained for One – Way ANOVA analysis using RStudio, comparing the CNs obtained from samples from LDPE bags, subjected to different combinations of DNA recovery and DNA extraction workflow.

```
> summary(anova)
                    Df    Sum Sq   Mean Sq F value   Pr(>F)
factor(Bags_6.5.2$V1)  3 1.106e+13 3.686e+12   23.51 6.16e-09 ***
Residuals             40 6.270e+12 1.567e+11
---
Signif. codes:  0 ‘***’ 0.001 ‘**’ 0.01 ‘*’ 0.05 ‘.’ 0.1 ‘ ’ 1
```

Table 34: Raw data obtained for Tukey Post – hoc test using RStudio, comparing the CNs obtained from samples from LDPE bags, subjected to different combinations of DNA recovery and DNA extraction workflow. SE denotes samples subjected to swabbing followed by commercial spin

column DNA extraction, SA denotes samples subjected to swabbing followed by commercial alkaline lysis DNA extraction, TE denotes samples subjected to tape - lifting followed by commercial spin column DNA extraction, TA denotes samples subjected to tape - lifting followed by commercial alkaline lysis DNA extraction.

```
> TukeyHSD(anova)
  Tukey multiple comparisons of means
    95% family-wise confidence level

Fit: aov(formula = Bags_6.5.2$V2 ~ factor(Bags_6.5.2$V1))

$`factor(Bags_6.5.2$V1)`
            diff        lwr       upr     p adj
SE-SA  1148571.8   696068.4 1601075.2 0.0000002
TA-SA  -110012.0  -562515.4  342491.4 0.9143488
TE-SA   135036.6  -317466.8  587540.1 0.8540401
TA-SE -1258583.8 -1711087.2 -806080.4 0.0000000
TE-SE -1013535.2 -1466038.6 -561031.8 0.0000027
TE-TA   245048.6  -207454.8  697552.0 0.4756502
```

6.5.3 Discussion of Results and the Optimal DNA Recovery and Extraction Workflow

This chapter demonstrated the deposition of latent DNA from processed *M. javanica* scales onto the plastic bags that they were stored in for a period of seven days. The laboratory-controlled experiment conducted showed that the highest amount of DNA was isolated from the bottom of the bag where the highest amount of contact between the scales and surfaces took place over the storage period. Although the contact period between the scales and the plastic bags was very brief during the pouring of scales in and out of the bags, the presence of latent DNA demonstrated through the fluorescence staining on the middle and top portion of the bag indicated that latent DNA could be deposited when scales were poured in and out of the bags.

Subsequently, the optimal workflow to recover and extract the latent DNA from the surfaces of plastic bags was determined through the use of conventional PCR and qPCR. DNA samples extracted using commercial spin column kits achieved a 100% positive amplification rate, however, DNA samples extracted using alkaline lysis extraction method achieved only 53.33% positive amplification rate. Although the positive amplification rate of DNA samples extracted using alkaline lysis extraction method improved tremendously after the samples were diluted 10x, DNA samples extracted using commercial spin column extraction method still had a higher positive amplification rate, indicating that commercial spin column extract method was a more effective DNA extraction method for use to extract latent DNA from processed *M. javanica* scales.

DNA samples recovered using swabbing achieved a positive amplification rate of 60%, while DNA samples recovered using tape – lifting achieved a positive amplification rate of 93.33%. However, upon dilution of the thirty DNA samples obtained using swabs followed with alkaline lysis extraction method, the positive amplification rate of all DNA samples obtained using swabbing increased to 96.67%. This indicated that PCR inhibitors might be present in samples recovered from such scenarios and where possible, DNA samples should be diluted to minimise the effects of PCR inhibition should DNA concentration be deemed to be sufficient.

The results from the conventional PCR demonstrated that both swabbing and tape – lifting could recover sufficient DNA for conventional PCR amplification, however, the commercial spin column extraction method was far more effective in this scenario than the alkaline lysis extraction method.

The CNs obtained for DNA samples isolated from bottom of each plastic bags indicated that the highest amount of DNA could be obtained using swabbing followed by commercial spin column extraction method. The result correlated well with the results obtained from conventional PCR in this chapter, where swabbing followed by commercial spin column extraction method had also achieved the highest positive PCR amplification rate. The DNA samples, obtained from tape – lifting followed by commercial spin column extraction method which also had also achieved a positive PCR amplification rate of 100%, had the second highest mean CNs. The DNA samples obtained from tape – lifting followed by alkaline lysis extraction method had the lowest mean CN, suggesting they contained the lowest amount of DNA in the samples.

In conclusion, the results from this chapter indicated that swabbing coupled with commercial spin column DNA extraction methods would be the most effective method to be used for isolating latent DNA deposited by *M. javanica* scales onto surfaces of plastic bag that the scales were stored in.

CHAPTER SEVEN: CONCLUSION

7.1 Concluding Remarks

It has long been hypothesised that latent DNA could be recovered from packagings that once containedwildlife products as wildlife products are usually animal parts, such as bones, skins and horns. When in contact with surfaces, the DNA from these processed animal parts may possibly deposit latent DNA onto the contact surfacesthrough the introduction of friction between the products and contact surfaces through movement of the consignment. Th recovered latent DNA can then be used for species identification to aid in wildlife trade enforcement. However, a search on the internet yielded no published evidence of such nature.

Two examples of how latent DNA can help in wildlife trade enforcement. Firstly, the isolation of latent DNA could help enforcement officers to prove that an alleged packaging (such as luggage or plastic bags) may once contained the wildlife product to a wildlife product. Secondly, latent DNA may also be used to determine the presence of concealed wildlife products. A mentioned in section 6.3 - most illegal wildlife goods are typically concealed during transportation to avoid visual inspections and the access to these IWT goods is often met with many difficulties. Latent DNA, if determined to be present, can help to circumvent the access problem and help to provide indication if wildlife products are hidden in concealed areas. The use of DD to visualise latent DNA in such scenarios will help to guide operational or enforcement officers to conduct targeted DNA sampling in a large area so that the samples collected will have a higher possibly of containing the DNA that is representative of the alleged wildlife product.

The work done in this thesis demonstrated that latent DNA could be deposited by pangolin scales that have been processed for distribution in markets. Such pangolin scales were typically processed by drying, and therefore, contained highly degraded DNA. Although the amount of DNA deposited were demonstrated to be very low , this amount was still sufficient to allow positive amplifications using conventional PCR and qPCR in this project and all positive amplicons were correctly identified to be of *M. javanica* origin.

Additionally, work conducted in this project had also demonstrated that latent *M. javanica* DNA deposited on the surfaces of non-porous glass surfaces and plastic bags could be recovered using both swabs and tape – liftings. Although alkaline lysis DNA extraction method is a rapid and cheap way of extracting DNA, the use of commercial spin column DNA extraction method was still the preferred method to extract for the latent *M. javanica* DNA on the swab or tape – lift as more DNA can obtained.

The workflow presented in this project utilises DNA recovery techniques – swabbing and tape – lifting, that are commonly used in human forensic sciences. Such techniques can typically be

carried out by operations or enforcement officers without specialised molecular training. Subsequent DNA extraction and amplification workflow utilises general molecular techniques, such as PCR and Sanger sequencing, that can be found in most molecular laboratories. This makes the whole latent DNA workflow easily implementable for most molecular laboratories.

7.1.1 Limitations

It was demonstrated in the experiments conducted that qPCR targeting a much smaller cyt B region of 100bp mtDNA was able to detect pangolin DNA in more samples than the conventional PCR which targeted a 350bp cyt B mtDNA. This suggested that the isolated latent DNA might be highly degraded, indicating that the latent DNA isolated in the experiment may not be useful for more in genetic analysis where a longer DNA read is more desirable.

Additionally, we should also note that in real case scenarios latent DNA recovered from contact surfaces is highly likely to be of mixed origins, consisting of DNA from various sources such as humans, other vertebrates, invertebrates or even bacteria and plant from the environment. The use of qPCR and conventional PCR demonstrated in this project may not provide sufficient granularity to resolve DNA mixture and hence, the use of next generation sequencing or metabarcoding may have to be evaluated for their suitability for use in such scenarios.

It should also be noted that the use of DD may be limited in some cases. DD might not be able to be visualised clearly on certain surfaces due to background fluorescence (Kanokwongnuwut et al., 2020b)

7.2 Future Work

7.2.1 Deposition of Latent DNA on Different Contact Surface by Various Wildlife Products

The work done in this thesis studied the deposition of DNA from only a single species - the *M. javanica* scales. As the markets turning to the Africa pangolins due to the declining populations of Asian pangolins (Challender et al., 2020; Heinrich et al., 2016), the ability to deposit latent DNA onto contact surfaces by the scales from African pangolins should be also be verified.

The ability of pangolin scales to deposit latent DNA onto other substrates should also be investigated. The amount of background fluorescence with applying DD to various substrates should also be evaluation. Some of the substrates commonly encountered in IWT include canvas bags, gunny sacks, metal surfaces (shipping containers) etc. Such trials will provide us with a better understanding of the practicality of applying latent DNA to enforcements involving seizures of illegal wildlife products.

Apart from pangolin scales, some of the other seized wildlife products (excluding plants) in Singapore includes the ivory ("Singapore seizes record haul of ivory alongside pangolin scales in

S$66m shipment," 2019), rhino horns ("Singapore: Singapore makes biggest seizure of rhino horns," 2022), shark fins and sea cucumbers (Ong & Teng, 2022) etc. Such wildlife products are typically stored in various types of packaging materials during transport and sales. The ability of other wildlife products to deposit latent DNA should also be studied.

7.2.2 Persistence of Latent DNA in Varying Environmental Conditions

This project was conducted in a sheltered, controlled laboratory condition. In reality, it is highly possible that latent DNA deposited by the wildlife products would be exposed to varying environmental conditions such as temperature, rainfall, sunlight, and humidity. Such varying conditions can accelerate the degradation of latent DNA deposited on contact surfaces. Therefore, the persistence of trace amount of latent DNA in varying conditions to ensure that the latent DNA technology should be studied to ensure its deployability in real casework.

7.2.3 Identification of Human Individuals from Latent DNA from IWT Casework

The use of latent DNA deposited on surfaces of tools used in poaching, trapping and snaring of animals has been studied and it showed that latent DNA could be used to link the perpetrators to an illegal animal poaching or trapping activity (Kanokwongnuwut et al., 2020a). Similarly, it is highly possible that human DNA can also be isolated from contact surfaces of an illegal wildlife product consignment and such latent DNA could be used to investigate and link the criminal network involved in the illegal wildlife trade. Metabarcoding or NGS technologies can also be studied to sequence the difference DNA isolated from the contact surfaces to provide a more in-depth information of the illegal consignment.

7.2.4 Validation of Latent DNA for IWT caseworks

Latent or touch DNA has been much widely used on human forensic sciences than the wildlife forensic science and hence, more studies have been conducted using human caseworks as a basis, providing more information on the representativeness and validity of latent DNA is in a casework.

Such validation is also important in wildlife forensic sciences in order to ensure that evidence provided by latent DNA can be admissible in wildlife forensic casework. More validation studies (such as reproducibility and repeatability studies) would have to be conducted.

BIBLIOGRAPHY

't Sas-Rolfes, M., Challender, D. W. S., Hinsley, A., Veríssimo, D., & Milner-Gulland, E. J. (2019). Illegal Wildlife Trade: Scale, Processes, and Governance. *Annual Review of Environment and Resources*, *44*(1), 201-228. https://doi.org/10.1146/annurev-environ-101718-033253

AFP. (2019, Apr 10, 2019). Singapore in second major pangolin seizure in a week. *AFP International Text Wire in English; Washington*. https://www.proquest.com/wire-feeds/singapore-second-major-pangolin-seizureweek/docview/2206028729/se-2?accountid=10910

Alketbi, S. K., & Goodwin, W. (2019). The effect of surface type, collection and extraction methods on touch DNA. *Forensic Science International: Genetics Supplement Series*, *7*(1), 704-706. https://doi.org/10.1016/j.fsigss.2019.10.145

Andersson, A. A., Tilley, H. B., Lau, W., Dudgeon, D., Bonebrake, T. C., & Dingle, C. (2021). CITES and beyond: Illuminating 20 years of global, legal wildlife trade. *Global Ecology and Conservation*, *26*. https://doi.org/10.1016/j.gecco.2021.e01455

Arya, M., Shergill, I. S., Williamson, M., Gommersall, L., Arya, N., & Patel, H. R. (2005). Basic principles of real-time quantitative PCR. *Expert Review of Molecular Diagnostics*, *5*(2), 209-219. https://doi.org/10.1586/14737159.5.2.209

Beasley, J., Shorrock, G., Neumann, R., May, C. A., & Wetton, J. H. (2021). Massively parallel sequencing and capillary electrophoresis of a novel panel of falcon STRs: Concordance with minisatellite DNA profiles from historical wildlife crime. *Forensic Science International Genetics*, *54*, 102550. https://doi.org/10.1016/j.fsigen.2021.102550

Berger, B., Berger, C., Hecht, W., Hellmann, A., Rohleder, U., Schleenbecker, U., & Parson, W. (2014). Validation of two canine STR multiplex-assays following the ISFG recommendations for non-human DNA analysis. *Forensic Science International Genetics*, *8*(1), 90-100. https://doi.org/10.1016/j.fsigen.2013.07.002

Biotium. (2021). GelRed® Nucleic Acid Gel Stain, 10,000X. In.

Borst, P. (2005). Ethidium DNA agarose gel electrophoresis: how it started. *IUBMB Life*, *57*(11), 745-747. https://doi.org/10.1080/15216540500380855

Boscari, E., Barmintseva, A., Pujolar, J. M., Doukakis, P., Mugue, N., & Congiu, L. (2014). Species and hybrid identification of sturgeon caviar: a new molecular approach to detect illegal trade. *Molecular Ecology Resources*, *14*(3), 489-498. https://doi.org/10.1111/1755-0998.12203

Bourgeois, S., Kaden, J., Senn, H., Bunnefeld, N., Jeffery, K. J., Akomo-Okoue, E. F., Ogden, R., & McEwing, R. (2019). Improving cost-efficiency of faecal genotyping: New tools for elephant species. *PLoS One*, *14*(1), e0210811. https://doi.org/10.1371/journal.pone.0210811

Bourzac, K. M., LaVine, L. J., & Rice, M. S. (2003). Analysis of DAPI and SYBR Green I as Alternatives to Ethidium Bromide for Nucleic Acid Staining in Agarose Gel Electrophoresis. *Journal of Chemical Education*, *80*(11), 1292-1296.

Bruijns, B. B., Tiggelaar, R. M., & Gardeniers, H. (2018). The Extraction and Recovery Efficiency of Pure DNA for Different Types of Swabs. *Journal of Forensic Sciences*, *63*(5), 1492-1499. https://doi.org/10.1111/1556-4029.13837

Bucevičius, J., Lukinavičius, G., & Gerasimaitė, R. (2018). The Use of Hoechst Dyes for DNA Staining and beyond. *Chemosensors*, *6*(2). https://doi.org/10.3390/chemosensors6020018

Burrill, J., Daniel, B., & Frascione, N. (2019). A review of trace "Touch DNA" deposits: Variability factors and an exploration of cellular composition. *Forensic Science International Genetics*, *39*, 8-18. https://doi.org/10.1016/j.fsigen.2018.11.019

Burrill, J., Daniel, B., & Frascione, N. (2020). Illuminating touch deposits through cellular characterization of hand rinses and body fluids with nucleic acid fluorescence. *Forensic Science International Genetics*, *46*, 102269. https://doi.org/10.1016/j.fsigen.2020.102269

Burrill, J., Kombara, A., Daniel, B., & Frascione, N. (2021). Exploration of cell-free DNA (cfDNA) recovery for touch deposits. *Forensic Science International Genetics*, *51*, 102431. https://doi.org/10.1016/j.fsigen.2020.102431

Candi, E., Knight, R. A., Panatta, E., Smirnov, A., & Melino, G. (2016). Cornification of the Skin: A Non-apoptotic Cell Death Mechanism. In *eLS* (pp. 1-10). https://doi.org/10.1002/9780470015902.a0021583.pub2

Cardeñosa, D., Chapman, D. D., Robles, Y. L., Ussa, D. A., & Caballero, S. (2021). Rapid species and river-of-origin determination for matamata turtles (Chelus sp.) using real-time PCR: Facilitating rapid return of trafficked specimens back to the wild. *Aquatic Conservation: Marine and Freshwater Ecosystems*, *31*(9), 2586-2593. https://doi.org/10.1002/aqc.3613

Cardenosa, D., Quinlan, J., Shea, K. H., & Chapman, D. D. (2018). Multiplex real-time PCR assay to detect illegal trade of CITES-listed shark species. *Scientific Reports*, *8*(1), 16313. https://doi.org/10.1038/s41598-018-34663-6

Carpi, F. M., Di Pietro, F., Vincenzetti, S., Mignini, F., & Napolioni, V. (2011). Human DNA extraction methods: patents and applications. *Recent Patents on DNA & Gene Sequences*, *5*(1), 1-7. https://doi.org/10.2174/187221511794839264

Castella, V., & Mangin, P. (2008). DNA profiling success and relevance of 1739 contact stains from caseworks. *Forensic Science International: Genetics Supplement Series*, *1*(1), 405-407. https://doi.org/10.1016/j.fsigss.2007.10.071

Challender, D. W. S., Harrop, S. R., & MacMillan, D. C. (2015). Understanding markets to conserve trade-threatened species in CITES. *Biological Conservation*, *187*, 249-259. https://doi.org/10.1016/j.biocon.2015.04.015

Challender, D. W. S., Heinrich, S., Shepherd, C. R., & Katsis, L. K. D. (2020). International trade and trafficking in pangolins, 1900–2019. In *Pangolins* (pp. 259-276). https://doi.org/10.1016/b978-0-12-815507-3.00016-2

Challender, D. W. S., & O'Criodain, C. (2020). Addressing trade threats to pangolins in the Convention on International Trade in Endangered Species of Wild Fauna and Flora (CITES). In *Pangolins* (pp. 305-320). https://doi.org/10.1016/b978-0-12-815507-3.00019-8

Challender, D. W. S., Waterman, C., & M., B. J. E. (2014). Scaling up pangolin conservation. UCN SSC Pangolin Specialist Group Conservation Action Plan, London, UK.

Champion, J., Kanokwongnuwut, P., van Oorschot, R. A. H., Taylor, D., & Linacre, A. (2021). Evaluation of a fluorescent dye to visualize touch DNA on various substrates. *Journal of Forensic Sciences*, *66*(4), 1435-1442. https://doi.org/10.1111/1556-4029.14695

Chong, J. L., Panjang, E., Willcox, D., Nash, H. C., Semiadi, G., Sodsai, W., Lim, N. T. L., Fletcher, L., Kurniawan, A., & Cheema, S. (2020). Sunda pangolin Manis javanica (Desmarest, 1822). In *Pangolins* (pp. 89-108). https://doi.org/10.1016/b978-0-12-815507-3.00006-x

Cicinnati, V. R., Shen, Q., Sotiropoulos, G. C., Radtke, A., Gerken, G., & Beckebaum, S. (2008). Validation of putative reference genes for gene expression studies in human hepatocellular carcinoma using real-time quantitative RT-PCR. *BMC Cancer*, *8*, 350. https://doi.org/10.1186/1471-2407-8-350

CITES. *List of Parties to the Convention*. Retrieved 17 April 2023 from https://cites.org/eng/disc/parties/index.php

CITES. *What is CITES?* Retrieved 14 April 2023 from https://cites.org/eng/disc/what.php

Clarke, S. (2019, Jul 24, 2019). Singapore Officials Seize Elephant Ivory, Pangolin Scales in Record Haul. *University Wire; Carlsbad*. https://www.proquest.com/wire-feeds/singapore-officials-seize-elephant-ivorypangolin/docview/2262901456/se-2?accountid=10910

Comment, D., Gouy, A., Zingg, C., & Zieger, M. (2023). A holistic approach for the selection of forensic DNA swabs. *Forensic Science International*, *348*, 111737. https://doi.org/10.1016/j.forsciint.2023.111737

Comte, J., Baechler, S., Gervaix, J., Lock, E., Milon, M. P., Delemont, O., & Castella, V. (2019). Touch DNA collection - Performance of four different swabs. *Forensic Science International Genetics*, *43*, 102113. https://doi.org/10.1016/j.fsigen.2019.06.014

Consideration of Proposals for Amendment of Appendices I and II. (2016). CITES: Seventeenth meeting of the Conference of the Parties, Johannesburg (South Africa).

Conte, J., Potoczniak, M. J., Mower, C., & Tobe, S. S. (2019). ELEquant: a developmental framework and validation of forensic and conservation real-time PCR assays. *Molecular Biology Reports*, *46*(2), 2093-2100. https://doi.org/10.1007/s11033-019-04660-7

Crisafuli, F. A., Ramos, E. B., & Rocha, M. S. (2015). Characterizing the interaction between DNA and GelRed fluorescent stain. *European Biophysics Journal*, *44*(1-2), 1-7. https://doi.org/10.1007/s00249-014-0995-4

Davoust, B., Mary, C., & Marie, J. L. (2014). Detection of Leishmania in red foxes (Vulpes vulpes) from southeastern France using real-time quantitative PCR. *Journal of Wildlife Diseases*, *50*(1), 130-132. https://doi.org/10.7589/2013-07-190

Dawnay, N., Ogden, R., Thorpe, R. S., Pope, L. C., Dawson, D. A., & McEwing, R. (2008). A forensic STR profiling system for the Eurasian badger: a framework for developing profiling systems for wildlife species. *Forensic Sci Int Genet*, *2*(1), 47-53. https://doi.org/10.1016/j.fsigen.2007.08.006

Deliveyne, N., Cassey, P., Linacre, A., Delean, S., Austin, J. J., & Young, J. M. (2022). Recovering trace reptile DNA from the illegal wildlife trade. *Forensic Science International: Animals and Environments*, *2*. https://doi.org/10.1016/j.fsiae.2021.100040

Dobbin, C. (2017). An Industrial Chronology of Polyethylene. In *Handbook of Industrial Polyethylene and Technology* (pp. 1-23). https://doi.org/10.1002/9781119159797.ch1

Dragan, A. I., Pavlovic, R., McGivney, J. B., Casas-Finet, J. R., Bishop, E. S., Strouse, R. J., Schenerman, M. A., & Geddes, C. D. (2012). SYBR Green I: fluorescence properties and interaction with DNA. *Journal of Fluorescence*, *22*(4), 1189-1199. https://doi.org/10.1007/s10895-012-1059-8

Eikelboom, J. A. J., Nuijten, R. J. M., Wang, Y. X. G., Schroder, B., Heitkonig, I. M. A., Mooij, W. M., van Langevelde, F., & Prins, H. H. T. (2020). Will legal international rhino horn trade save wild rhino populations? *Global Ecology and Conservation*, *23*, e01145. https://doi.org/10.1016/j.gecco.2020.e01145

Ewart, K. M., Frankham, G. J., McEwing, R., Webster, L. M. I., Ciavaglia, S. A., Linacre, A. M. T., The, D. T., Ovouthan, K., & Johnson, R. N. (2018). An internationally standardized species identification test for use on suspected seized rhinoceros horn in the illegal wildlife trade. *Forensic Science International Genetics*, *32*, 33-39. https://doi.org/10.1016/j.fsigen.2017.10.003

Ewart, K. M., Lightson, A. L., Sitam, F. T., Rovie-Ryan, J., Nguyen, S. G., Morgan, K. I., Luczon, A., Anadon, E. M. S., De Bruyn, M., Bourgeois, S., Ouitavon, K., Kotze, A., Bakar, M. S. A., Salgado-Lynn, M., & McEwing, R. (2021). DNA analyses of large pangolin scale seizures: Species identification validation and case studies. *Forensic Science International: Animals and Environments*, *1*. https://doi.org/10.1016/j.fsiae.2021.100014

Farrell, R. E. (2017). Quantitative PCR Techniques. In *RNA Methodologies* (pp. 283-328). https://doi.org/10.1016/b978-0-12-804678-4.00009-9

Fey, A., Eichler, S., Flavier, S., Christen, R., Hofle, M. G., & Guzman, C. A. (2004). Establishment of a real-time PCR-based approach for accurate quantification of bacterial RNA targets in water, using Salmonella as a model organism. *Applied Environment Microbiology*, *70*(6), 3618-3623. https://doi.org/10.1128/AEM.70.6.3618-3623.2004

Finaughty, C., Heathfield, L. J., Kemp, V., & Marquez-Grant, N. (2023). Forensic DNA extraction methods for human hard tissue: A systematic literature review and meta-analysis of technologies and sample type. *Forensic Science International Genetics*, *63*, 102818. https://doi.org/10.1016/j.fsigen.2022.102818

Fu, J., & Allen, R. W. (2019). A method to estimate the age of bloodstains using quantitative PCR. *Forensic Science International Genetics*, *39*, 103-108. https://doi.org/10.1016/j.fsigen.2018.12.004

Fukushima, C. S., Mammola, S., & Cardoso, P. (2020). Global wildlife trade permeates the Tree of Life. *Biology Conservation*, *247*, 108503. https://doi.org/10.1016/j.biocon.2020.108503

Funes-Huacca, M. E., Opel, K., Thompson, R., & McCord, B. R. (2011). A comparison of the effects of PCR inhibition in quantitative PCR and forensic STR analysis. *Electrophoresis*, *32*(9), 1084-1089. https://doi.org/10.1002/elps.201000584

Gao, Y., & Clark, S. G. (2014). Elephant ivory trade in China: Trends and drivers. *Biological Conservation*, *180*, 23-30. https://doi.org/10.1016/j.biocon.2014.09.020

Gaubert, P., Njiokou, F., Ngua, G., Afiademanyo, K., Dufour, S., Malekani, J., Bi, S. G., Tougard, C., Olayemi, A., Danquah, E., Djagoun, C. A., Kaleme, P., Mololo, C. N., Stanley, W., Luo, S. J., & Antunes, A. (2016). Phylogeography of the heavily poached African common pangolin (Pholidota, Manis tricuspis) reveals six cryptic lineages as traceable signatures of Pleistocene diversification. *Molecular Ecology*, *25*(23), 5975-5993. https://doi.org/10.1111/mec.13886

Gaubert, P., Wible, J. R., Heighton, S. P., & Gaudin, T. J. (2020). Phylogeny and systematics. In *Pangolins* (pp. 25-39). https://doi.org/10.1016/b978-0-12-815507-3.00002-2
Gehrig, C., Kummer, D., & Castella, V. (2009). Automated DNA extraction using the QIAsymphony platform: Estimation of DNA recovery from simulated forensic stains. *Forensic Science International: Genetics Supplement Series*, *2*(1), 85-86. https://doi.org/10.1016/j.fsigss.2009.07.009
Goncharova, E. A., Dedkov, V. G., Dolgova, A. S., Kassirov, I. S., Safonova, M. V., Voytsekhovskaya, Y., & Totolian, A. A. (2021). One-step quantitative RT-PCR assay with armored RNA controls for detection of SARS-CoV-2. *Journal of Medical Virology*, *93*(3), 1694-1701. https://doi.org/10.1002/jmv.26540
Gouda, S., Kerry, R. G., Das, A., & Chauhan, N. S. (2020). Wildlife forensics: A boon for species identification and conservation implications. *Forensic Science International*, *317*, 110530. https://doi.org/10.1016/j.forsciint.2020.110530
Griffiths, J. (2019, Apr 8, 2019). 14 tons of pangolin scales seized in Singapore in a single smuggling bust. *CNN Wire Service; Atlanta*. https://www.proquest.com/wire-feeds/14-tons-pangolin-scales-seized-singaporesingle/docview/2204950711/se-2?accountid=10910
Griffiths, L., & Chacon-Cortes, D. (2014). Methods for extracting genomic DNA from whole blood samples: current perspectives. *Journal of Biorepository Science for Applied Medicine*. https://doi.org/10.2147/bsam.S46573
Haines, A. M., Tobe, S. S., Kobus, H. J., & Linacre, A. (2015a). Duration of in situ fluorescent signals within hairs follicles. *Forensic Science International: Genetics Supplement Series*, *5*, e175-e176. https://doi.org/10.1016/j.fsigss.2015.09.070
Haines, A. M., Tobe, S. S., Kobus, H. J., & Linacre, A. (2015b). Effect of nucleic acid binding dyes on DNA extraction, amplification, and STR typing. *Electrophoresis*, *36*(20), 2561-2568. https://doi.org/10.1002/elps.201500170
Haines, A. M., Tobe, S. S., Kobus, H. J., & Linacre, A. (2015c). Finding DNA: Using fluorescent in situ detection. *Forensic Science International: Genetics Supplement Series*, *5*, e501-e502. https://doi.org/10.1016/j.fsigss.2015.09.198
Haines, A. M., Tobe, S. S., Kobus, H. J., & Linacre, A. (2015d). Properties of nucleic acid staining dyes used in gel electrophoresis. *Electrophoresis*, *36*(6), 941-944. https://doi.org/10.1002/elps.201400496
Haines, A. M., Tobe, S. S., & Linacre, A. (2016). Optimization of Diamond Nucleic Acid Dye for quantitative PCR. *Biotechniques*, *61*(4), 183-189. https://doi.org/10.2144/000114458
Hall, T. A. (1999). BioEdit: A User-Friendly Biological Sequence Alignment Editor and Analysis Program for Windows 95/98/NT. *Nucleic Acids Symposium Series*, *41*, 95-98.
Hansson, O., Finnebraaten, M., Heitmann, I. K., Ramse, M., & Bouzga, M. (2009). Trace DNA collection—Performance of minitape and three different swabs. *Forensic Science International: Genetics Supplement Series*, *2*(1), 189-190. https://doi.org/10.1016/j.fsigss.2009.08.098
Harper, C. K., Vermeulen, G. J., Clarke, A. B., de Wet, J. I., & Guthrie, A. J. (2013). Extraction of nuclear DNA from rhinoceros horn and characterization of DNA profiling systems for white (Ceratotherium simum) and black (Diceros bicornis) rhinoceros. *Forensic Science International Genetics*, *7*(4), 428-433. https://doi.org/10.1016/j.fsigen.2013.04.003
Hartless, S., Walton-Williams, L., & Williams, G. (2019). Critical evaluation of touch DNA recovery methods for forensic purposes. *Forensic Science International: Genetics Supplement Series*, *7*(1), 379-380. https://doi.org/10.1016/j.fsigss.2019.10.020
Hedman, J., Jansson, L., Akel, Y., Wallmark, N., Gutierrez Liljestrand, R., Forsberg, C., & Ansell, R. (2020). The double-swab technique versus single swabs for human DNA recovery from various surfaces. *Forensic Science International Genetics*, *46*, 102253. https://doi.org/10.1016/j.fsigen.2020.102253
Hefetz, I., Einot, N., Faerman, M., Horowitz, M., & Almog, J. (2019). Touch DNA: The effect of the deposition pressure on the quality of latent fingermarks and STR profiles. *Forensic Science International Genetics*, *38*, 105-112. https://doi.org/10.1016/j.fsigen.2018.10.016
Heinrich, S., Wittmann, T. A., Prowse, T. A. A., Ross, J. V., Delean, S., Shepherd, C. R., & Cassey, P. (2016). Where did all the pangolins go? International CITES trade in pangolin species. *Global Ecology and Conservation*, *8*, 241-253. https://doi.org/10.1016/j.gecco.2016.09.007

Hellberg, R. S., Isaacs, R. B., & Hernandez, E. L. (2019). Identification of shark species in commercial products using DNA barcoding. *Fisheries Research*, *210*, 81-88. https://doi.org/10.1016/j.fishres.2018.10.010

Hess, S., & Haas, C. (2017). Recovery of Trace DNA on Clothing: A Comparison of Mini-tape Lifting and Three Other Forensic Evidence Collection Techniques. *Journal of Forensic Science*, *62*(1), 187-191. https://doi.org/10.1111/1556-4029.13246

Heymans, R., Vila, A., van Heerwaarden, C. A. M., Jansen, C. C. C., Castelijn, G. A. A., van der Voort, M., & Biesta-Peters, E. G. (2018). Rapid detection and differentiation of Salmonella species, Salmonella Typhimurium and Salmonella Enteritidis by multiplex quantitative PCR. *PLoS One*, *13*(10), e0206316. https://doi.org/10.1371/journal.pone.0206316

Hughes, A. C. (2021). Wildlife trade. *Current Biology Magazine*, *31*(19), R1218-R1224. https://doi.org/10.1016/j.cub.2021.08.056

Hughes, D. A., Szkuta, B., van Oorschot, R. A. H., & Conlan, X. A. (2022). "Technical Note:" Optimisation of Diamond Nucleic Acid Dye preparation, application, and visualisation, for latent DNA detection. *Forensic Science International*, *330*, 111096. https://doi.org/10.1016/j.forsciint.2021.111096

Idris, B., & Goodwin, W. (2015). Comparison of Chelex ® -100 with two solid phase DNA extraction techniques. *Forensic Science International: Genetics Supplement Series*, *5*, e274-e275. https://doi.org/10.1016/j.fsigss.2015.09.109

IUCN. (2016). The Statues, Trade and Conservation of Pangolins (Manis spp.). 17th Meeting of the Conference of the Partiesto CITES, Johannsberg, South Africa.

IUCN. (2021). *The IUCN Red List of Threatened Species*. Retrieved 14/03/2022 from https://www.iucnredlist.org/search/list?query=pangolin&searchType=species

Joël, J., Glanzmann, B., Germann, U., & Cossu, C. (2015). DNA extraction of forensic adhesive tapes—A comparison of two different methods. *Forensic Science International: Genetics Supplement Series*, *5*, e579-e581. https://doi.org/10.1016/j.fsigss.2015.09.229

Johnson, R. N., Wilson-Wilde, L., & Linacre, A. (2014). Current and future directions of DNA in wildlife forensic science. *Forensic Science International Genetics*, *10*, 1-11. https://doi.org/10.1016/j.fsigen.2013.12.007

Kaesler, T., Kirkbride, K. P., & Linacre, A. (2022). DNA deposited in whole thumbprints: A reproducibility study. *Forensic Science International Genetics*, *58*, 102683. https://doi.org/10.1016/j.fsigen.2022.102683

Kaesler, T., Kirkbride, K. P., & Linacre, A. (2023). Persistence of touch DNA on commonly encountered substrates in different storage conditions. *Forensic Science International*, *348*, 111728. https://doi.org/10.1016/j.forsciint.2023.111728

Kanokwongnuwut, P., Kirkbride, K. P., & Linacre, A. (2020a). Detecting latent DNA in wildlife forensic science investigations. *Science & Justice*, *60*(4), 358-362. https://doi.org/10.1016/j.scijus.2020.02.001

Kanokwongnuwut, P., Kirkbride, P., & Linacre, A. (2018a). Detection of latent DNA. *Forensic Science International Genetics*, *37*, 95-101. https://doi.org/10.1016/j.fsigen.2018.08.004

Kanokwongnuwut, P., Kirkbride, P., & Linacre, A. (2018b). Visualising latent DNA on swabs. *Forensic Science International*, *291*, 115-123. https://doi.org/10.1016/j.forsciint.2018.08.016

Kanokwongnuwut, P., Kirkbride, P. K., & Linacre, A. (2020b). An assessment of tape-lifts. *Forensic Science International Genetics*, *47*, 102292. https://doi.org/10.1016/j.fsigen.2020.102292

Kanokwongnuwut, P., Martin, B., Taylor, D., Kirkbride, K. P., & Linacre, A. (2021). How many cells are required for successful DNA profiling? *Forensic Science International Genetics*, *51*, 102453. https://doi.org/10.1016/j.fsigen.2020.102453

Kapuscinski, J. (1995). DAPI: a DNA-specific fluorescent probe. *Biotechnic & Histochemistry*, *70*(5), 220-233. https://doi.org/10.3109/10520299509108199

Kissin, Y. V. (2020). Educational Minimum: Synthesis, Structure, and Properties of Polyethylene Resins. In Y. V. Kissin (Ed.), *Polyethylene* (2 ed., pp. 1-41). Hanser.

Kita, T., Yamaguchi, H., Yokoyama, M., Tanaka, T., & Tanaka, N. (2008). Morphological study of fragmented DNA on touched objects. *Forensic Science International Genetics*, *3*(1), 32-36. https://doi.org/10.1016/j.fsigen.2008.09.002

Kitano, T., Umetsu, K., Tian, W., & Osawa, M. (2007). Two universal primer sets for species identification among vertebrates. *International Journal of Legal Medicine*, *121*(5), 423-427. https://doi.org/10.1007/s00414-006-0113-y

Kubista, M., Andrade, J. M., Bengtsson, M., Forootan, A., Jonak, J., Lind, K., Sindelka, R., Sjoback, R., Sjogreen, B., Strombom, L., Stahlberg, A., & Zoric, N. (2006). The real-time polymerase chain reaction. *Aspects of Molecular Medicine*, *27*(2-3), 95-125. https://doi.org/10.1016/j.mam.2005.12.007

Lim, N. T. L., & Ng, P. K. L. (2008). Home range, activity cycle and natal den usage of a female Sunda pangolin Manis javanica (Mammalia: Pholidota) in Singapore. *Endangered Species Research*, *4*, 233-240. https://doi.org/10.3354/esr00032

Linacre, A. (2021). Animal Forensic Genetics. *Genes (Basel)*, *12*(4). https://doi.org/10.3390/genes12040515

Loontiens, F. G., Regenfuss, P., Zechel, A., Dumortier, L., & Clegg, R. M. (1990). Binding Characteristics of Hoechst 33258 with Calf Thymus DNA, Poly[d(A-T)], and d(CCGGAATTCCGG): Multiple Stoichiometries and Determination of Tight Binding with a Wide Spectrum of Site Affinities. *Biochemistry*, *29*, 9029-9039.

Mapes, A. A., Kloosterman, A. D., & de Poot, C. J. (2015). DNA in the Criminal Justice System: The DNA Success Story in Perspective. *Journal of Forensic Science*, *60*(4), 851-856. https://doi.org/10.1111/1556-4029.12779

Mardan-Nik, M., Saffar Soflaei, S., Biabangard-Zak, A., Asghari, M., Saljoughian, S., Tajbakhsh, A., Meshkat, Z., Ferns, G. A., Pasdar, A., & Ghayour-Mobarhan, M. (2019). A method for improving the efficiency of DNA extraction from clotted blood samples. *Journal of Clinical Laboratory Analysis*, *33*(6), e22892. https://doi.org/10.1002/jcla.22892

Maxwell, S., Fuller, R., Brooks, T., & Watson, J. (2016). Biodiversity: The ravages of guns, nets and bulldozers. *Nature*, *536*, 143–145. https://doi.org/https://doi.org/10.1038/536143a

McCartney, H. A., Foster, S. J., Fraaije, B. A., & Ward, E. (2003). Molecular diagnostics for fungal plant pathogens. *Pest Management Science*, *59*(2), 129-142. https://doi.org/10.1002/ps.575

McGaughey, K. D., Yilmaz-Swenson, T., Elsayed, N. M., Cruz, D. A., Rodriguez, R. R., Kritzer, M. D., Peterchev, A. V., Gray, M., Lewis, S. R., Roach, J., Wetsel, W. C., & Williamson, D. E. (2018). Comparative evaluation of a new magnetic bead-based DNA extraction method from fecal samples for downstream next-generation 16S rRNA gene sequencing. *PLoS One*, *13*(8), e0202858. https://doi.org/10.1371/journal.pone.0202858

Meredith, E. P., Adkins, J. K., & Rodzen, J. A. (2020). UrsaPlex: An STR multiplex for forensic identification of North American black bear (Ursus americanus). *Forensic Science International Genetics*, *44*, 102161. https://doi.org/10.1016/j.fsigen.2019.102161

Mitra, I., Roy, S., & Haque, I. (2018). Application of Molecular Markers in Wildlife DNA Forensic Investigations. *Journal of Forensic Science and Medicine*, *4*(3), 156-160. https://doi.org/10.4103/jfsm.jfsm_23_18

Morton, O., Scheffers, B. R., Haugaasen, T., & Edwards, D. P. (2021). Impacts of wildlife trade on terrestrial biodiversity. *Nature Ecology & Evolution*, *5*(4), 540-548. https://doi.org/10.1038/s41559-021-01399-y

Mure, C. R. (2017). Rigid Packaging Applications. In *Handbook of Industrial Polyethylene and Technology* (pp. 1091-1107). https://doi.org/10.1002/9781119159797.ch41

Nash, H. C., Lee, P. B., Lim, N. T. L., Luz, S., Li, C., Chung, Y. F., Olsson, A., Boopal, A., Strange, B. C. N., & Rao, M. (2020). The Sunda pangolin in Singapore: a multi-stakeholder approach to research and conservation. In *Pangolins* (pp. 411-425). https://doi.org/10.1016/b978-0-12-815507-3.00026-5

Nash, H. C., Wirdateti, Low, G. W., Choo, S. W., Chong, J. L., Semiadi, G., Hari, R., Sulaiman, M. H., Turvey, S. T., Evans, T. A., & Rheindt, F. E. (2018). Conservation genomics reveals possible illegal trade routes and admixture across pangolin lineages in Southeast Asia. *Conservation Genetics*, *19*(5), 1083-1095. https://doi.org/10.1007/s10592-018-1080-9

Nasiri, H., Forouzandeh, M., Rasaee, M. J., & Rahbarizadeh, F. (2005). Modified salting-out method: high-yield, high-quality genomic DNA extraction from whole blood using laundry detergent. *Journal of Clinical Laboratory Analysis*, *19*(6), 229-232. https://doi.org/10.1002/jcla.20083

Nylund, L., Heilig, H. G., Salminen, S., de Vos, W. M., & Satokari, R. (2010). Semi-automated extraction of microbial DNA from feces for qPCR and phylogenetic microarray analysis. *Journal of Microbiological Methods*, *83*(2), 231-235. https://doi.org/10.1016/j.mimet.2010.09.003

Omifolaji, J. K., Ikyaagba, E. T., Jimoh, S. O., Ibrahim, A. S., Ahmad, S., & Luan, X. (2020). The emergence of Nigeria as a staging ground in the illegal pangolin exportation to South East Asia. *Forensic Science International: Reports*, *2*. https://doi.org/10.1016/j.fsir.2020.100138

Ong, E. J., & Teng, C. S. (2022). *A Rapid Assessment of Online Trade in Sea Cucumber and Fish Maw in Malaysia and Singapore*.

Oswald, N. (2015, November 2020). *What Is a Cq (Ct) Value?* Retrieved 30 May 2023 from https://bitesizebio.com/24581/what-is-a-ct-value/

Owczarzy, R., Tataurov, A. V., Wu, Y., Manthey, J. A., McQuisten, K. A., Almabrazi, H. G., Pedersen, K. F., Lin, Y., Garretson, J., McEntaggart, N. O., Sailor, C. A., Dawson, R. B., & Peek, A. S. (2008). IDT SciTools: a suite for analysis and design of nucleic acid oligomers. *Nucleic Acids Research*, *36*(Web Server issue), W163-169. https://doi.org/10.1093/nar/gkn198

Panjaruang, P., Romgaew, T., & Aobaom, S. (2022). Detection of touch DNA evidence on swab by SYBR(R)Green I Nucleic Acid Gel Stain. *Forensic Science International*, *341*, 111477. https://doi.org/10.1016/j.forsciint.2022.111477

Patel, R. M. (2017). Types and Basics of Polyethylene. In *Handbook of Industrial Polyethylene and Technology* (pp. 105-138). https://doi.org/10.1002/9781119159797.ch4

Phillips, K., McCallum, N., & Welch, L. (2012). A comparison of methods for forensic DNA extraction: Chelex-100(R) and the QIAGEN DNA Investigator Kit (manual and automated). *Forensic Science International Genetics*, *6*(2), 282-285. https://doi.org/10.1016/j.fsigen.2011.04.018

Quinones, I., & Daniel, B. (2012). Cell free DNA as a component of forensic evidence recovered from touched surfaces. *Forensic Science International Genetics*, *6*(1), 26-30. https://doi.org/10.1016/j.fsigen.2011.01.004

Raymond, J. J., van Oorschot, R. A., Gunn, P. R., Walsh, S. J., & Roux, C. (2009). Trace evidence characteristics of DNA: A preliminary investigation of the persistence of DNA at crime scenes. *Forensic Science International Genetics*, *4*(1), 26-33. https://doi.org/10.1016/j.fsigen.2009.04.002

Sauer, E., Reinke, A. K., & Courts, C. (2016). Differentiation of five body fluids from forensic samples by expression analysis of four microRNAs using quantitative PCR. *Forensic Science International Genetics*, *22*, 89-99. https://doi.org/10.1016/j.fsigen.2016.01.018

Schefe, J. H., Lehmann, K. E., Buschmann, I. R., Unger, T., & Funke-Kaiser, H. (2006). Quantitative real-time RT-PCR data analysis: current concepts and the novel "gene expression's CT difference" formula. *Journal of Molecular Medicine*, *84*(11), 901-910. https://doi.org/10.1007/s00109-006-0097-6

Scheffers, B., Brunno, F. O. B., Lamb, I., & Edwards, D. (2019). Global wildlife trade across the tree of life. *Science*, *366*(6461), 71-76. https://doi.org/10.1126/science.aav5327

Schneider, C. A., Rasband, W. S., & Eliceiri, K. W. (2012). NIH Image to ImageJ: 25 years of image analysis. *Nature methods*, *9*(7), 671-675. https://doi.org/10.1038/nmeth.2089

Schury, N., Schleenbecker, U., & Hellmann, A. P. (2014). Forensic animal DNA typing: Allele nomenclature and standardization of 14 feline STR markers. *Forensic Science International Genetics*, *12*, 42-59. https://doi.org/10.1016/j.fsigen.2014.05.002

Sewell, J., Quinones, I., Ames, C., Multaney, B., Curtis, S., Seeboruth, H., Moore, S., & Daniel, B. (2008). Recovery of DNA and fingerprints from touched documents. *Forensic Science International Genetics*, *2*(4), 281-285. https://doi.org/10.1016/j.fsigen.2008.03.006

Shaik, M., Shivanna, D. K., Kamate, M., Ab, V., & Tp, K. V. (2016). Single Lysis-Salting Out Method of Genomic DNA Extraction From Dried Blood Spots. *Journal of Clinical Laboratory Analysis*, *30*(6), 1009-1012. https://doi.org/10.1002/jcla.21972

Shea, K. H., & To, A. W. L. (2017). From boat to bowl: Patterns and dynamics of shark fin trade in Hong Kong — implications for monitoring and management. *Marine Policy*, *81*, 330-339. https://doi.org/10.1016/j.marpol.2017.04.016

Singapore seizes record haul of ivory alongside pangolin scales in S$66m shipment. (2019, 23/07/2019). *CNA*. https://www.channelnewsasia.com/singapore/singapore-seizes-record-ivory-pangolin-scales-congo-vietnam-1312516

Singapore: Singapore makes biggest seizure of rhino horns. (2022, 10 Oct 2022). *Asia News Monitor*.

Singer, V. L., Lawlor, T. E., & Yue, S. (1999). Comparison of SYBR® Green I nucleic acid gel stain mutagenicity and ethidium bromide mutagenicity in the Salmonella/mammalian microsome reverse mutation assay (Ames test). *Mutation Research/Genetic Toxicology and Environmental Mutagenesis*, *439*(1), 37-47. https://doi.org/https://doi.org/10.1016/S1383-5718(98)00172-7

Singh, U. A., Kumari, M., & Iyengar, S. (2018). Method for improving the quality of genomic DNA obtained from minute quantities of tissue and blood samples using Chelex 100 resin. *Biological Procedures Online*, *20*, 12. https://doi.org/10.1186/s12575-018-0077-6

Smith, C. J., & Osborn, A. M. (2009). Advantages and limitations of quantitative PCR (Q-PCR)-based approaches in microbial ecology. *FEMS Microbiol Ecology*, *67*(1), 6-20. https://doi.org/10.1111/j.1574-6941.2008.00629.x

Soewu, D. A., & Sodeinde, O. A. (2015). Utilization of pangolins in Africa: Fuelling factors, diversity of uses and sustainability. *International Journal of Biodiversity and Conservation*, *7*(1), 1-10. https://doi.org/10.5897/ijbc2014.0760

Staats, M., Arulandhu, A. J., Gravendeel, B., Holst-Jensen, A., Scholtens, I., Peelen, T., Prins, T. W., & Kok, E. (2016). Advances in DNA metabarcoding for food and wildlife forensic species identification. *Analytical and Bioanalytical Chemistry*, *408*(17), 4615-4630. https://doi.org/10.1007/s00216-016-9595-8

Sweet, D., Lorente, M., Lorente, J. A., Valenzuela, A., & Villanueva, E. (1997). An improved method to recover saliva from human skin: the double swab technique. *Journal of Forensic Sciences*, *42*(2), 320-322.

Symes, W. S., McGrath, F. L., Rao, M., & Carrasco, L. R. (2018). The Gravity of Wildlife Trade. *Biological Conservation*, *218*, 268-276. https://doi.org/10.1016/j.biocon.2017.11.007

ThermofisherScientific. *Nucleic Acid Stains—Section 8.1*. Retrieved 15/03/2022 from https://www.thermofisher.com/sg/en/home/references/molecular-probes-the-handbook/nucleic-acid-detection-and-genomics-technology/nucleic-acid-stains.html

ThermoFisherScientificInc. (2018). Qubit dsDNA assay specificity in the presence of single-stranded DNA. In T. F. S. Inc. (Ed.).

Tobe, S. S., Kitchener, A. C., & Linacre, A. M. (2010). Reconstructing mammalian phylogenies: a detailed comparison of the cytochrome B and cytochrome oxidase subunit I mitochondrial genes. *PLoS One*, *5*(11), e14156. https://doi.org/10.1371/journal.pone.0014156

Tonkrongjun, P., Thanakiatkrai, P., Phetpeng, S., Asawutmangkul, W., Sotthibandhu, S., & Kitpipit, T. (2017). Touch DNA localization and direct PCR: An improved workflow for STR typing from improvise explosive devices. *Forensic Science International: Genetics Supplement Series*, *6*, e610-e612. https://doi.org/10.1016/j.fsigss.2017.09.228

TRAFFIC. (2022). *Illegal wildlife trade: enhancing responses to wildlife crime and illegal trade*. TRAFFIC. Retrieved 14/03/2022 from https://www.traffic.org/about-us/illegal-wildlife-trade/

Truman, A., Hook, B., & Hendricksen, A. (2013). *Diamond™ Nucleic Acid Dye: A Sensitive Alternative to SYBR® Dyes*. Retrieved 25/03/2022 from https://www.promega.sg/resources/pubhub/diamond-nucleic-acid-dye-is-a-safe-and-economical-alternative-to-ethidium-bromide/

van Oorschot, R. A., Ballantyne, K. N., & Mitchell, R. J. (2012). Forensic trace DNA: a review. *Investigative Genetics*, *1*(14), 1-17. https://doi.org/https://doi.org/10.1186/2041-2223-1-14

Verdon, T. J., Mitchell, R. J., & van Oorschot, R. A. (2014a). Evaluation of tapelifting as a collection method for touch DNA. *Forensic Science International Genetics*, *8*(1), 179-186. https://doi.org/10.1016/j.fsigen.2013.09.005

Verdon, T. J., Mitchell, R. J., & van Oorschot, R. A. (2014b). Swabs as DNA collection devices for sampling different biological materials from different substrates. *Journal of Forensic Science*, *59*(4), 1080-1089. https://doi.org/10.1111/1556-4029.12427

Walsh, P. S., Metzger, D. A., & Higuchi, R. (2013). Chelex 100 as a Medium for Simple Extraction of DNA for PCR-Based Typing from Forensic Material. *Biotechniques*, *54*(3), 134-139. https://doi.org/10.2144/000114018

Wang, B., Yang, W., Sherman, V. R., & Meyers, M. A. (2016). Pangolin armor: Overlapping, structure, and mechanical properties of the keratinous scales. *Acta Biomaterialia*, *41*, 60-74. https://doi.org/10.1016/j.actbio.2016.05.028

Wang, Y., Turvey, S. T., & Leader-Williams, N. (2022). Global biodiversity conservation requires traditional Chinese medicine trade to be sustainable and well regulated. *Global Change Biology*, *28*(23), 6847-6856. https://doi.org/10.1111/gcb.16425

Wasser, Brown L., Mailand C., Mondol S., C. W., Laurie C., & B.S, W. (2015). Genetic assignment of large seizures of elephant ivory reveals Africa's major poaching hotspots. *Science*, *349*(6243), 84-87. https://doi.org/10.1126/science.aaa2457

Williamson, A. L. (2012). Touch DNA: Forensic Collection and Application to Investigations. *Journal of Associated Crime Scene Reconstruction* (18), 1-5.

Wood, I., Park, S., Tooke, J., Smith, O., Morgan, R. M., & Meakin, G. E. (2017). Efficiencies of recovery and extraction of trace DNA from non-porous surfaces. *Forensic Science International: Genetics Supplement Series*, *6*, e153-e155. https://doi.org/10.1016/j.fsigss.2017.09.022

Wooster, J., & Martin, J. (2017). Flexible Packaging Applications of Polyethylene. In *Handbook of Industrial Polyethylene and Technology* (pp. 1071-1090). https://doi.org/10.1002/9781119159797.ch40

Wozney, K. M., & Wilson, P. J. (2012). Real-time PCR detection and quantification of elephantid DNA: species identification for highly processed samples associated with the ivory trade. *Forensic Science International*, *219*(1-3), 106-112. https://doi.org/10.1016/j.forsciint.2011.12.006

Xie, K. (2015). Crime Gone Wild: The Dangers of the International Illegal Wildlife Trade. *Harvard International Review*, *36*(4), 60-63.

Xing, S., Bonebrake, T. C., Cheng, W., Zhang, M., Ades, G., Shaw, D., & Zhou, Y. (2020). Meat and Medicine: Historic and Contemporary Use in Asia. In *Pangolins* (pp. 227-239). https://doi.org/10.1016/b978-0-12-815507-3.00014-9

Xu, M., Arku, B., Jartti, T., Koskinen, J., Peltola, V., Hedman, K., & Soderlund-Venermo, M. (2017). Comparative Diagnosis of Human Bocavirus 1 Respiratory Infection With Messenger RNA Reverse-Transcription Polymerase Chain Reaction (PCR), DNA Quantitative PCR, and Serology. *Journal of Infectious Diseases*, *215*(10), 1551-1557. https://doi.org/10.1093/infdis/jix169

Zain, S., Melisch, R., & Timoshyna, A. (2017). *Complementary approaches: the role in tackling illegal wildlife trade*.

Zemb, O., Achard, C. S., Hamelin, J., De Almeida, M. L., Gabinaud, B., Cauquil, L., Verschuren, L. M. G., & Godon, J. J. (2020). Absolute quantitation of microbes using 16S rRNA gene metabarcoding: A rapid normalization of relative abundances by quantitative PCR targeting a 16S rRNA gene spike-in standard. *Microbiologyopen*, *9*(3), e977. https://doi.org/10.1002/mbo3.977

Zhang, F., Wu, S., Yang, L., Zhang, L., Sun, R., & Li, S. (2015). Reproductive parameters of the Sunda pangolin,Manis javanica. *Folia Zoologica*, *64*(2), 129-135. https://doi.org/10.25225/fozo.v64.i2.a6.2015

Zhang, H., Ades, G., Miller, M. P., Yang, F., Lai, K., & Fischer, G. A. (2020). Genetic identification of African pangolins and their origin in illegal trade. *Global Ecology and Conservation*, *23*. https://doi.org/10.1016/j.gecco.2020.e01119

Zhang, X. X., Brantley, S. L., Corcelli, S. A., & Tokmakoff, A. (2020). DNA minor-groove binder Hoechst 33258 destabilizes base-pairing adjacent to its binding site. *Communications Biology*, *3*(1), 525. https://doi.org/10.1038/s42003-020-01241-4

Zhao, F., Bulin, L., Fricker-Hidalgo, H., Renaut, Q., Robert, M. G., Garnaud, C., Pelloux, H., & Brenier-Pinchart, M. P. (2020). Molecular diagnosis of toxoplasmosis: evaluation of automated DNA extraction using eMAG(R) (bioMerieux) on buffy coat, cerebrospinal and bronchoalveolar lavage fluids. *Clinical Chemistry and Laboratory Medicine*, *58*(3), e91-e93. https://doi.org/10.1515/cclm-2019-0753

Zipper, H., Brunner, H., Bernhagen, J., & Vitzthum, F. (2004). Investigations on DNA intercalation and surface binding by SYBR Green I, its structure determination and methodological implications. *Nucleic Acids Research*, *32*(12), e103. https://doi.org/10.1093/nar/gnh101

APPENDICES

Appendix A: Additional illustrations for Section 2.3.2: Staining of Cellular Material Deposited by *M. javanica* Scales via Friction

Figure A1: Particle length measurements for slide with thumbprint deposited.

Figure A2: Particle length measurements for slide with scale A deposited.

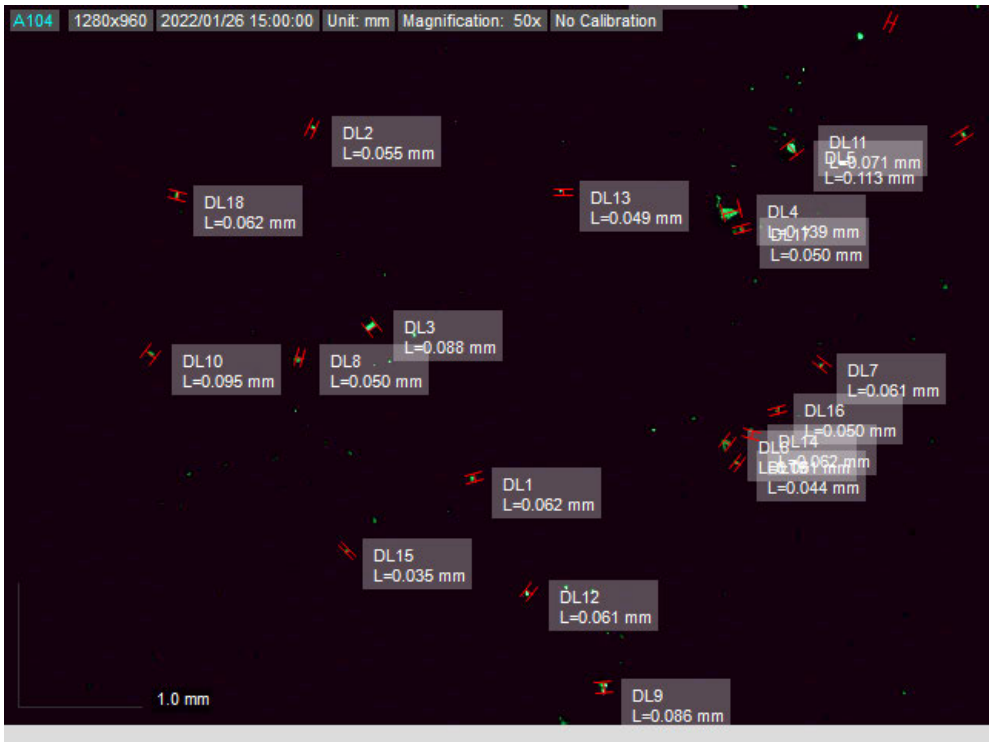

Figure A3: Particle length measurements for slide with scale B deposited.

Figure A4: Particle length measurements for slide with scale C deposited.

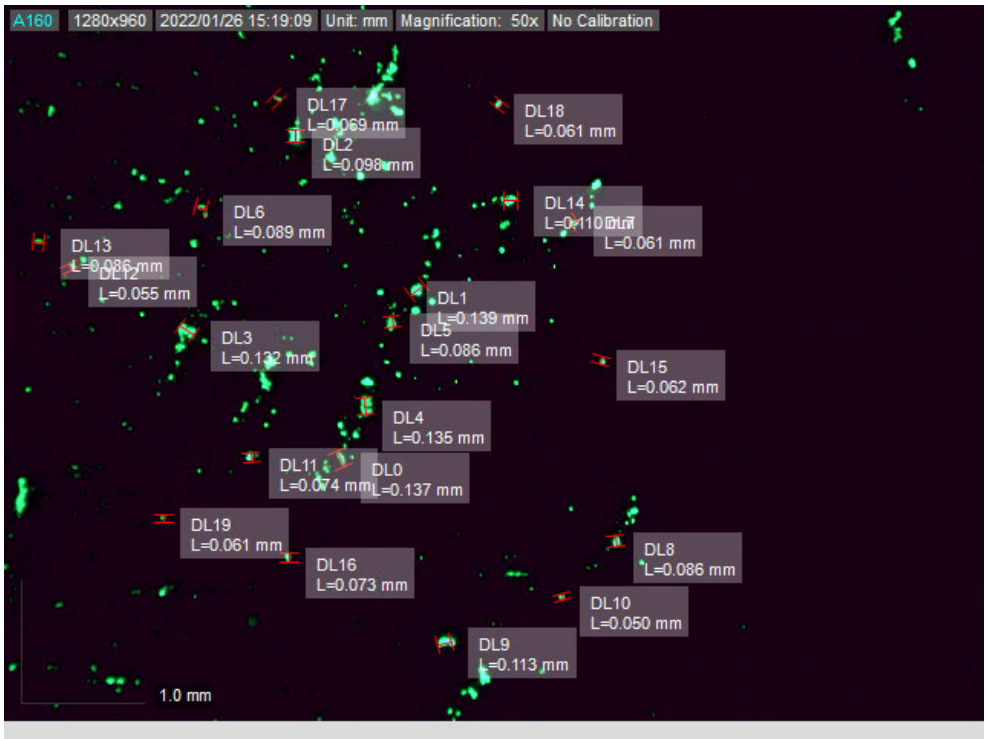

Figure A5: Particle length measurements for slide with scale D deposited.

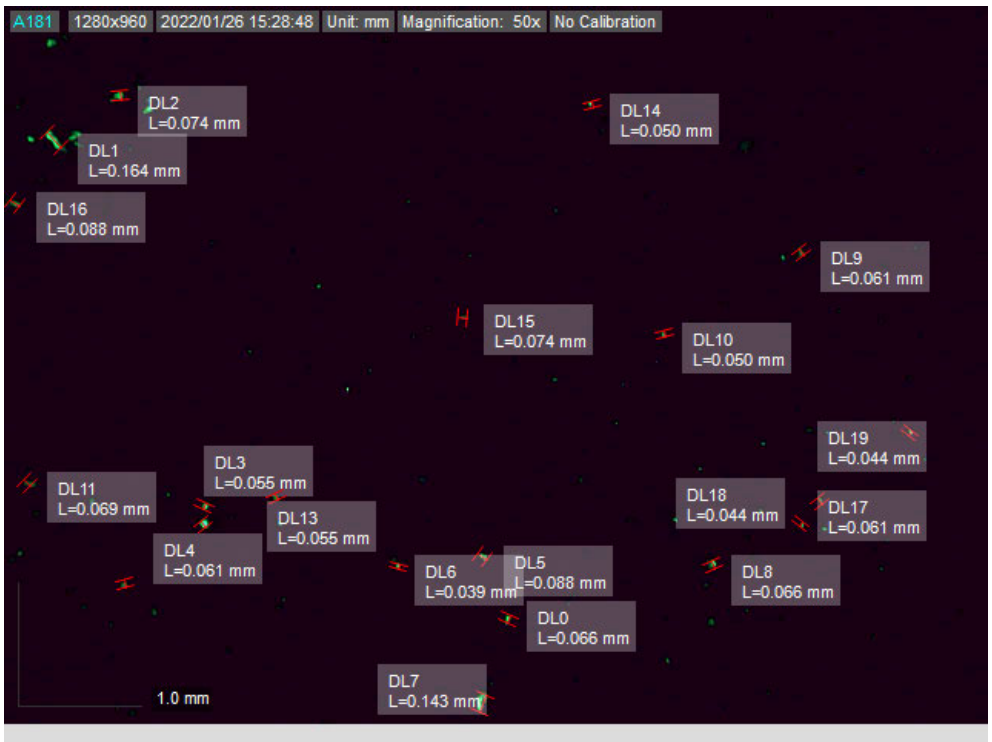

Figure A6: Particle length measurements for slide with scale E deposited.

```
> summary(anova_particleLength)
                              Df  Sum Sq  Mean Sq F value  Pr(>F)
factor(Particle.length$Slide)  5 0.01997 0.003994   4.087 0.00189 **
Residuals                    114 0.11141 0.000977
---
Signif. codes:  0 ‘***’ 0.001 ‘**’ 0.01 ‘*’ 0.05 ‘.’ 0.1 ‘ ’ 1
```

Table A1: Raw data from One Way Anova analysis generated by RStudio.

```
> TukeyHSD(anova_particleLength)
  Tukey multiple comparisons of means
    95% family-wise confidence level

Fit: aov(formula = Particle.length$Particle.length ~ factor(Particle.length$Sli
de))

$`factor(Particle.length$Slide)`
                 diff          lwr          upr     p adj
B-A          -0.02400 -0.052655986  0.004655986 0.1555070
C-A          -0.01170 -0.040355986  0.016955986 0.8438525
D-A          -0.00260 -0.031255986  0.026055986 0.9998251
E-A          -0.02075 -0.049405986  0.007905986 0.2952285
Thumbprint-A -0.03740 -0.066055986 -0.008744014 0.0033154
C-B           0.01230 -0.016355986  0.040955986 0.8140491
D-B           0.02140 -0.007255986  0.050055986 0.2624725
E-B           0.00325 -0.025405986  0.031905986 0.9994780
Thumbprint-B -0.01340 -0.042055986  0.015255986 0.7531997
D-C           0.00910 -0.019555986  0.037755986 0.9404978
E-C          -0.00905 -0.037705986  0.019605986 0.9418236
Thumbprint-C -0.02570 -0.054355986  0.002955986 0.1056915
E-D          -0.01815 -0.046805986  0.010505986 0.4470727
Thumbprint-D -0.03480 -0.063455986 -0.006144014 0.0079737
Thumbprint-E -0.01665 -0.045305986  0.012005986 0.5449556
```

Table A2: Raw data from Post Tukey analysis generated by Rstudio.

	Image no.	Blank Slide	Thumbprint	A	B	C	D	E
Row 1	1	23	0	27	23	28	210	64
	2	4	2	4	16	15	138	202
	3	0	19	161	27	24	118	66
	4	0	32	78	16	16	25	42
	5	0	10	175	94	30	99	167
	6	0	27	32	85	55	241	206
	7	3	13	47	37	39	274	52
Row 2	8	58	28	76	45	74	146	88
	9	2	44	51	60	118	557	317
	10	0	112	264	23	185	332	272
	11	0	183	95	51	123	108	96
	12	0	202	355	162	45	64	99
	13	0	23	221	136	201	22	163
	14	0	1	73	60	326	228	309
Row 3	15	24	70	97	56	67	124	89
	16	2	181	831	90	396	921	333
	17	0	368	554	19	294	827	109
	18	1	509	988	72	117	282	55
	19	1	240	385	49	40	123	64
	20	3	60	1284	61	101	141	219
	21	1	7	346	203	247	262	183
Row 4	22	25	115	48	55	51	36	22
	23	3	218	1338	105	233	253	170
	24	1	313	871	333	111	471	264
	25	0	408	1605	76	106	76	96
	25	0	202	953	98	179	30	188
	27	1	15	265	20	222	140	275
	28	0	2	397	3	103	179	213
	Total	152	3404	11621	2075	3546	6427	4423

Table A3: Fluorescent particle count for each image obtained from slides deposited with *M. javanica* scales via friction.

Appendix B: Additional illustrations for Section 2.3.3: Staining of Cellular Material Deposited by *M. javanica* Scales via Pressure

Figure B1: Particle length measurements for slide with scale A, Ventral side deposited via pressure.

Figure B2: Particle length measurements for slide with scale B, Ventral side deposited via pressure.

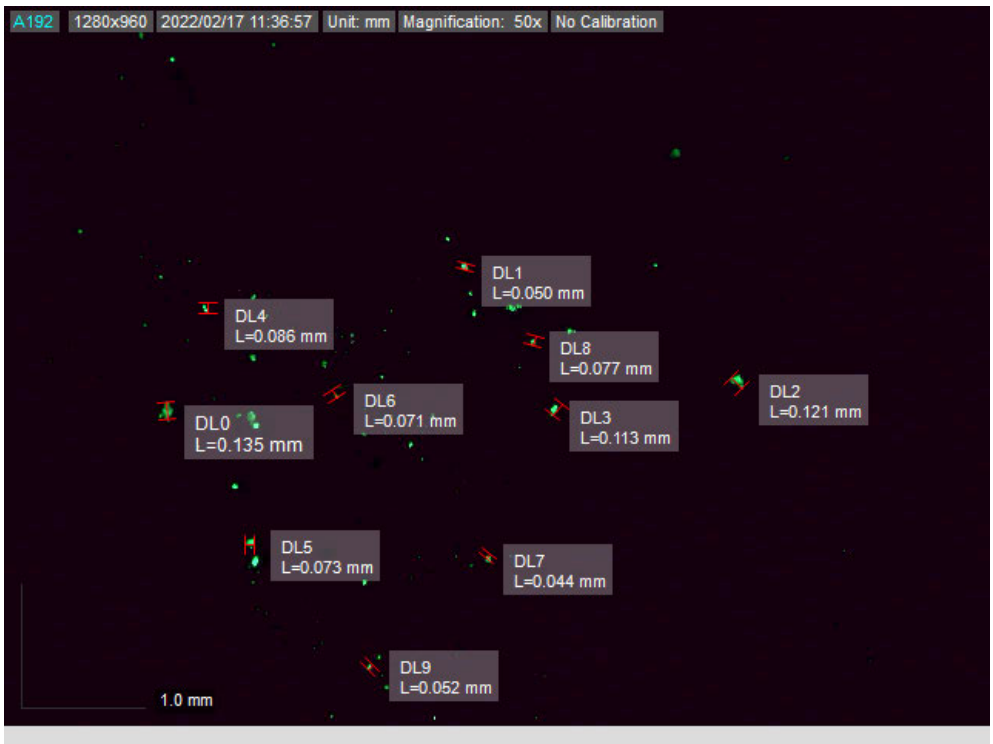

Figure B3: Particle length measurements for slide with scale C, Ventral side deposited via pressure.

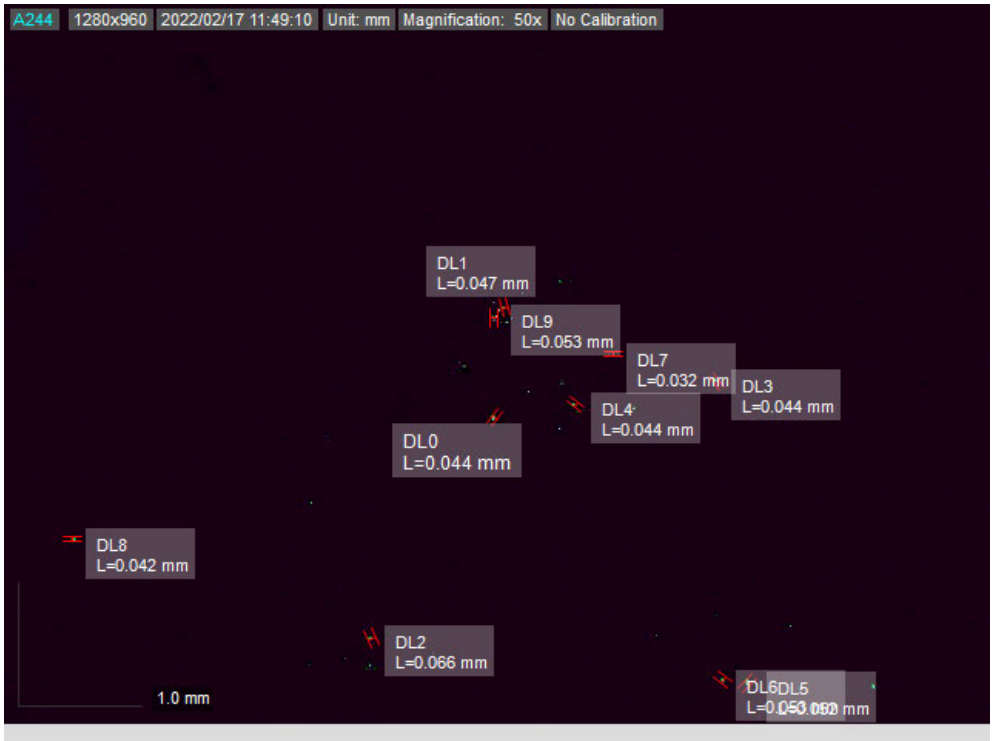

Figure B4: Particle length measurements for slide with scale D, Ventral side deposited via pressure.

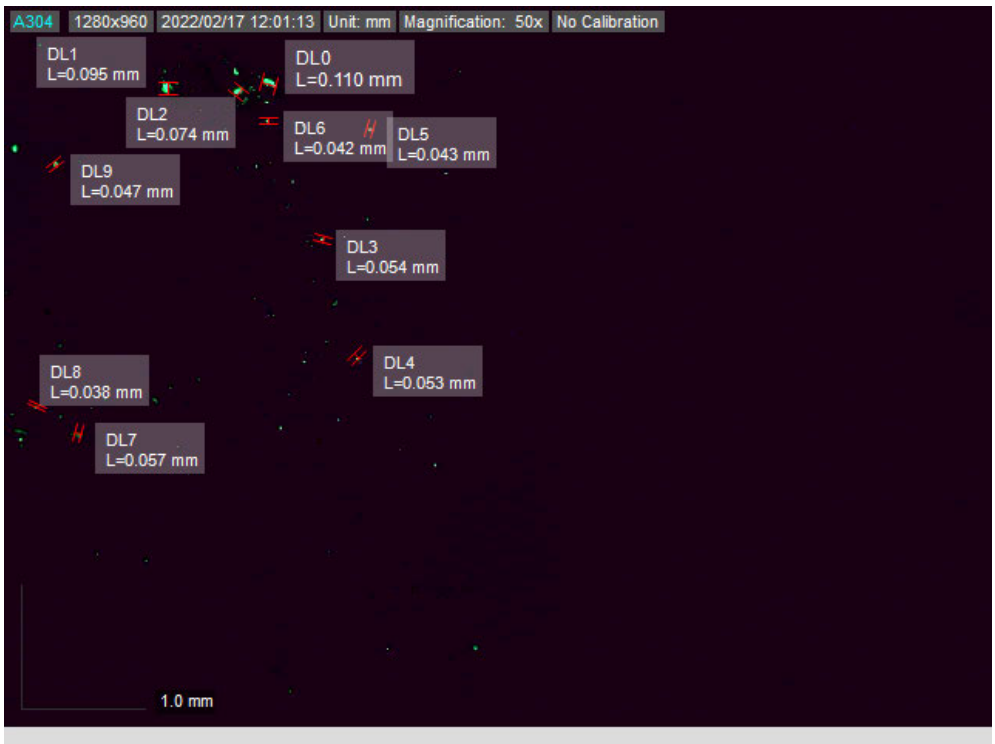

Figure B5: Particle length measurements for slide with scale E, Ventral side deposited via pressure.

Table B1: Raw data from One Way Anova analysis generated by RStudio.

```
                                Df  Sum Sq   Mean Sq F value  Pr(>F)
factor(particle.length_pressure$Slide)  5 0.01340 0.0026807   4.265 0.00243 **
Residuals                              54 0.03394 0.0006286
---
Signif. codes:  0 ‘***’ 0.001 ‘**’ 0.01 ‘*’ 0.05 ‘.’ 0.1 ‘ ’ 1
```

Table B2: Raw data from Post Tukey analysis generated by Rstudio.

```
Tukey multiple comparisons of means
    95% family-wise confidence level

Fit: aov(formula = particle.length_pressure$Particle.Length ~ factor(particle.l
ength_pressure$Slide))

$`factor(particle.length_pressure$Slide)`
                          diff         lwr           upr     p adj
B, Ventral-A, Ventral -0.0054 -0.03852723  0.0277272291 0.9966221
C, Ventral-A, Ventral -0.0016 -0.03472723  0.0315272291 0.9999912
D, Ventral-A, Ventral -0.0361 -0.06922723 -0.0029727709 0.0251253
E, Ventral-A, Ventral -0.0225 -0.05562723  0.0106272291 0.3521392
Thumbprint-A, Ventral -0.0339 -0.06702723 -0.0007727709 0.0420236
C, Ventral-B, Ventral  0.0038 -0.02932723  0.0369272291 0.9993749
D, Ventral-B, Ventral -0.0307 -0.06382723  0.0024272291 0.0841657
E, Ventral-B, Ventral -0.0171 -0.05022723  0.0160272291 0.6499358
Thumbprint-B, Ventral -0.0285 -0.06162723  0.0046272291 0.1302404
D, Ventral-C, Ventral -0.0345 -0.06762723 -0.0013727709 0.0366265
E, Ventral-C, Ventral -0.0209 -0.05402723  0.0122272291 0.4349560
Thumbprint-C, Ventral -0.0323 -0.06542723  0.0008272291 0.0599720
E, Ventral-D, Ventral  0.0136 -0.01952723  0.0467272291 0.8286764
Thumbprint-D, Ventral  0.0022 -0.03092723  0.0353272291 0.9999574
Thumbprint-E, Ventral -0.0114 -0.04452723  0.0217272291 0.9103425
```

Table B3: Fluorescent particle count for each image obtained from slides deposited with *M. javanica* scales via pressure.

Image no.	Neg Ctrl (B)	Neg Ctrl (T)	AV	AD	BV	BD	CV	CD	DV	DD	EV	ED
2	0	1	10	4	1	7	9	0	3	10	2	5
3	3	1	3	3	1	2	42	4	1	4	11	1
4	1	1	5	2	2	0	55	0	1	9	1	5
5	0	1	5	1	4	0	5	0	0	1	1	3
6	0	0	1	3	4	3	12	0	3	1	0	1
7	1	0	0	2	2	0	19	2	4	1	3	0
9	0	2	2	3	2	0	11	1	4	4	1	2
10	0	1	29	8	2	38	13	3	6	7	4	1
11	1	0	2	1	0	0	31	2	3	5	2	12
12	1	0	0	2	0	1	25	3	9	0	41	5
13	0	0	1	1	0	2	9	1	5	0	6	1
14	0	0	6	1	1	0	6	0	9	2	17	0
16	0	0	27	3	1	0	85	1	48	0	3	2
17	0	0	27	1	0	8	21	1	9	6	6	2
18	3	0	1	1	4	1	3	2	12	7	6	0
19	0	0	4	5	1	1	50	1	3	0	51	0
20	0	0	6	0	0	2	96	0	44	1	85	1
21	0	0	2	1	0	1	3	2	15	6	4	0
23	0	1	14	0	27	3	12	3	3	0	14	2
24	0	1	4	2	7	6	14	5	4	2	81	0
25	0	0	0	0	2	2	7	1	0	0	3	0
25	0	0	0	0	13	1	23	2	5	1	2	0
27	0	0	1	0	3	1	12	0	1	1	8	2
28	1	2	3	1	1	1	9	0	10	0	8	0
Total	11	11	153	45	78	80	572	34	202	68	360	45

Appendix C: Co – Authorship Approval Form

STUDENT DETAILS

Student Name	Hee Joo Amy Chan
Student ID	2021749
College	College of Science and Engineering
Degree	Master of Science by research
Title of Thesis	Visualisation and Detection of Latent DNA in the Wildlife Trade: Pangolins as a Model Species

PUBLICATION 1

This section is to be completed by the student and co-authors. If there are more than four co-authors (student plus 3 others), only the three co-authors with the most significant contributions are required to sign below.

Please note: A copy of this page will be provided to the Examiners.

Full Publication Details	Disrupting the illegal trade in pangolins: Visualisation and Detection of Latent DNA Deposited by Pangolin Scales
Section of thesis where publication is referred to	Section 6.3

Student's contribution to the publication	70	%	Research design
	100	%	Data collection and analysis
	60	%	Writing and editing

Outline your (the student's) contribution to the publication:

Student designed the project plan and performed the project. Data used in the published was generated from the project carried out by the student and was collected and analysed by the student. The first draft of the publication was written by the student and subsequently vetted by the co – authors.

APPROVALS

By signing the section below, you confirm that the details above are an accurate record of the student's contribution to the work.

Name of Co-Author 1	Prof. Adrian Linacre	Signed		Date	28/08/2023
Name of Co-Author 2	Prof. Michael G. Gardner	Signed		Date	29/08/2023